

Iron Catalysis in Synthetic Chemistry

**SUJOY RANA, ATANU MODAK, SOHAM MAITY,
TUHIN PATRA, AND DEBABRATA MAITI**

*Department of Chemistry, Indian Institute of Technology Bombay,
Powai, Mumbai, India*

CONTENTS

- I. INTRODUCTION
- II. ADDITION REACTIONS
 - A. Cycloadditions
 - 1. The [2 + 2] Cycloaddition
 - 2. The [3 + 2] Cycloaddition
 - 3. The [2 + 2 + 2] Cycloaddition
 - 4. The [4 + 2] Cycloaddition
 - B. Cyclopropanation
 - C. Aziridination and Aziridine Ring-Opening Reactions
 - D. Carbometalation of C–C Unsaturation Bond
 - E. Michael Addition
 - F. Barbier-Type Reaction
 - G. Kharasch Reaction
- III. THE C–C BOND FORMATIONS VIA C–H FUNCTIONALIZATION
 - A. The C–H Arylation
 - 1. Direct Arylation With Organometallic Reagents
 - 2. Direct Arylation With Aryl Halides
 - B. The C–C Bond Formation Via Cross-Dehydrogenative Coupling
 - 1. The CDC Between Two sp^3 C–H Bonds
 - 2. The CDC Between sp^3 and sp^2 C–H Bonds
 - 3. The CDC Between sp^3 and sp C–H Bonds
 - C. The C–C Bond Formation via Cross-Decarboxylative Coupling
 - D. The C–C Bond Formation via Alkene Insertion
 - E. Oxidative Coupling of Two C–H Bonds
- IV. THE C–H BOND OXIDATION
 - A. Hydroxylation

- B. Epoxidation
- C. cis-Dihydroxylation

V. CROSS-COUPLING REACTIONS

- A. Alkenyl Derivatives as Coupling Partners
- B. Aryl Derivatives as Coupling Partners
- C. Alkyl Derivatives as Coupling Partners
 - 1. Low-Valent Iron Complex in Cross-Coupling Reactions
- D. Acyl Derivatives as Coupling Partners
- E. Iron-Catalyzed C–O, C–S, and C–N Cross-Coupling Reaction
- F. Iron-Catalyzed Mizoraki–Heck Reaction
- G. Iron-Catalyzed Negishi Coupling Reaction
- H. Suzuki–Miyaura Coupling Reaction
- I. Sonogashira Reaction
- J. Mechanism of Cross-Coupling Reactions
- K. Hydrocarboxylation
- L. Enyne Cross-Coupling Reaction

VI. DIRECT C–N BOND FORMATION VIA C–H OXIDATION

VII. IRON-CATALYZED AMINATION

- A. Allylic Aminations
- B. Intramolecular Allylic Amination

VIII. SULFOXIDATIONS AND SYNTHESIS OF SULFOXIMINES, SULFIMIDES, AND SULFOXIMIDES

- A. Sulfoxidation
- B. Synthesis of Sulfoximines, Sulfimides, and Sulfoximides
 - 1. Mechanism

IX. REDUCTION REACTIONS

- A. Hydrosilylation of Alkenes
- B. Hydrosilylation of Aldehydes and Ketones
- C. Hydrogenation of C–C Unsaturated Bonds
- D. Hydrogenation of Ketones
- E. Hydrogenation of Imines
- F. Reduction of Nitroarene to Anilines
- G. Hydrogenation of Carbon Dioxide and Bicarbonate
- H. Amide Reduction
- I. Reductive Aminations

X. TRIFLUOROMETHYLATION

XI. CONCLUSION

ACKNOWLEDGMENTS

ABBREVIATIONS

REFERENCES

I. INTRODUCTION

During the last few decades, transition metal catalysts, especially those on precious metals [e.g., palladium (Pd), rhodium (Rh), iridium (Ir), and ruthenium (Ru)] have proven to be efficient for a large number of applications. The success of transition metal based organometallic catalysts lies in the easy modification of their environment by ligand exchange. A very large number of different types of ligands can coordinate to transition metal ions. Once the ligands are coordinated, the reactivity of the metals may change dramatically. However, the limited availability of these metals, in order of decreasing risk (depletion): Au > Ir, Rh, Ru > Pt, Re, Pd), as well as their high price (Fig. 1) and significant toxicity, makes it desirable to search for more economical and environmental friendly alternatives. A possible solution to this problem could be the increased use of catalysts based on first-row transition metals, especially iron (Fe) (1). In contrast to synthetic precious metal catalysts, iron takes part in various biological systems as an essential key element and electron-transfer reactions.

Due to its abundance, inexpensiveness, and environmentally benign nature, use of iron has increased significantly in the last two decades for synthetic transformation both in asymmetric synthesis and reaction methodology. This development encouraged us to summarize the use of iron catalysis in organic synthesis, which includes cycloadditions, C–C, C–N bond formation, redox, and other reactions. This chapter has been divided into different sections based on the reaction type.

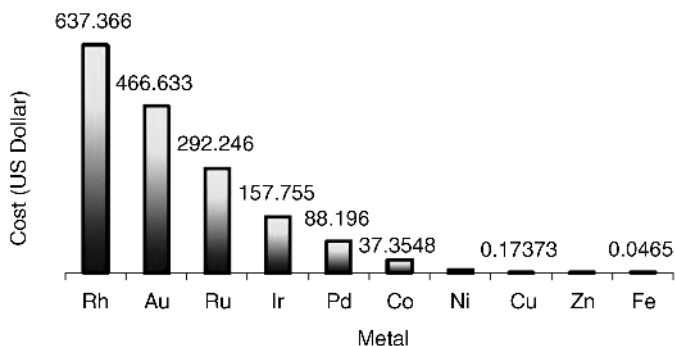


Figure 1. Comparison of prices for different transition metals (Sigma Aldrich).

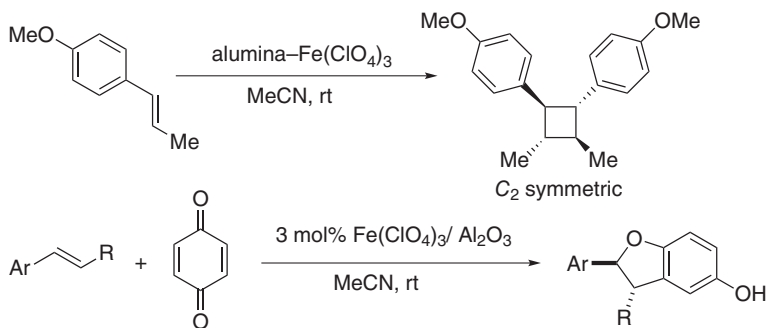
II. ADDITION REACTIONS

A. Cycloadditions

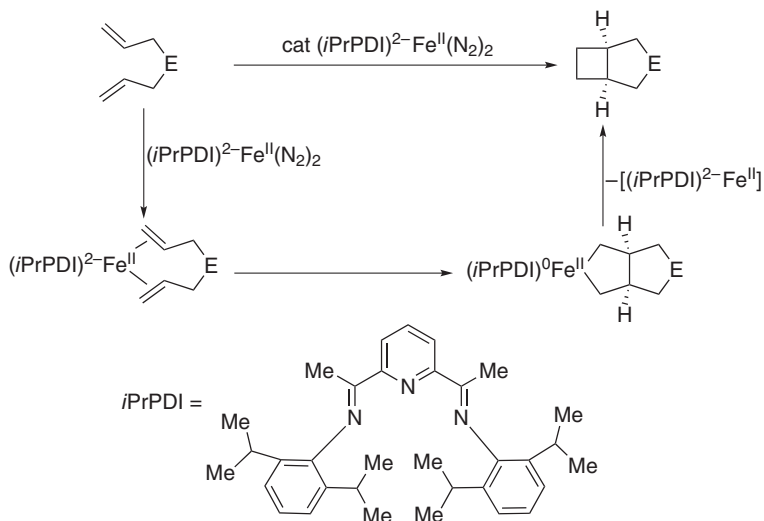
1. The [2 + 2] Cycloaddition

In 2001, Itoh and co-workers (2) demonstrated the [2 + 2] cyclodimerization of *trans*-anethol catalyzed by alumina supported iron(III) perchlorate. A C_2 symmetric cyclobutane derivative was obtained in excellent yield (92%) at room temperature (rt), though longer reaction time was required. They applied the same catalytic system for the cycloaddition of styrenes and quinones. However, 2,3-dihydrobenzofuran derivatives were obtained in excellent yields in place of the desired [2 + 2] cycloadduct (Scheme 1) (3). Earlier, in 1982, Rosenblum and Scheck (4) showed that the $CpFe(CO)_2$ cation, where Cp = cyclopentadienyl, could afford the unsaturated bicycle through the reaction of alkenes and methyl tetrolate, though the yields obtained were inferior.

Significant improvement in iron-catalyzed [2 + 2] cycloaddition was achieved in 2006 by Chirik and co-workers (5). They reported an intramolecular [2 + 2] cycloaddition of the dienes resulting in the formation of [0.2.3] heptane derivatives catalyzed by a bis(imino)-pyridine iron(II) bis(dinitrogen) complex and only *cis* product was obtained. Further, labeling experiments confirmed the reaction to be stereospecific. A number of dienes containing different amine and ester functional groups reacted efficiently, but the presence of secondary amine and an $SiMe_2$ group inhibited the reaction. This reaction can also be performed in the dark, clearly indicating the process to be thermally driven, rather than a photochemical one. A mechanism of this catalytic process was proposed where iron is assumed to maintain its ferrous oxidation state throughout the reaction with the help of redox active *i*PrPDI ligand (Scheme 2).

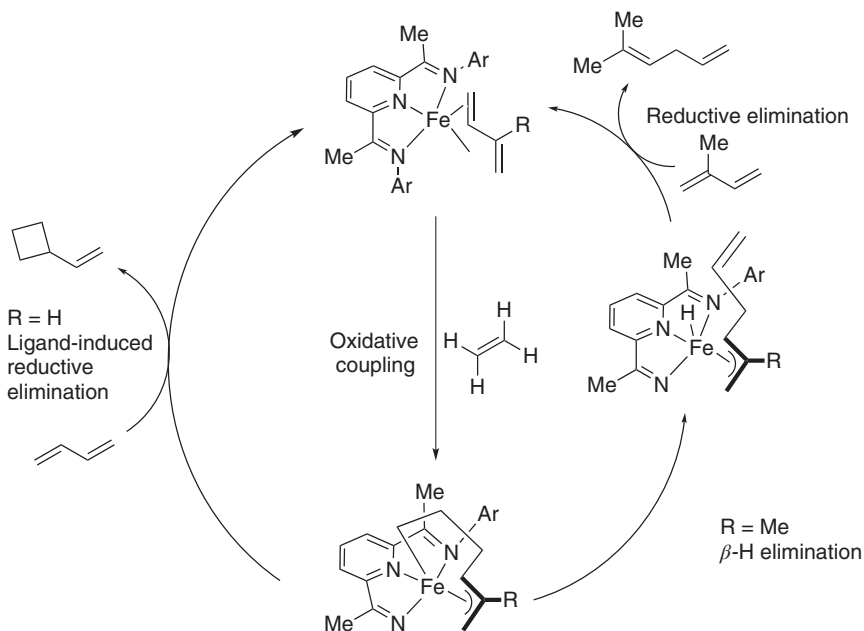


Scheme 1. Early examples of iron-catalyzed [2 + 2] cycloaddition.



Scheme 2. Plausible mechanism involving the iron(II) oxidation state [PDI = (*N,N*,*E,N,N*,*E*)-*N,N'*-(1,1')-(pyridine-2,6-diyl)bis(ethan-1-yl-1-ylidene)bis(2,6-diisopropylaniline)].

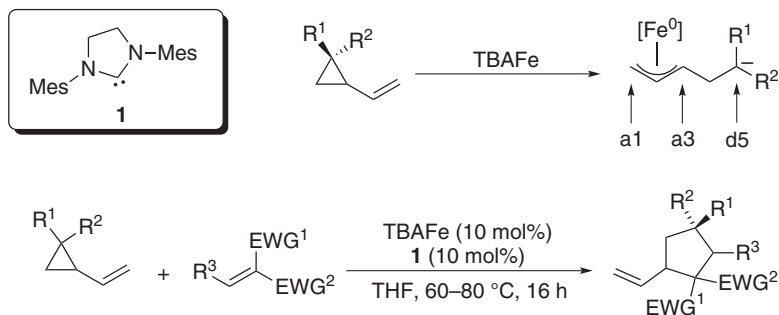
A combination of ethylene and butadiene resembles a thermally allowed [4 + 2] cycloaddition reaction, namely, the Diels–Alder reaction. Using their redox-active bis(imino)-pyridine supported iron catalysts, Chirik and co-workers (6) reported the more challenging [2 + 2] cycloaddition from the same set of starting materials that furnished vinylcyclobutane in an excellent 95% yield. The protocol turned out to be substrate specific, as with insertion of a methyl group in the 2- position of diene, no cycloadduct was observed; rather it resulted in a 1,4-addition product. To shed light on their plausible mechanism, several labeling experiments were carried out with different substrates. They were successful in intercepting one iron metallocyclic intermediate, which resulted from ethylene insertion into the coordinated diene. The same species was also prepared by reacting vinylcyclobutane, the product of the [2 + 2] cycloaddition, with the iron catalyst. Thus the reaction proved to be reversible with iron metallocycle as an intermediate, and the backward reaction demonstrated a rare example of sp^3 – sp^3 C–C bond activation with an iron catalyst under mild conditions. Isolation of the metallocycle intermediate and labeling experiments led to a proposed mechanism for [2 + 2] cycloaddition and 1,4-addition. The reaction initiated by displacement of dinitrogen ligands by diene an η^4 complex, and ethylene insertion, which furnished the isolable metallocycle intermediate. In the next step, butadiene-induced reductive-elimination resulted in vinylcyclobutane along with regeneration of an iron butadiene intermediate. However, with isoprene, β -hydrogen elimination followed by C–H reductive elimination resulted in the 1,4-addition product (Scheme 3).



Scheme 3. Proposed mechanism for [2+2] cycloaddition of ethylene and butadiene.

2. The [3+2] Cycloaddition

In 2012, Plietker and co-workers (7) reported an iron-catalyzed [3+2] cycloaddition of vinylcyclopropanes (VCP) and activated olefins or *N*-tosyl imines to generate functionalized vinylcyclopentanes and cyclopyrrolidines in high yields and regioselectivities. The activation of VCP by the electron-rich ferrate, $\text{Bu}_4\text{N}[\text{Fe}(\text{CO})_3(\text{NO})]$ (TBAFe) (TBA = tetrabutylammonium), resulted in the formation of an intermediate allyl-Fe complex, which can be regarded as an a1, a3, d5-synthon (Scheme 4). Subsequent Michael addition onto activated olefins generated another carbanion, which readily attacked the carbocationic part of the intermediate to generate VCP derivatives. The scope of VCPs was tested with 1,1-bis(phenylsulfonyl)ethylene as the Michael acceptor where different functional groups like esters, nitriles, and amides were tested. Likewise, a variety of Michael acceptors containing esters, sulfones, nitriles, amides, and ketones were successfully employed in this reaction. Further, they tried to incorporate imines as the Michael acceptor to extend their methodology. However, only *N*-tosylarylimines reacted successfully while *N*-Ph and *N*-Boc protected imines gave no or undesired products. Notably, activation of a carbon-carbon bond of VCP by an inexpensive iron catalyst would encourage further investigation on other strained systems (e.g., cyclobutanes, aziridines, and oxiranes).

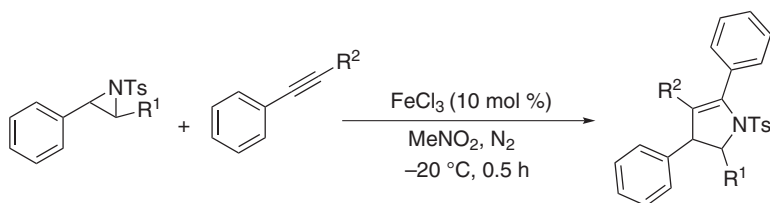


Scheme 4. Iron-catalyzed [3+2] cycloaddition of VCPs and activated olefins [Mes = mesylate, EWG = electron-withdrawing group, THF = tetrahydrofuran (solvent)].

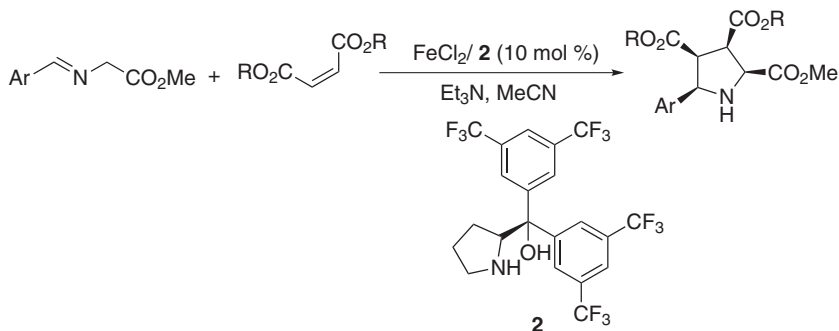
Simple FeCl_3 acts as a Lewis acid catalyst to assist the ring opening of another strained system, *N*-tosylaziridines (NTs), which in the presence of base reacts efficiently with terminal aryl alkynes to generate substituted 2-pyrrolines (Scheme 5) (8).

Further, a one-pot synthesis of γ -amino ketones from 2-pyrrolines was achieved by treatment with H_2O at rt for 12 h. However, the scope of the reaction was limited to Cl, F, and OMe containing arylalkynes and only NTs reacted successfully. Internal alkyne resulted in a lower yield (48%), while alkylalkyne, as well as electron-deficient aziridines, gave no product. Recently, Wang and co-workers (9) reported an Fe(II)/N, O ligand-catalyzed asymmetric [3+2] cycloaddition reaction of *in situ* generated azomethine ylides and electron-deficient alkenes (Scheme 6). Only 10 mol% FeCl_2 in the presence of diarylprolinol and Et_3N efficiently catalyzed the cycloaddition to afford a five-membered heterocyclic endo adduct stereoselectively in good-to-moderate yield.

In 2002, Kundig et al. (10) reported the first asymmetric [3+2] cycloaddition of nitrones and enals to generate isooxazolidines catalyzed by the Lewis acidic iron complex (*R,R*)-**3** (Scheme 7). The role of a Lewis acid was crucial as an α,β -unsaturated aldehyde had to be activated in preference to stronger Lewis basic nitrones having two coordination sites against one point coordinating enals. However, they were successful in discovering such a reactive yet selective



Scheme 5. Iron chloride acts as a Lewis acid catalyst in [3+2] cycloaddition.



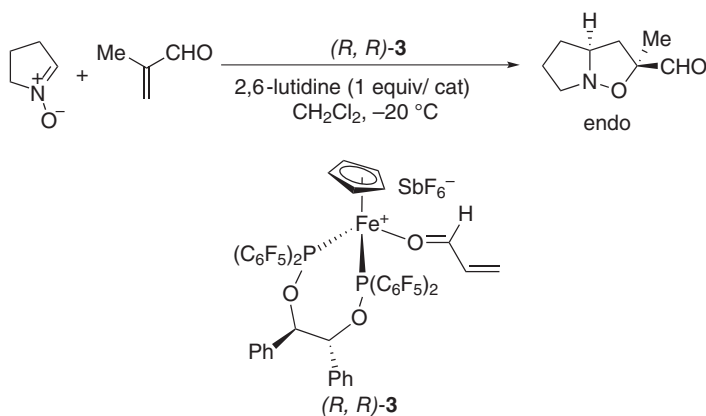
Scheme 6. Iron(II)/N, O ligand-catalyzed asymmetric [3+2] cycloaddition.

iron- and ruthenium-based Lewis acidic complex. The iron complex turned out to be the more beneficial choice.

In the presence of 2, 6-lutidine, which acts as a scavenger of acidic impurities, C, N diarylnitrones and heterocyclic *N*-oxides reacted efficiently with methacrolein to generate an endo adduct selectively. Notably, this transformation was also achieved by an elegant organocatalytic pathway with a high degree of enantioselectivity by the MacMillan group in 2000 (11).

3. The [2+2+2] Cycloaddition

Inter- and intramolecular [2+2+2] cycloaddition reactions of alkynes and nitriles catalyzed by transition metals have been considered as the most straightforward and convenient approach to synthesize six-membered arenes and highly

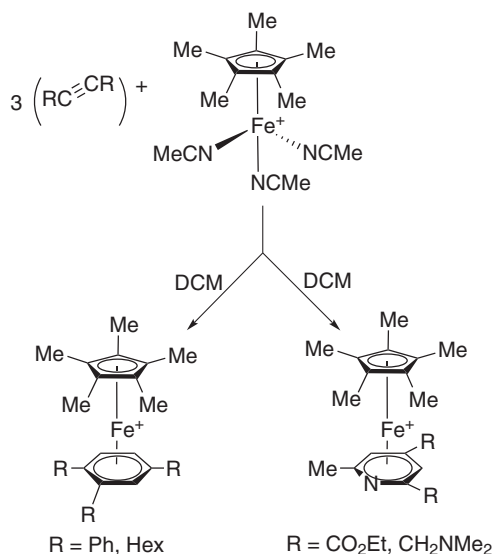


Scheme 7. Iron-catalyzed [3+2] cycloaddition of nitrones and enals.

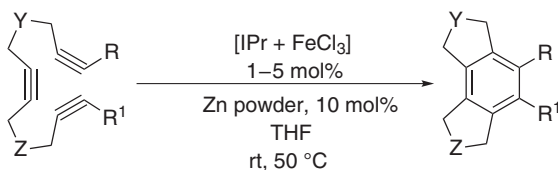
substituted pyridines. Importantly, a number of functional groups (e.g., alcohols, amines, ethers, esters, and halogens) can be tolerated while several C–C bonds are formed in a single step. For these transformations, several transition metals ranging from Co, Ru, Rh, Ni, Ti to bimetallic systems (e.g., Zr/Ni and Zr/Cu) have been used in recent decades. Iron catalysis has also played a crucial role in this reaction, though until very recently, methods were limited by poor chemo- and regioselectivity, as well as difficulty in preparation and handling of the catalysts.

In 2000, Pertici and co-workers (12) reported a cyclotrimerization reaction of terminal alkynes catalyzed by $\text{Fe}(\eta^6\text{-CHT})(\eta^4\text{-COD})$, where CHT = cyclohepta-1,3,5-triene and COD = 1,5-cyclooctadiene, respectively, to generate various multisubstituted benzene derivatives. The method lacked regioselectivity as a mixture of two regioisomers was formed for most of the terminal alkynes in an ~1:1 ratio. Meanwhile, Zenneck and co-workers (13) developed a [2+2+2] cycloaddition reaction of two molecules of alkynes and nitriles catalyzed by an Fe(0) complex to generate pyridines. This reaction was also limited by poor chemoselectivity, as well as a complex procedure of catalyst preparation.

However, better chemoselectivity was achieved by Guerchais and co-workers in 2002 (14) as they employed iron bis(acetonitrile) and tris(acetonitrile) complexes to catalyze the cycloaddition reactions of carbon–carbon and carbon–nitrogen triple bonds (Scheme 8). Three equivalents of alkynes cyclotrimerized to



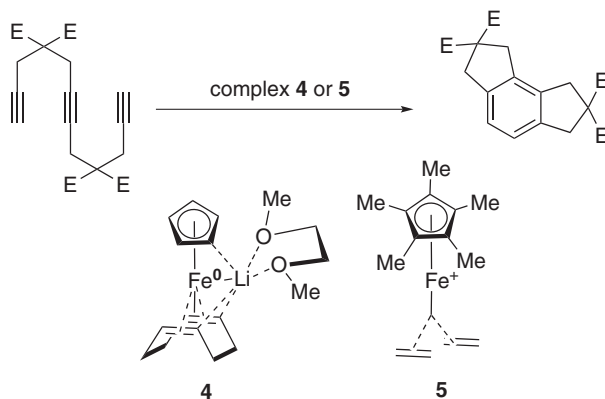
Scheme 8. Iron-catalyzed cycloaddition reaction of C–C and C–N triple bonds (DCM = dichloromethane, CH₂Cl₂).



Scheme 9. Intramolecular cyclotrimerization of triynes catalyzed by bench-stable iron salt [IPr = 1,3-bis(2,6-diisopropylimidazolium)-2,3-dehydro-1*H*-imidazole].

produce arene complexes in the presence of an iron tris(acetonitrile) complex in CH_2Cl_2 solvent at rt. Under the same condition, alkynes having heteroatoms bonded to the propargylic position afforded pyridine complexes instead of previously observed arene complexes, by the heterocyclotrimerization of two alkynes and one metal-bound acetonitrile ligand. When MeCN was used as solvent, in place of CH_2Cl_2 , only ethyl propiolate reacted among the alkynes as the carbonyl group successfully coordinated with the metal center competing with inhibiting acetonitriles to provide a free pyridine derivative in 73% yield, rather than generating the metal–pyridine complex. It was evident that nature of the solvent had dramatically altered the outcome of the reaction as no organometallic product was detected in this case.

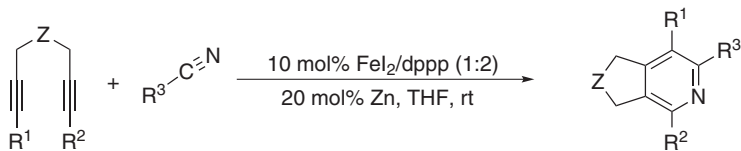
On the other hand, in 2005 iron-catalyzed intramolecular cyclotrimerization of triynes was reported by Okamoto and co-workers (15), which was less problematic in terms of regioselectivity (Scheme 9). So far, the iron catalysts that have been discussed are based on iron arene or iron 1,5-cylooctadiene and cycloheptatriene complexes. An alternate approach with simple iron salts is advantageous, as preparation and storage of expensive organometallic iron complexes can be avoided. Further, this approach rendered the related processes much more economical, as a fewer stabilizing ligands were required while reactions were performed under milder condition with high efficiency. Inspired by such an approach, Okamoto and co-workers (15) preferred commercially available iron and cobalt salts, which in the presence of suitable ligands and reducing agent can act as efficient catalysts for such transformations. They tested a number of commercially available iron, cobalt, and nickel salts in the presence of an imidazolium carbene ligand, and observed that cyclotrimerization occurred efficiently only at rt or at 50 °C under a reducing condition. Zinc powder was the reducing agent of choice, which supposedly converted the *in situ* generated metal complexes to their corresponding low-valent complexes so as to initiate the process by formation of a metallacycle intermediate. Further, they showed the advantages of their method by efficient formation of carbocyclic, *O*-heterocyclic and biaryl compounds. In another report from the same group, N-based bidentate ligands (e.g., 1,2-diimines or 2-iminomethylpyridines) were utilized in iron-catalyzed chemo- and regioselective cyclotrimerization of triynes (16).



Scheme 10. Cyclotrimerization catalyzed by low-valent iron-olefin complexes.

Recently, Furstner et al. (17) synthesized a fine blend of iron complexes of formal oxidation states -2 , 0 and $+1$ from readily available ferrocene. Among these low-valent iron olefin complexes, complex **4** turned out to be a very efficient catalyst in the cyclotrimerization reaction. This outcome is not surprising as $\text{Fe}(0)$ complexes are isoelectronic with $\text{Co}(\text{I})$ and $\text{Rh}(\text{I})$ species, which are arguably the most widely used catalysts in transition metal catalyzed $[2 + 2 + 2]$ cycloaddition reactions. Interestingly, complex **5** with a formal oxidation state of $(+1)$ is also found to be effective, though a higher catalyst loading and longer reaction time is required (Scheme 10). To gain mechanistic insights, 1,2-diphenylacetylene (toluene) was reacted with a series of iron complexes.

Although significant advances have been made in recent years regarding transition metal catalyzed $[2 + 2 + 2]$ cycloaddition, an efficient iron-catalyzed protocol for chemoselective synthesis of pyridines eluded the researchers for a long time. The crucial role of low-valent iron complexes in realizing efficient $[2 + 2 + 2]$ cycloaddition lies in the fact that it facilitates the formation of a metallocyclic intermediate by oxidative cyclization, subsequent reductive elimination that generate arenes or pyridines. In 2006, Holland and co-workers (18) revealed that alkyne binding to a low-valent iron metal center is particularly stronger than that of phosphine. Inspired by this report, Wan and co-workers (19) developed an iron catalyst comprising of readily available FeI_2 and dppp [1,3-bis(diphenylphosphino)propane] as the phosphine ligand in the presence of Zn dust, which served as the reducing agent (Scheme 11). Efficient synthesis of pyridines was observed only at rt starting from diynes and a slight excess of nitriles in THF solvent. They initially postulated that both ferracyclopentadiene, as well as the azaferracyclopentadiene intermediate, might be operating in the catalytic system and two plausible pathways were proposed. A competitive experiment using



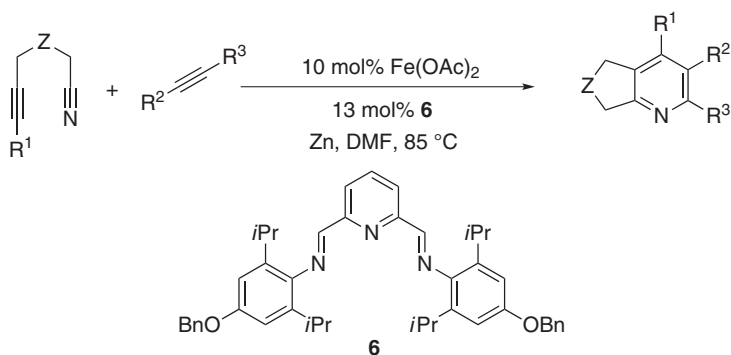
Scheme 11. An efficient iron-catalyzed [2 + 2 + 2] cycloaddition for pyridine synthesis.

an unsymmetrical diyne and acetonitrile indicated a ferracyclopentadiene intermediate that might not be involved in the overall catalytic system. Further, another competitive experiment with acetonitrile and 3 equiv alkynes confirmed that formation of such a ferracyclopentadiene intermediate is inhibited in the presence of nitriles.

At the same time, Louie and co-workers (20) reported another efficient method of iron-catalyzed pyridine synthesis. The $\text{Fe}(\text{OAc})_2$ in the presence of a sterically hindered bis(imino)pyridine ligand catalyzes the cycloaddition of a different substrate class, alkyne nitriles and alkynes, to form a number of pyridine derivatives (Scheme 12).

4. The [4 + 2] Cycloaddition

The [4 + 2] cycloaddition reaction serves as an efficient and powerful tool for synthesizing six-membered ring compounds by forming carbon–carbon and carbon–heteroatom bonds. According to the Woodward–Hoffmann rule, the concerted suprafacial $[\pi 4_s + \pi 2_s]$ addition of diene with a dienophile is thermally allowed and the reaction rate or feasibility of the reaction is strongly dependent on



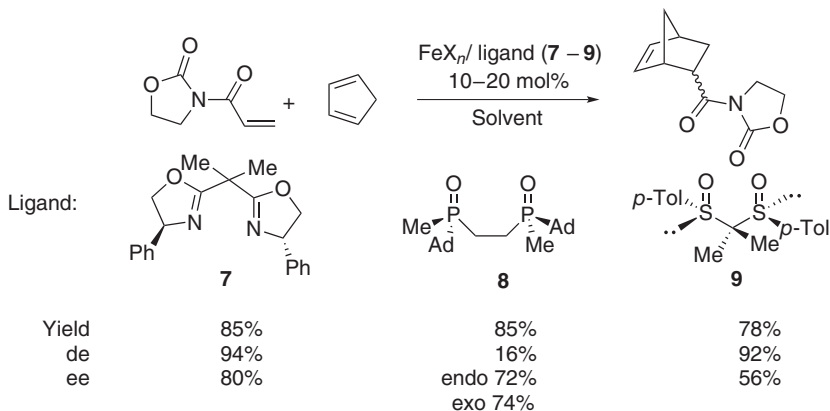
Scheme 12. Pyridine synthesis by iron-catalyzed [2 + 2 + 2] cycloaddition of alkyne nitriles and alkynes (DMF = *N,N*-dimethylformamide).

the energy gap of the frontier orbitals of the reacting species. Generally, it is classified into two distinct categories: a normal Diels–Alder reaction that involves interaction between highest occupied molecular orbital (HOMO) of the diene and lowest unoccupied molecular orbital (LUMO) of the dienophile and Diels–Alder reaction with inverse electron demand involving the HOMO of the dienophile and the LUMO of the diene. In a normal Diels–Alder reaction, if the LUMO of the dienophile can be further lowered in energy, the reaction would be much faster and can proceed at a significantly lower temperature. One way to lower the energy is to coordinate the heteroatom present in the EWG of the dienophile by Brønsted or Lewis acids. In this regard, transition metal complexes (e.g., iron complexes) can facilitate the reaction by applying the same concept and can also induce chirality into the reaction by using stabilizing chiral ligands. However, only a few reports are in the literature regarding an iron-catalyzed Diels–Alder reaction.

In 1991, Corey et al. (21) reported the first iron-catalyzed asymmetric Diels–Alder reaction between cyclopentadiene and 3-acryloyl-1,3-oxazolidin-2-one. For this asymmetric catalytic system, FeX_3 was chosen as the Lewis acidic metal component, along with a C_2 symmetric bis(oxazoline) ligand, which imposed the chiral environment. This metal–ligand (FeI_3) complex, was further activated by insertion of molecular I_2 into the reaction mixture, which significantly accelerated the rate of the reaction even at -50°C . The endo adduct was preferentially obtained in preparatively useful yield (85%). Further, the chiral ligand was found to be readily recoverable and recyclable, which emphasized the synthetic utility of this protocol. Use of a fluxional additive with a similar catalyst system comprising of $\text{Fe}(\text{ClO}_4)_2$ and the ligand improved the enantioselectivity further (up to 91% ee) (22). Here ee = enantiomeric excess. Khir (23) in 1993 and Imamoto and co-workers (24) in 2000 devised other bidentate ligands, such as C_2 symmetric bis(sulfoxides) and diphosphine oxides, respectively, for an asymmetric Diels–Alder reaction that resulted in lower diastereo- and enantioselectivity for the reaction (Scheme 13).

Practical utility of the asymmetric Diels–Alder reaction was further enhanced when Kanemasa et al. (25, 26) unveiled a series of cationic aqua. complexes comprising of transition metal perchlorates and C_2 symmetric tridentate ligand DBFOX/Ph (**10**) (Scheme 14). The use of a tridentate ligand was particularly beneficial as it remained strongly bound to the metal by competitive coordination with the substrate and created an attractive chiral environment in which the metal was embodied. This in turn disfavored the aggregation or oligomerization of the complex, yet it induced a high degree of asymmetry in the reaction outcome. Further, the stability of the complexes in water made this catalytic system advantageous.

In 2004, Shibasaki and co-workers (27) devised an efficient iron-catalyzed Diels–Alder reaction that resulted in the formation of highly substituted acyl cyclohexene derivatives in high enantiomeric purity (up to 92% ee) (Scheme 15).

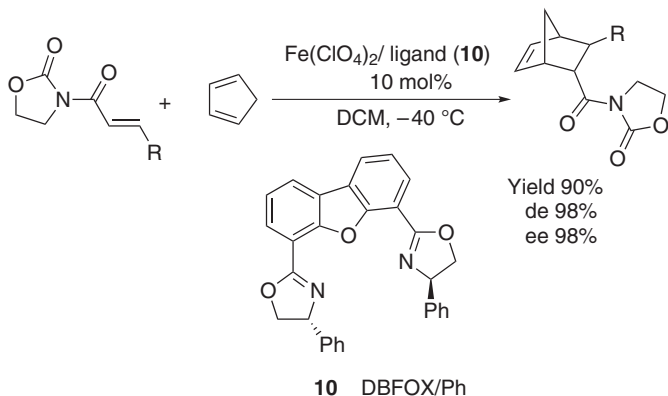


Corey, (1991) (21) Imamoto co-workers (2000) (24) Khiar et al. (1993) (23)

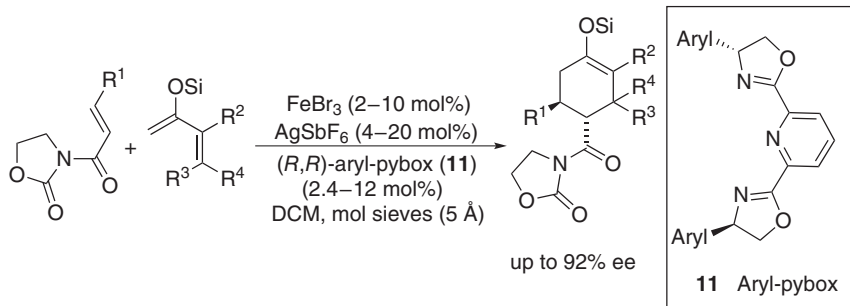
Scheme 13. The N, P, and S based ligand system for iron-catalyzed [4 + 2] cycloaddition (Diastereometric excess = de, Tol = tolyl, Ad = adamantyl).

A 1.2:1 combination of tridentate aryl-pybox ligands (**11**) and FeBr_3 in conjunction with AgSbF_6 provided an efficient catalyst that reacted with trisubstituted and tetrasubstituted diene with equal ease. Further, this protocol was successfully applied in the synthesis of biologically relevant natural product *ent*-hyperforin by the same group in 2010 (28).

In search of an efficient asymmetric Diels–Alder reaction, Kundig and co-worker (29) prepared a series of chiral phosphine ligands from an iron–



Scheme 14. Asymmetric Diels–Alder reaction-catalyzed cationic iron aquo complexes [DBFOX = 4,6-dibenzofurandilyl-2,2'-bis(4-phenyloxazoline)].



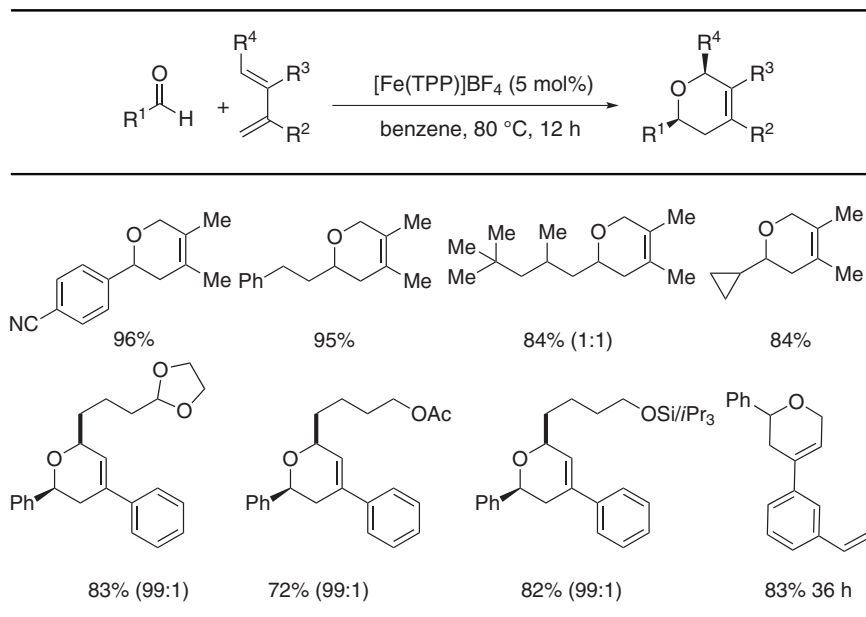
Scheme 15. An efficient iron-catalyzed Diels–Alder reaction [pybox = bis(oxazolonyl)pyridine].

cyclopentadienyl complex with a cyclopentane diol and a hydrobenzoin backbone. These C_2 symmetric ligand systems were compatible with iron, as well as with ruthenium, and cycloaddition between cyclopentadiene and enals were realized in high diastereo- and enantioselectivity.

Alkynes were used as the dienophile as well. In 1992, Jacobsen and co-workers (30) reported an iron-catalyzed [4 + 2] cycloaddition of 1,3-butadiene and alkynes involving a “bare” Fe^+ cation. Experiments were performed in a Fourier transform mass spectrometer (Nicolet FTMS-1000), where Fe^+ was generated by laser desorption–ionization from a high-purity iron foil. The *in situ* generated $Fe(1,3\text{-butadiene})^+$ reacted rapidly with ethyne (and propyne) via a proposed η^3 -complex to form $Fe(1,4\text{-hexadiene})^+$, which upon subsequent dehydrogenation yielded the $Fe(\text{benzene})^+$ complex. However, with alkenes or nitriles, no cycloaddition was observed in this case. Alkynes were also used in a stoichiometric reaction with vinylketeneiron (0) to generate catechol derivatives in moderate yields and regioselectivity.

The Hetero-Diels–Alder reaction, which is regarded as a convenient route to access six-membered heterocyclic compounds between aldehydes and dienes, are limited by the usage of either activated aldehydes (e.g., glyoxylates) or electron-rich dienes e.g., Danishefsky’s diene and Rawal’s diene. Further, strong Brønsted or Lewis acid had to be employed to overcome the poor reactivity of unactivated dienes. These drawbacks were successfully addressed by Matsubara and co-workers (31) in 2012, as they reported an unprecedented [4 + 2] cycloaddition of unactivated aldehydes and simple dienes catalyzed by iron(III)–porphyrin complex under mild and neutral conditions. A wide array of aldehydes and dienes containing various functional groups were reacted efficiently in the presence of 5 mol% of $[Fe(\text{TPP})]BF_4$. In addition, highly substituted pyran scaffolds were generated in excellent yields and diastereoselectivities (Table I). High chemoselectivity, tolerance of water in the reaction medium, and mild reaction conditions made this method advantageous.

TABLE I
Scope of Hetero-Diels–Alder Reaction Catalyzed by $[\text{Fe}(\text{TPP})]\text{BF}_4^a$



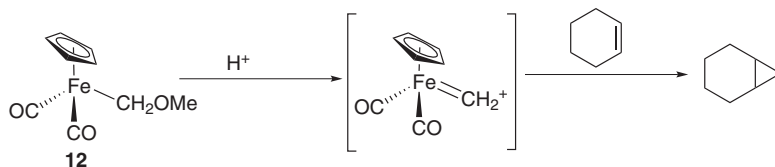
^aHere TPP = tetraphenylporphyrin.

B. Cyclopropanation

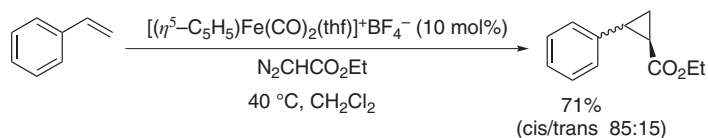
Small ring molecules are potentially important to influence the pharmaceutical properties of many bioactive drugs (32). In this respect, cyclopropyl moieties achieved more attention due to its ubiquitous presence in many natural products (33), insecticides, modern pharmaceuticals, and in critical synthetic intermediates (34). So far, the traditional process of cyclopropanation is the [2 + 1] addition of different carbenes with olefins via radical pathways (35). In this respect, transition metal (35) (Ru, Rh, Co, Cr, Mo, W, the Fischer–Tropsch carbene-transfer process) mediated transfer of carbene to olefin from the stoichiometric carbene source is one of the efficient pathways.

In 1966, Jolly and Pettit (36) first reported cyclopropanation (Scheme 16) by an iron complex to an olefin. Importantly, this was the first example of a metal–carbene complex acting as a carbene-transfer agent. Treatment of cyclohexene in the presence of $\text{CpFe}(\text{CO})_2\text{CH}_2\text{OMe}$ (**12**) and acid gave norcarane in 46% yield. It was proposed that the reaction was accomplished by the intermediacy of $\text{CpFe}(\text{CO})_2\text{CH}_2^+$.

Recently, the cyclopropanation reaction was further developed. Most of the time, the process of carbene transfer was hampered by low selectivity with the different types of catalysts used. In 1993, Hossain and co-workers (37) developed the first iron-based cyclopropanation reaction in a catalytic manner (Scheme 17). The Lewis



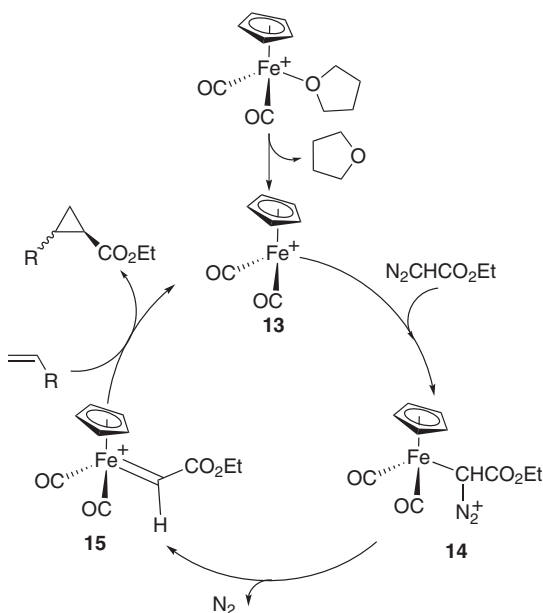
Scheme 16.



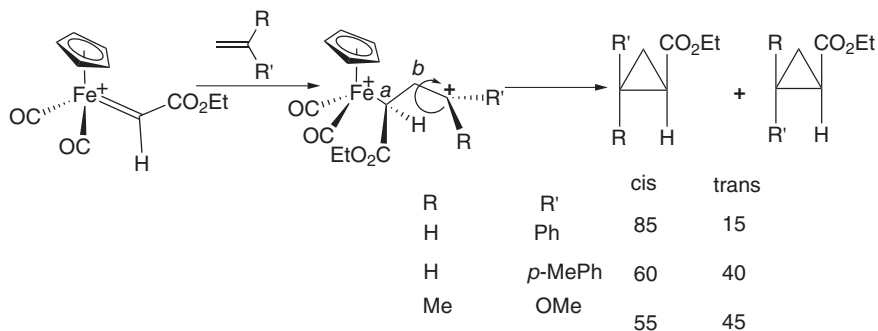
Scheme 17.

acidic iron center in $[(\eta^5\text{-C}_5\text{H}_5)\text{Fe}(\text{CO})_2(\text{thf})]^+\text{BF}_4^-$ can act as an efficient catalyst to cyclopropanate styrene analogues in the presence of ethyldiazoacetate (EDA) as the carbene source. After several rounds of optimization, it was found that 10 mol% of catalyst at 40°C with 5 equiv of styrene were the optimal requirement.

In the proposed mechanism (Scheme 18), THF was dissociated first from the iron Lewis acid to generate cationic intermediate (**13**), which reacted with EDA to form



Scheme 18.



Scheme 19.

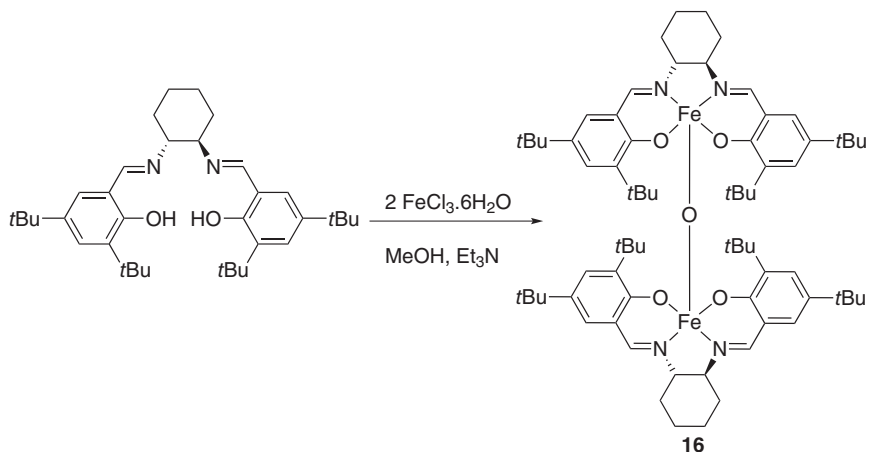
an intermediate complex (**14**) followed by extrusion of nitrogen to give an extremely reactive iron–carbene complex (**15**). The new complex readily transferred the carbene moiety to styrene. Several controlled experiments further supported this plausible mechanism.

The iron–carbene complex reacted with styrene to form a 5.6:1 mixture of *cis/trans*-1-phenyl-2-carboxycyclopropane (Scheme 19). This reaction indicated the presence of the short-lived γ -carbocation, which was rearranged to give the expected product. The ratio of *cis* and *trans* products was mainly dependent on the electronic property of the substituents attached to the intermediate. When electron-donating groups were present, the rotation of the C_β – C_γ bond was greater. Consequently, the *cis/trans* selectivity was less for *p*-methylstyrene and 2-methoxypropene.

In 2002, Nguyen and co-workers (38) reported the olefin cyclopropanation using μ -oxo-bis[(salen)iron(III)] complexes [salen = *N,N'*-bis(3,5-di-*tert*-butylsalicylidene)-1,2-cyclohexanediamine] (**16–20**) (Scheme 20). Thus, this (salen)iron complex (**16**) can be used as an efficient, selective, and inexpensive metal alternative to a widely used ruthenium(II) salen complex.

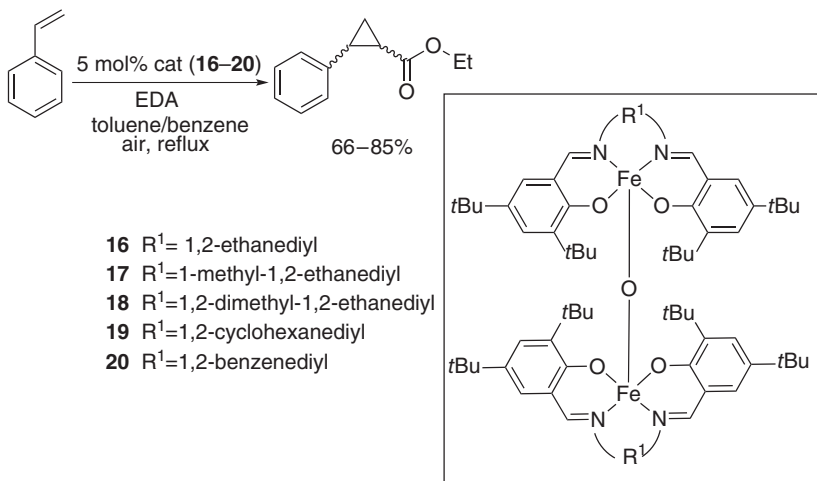
The ethyldiazoacetate can act as an efficient reducing agent, and can break the μ -oxo bridge to produce the active (salen)iron(II) complex (**16**) for cyclopropanation. An optimized condition for cyclopropanation referred 5 mol% of catalyst with dry benzene or toluene as the solvent under refluxing temperature (Scheme 21) (38). By varying the diamine backbone of the complex, different yields of the product were obtained with subsequent increased or decreased reactivities. The reaction was fastest with the least sterically hindered backbone (e.g., 1,2-ethanediamine). But a bulkier 1,2-dimethyl-1,2-ethanediamine backbone gave the slowest reaction.

In 2002, Morise et al. (39) reported the cyclopropanation reaction using *trans*-[(CO)₃Fe(μ -L^{P,N})₂Cu]BF₄ (**21**), which was the first metal–metal bonded six-membered ring system with P,N donors (Scheme 22). In this complex, formally

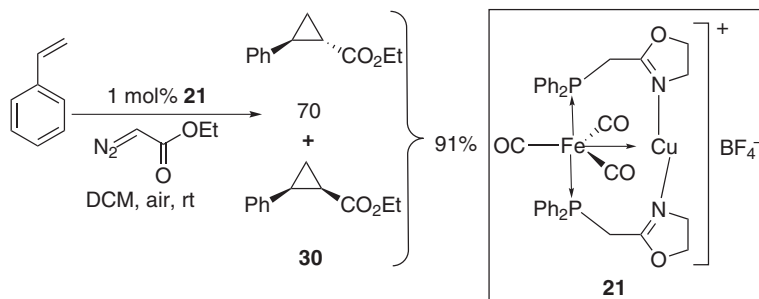


Scheme 20.

a zero-valent Fe center became attached to the Cu(I) center via the nitrogen of the flanked oxazoline moiety from the phosphine group. This complex can be used as an efficient catalyst for the cyclopropanation of styrene with ethyl diazoacetate. The reaction was carried out using 1 mol% of the catalyst with DCM as solvent at rt. The *trans*- and *cis*- ethyl-2-phenyl-1-cyclopropanecarboxylates were obtained in 91% isolated yield in a 70:30 ratio. The complex **21** was the first metal–metal bonded heterometallic catalyst for cyclopropanation.



Scheme 21.

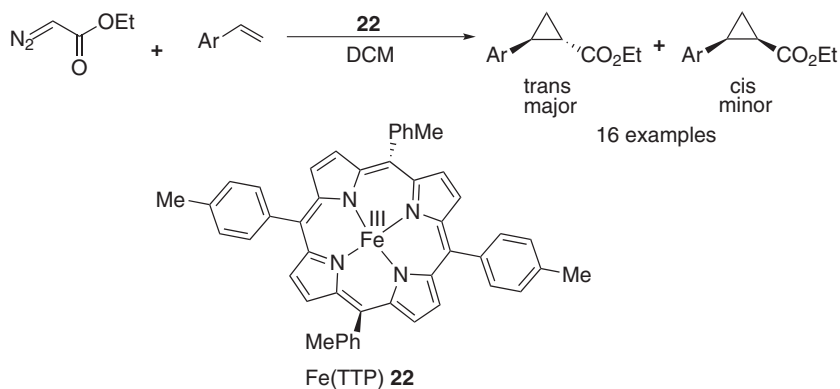


Scheme 22.

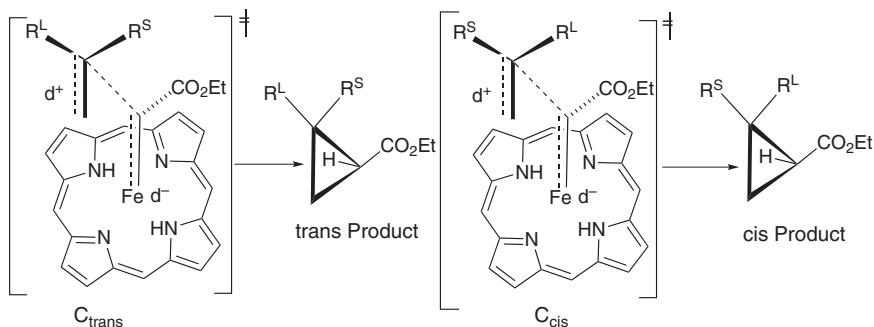
In 1995, Woo and co-workers (40) reported the asymmetric cyclopropanation reaction of styrenes using different iron(II) complexes with chiral macrocyclic (porphyrin-based) ligands (Scheme 23). These ligands provided the auxiliary stereogenic centers in close proximity to the active metal sites and also made those complexes as an efficient catalyst. The reaction was useful for the production of industrially important trans cyclopropyl ester derivatives.

In order to get the mechanistic insight into the reaction, labeling experiments were performed for styrene and styrene- d_8 . The reaction was presumed to go via iron(II), which was originally *in situ* generated by the reductant ethyl diazo acetate. In contrast to other cyclopropanating catalysts, iron(II)(TTP) where TTP = *meso*-tetra-*p*-tolylporphyrin, was less electrophilic. In the transition state, the alkene possesses some carbocataionic character, which was in accordance with the reverse secondary kinetic isotopic effect (KIE).

According to the proposed transition state (Scheme 24), the selectivity was mainly dependent on the orientation of the alkene with the porphyrin plane. The shape selectivity of the alkene was mainly dependent on the presence of the



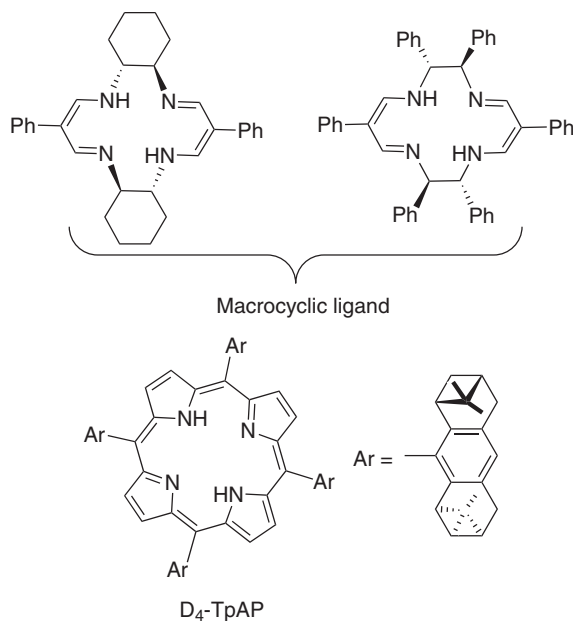
Scheme 23.



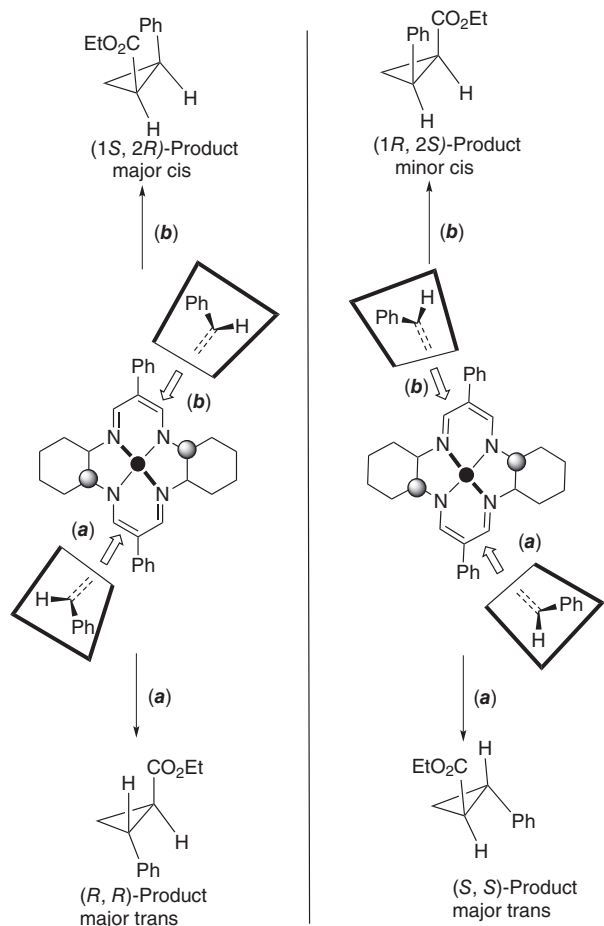
Scheme 24.

substituents on the nearest carbon to the macrocyclic plane. The trans product was dominated due to the interaction between macrocycle and the large group (R_L). The proposed model also depicted the increasing trans/cis ratio in some donor solvents, which could coordinate axially to iron. Such coordination can reduce the electrophilicity of the complex and therefore trans selectivity can be increased.

In 2002, the same group (41) developed some iron(II) complexes with different macrocyclic ligands and iron(II) porphyrin complexes, like iron(II) (D_4 -TpAP) and Fe($\alpha_2\beta_2$ -BNP) for asymmetric cyclopropanation (Scheme 25, BNP = bis



Scheme 25.



Scheme 26.

(binaphthylporphyrin)) with EDA. The reactions were carried out using 0.1–0.4 mol% of an Fe–porphyrin catalyst and 1–2 mol% of an Fe–macrocycle catalysts. Predominantly trans products were obtained compared to cis.

The enantioselectivity for this reaction was solely attributed to the orientation of carbene, as well as the olefins. For the catalysts containing macrocycles, selectivity appeared due to the parallel orientation of the C=C axis with the M=C bond (Scheme 26). Minimized steric interactions between the ester group and the axial proton of the chiral cyclohexyl group were achieved, when the olefin approached from path *a*. Thus, the observed product had an (*R,R*) configuration and was

TABLE II
Cyclopropanation Using the Halterman Catalyst

23
Fe-Halterman catalyst

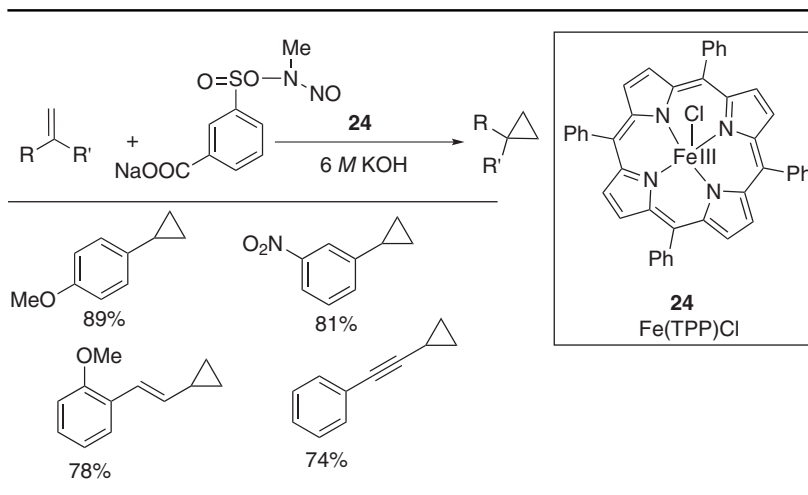
Substrate				
	53%	58%	58%	58%
trans/cis	96:4	93:7	94:6	92:8

obtained as a major trans isomer. A similar sense of chirality was introduced when Fe-porphyrin catalysts were used. The olefin approached from the right side of the carbene plane and as a result both (*S,S*) and (*R,R*) products were favored.

In 2009, Simonneaux and co-workers (42) reported the asymmetric intermolecular cyclopropanation of styrene analogues using an aryl diazoketone as the carbene source and a chiral Halterman iron-porphyrin complex (**23**) as catalyst. The initial attempt was made using the iron chloride Fe(TPP)Cl as a catalyst at rt. But low yield and major side products made those attempts unsuccessful. When the Fe-Halterman catalyst was applied the yields, as well as the selectivity (76% for trans), were increased. Different electronically and sterically demanding substrates were successful in that process, with moderate-to-good yield (Table II).

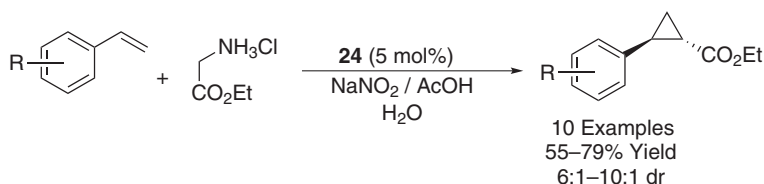
Safe and environmentally benign methodologies are always in demand for synthetic chemistry. Especially when the reactive intermediates are toxic and explosive. Considering these facts, Morandi and Carreira recently developed (43) a new procedure for cyclopropanation that minimized the risk as well as the time and

TABLE III
Cyclopropanation Using an Iron–Porphyrin Complex in Water



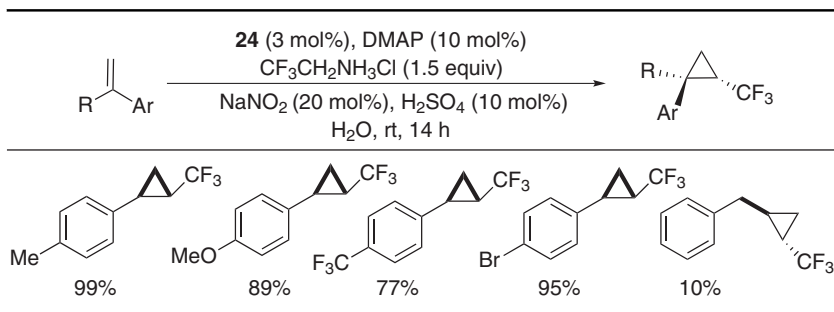
effort. A water-soluble diazald derivative (i.e., *N*-methyl-*N*-nitroso-*p*-toluenesulfonamide), which showed low toxicity compared to other diazomethane precursors, released diazomethane *in situ* on treatment with a 6 molar KOH solution. Tandem cyclopropanation occurred in the presence of the $Fe(TPP)Cl$ catalyst (**24**) when the ejected diazomethane was transferred to the organic layer. Except for being hydrophilic, both the electron-rich and the electron-poor substrates were well tolerated under optimal reaction condition (Table III).

Carreira and co-workers (44) developed a cyclopropanation reaction (Scheme 27, dr = diastereomeric ratio) using the same catalyst $Fe(TPP)Cl$ (**24**) and glycine ethyl ester hydrochloride as the inexpensive and safe carbene source to yield the *trans*-cyclopropyl ester selectively.



Scheme 27.

TABLE IV
Iron-Catalyzed Cyclotrifluoromethylation^a



^a 4-Dimethylaminopyridine = DMAP.

Trifluoromethylated cyclopropanes are important compounds in drug delivery (45), though very few synthetic methods were reported for their preparation. Carreira and co-workers (46, 47) recently reported potentially applicable methods for the synthesis of trifluoromethylated cyclopropanes by using trifluoroethylamine hydrochloride as the carbene source. Tandem cyclopropanation occurred in the presence of 3 mol% $\text{Fe}(\text{TPP})\text{Cl}$ (**24**) and saturated NaNO_2 solution to generate carbene. Both electron-rich and electron-deficient dienes were good substrates (Table IV) for this transformation, but it was unable to cyclopropanate 1,2-transubstituted double bonds.

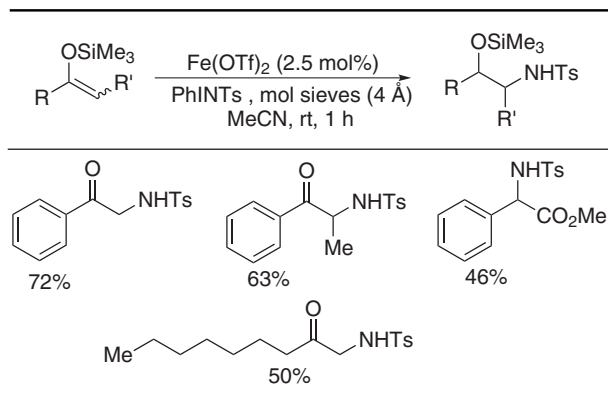
C. Aziridination and Aziridine Ring-Opening Reactions

Synthesis of various nitrogen-based compounds, particularly α -amido ketones, can be achieved by ring-opening aziridination (48). Therefore, development of sustainable and effective methods for aziridination is highly desirable. Bolm and co-workers (49) developed iron-catalyzed aziridination. They synthesized α -*N*-arylamido ketones by using 2.5 mol% $\text{Fe}(\text{OTf})_2$ as catalyst and PhINTs as a nitrene source (Table V), where OTf = trifluoromethanesulfonate.

Reaction conditions for a 0.25-mmol scale: $\text{Fe}(\text{OTf})_2$ (2.5 mol%), enol silyl ether (2 equiv), MeCN (1 mL), rt, 1 h.

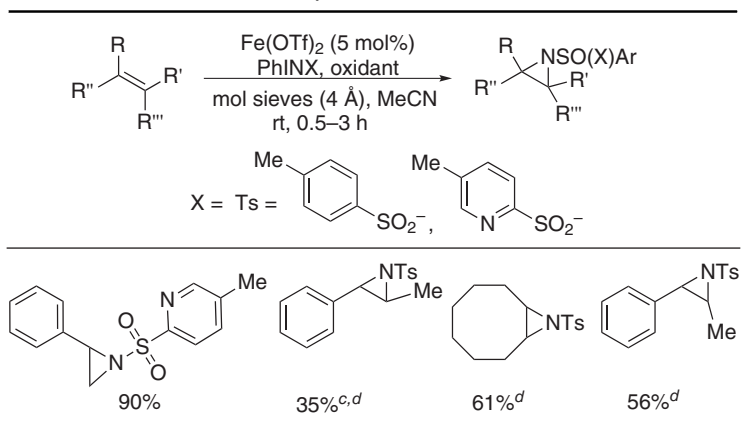
Sulfonamide and iodostyrene or iodobenzene diacetate in the presence of magnesium oxide gave styrene aziridine derivatives in good yields. Use of MgO could be avoided by using less acetonitrile. The reaction gave moderate-to-good yields for styrene derivatives as substrates and moderate yields for internal olefins (Table VI).

TABLE V
Synthesis of α -*N*-Arylamido Ketones^a



^a *N*-Tosyliminobenzylidiane = PhINTs.

TABLE VI
Iron-Catalyzed Aziridination^{a,b,c,d}



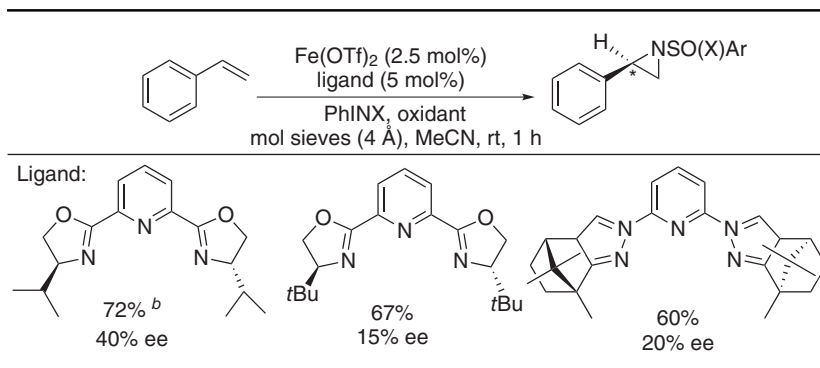
^a Reaction conditions for a 0.25-mmol scale: Fe(OTf)₂ (2.5 mol%), enol silyl ether 1 (2 equiv), MeCN (1 mL) rt, 1 h. Ts = tosyl.

^b The known products were identified by comparison of their analytical data with those of previous reports.

^c Only trans-product was obtained selectively.

^d Use of 10 mol% of Fe(OTf)₂.

TABLE VII
Asymmetric Aziridination of Styrenes^a



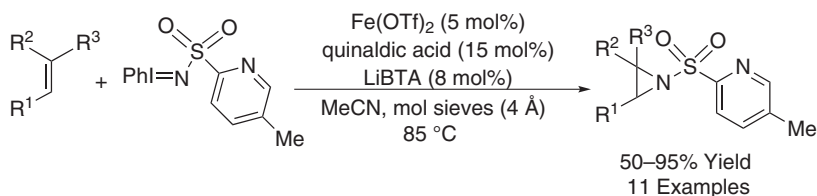
^a Reaction conditions for a 0.25-mmol scale: $\text{Fe}(\text{OTf})_2$ (2.5 mol%), ligand (5 mol%), styrene (20 equiv), MeCN (1 mL), rt, 1 h.

^b Both $\text{Fe}(\text{OTf})_2$ (5 mol%) and a chiral ligand (30 mol%) were used.

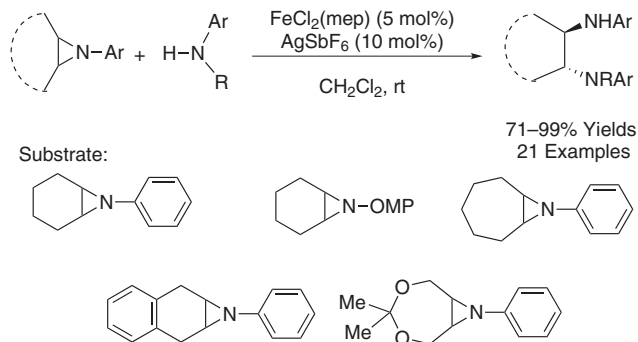
Asymmetric synthesis of aziridine was achieved in the presence of chiral nitrogen ligands based on 2,6-bis(*N*-pyrazolyl)pyridines (Table VII). A radical mechanism was proposed from observed isomerization of *cis*-stilbene to the *cis* and *trans* isomer under the reaction condition.

Further improvement in yield was obtained by using quinaldic acid in the presence of ionic liquids, such as ethyl methyl imidazolium bis[(trifluoromethyl) sulfonyl]-amide (emim BTA) or LiBTA (Scheme 28) (50).

Ring opening of aziridines by a nucleophile can generate stereospecific β -functionalized amines. In this context, Schneider and co-workers (51) developed an iron-catalyzed method to synthesize β -functionalized amines (Scheme 29). Different *N*-substituted aziridines and aniline derivatives were tolerated under this reaction condition.



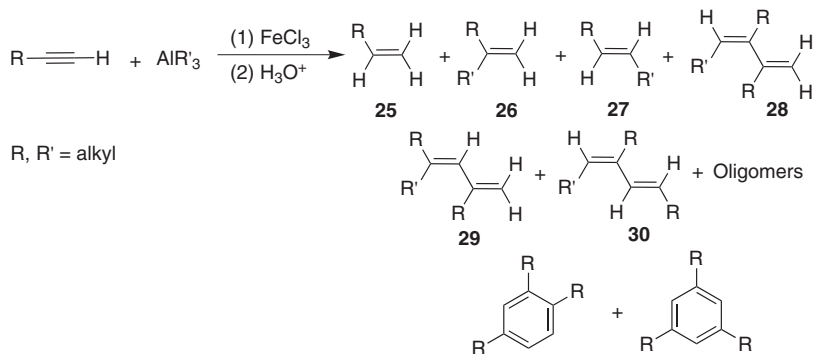
Scheme 28. Effect of ionic liquid in aziridination reaction.



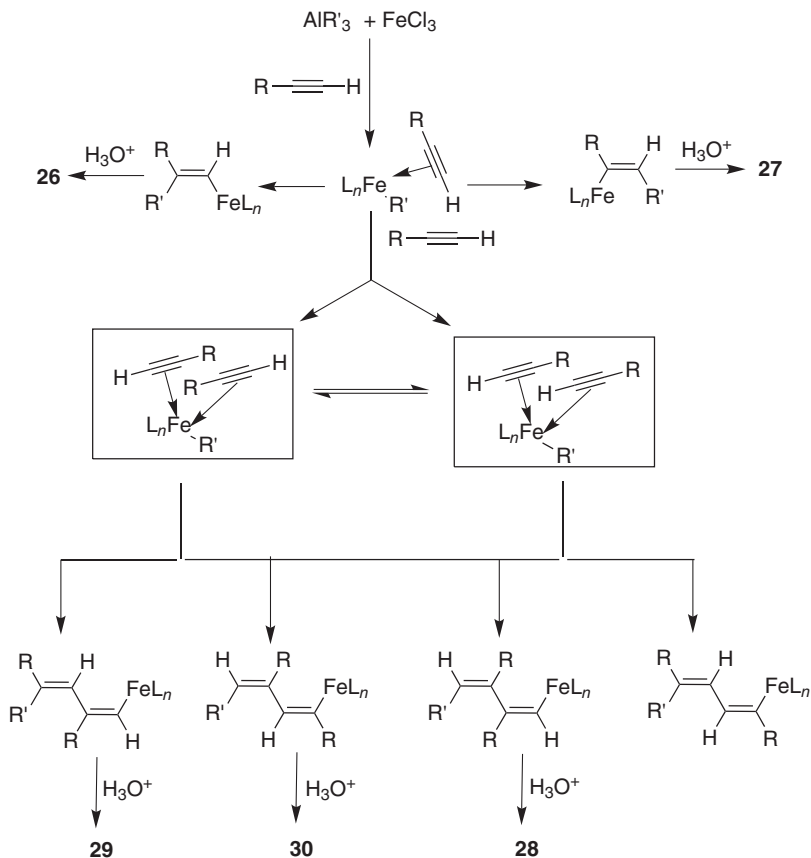
Scheme 29. Reaction scheme of ring-opening aziridination [mep = *N,N'*-dimethyl-*N,N'*-bis(2-pyridylmethyl)-ethane, OMP = *o*-methoxyphenyl].

D. Carbometalation of C–C Unsaturated Bond

A carbometalation reaction is an addition reaction of an organometallic compound to an unsaturated carbon–carbon bond resulting in a new carbon–carbon and carbon–metal bond formation. Generally, catalytic iron salt in the presence of an organometallic compound forms an organo-iron species, which accelerates the addition reaction to the unsaturated C–C bond. In 1977 Lardicci and co-workers (52) first used FeCl_3 as a catalyst in the alkylation of hex-1-yne by organoaluminium compounds. This protocol showed regioselectivity toward 2-alkyl-alk-1-ene (**26**) and trialkylbuta-1,3-dienes (**29**) with a small amount of oligomer and other cyclic trimers. With an optically active alkyl substituent at the α -position of the triple bond, high stereospecificity was noticed upon carbometalation. With [1- D]hex-1-yne, no deuterium transfer was detected after hydrolysis (Scheme 30).

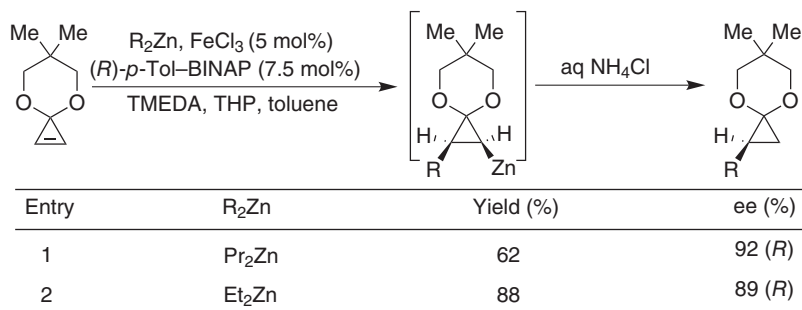


Scheme 30. Iron-catalyzed organoalumination of aliphatic alk-1-yne.



Scheme 31. Proposed pathways for iron-catalyzed organoaluminumation of aliphatic alk-1-ynes.

To begin with, the iron center performed ligand exchange with an excess of organoaluminium compound, which underwent a cis-addition to the triple bond forming an iron–carbon single bond. Compound **26** was preferentially formed over **27** due to steric and electronic reasons. According to the proposed mechanism, the diene species were formed from two probable π -alkyne–iron species, which resulted in four organoiron compounds. Among them, compound **29** was more favorable due to stereoelectronic factors. Alkylation to the alkyne played a competitive role with cyclic trimer formation. Finally, increased steric hindrance on the alkyne moiety led to cyclization (Scheme 31) (52b).

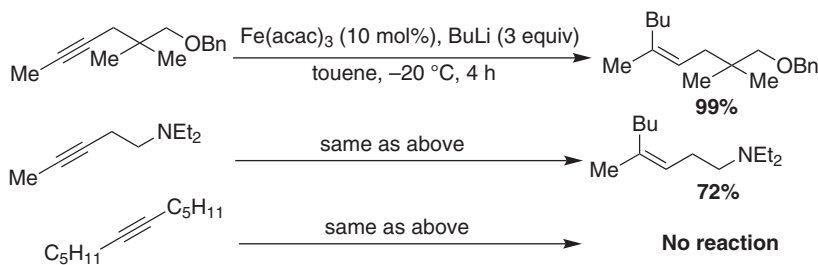


Scheme 32. Iron-catalyzed olefin carbometalation (THP = tetrahydropyran).

In 2000, Nakamura et al. (53) reported FeCl₃ catalyzed olefin carbometalation using a Grignard reagent or organozinc complexes (Scheme 32). A cyclopropene moiety was easily carbometalated by this method. The carbometalated intermediate was also trapped with different carbon electrophiles. Enantioselective carbocation was achieved by applying a number of bidentate phosphine ligands. The optimized condition with (*R*)-*p*-Tol-BINAP (2,2'-bis(diphenylphosphino)-1,1'-binaphthyl) and TMEDA [*N,N,N',N'*-tetramethylethane-1,2-diamine (solvent)] produced carbometalation with high enantioselectivity.

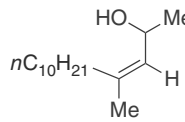
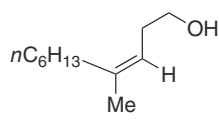
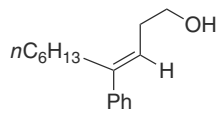
Hosomi's and co-workers (54) reported iron-catalyzed stereo- and regioselective carbolithiation of alkynes using a catalytic amount of Fe(acac)₃ (Scheme 33). They proposed that iron catalysis was going through an iron-ate complex. Under this reaction condition, alkynyl ether and alkynyl amines were well tolerated, but reaction with a simple alkyne (e.g., 6-dodecyne) totally failed.

Through iron-catalyzed alkyne carbometalation of propargylic and homo-propargylic alcohol with Grignard reagent, a class of substituted allylic and



Scheme 33. Iron-catalyzed region- and stereoselective carbolithiation of alkynes (acac = acetylacetonate).

TABLE VIII
Stereo- and Regioselective Carbometalation of Propargylic and Homopropargylic Alcohol^a

Entry	Condition	Product	Yield (%)
$\text{R}^1-\text{C}\equiv\text{C}-\left(\text{CH}_2\right)_n-\text{C}(\text{OH})\text{R}^2 + \text{R}^3\text{MgBr} \xrightarrow[\text{THF, 0 }^\circ\text{C, 7 h,}]{\text{cat Fe(III)}} \text{R}^3-\text{C}(\text{R}^1)=\text{C}(\text{H})-\left(\text{CH}_2\right)_n-\text{C}(\text{OH})\text{R}^2$ <p style="text-align: center;">$n = 0-1$ (5 equiv)</p>			
1	Fe(ehx) ₃ (0.2 equiv) dppe (0.2 equiv)		75
2	Fe(acac) ₃ (0.2 equiv)		75
3	Fe(acac) ₃ (0.4 equiv)		63

^a 1,2-Bis(diphenylphosphino) ethane = dppe; ehx = 2-ethylhexanoate.

homoallylic substrates were synthesized stereoselectively (Table VIII). In 2005, Zhang and Ready (55) demonstrated regio- and stereoselective carbometalation by use of a catalytic amount of iron(III) salt. A small amount of dialkylated alkene and, in some cases, a hydrometalated species, was detected as a side product. Further, a vinyl Grignard intermediate was trapped with a different electrophile to produce tetrasubstituted allylic or homoallylic alcohols (Table IX).

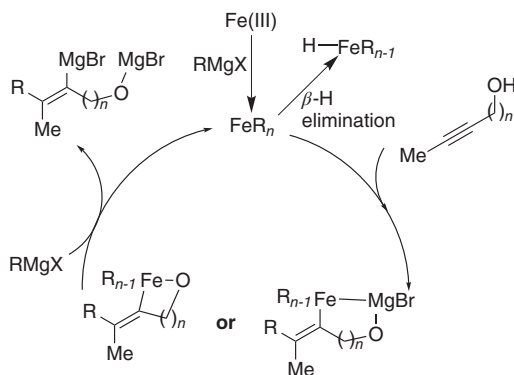
The iron(III) center is reduced through a fast ligand-exchange process with the Grignard reagent. Then alkoxide directed carbometalation occurred forming a cyclic vinyl-iron intermediate. Subsequent metathesis with the Grignard reagent formed a vinyl-magnesium species, which was responsible for electrophilic substitution. After β -hydride elimination from the FeR_n species, an iron-hydride complex was generated that performed the hydrometalation of the alkyne moiety (Scheme 34) (55).

With the prospect of alkyne carbometalation, in 2005, Hayashi and co-workers (56) reported an iron-copper cooperative catalytic system, which successively

TABLE IX
Intermediate Trapping of an Electrophile of a Carbometalation Reaction^a

Entry	E ⁺ ^a	Product	Yield (%)
1			75 (92 D)
2	ZnCl ₂ .NBS		65
3	DMF		50
4	CuCN.LiCl. allyl bromide		61

^a *N*-Bromosuccinimide = NBS.



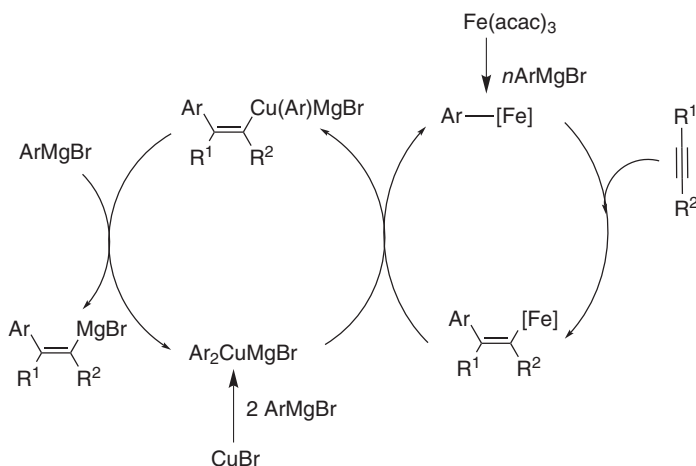
Scheme 34. Proposed mechanism for the carbometalation of propargylic and homopropargylic alcohol.

TABLE X
Alkyne Carbometalation Using an Iron–Copper Cooperative Catalytic System

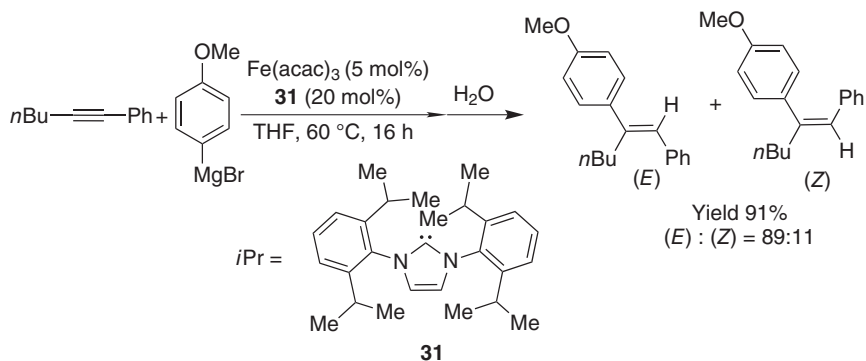
Entry	Ar	R ¹	R ²	Yield (%)	(E):(Z)
1	Ph	Pr	Pr	62	97:3
2	3-MeC ₆ H ₄	Pr	Pr	70	95:5
3	3-OMeC ₆ H ₄	Pr	Pr	56	97:3
4	4-FC ₆ H ₄	Pr	Pr	40	95:5
5	3,5-Me ₂ C ₆ H ₃	H	Ph	34	91:5
6	3,5-Me ₂ C ₆ H ₃	Me	SiMe ₃	56	72:26

performed aryl magnesiation with a Grignard reagent (Table X). An aryl magnesium bromide with an electron-donating as well as electron-withdrawing aryl group was successfully employed.

An aryl–iron species was proposed through the ligand exchange between the iron salt and the arylmagnesium bromide. The aryl–iron complex accomplished a *cis* addition with the alkyne forming vinyl–iron complex. Upon transmetalation this complex gave vinyl–cuprate. A subsequent transmetalation with a Grignard reagent formed the alkenylmagnesium bromide (Scheme 35) (56, 57).



Scheme 35. Mechanism of arylmagnesiation of alkynes with an Fe/Cu cooperative catalytic system.



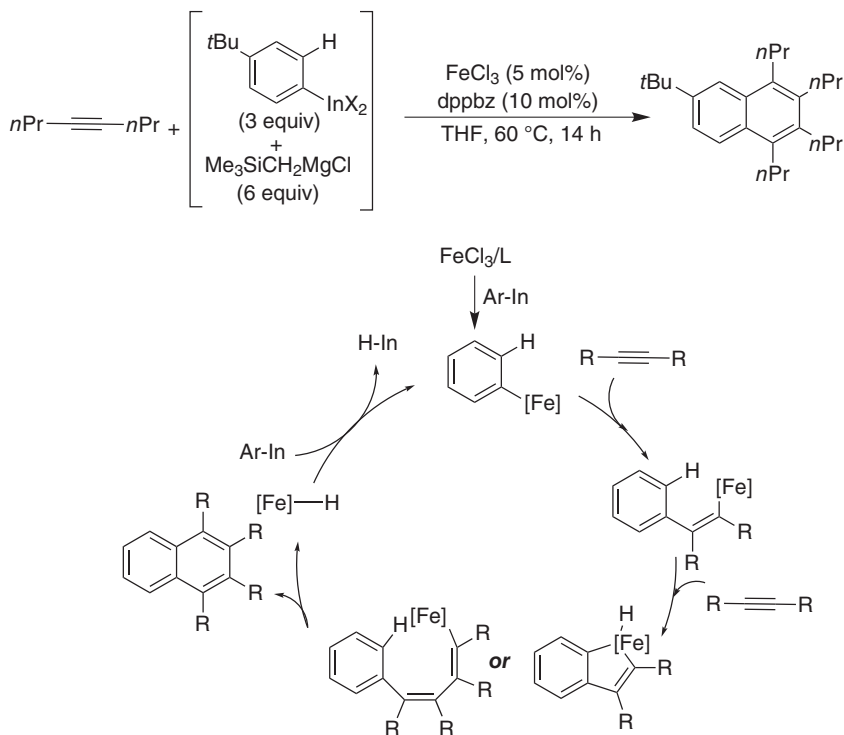
Scheme 36. Iron-catalyzed arylmagnesiation of alkynes in the presence of the NHC ligand.

In 2007, the same group reported arylmagnesiation of aryl(alkyl)acetylenes in the presence of a catalytic amount of $\text{Fe}(\text{acac})_3$ and an N-heterocyclic carbene (NHC) ligand (Scheme 36) (58). The aryl–iron species preferentially promoted cis addition to the alkyne forming an alkenyliron intermediate. The NHC ligated intermediate gave the desired product upon transmetalation with Grignard reagent.

Again in 2009, Hiyashi and co-workers (59) reported iron-catalyzed carbolithiation of alkynes in the presence of a catalytic amount of TMEDA (Table XI). In this system, they demonstrated alkyllithiation of aliphatic and aromatic substituted alkyne with good yield and stereoselectivity. The alkene-lithiated intermediate was

TABLE XI
Carbolithiation of Alkynes in the Presence of a Catalytic Amount of TMEDA

Entry	R ¹	R ¹	R ³	Time (h)	Yield (%)	A: B
1	Bu	Bu	Ph	1.5	81	
2	Bu	Bu	3-CF ₃ C ₆ H ₄	1.5	82	
3	Bu	Bu	2-MeOC ₆ H ₄	1.5	82	
4	Bu	Et	Ph	1.0	81	98:2
5	<i>i</i> Bu	Me	Ph	0.25	72	>99:1

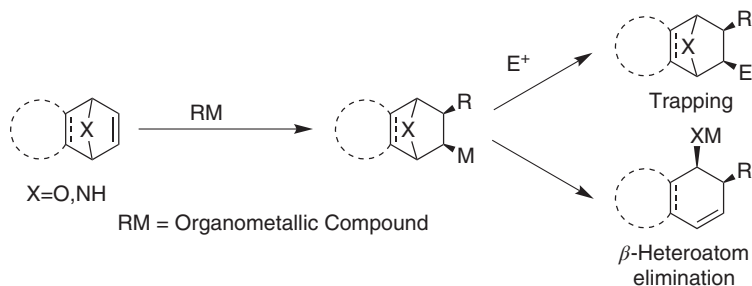


Scheme 37. Iron-catalyzed annulation reaction of aryllindium reagents and alkynes (dppbz = 1,2-bis(diphenylphosphino)benzene)

also used for further electrophilic substitution with aldehyde, alkyl bromide, and so on.

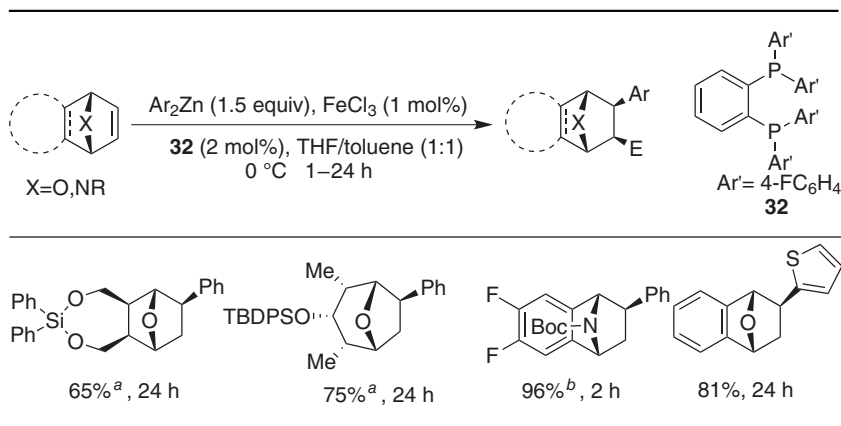
An aromatic ring can be constructed through carbometalation of two alkynes in the presence of a catalytic amount of iron chloride. Upon formation of an aryl-iron complex from an aryllindium reagent, reaction with alkyne was generated from an alkenyl-iron species. An intramolecular C-H activation involving another alkyne resulted in ring annulations (Scheme 37) (60).

Carbometalation in oxa- and azabicyclic alkene moieties are often problematic due to the ring-opening reaction through β -heteroatom elimination (Scheme 38). Ito and Nakamura (61) reported an iron-catalyzed diastereoselective organozincation of oxa- and azabicyclic alkenes in the presence of dppbz based ligands with much less conversion to the ring-opening product (Table XII).



Scheme 38. Schematic diagram for carbometalation of oxa- and azabicyclic alkene.

TABLE XII
Carbometalation in Oxa- and Azabicyclic Alkene Moieties^{a,b}

^a At 40 °C, FeCl₃ (3 mol%), ligand (6 mol%).^b At 25 °C (Boc = *tert*-Butyloxycarbonyl; TBDPS = *tert*-butyldiphenylsilane).

E. Michael Addition

The Michael addition is a useful pathway for C–C bond formation in the synthesis of an organic molecule. The convenient base-catalyzed Michael addition affords a number of side-product formations. To avoid the use of base, several methods using a transition metal have been developed. A number of homogeneous, as well as heterogeneous, iron-catalyzed Michael addition reactions have enriched this field with prospects for the future.

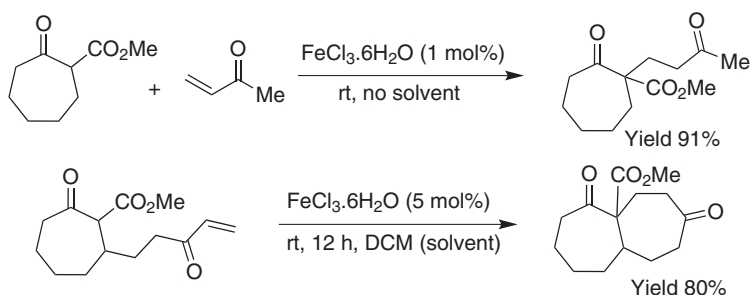
TABLE XIII
Michael Addition of Amines onto Acrylate Acceptors

Entry	Amines	X	Yield (%)
1	Diethylamine	OEt	96
2	Diethylamine	H	Polymerization
3	Piperidine	OEt	97
4	Morpholine	OEt	90
5	Pyrrolidine	OEt	95
6	<i>n</i> -Butylamine	OEt	79

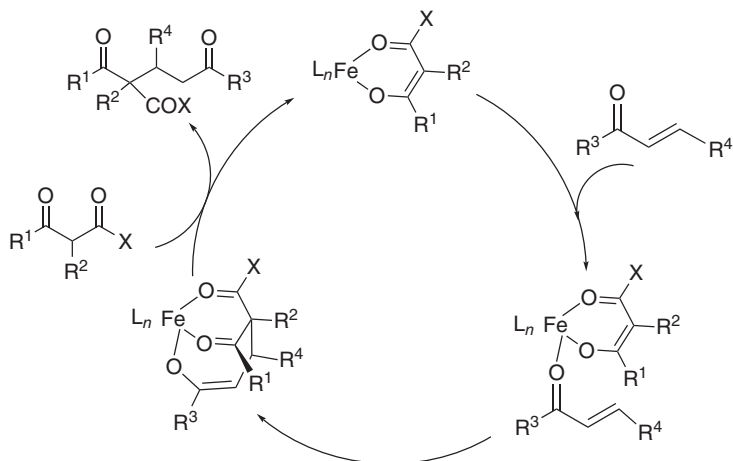
In 1989, Laszlo et al. (62) reported an FeCl_3 catalyzed Michael addition of amines onto acrylate acceptors (Table XIII). Herein, FeCl_3 acted as a Lewis acid, which coordinated with the carbonyl oxygen of the acrylate acceptor and catalyzed the reaction toward a thermodynamically favored 1,4- addition.

Iron(III) salts have proven to be an effective catalyst for Michael addition between 1,3-dicarbonyl compounds and vinyl ketones. In 1997, Christoffers (63) reported the FeCl_3 catalyzed Michael addition reaction at rt (Scheme 39).

First, the enone substrate interacted with the iron center through a vacant coordination site of a 1,3-dicarbonyl ligated iron complex. Then the center carbon of the dienato ligand performed the nucleophilic attack to the enone in 1,4-fashion. Since an olefin moiety should be in close contact with the dienato ligand for the alkylation of enone, the (*S*)-trans enone strongly disfavored the reaction (Scheme 40) (64).

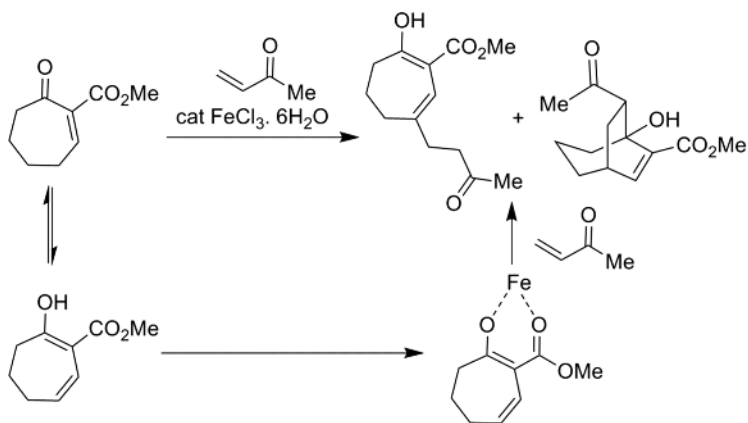


Scheme 39. Iron-catalyzed Michael reaction of 1,3-dicarbonyl compounds and enones.

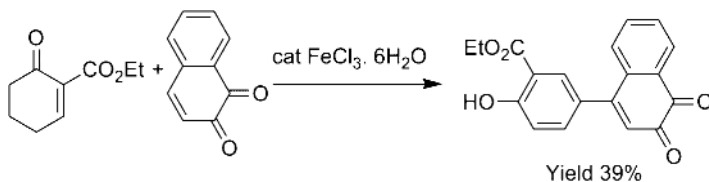


Scheme 40. Proposed mechanism for an iron-catalyzed Michael reaction of 1,3-dicarbonyl compounds and enones (COX = acyl halide).

A new class of Michael addition product was generated. The 2-acceptor substituted cycloalkenones with an iron salt formed a stable enolate, which acted as a Michael vinylogous donor toward the acceptor methyl vinyl ketone. Some amount of aldol product of the desired Michael addition was also formed as a side product (Scheme 41) (65).



Scheme 41. Iron-catalyzed Michael reaction with a vinylogous donor molecule.



Scheme 42. Synthesis of biaryl compounds by iron-catalyzed Michael reaction.

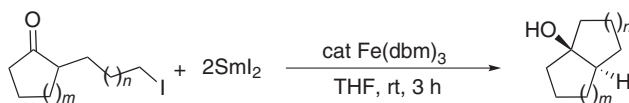
By using a quinine derivative as the acceptor of a vinylogous Michael addition, biaryl cross-coupled products were formed after overoxidation of the donor and acceptor moieties of the addition product (Scheme 42) (66).

Asymmetric Michael reaction with a chiral ligand was reported by Christoffers and co-workers (67). In 2003, an iron-catalyzed Michael reaction on a solid support was reported by Kitayama and co-worker (68).

F. Barbier-Type Reaction

Another popular way to construct a C–C bond is to attack the carbonyl center with a nucleophilic carbon center. In this regard, the Barbier reaction has drawn much attention for the preparation of alcohols from carbonyl compounds with simultaneous C–C bond formation. Generally, the nucleophilic carbon center is generated *in situ* from an alkyl or aryl halide, using various reducing agents (e.g., alkali and alkaline earth metals or lanthanides and their salts). Among various lanthanides, Molander and Harris (69) found SmI_2 and YbI_2 , to be very effective in promoting various types of intramolecular Barbier-type reactions in the presence of an iron catalyst. Several 2-(*n*-iodoalkyl) afforded good-to-excellent yield of the corresponding bicyclic alcohols in the presence of SmI_2 and catalytic iron tris(dibenzoylmethane) $[\text{Fe}(\text{dbm})_3]$ (Scheme 43, DBM = dibenzoylmethane) (70).

In particular, entries 1 and 4 in Table XIV show almost exclusive formation of one stereoisomer. Lack of stereoselectivity for entry 2 is due to the ease of attack from both the equatorial and axial side for equatorial side chains, whereas an axial side has only one option for equatorial attack, leading to a single diastereomer (Scheme 44) (70a).

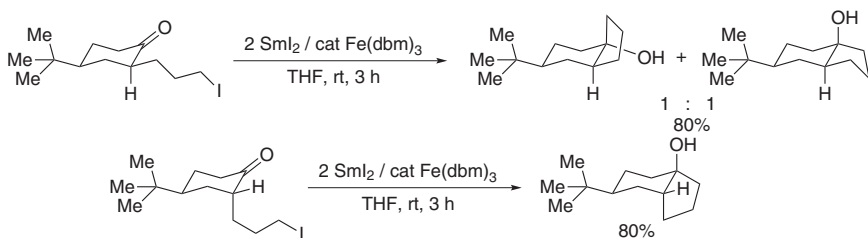


Scheme 43.

TABLE XIV
Iron-Catalyzed Intramolecular Barbier Reaction

Entry	<i>m</i>	<i>n</i>	% GC Yield (Isolated Yield) ^a	cis: trans
1	1	1	90 (60)	>99.5:<0.5
2	2	1	100 (75)	1.3: 1
3	3	1	85 (77)	2.0: 1
4	1	2	67	18: 1
5	2	2	95 (75)	1: 1.5
6	3	2	(83)	1: 2.3

^aGas chromatography = GC.

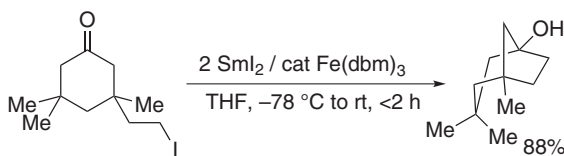


Scheme 44.

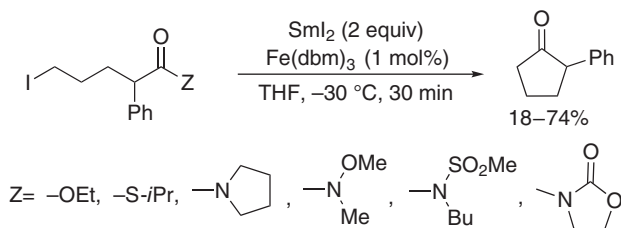
Even for the 3-(alkyl)cycloalkanones, the desired intramolecular rearranged bicyclic product was obtained in moderate-to-good yield (71). In all these cases, Fe(dbm)₃ was used as an effective catalyst due to its nonhygroscopic, air-stable nature and easy solubility in THF. In addition, other iron complexes including FeCl₂, FeCl₃, and Fe(acac)₃ were found to catalyze this reaction quite effectively (Scheme 45).

Acyclic acyl derivatives (e.g., esters, amides, and thioesters) were successfully converted into cyclic ketones (Scheme 46) (72).

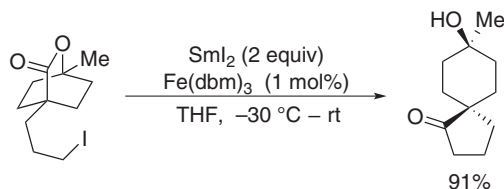
Cyclization by C–C bond formation followed by lactone ring opening via C–O bond cleavage can be obtained via intramolecular nucleophilic acyl substitution (INAS) with specific stereoselectivity (Scheme 47) (73).



Scheme 45.



Scheme 46.



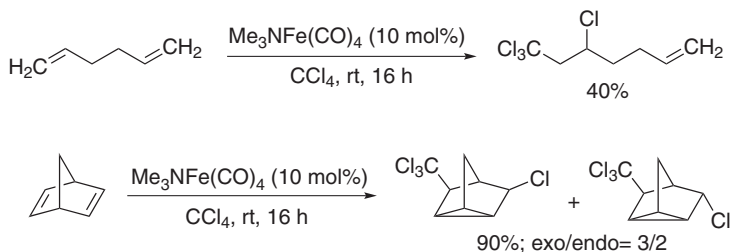
Scheme 47.

G. Kharasch Reaction

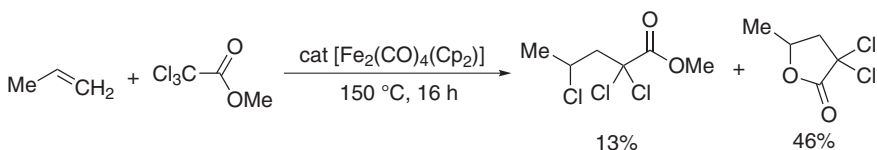
Construction of a new C–C bond can also be done by simple addition of polyhalogenated compounds with an alkenyl double bond by cleaving a C–X (X = Cl, Br, I) bond to form new geminal C–X and C–C single bonds (74). This type of transformation, popularly known as the Kharasch reaction, mainly goes through a radical pathway and starts by homolytic cleavage of a C–X bond in the presence of a radical initiator. Then newly generated alkyl radical attacks the alkene followed by final abstraction of a halide radical from a new polyhalide molecule leading to the final coupled product. Due to this radical pathway, several iron catalysts were found to be particularly efficient to initiate this transformation.

The first breakthrough in an iron-catalyzed Kharasch-type reaction came from the Hogeveen group (75). In their study, $\text{Me}_3\text{NFe}(\text{CO})_4$ was preferred to $\text{Fe}_2(\text{CO})_9$ for addition of CCl_4 in various alkene (Scheme 48). Interestingly, a strained tricyclic compound was formed in excellent yield from norbornadiene (Scheme 48).

Dimeric $[\text{Fe}_2(\text{CO})_4(\text{Cp})_2]$ was also found to catalyze this reaction at an elevated temperature (76). A detailed kinetic study showed first-order dependence on halocarbon and a dimeric iron complex, but a more complex dependence over the concentration of alkene. Interestingly, when simple halocarbon was replaced



Scheme 48.



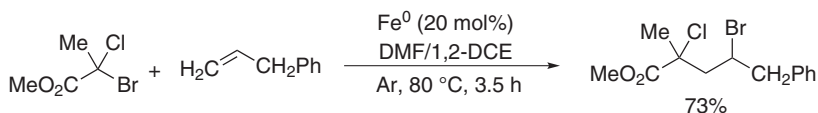
Scheme 49.

by methyltrichloroacetate, a mixture of products were obtained with lactone as the major product (Scheme 49) (76b).

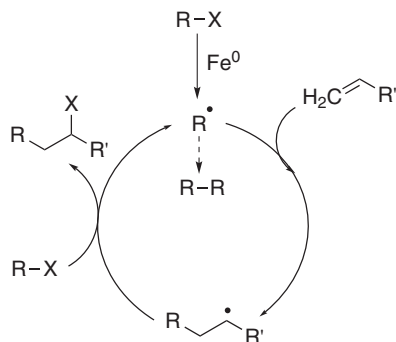
Elemental iron also has been found to catalyze this type of transformation. A bromo radical is preferred over chloro in this halogen-atom transfer radical addition to alkene process (Scheme 50 DCE = 1,2-dichloroethane) (77, 78).

At elevated temperature, α -dichloroester also can give the same type of compound by breakage of the C–Cl bond. The proposed mechanism involves single-electron transfer (SET) from Fe(0) to the LUMO of the haloester with concomitant expulsion of halide anion (Scheme 51) (78).

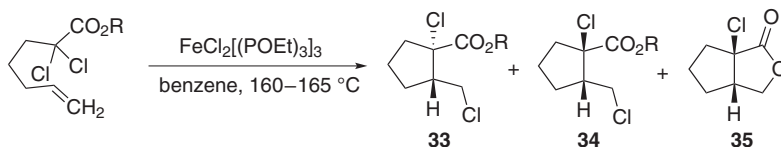
An intramolecular Kharasch-type reaction also can be performed by using a catalytic amount of $\text{FeCl}_2[(\text{P}(\text{OEt})_3)_3]$ from α,α -dichloroester in both diastereoisomers (79). Relative yields of the isomers depend on the catalyst loading and time. When haloacid was used in place of haloester, lactone was observed as the major product (Scheme 52).



Scheme 50.



Scheme 51.



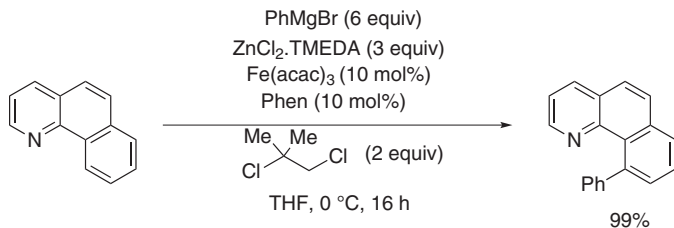
R	Catalyst (mol%)	Time (h)	33 Yield (%)	34 Yield (%)	35 Yield (%)
Et	5.7	8	51	24	0
Et	8.7	20	32	51	0
H	4.0	24	0	0	66

Scheme 52.

III. THE C–C BOND FORMATIONS VIA C–H FUNCTIONALIZATION

A. The C–H Arylation

Biaryl structural motifs are ubiquitous in nature as well as in synthetic chemistry. From the days of the Ullmann reaction to traditional cross-coupling reactions, transition metals have played the key role in forming biaryls through C–C coupling. With advancement in coupling reaction chemistry, chemists have devised a method where one organometallic reagent has been replaced by unactivated, simple arenes thereby minimizing the related preactivation, extra synthetic step, and waste. This approach is termed a “direct arylation” strategy. In recent decades, progress in this field has been achieved primarily with second- and



Scheme 53. Iron-catalyzed direct arylation, where Phen = 1,10-phenanthroline.

third-row transition metal catalysts (e.g., Pd, Rh, Ru). The utilization of first-row transition metals, which are less expensive and environmentally benign, is challenging, though in recent years significant improvements have been observed with Cu, Ni, or Fe catalysts. In Section III.A.1, recent advances in iron-catalyzed direct arylation of unactivated arenes will be discussed briefly.

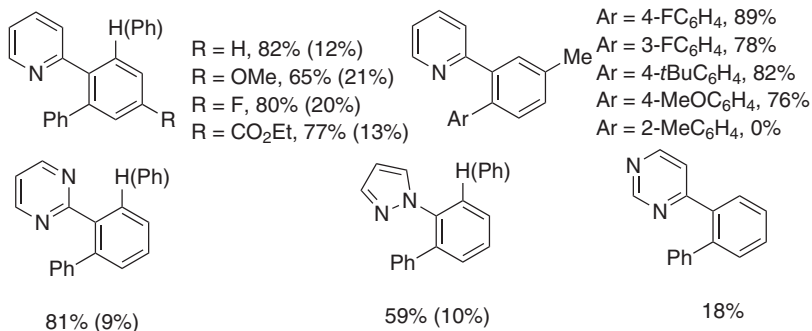
1. Direct Arylation With Organometallic Reagents

In 2008, Nakamura and co-workers (80) reported the first iron-catalyzed direct arylation with an *in situ* generated organozinc reagent in the presence of a suitable oxidant. Under optimized conditions, only 10 mol% Fe(acac)₃-phen resulted in an excellent yield of the desired product at a remarkably low temperature (0 °C) (Scheme 53).

The compounds FeCl₂ and FeCl₃ also were found to be equally reactive, but Fe(acac)₃ was chosen due to its ease of handling. Choice of a proper ligand system was extremely crucial, as Fe(acac)₃ alone was inefficient to catalyze the reaction. Bidentate nitrogen-based ligand phen was found to be the most efficient after extensive experimentations with various nitrogen-based bi- and tridentate ligands. Similarly, several dihalide oxidants were tested and 1,2-dichloroisobutane (DCIB) was found to promote this transformation in quantitative yield. Also, the combination of PhMgBr and ZnCl₂.TMEDA (in 2:1 ratio), was essential for the success of the reaction, as Ph₂Zn or PhZnBr were unable to promote the reaction.

Regioselectivity of arylation was determined by the presence of a nitrogen-atom in the substrates, which serves as the anchoring group for the metal. With benzoquinoline as the substrate, arylation was observed exclusively at the C10 position, as it was the only available position for arylation. With 2-phenylpyridine, an aryl group was inserted at the ortho position(s) only to give primarily the mono-arylated product, though diarylation was also observed to some extent with symmetrical substrates (Scheme 54).

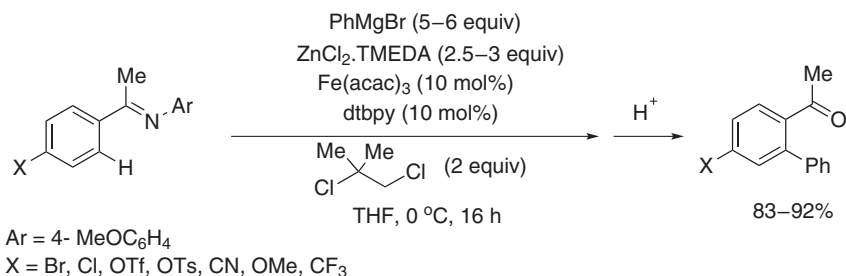
The variation of electronically different substituents on 2-phenylpyridine and in an aryl zinc reagent did not affect the yield of the desired product. However, the



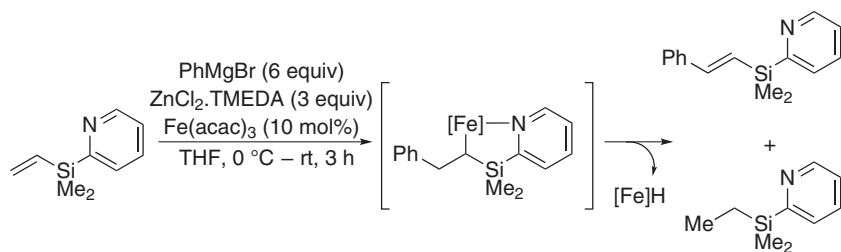
Scheme 54. Iron-catalyzed direct arylation of 2-aryl pyridine derivatives.

method was found to be very sensitive to the steric requirement of the substrate, as well as of the reagent. With a methyl group in the 3 position on the phenyl ring of 2-phenylpyridine, arylation occurred exclusively at the less hindered position and with 2-tolylzinc no product was observed.

In 2009, Nakamura and co-workers (81) also reported a related method, where the aryl group was selectively inserted into the ortho C–H bond of aryl imines (Scheme 55). In this report, dtbpy (4,4'-di-*tert*-butyl-2,2'-bipyridine) was used as the ligand in place of phen with $\text{Fe}(\text{acac})_3$. The 1,2-dichloroisobutane (DCIB) was used as the oxidant to generate arylated ketimines or the corresponding ketones. Mono-arylated products were obtained for a number of aryl and heteroaryl imines in excellent yields. Interestingly, under the applied condition traditional leaving groups of cross-coupling chemistry (e.g., Cl, Br, OTs, and even OTf) were tolerated, thus exhibiting the possibility of orthogonal arylation or sequential arylation–functionalization. This protocol was also found to be sensitive to the steric requirements of the substrates like the previous method. Now, the mechanism of this reaction remained unclear and a detailed investigation is still required. Further, they enhanced the applicability of their methods by replacing DCIB by



Scheme 55. Iron-catalyzed directed ortho arylation of aryl imines.

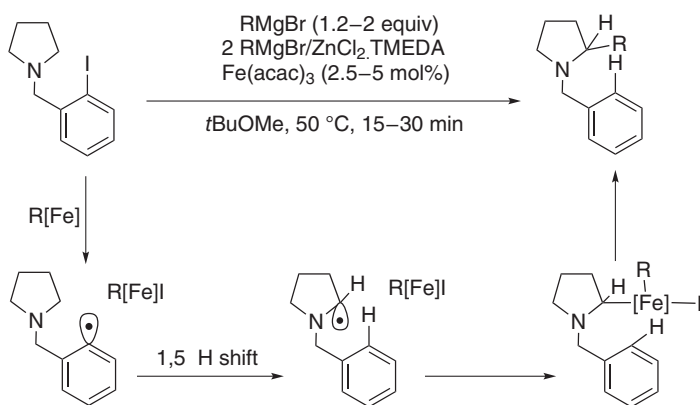


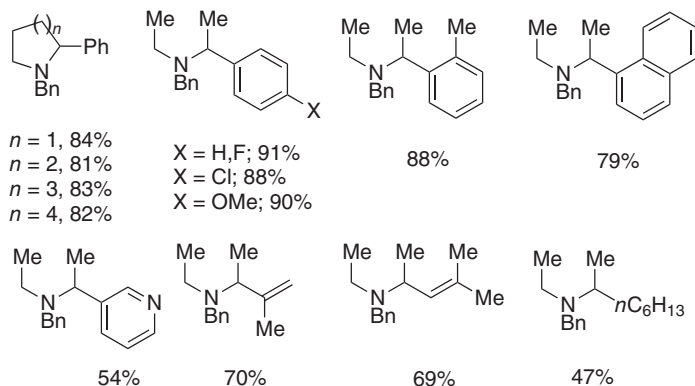
Scheme 56. Iron-catalyzed oxidative Heck reaction.

molecular oxygen as the stoichiometric oxidant, where sequential slow diffusion of oxygen into the reaction medium at 12-h intervals turned out to be advantageous.

In 2010, by applying similar conditions, Ilies et al. devised an oxidative Heck reaction in which the iron-catalyzed arylation of olefins was affected by organozinc and Grignard reagents through a proposed ferracycle intermediate (Scheme 56) (82). Here, 1-bromo-2-chloroethane was used as the optimal oxidant in place of DCIB to significantly suppress the reduced byproduct. Substrates without a directing group like 1-octene and styrene, as well as vinyl acetates or 2-vinyl pyridines, having a directing group, remained unreactive.

Encouraged by the success of iron-catalyzed sp^2 C–H functionalization, Nakamura and co-workers (83) further investigated the sp^3 C–H bond activation with an iron catalyst. In 2010, they reported an intermolecular coupling of aliphatic amines containing an *N*-(2-iodophenyl) methyl group (*N*-IBn) (acting as an internal trigger for C–H bond cleavage) and an organometallic reagent to generate an α -substituted product with an iron-based catalyst (Scheme 57). The reaction

Scheme 57. Proposed reaction pathway of an iron-catalyzed α -arylation of aliphatic amines.

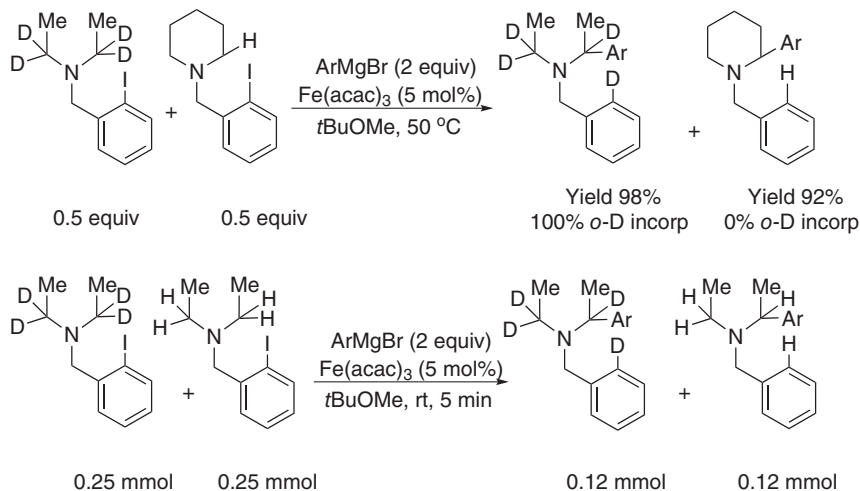
Scheme 58. Scope of an iron-catalyzed α -arylation of aliphatic amines.

proceeded by metal-mediated activation of a C–I bond, followed by intramolecular 1,5-hydrogen transfer and a subsequent C–C bond formation through a putative organoiron intermediate. Under optimized conditions, various cyclic and acyclic aliphatic amines reacted smoothly, though with a bromo analogue, lower yield of the desired product was observed (Scheme 58, Bn = benzyl). In the case of unsymmetrical aliphatic amines, arylation occurred preferentially at a more substituted position, thereby further enhancing the probability of a radical pathway.

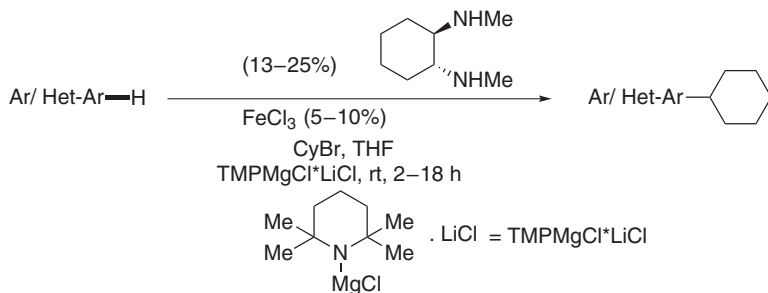
Control experiments suggested iron as the sole catalyst, as reaction occurred successfully with other iron sources (e.g., FeCl_3 or FeCl_2), but in the absence of the catalyst, no conversion was observed. Labeling experiments clearly indicated the 1,5-H shift to be strictly intramolecular and no H/D crossover was observed. Also, a competition experiment ruled out the possibility of C–H bond cleavage as the rate-determining step of the reaction (Scheme 59).

Tran and Daugulis (84) also reported an iron-catalyzed deprotonative alkylation of five- and six-membered heteroarenes (e.g., thiophenes, furans, pyridines, and electron-deficient arenes) in the presence of a Grignard reagent with alkyl halides (Scheme 60). Grignard reagent primarily serves as a proton abstractor and a number of alkyl bromides and iodides undergo the transformation successfully.

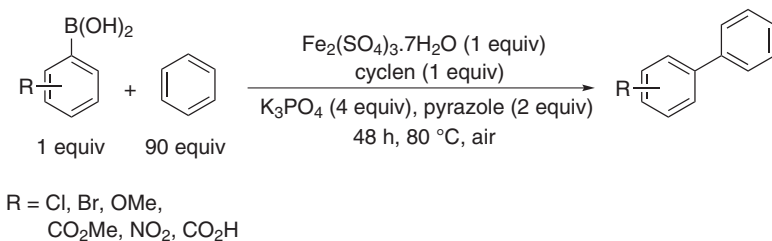
Without using Grignard–organozinc reagents, iron mediated direct arylation of unactivated arenes with boronic acids was reported by Yu and co-workers (85) for the first time in 2008 (Scheme 61). A number of substituted boronic acids and different unactivated arenes were coupled efficiently at a moderately high temperature. The mechanism for this reaction still remained unclear, though the intermediacy of radical species was ruled out by this investigation. However, this method needs further modification, as it requires a stoichiometric amount of iron salt and excess unactivated arenes.



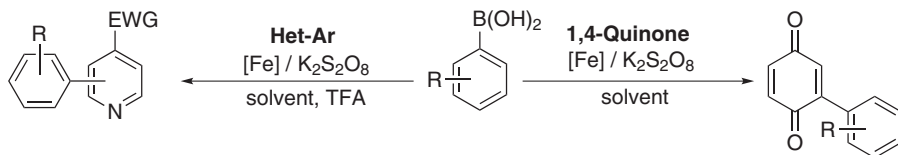
Scheme 59. Labeling experiments for mechanistic study.



Scheme 60. Iron-catalyzed deprotonative alkylation of heteroarenes (TMP = 2,2,6,6-tetramethylpiperidyl).



Scheme 61. Iron-mediated direct arylation of arenes by arylboronic acids (cyclen = 1,4,7,10-tetraazacyclododecane).



Scheme 62. Iron-catalyzed arylation of quinones and heteroarenes (TFA = trifluoroacetic acid).

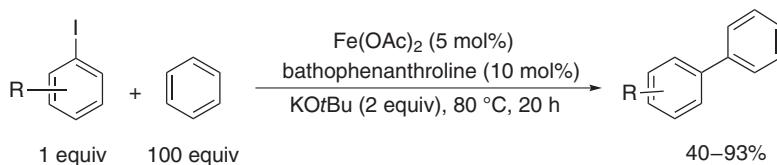
Recently, Yu and co-workers (85) reported an iron mediated C–C coupling reaction in 2012, that started from aryl boronic acids and electron-deficient pyridines and quinones (Scheme 62). In the presence of a suitable oxidizing agent, $\text{K}_2\text{S}_2\text{O}_8$, a number of quinone derivatives were efficiently arylated by FeS . Further, no exogenous ligand is required for the success of this reaction. Notably, all these transformations significantly improve the applicability of iron catalysis to achieve green and sustainable reaction protocols in coupling chemistry.

2. Direct Arylation With Aryl Halides

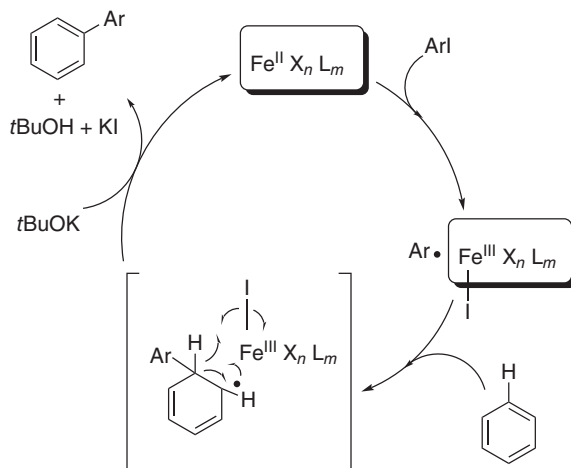
In 2010, Lei and Charette (86) independently reported iron-catalyzed direct arylation of unactivated arenes with aryl halides. In Charette's report, arylation with aryl iodides and simple arenes was affected efficiently without the need of any directing group or stoichiometric organometallic reagents (Scheme 63) (86).

The optimized condition required 5 mol% $\text{Fe}(\text{OAc})_2$ as the catalyst and bathophenanthroline (10 mol%) as the ligand in the presence of $\text{KO}t\text{Bu}$ (2 equiv) at 80°C . Even a 0.5 mol% catalyst loading was effective at an elevated temperature. Various aryl and heteroaryl iodides were found to give the desired product in moderate-to-excellent yields. Electron-rich iodides were found to be more reactive, as even at rt moderate yields were obtained with a prolonged reaction time. Notably, the protocol was efficient only with aryl iodides, as aryl bromide proved to be less reactive while aryl chloride remained unreactive.

In a preliminary mechanistic investigation, a KIE of 1.04 was found thus ruling out the possibility of C–H bond cleavage as the rate-determining step. A radical pathway was proposed and an iron(II)–iron(III) redox cycle was thought to be operative (Scheme 64).



Scheme 63. Iron-catalyzed direct arylation of arenes with aryl iodides.

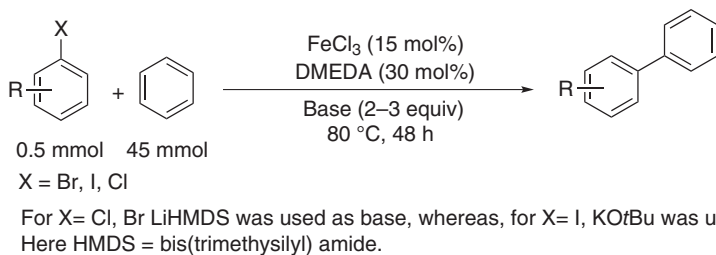


Scheme 64. Proposed catalytic cycle.

In this proposed mechanism, one-electron oxidation of the iron center activated the aryl–halogen bond and generated a radical species. In the next step, a radical addition on arene was followed by abstraction of a halogen atom from the metal center and KO*t*Bu quenched the resulting HI to form *t*BuOH, which had been detected in the reaction medium. This radical pathway was further supported by reactions with radical scavengers (e.g., TEMPO, 2,2,6,6-tetramethyl-piperidin-1-yl)oxyl, and galvinoxyl), which practically inhibited the reaction. Control experiments clearly indicated the prominent role of iron as the sole catalyst regardless of its purity and no product was obtained in the absence of Fe(OAc)₂.

A similar method was demonstrated by the Lei and co-workers (87) group in the same year, where FeCl₃ was the catalyst of choice along with *N,N*-dimethylethylenediamine (DMEDA) as the ligand (Scheme 13). At moderate temperature, aryl halides were efficiently reacted depending on the nature of the base used. With a strong base, LiHMDS (2 equiv), the less reactive aryl bromides exhibited good reactivity, while aryl chlorides were found to be moderately reactive (Scheme 65). In the presence of excess KO*t*Bu (3 equiv), more reactive aryl iodides reacted efficiently to form the desired product in satisfactory yields. Electron-rich aryl bromides gave a better result compared to electron-deficient ones. Also, substituent in the ortho position resulted in a lower yield, indicating that steric hindrance had a detrimental effect on reactivity. Notably, the same trend regarding the stereoelectronic effect of the substituents was observed with aryl iodides in Charette's report (86).

Detailed mechanistic studies were not conducted in this case, however, preliminary studies ruled out any intermediacy of a benzyne analogue. A labeling experiment with [*d*₆]-benzene yielded a KIE value of 1.7 and thus a radical



Scheme 65. Iron-catalyzed direct arylation of benzene with aryl halides.

pathway was considered. Also, in accordance with the report of Buchwald and Bolm (88), reaction was performed with ultrapure FeCl₃ under standard conditions and the same results were obtained. The arene coupling partner was required to be in excess for the reaction. In conclusion, in direct arylation chemistry these methods clearly indicate the significant development where less expensive iron salts exhibited unprecedented reactivity.

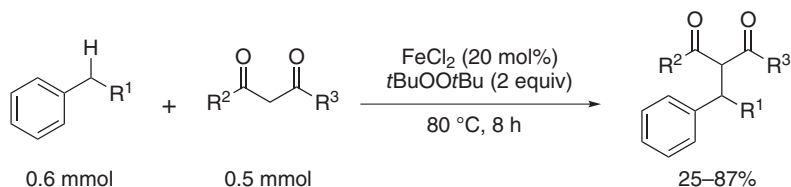
B. The C–C Bond Formation Via Cross-Dehydrogenative Coupling

A cross-coupling reaction is one of the most powerful tools in organic synthesis. Several approaches toward the desired cross-coupled products are known. The straightforward approach will be direct coupling of two different C–H bonds instead of using either organic halides–pseudohalides or organometallic partners or both (89). This technique is popularly known as cross-dehydrogenative coupling (CDC). Li (90) made a pioneering contribution in CDC by using a first-row transition metal catalyst. After their initial work with copper, first iron-catalyzed CDC was reported in 2007 and an iron catalyst was found to be more efficient than a copper catalyst (91).

1. The CDC Between Two *sp*³ C–H Bonds

Initially, diphenylmethane was used as one of the coupling partners for the double activation at the benzylic position. Similarly, another coupling partner was 1,3-dicarbonyl with an activated α -C–H bond. It was found that FeCl₂ was best among various iron salts and di(*tert*-butyl)peroxide (DTBP) replaced *tert*-butyl hydrogen peroxide (TBHP) with a further increase in yield (Scheme 66) (91).

The proposed mechanism involved homolysis of DTBP and a single-electron transfer from iron(II) with generation of a *tert*-butoxyl radical and a *tert*-butoxide anion, which was then followed by generation of an active benzyl radical and iron(III) enolate by proton abstraction. Then electrophilic radical attack led to the desired cross-coupled product with the regeneration of an iron(II) species to facilitate the catalytic cycle (Scheme 67) (91).

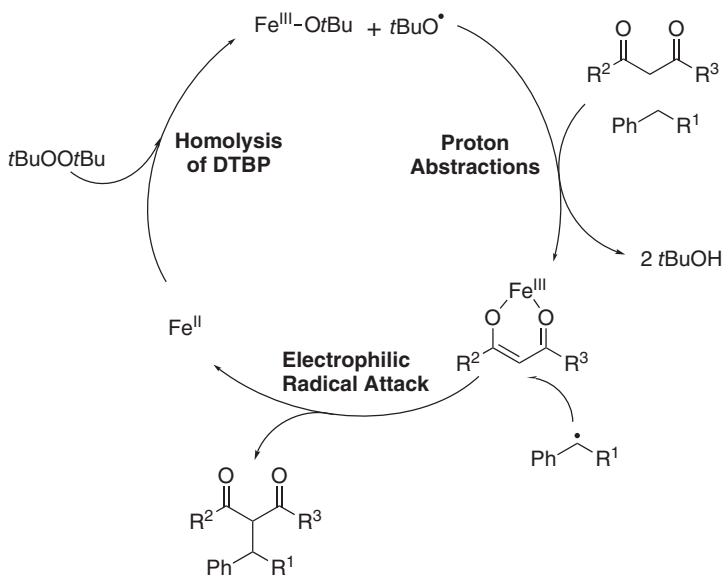


Scheme 66.

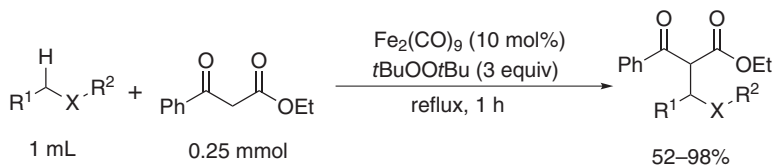
Instead of $\text{C}_{\text{sp}^3}\text{—H}$ at the activated benzylic position, the $\alpha\text{—C}_{\text{sp}^3}\text{—H}$ bond of nitrogen in amine or oxygen in ether can also be activated (90, 92) by using an iron catalyst. In this case, FeCl_2 , FeBr_2 , $\text{Fe}(\text{OAc})_2$, and $\text{Fe}_2(\text{CO})_9$ showed a catalytic property, but $\text{Fe}_2(\text{CO})_9$ was found to be the best in combination with DTBP as the oxidizing agent. Both acyclic and cyclic ether along with thioether and tertiary amine gave a moderate-to-excellent yield of the desired CDC product with 1,3-dicarbonyl compounds (Scheme 68) (93).

The presence of nitrogen or oxygen at the α -position was crucial due to the formation of iminium or oxonium ions as the key intermediate via SET. Further attack from a carbon nucleophile led to the product (Scheme 69) (90).

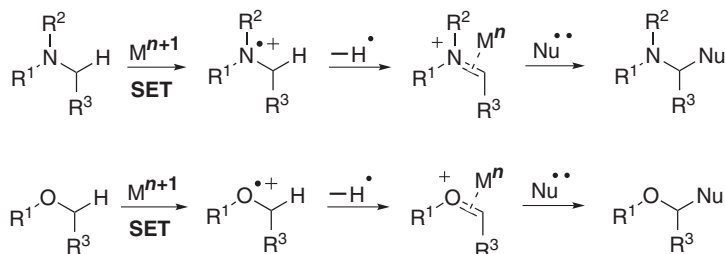
Extension of this work by Li et al. (94) using *N,N*-dimethylaniline as the source of the methylene group produced dialkylation with 1,3-dicarbonyl and a bridged bis-1,3-dicarbonyl compound was generated (Scheme 70).



Scheme 67.



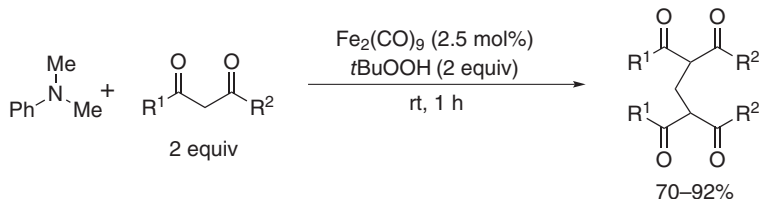
Scheme 68.



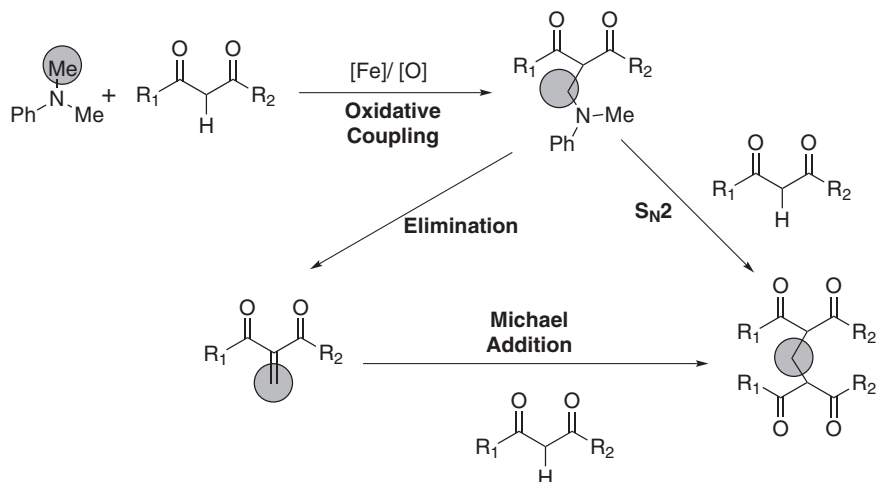
Scheme 69.

Several possible pathways were proposed for this transformation. In Li's proposal, first *N,N*-dimethylaniline underwent CDC with one molecule of the 1,3-dicarbonyl compound. Then, in one route direct S_2N attack might occur where *N*-methylaniline acted as a leaving group. In other route, cope elimination led to an α,β -unsaturated carbonyl moiety, where further Michael addition of a second 1,3-dicarbonyl compound led to the final product (94). Also *in situ* generation of formaldehyde from *N,N*-dimethylaniline and further coupling with two molecules of 1,3-dicarbonyl compound cannot be ruled out (Scheme 71).

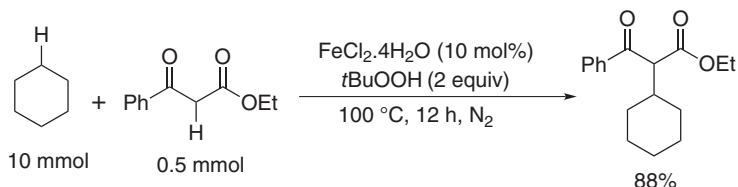
Activation of the alkylic $\text{C}_{\text{sp}^3}\text{-H}$ bond is most challenging due to low reactivity, selectivity problems, and the lack of a coordination site for the transition metal catalyst for $\text{C}_{\text{sp}^3}\text{-H}$ bonds. In all previous reports, both coupling partners had specific activated $\text{C}_{\text{sp}^3}\text{-H}$ bonds to participate in cross-coupling reactions. Till now, only one successful example with iron had been reported, where unactivated alkane was used as a substrate (Scheme 72) (95).



Scheme 70.



Scheme 71.

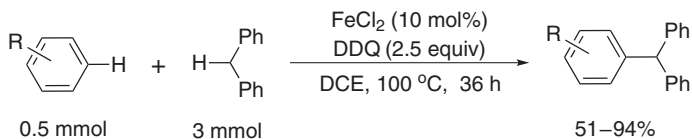


Scheme 72.

2. The CDC Between sp^3 and sp^2 C–H Bonds

In accordance with the mechanism of CDC between the 1,3-dicarbonyl compound and dibenzylmethane, as in Li's report, other nucleophiles can be considered to quench the intermediate formed from dibenzylmethane through the iron-catalyzed SET process. Shi and co-workers (96) reported the cross-dehydrogenative arylation (CDA) of dibenzylmethane with electron-rich arenes. Use of DDQ (dichlorodicyanobenzoquinone) in place of DTBP as oxidant gave a significant increase in yield, and DCE as solvent reduced the amount of dibenzylmethane used for the reaction. Excellent regioselectivity was observed for a class of electron-rich arenes, but double CDA was also observed for more electron-rich arenes (Scheme 73 DDQ = 2,3-dichloro-5,6-dicyano-1,4-benzoquinone).

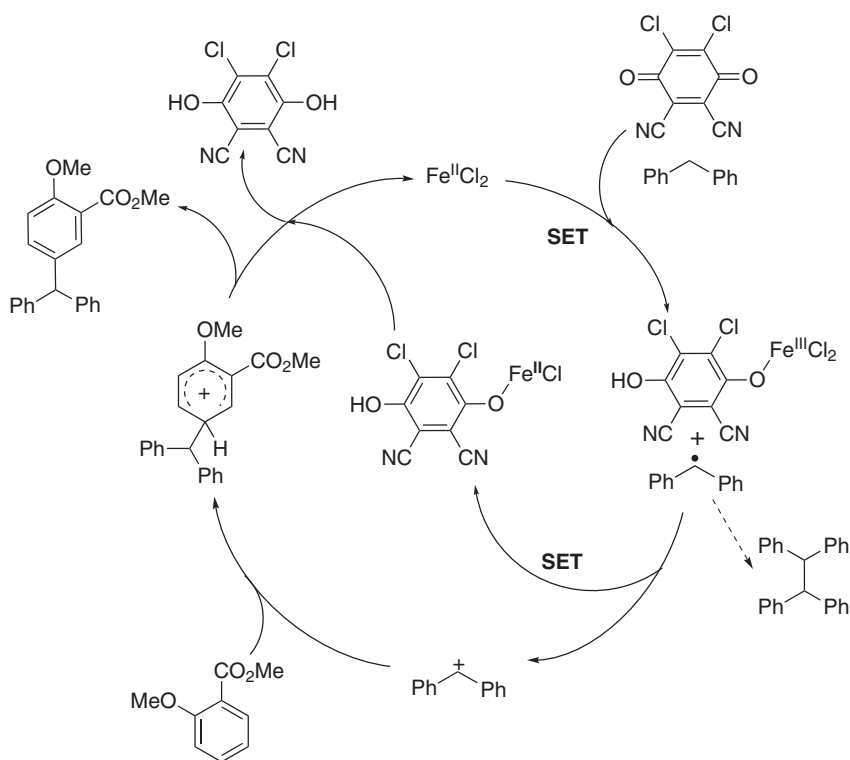
Based on preliminary mechanistic evidences by deuterium labeling, KIE, and the side products obtained, first iron(II) assisted SET oxidation was proposed to produce a dibenzyl radical and reduced quinone. Then again, dibenzyl cation was generated



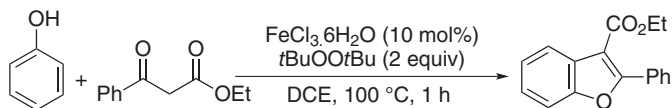
Scheme 73.

from dibenzyl radical through SET with regeneration of an iron(II) species. Finally, attack of this dibenzyl cation to an electron-rich arene followed by proton abstraction by reduced hydroquinone afforded the coupling product (Scheme 74) (96).

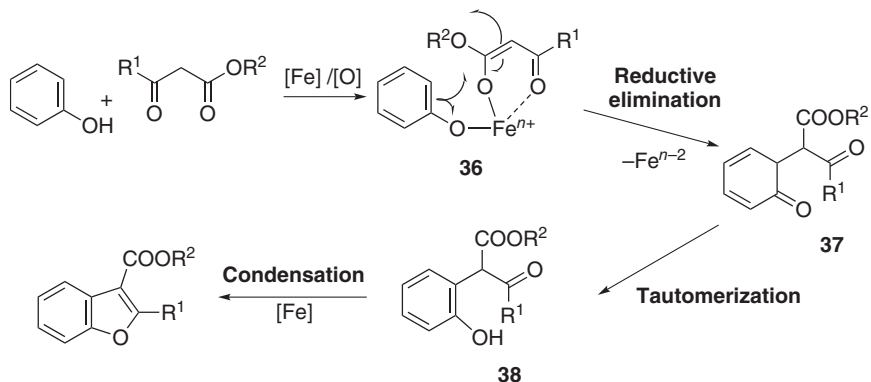
Similarly, electron-rich alkenes were considered as the active nucleophile in Shi's other report to quench the benzyl radical or cation. Surprisingly, only styrene was found to give the coupled product, but another styrene derivative did not give the desired product.



Scheme 74.



Scheme 77.



Scheme 78.

quenched by vinyl acetate. A proton-abstraction process may be involved in the rate-determining step in either pathway as indicated by an intermolecular isotopic competitive study ($K_{\text{H/D}} = 2.4$) (Scheme 76) (97).

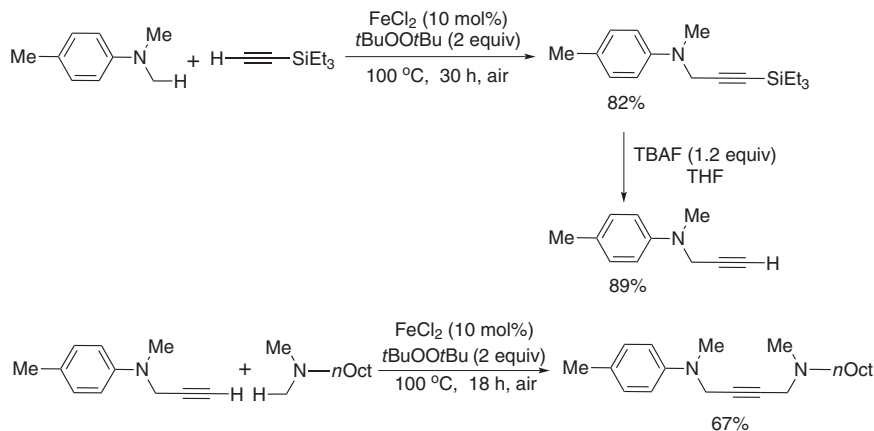
Yet another breakthrough came from Li and co-workers (98), wherein an iron-catalyzed CDC reaction and subsequent annulation of phenol and β -keto ester led to the polysubstituted benzofuran. Notably, various iron salts did not alter the yield too much, but the presence of water in an iron catalyst was crucial for a good yield (Scheme 77).

The hypothesized mechanism showed formation of an Fe^{n+} chelated complex, followed by reductive elimination, tautomerization, and condensation leading to the final product (98). Formation of the desired product from prepared compound **36** supported this hypothesis (Scheme 78).

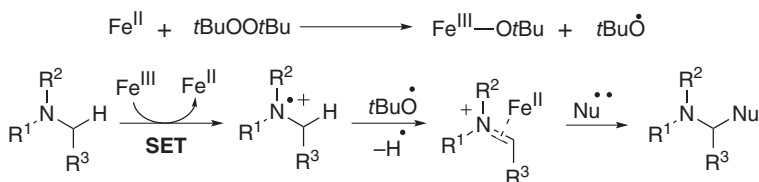
3. The CDC Between sp^3 and sp C–H Bonds

Besides aryl- and alkene-type substrates, terminal alkynes were also investigated. Instead of 1,3-dicarbonyl systems, an α - sp^3 C–H bond from nitrogen was found effective in CDC with terminal alkynes (Scheme 79) (99).

Both aromatic and aliphatic tertiary amines led to the desired product with FeCl_2 and DTBP combination. Iron-catalyzed SET led to generation of an iminium



Scheme 79.



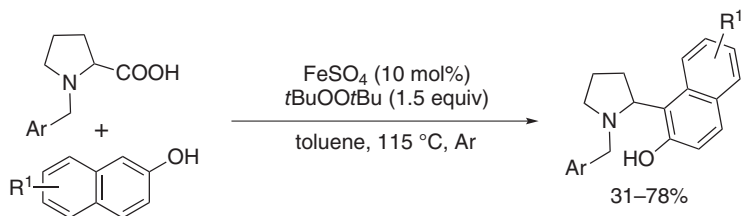
Scheme 80.

ion intermediate and quenching by an alkynyl carbanion proposed to be involved in this transformation (Scheme 80).

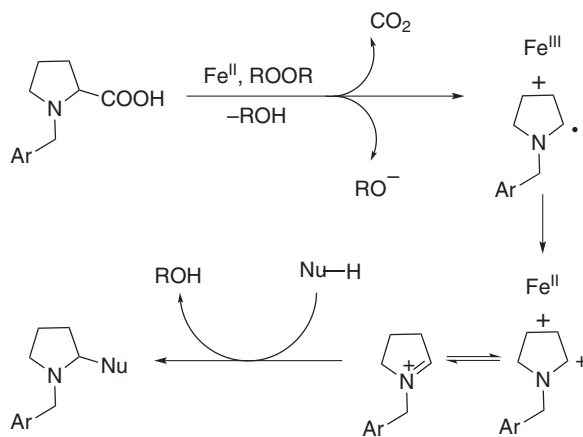
C. The C–C Bond Formation via Cross-Decarboxylative Coupling

Another potential approach for C–C bond formation is through C–H transformation and intermolecular–intramolecular decarboxylative coupling. The ready availability, low toxicity, low cost of carboxylic acids made it attractive as one of the coupling partners for selective cross-coupling (96, 100). A proline derivative was found to couple decarboxylatively with substituted β -naphthols in the presence of FeSO_4 and DTBP (101). Besides β -naphthols, electron-rich α -naphthols and indoles were also suitable nucleophiles for this decarboxylative coupling (Scheme 81).

The proposed mechanism involved homolysis of peroxide in the presence of iron(II) salts, followed by hydrogen-atom abstraction by a *tert*-butyl radical from the carboxylic acid to initiate decarboxylation with generation of 2-pyrrolidinyl



Scheme 81.

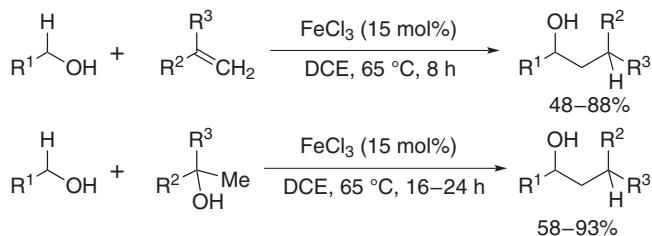


Scheme 82.

radical. In the presence of Iron(III), this radical was further oxidized to the 2-pyrrolidinium cation and was attacked by nucleophile generated by proton abstraction from electron-rich naphthols or indoles (Scheme 82) (101).

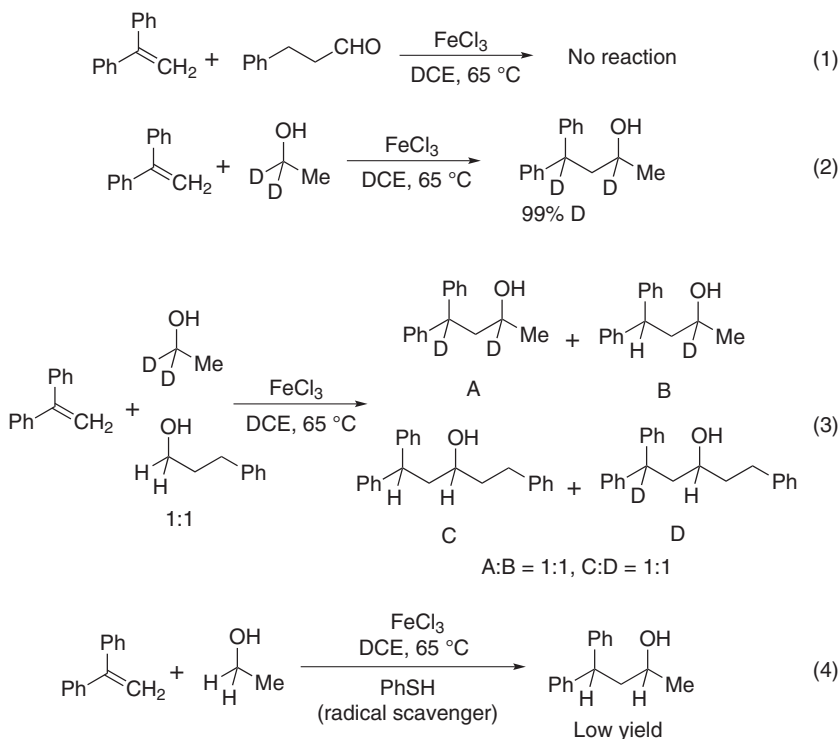
D. The C–C Bond Formation via Alkene Insertion

Another design for C–C bond formation relating to this well-known technique of radical or cation generation by iron-catalyzed SET processes followed by quenching by an electron-rich compound could be using unsaturated alkenes or alkynes instead of electron-rich arenes in the absence of any radical quencher. With the use of the relatively high activity of the α -C–H bond of a heteroatom, Tu and co-workers (102) reported this type of radical quenching using terminal alkenes (Scheme 83).

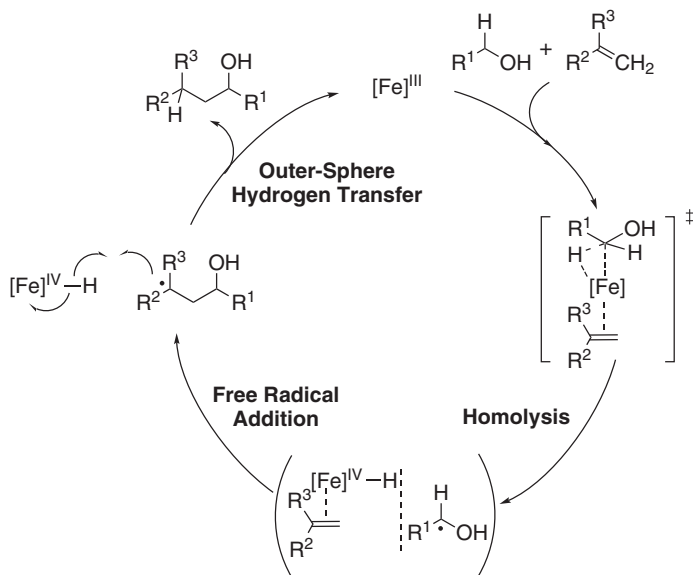


Scheme 83.

Controlled experiments, deuterium labeling, and cross-over experiments were conducted to give an idea about the possible mechanism. Failure of aldehyde to give the desired product indicated that the oxidation–hydroacylation–reduction pathway was not followed (Scheme 84, Eq. 1). Quantitative deuterium incorporation in alkene (Scheme 84, Eq. 2) and deuterium scrambling (Scheme 84, Eq. 3)



Scheme 84.



Scheme 85.

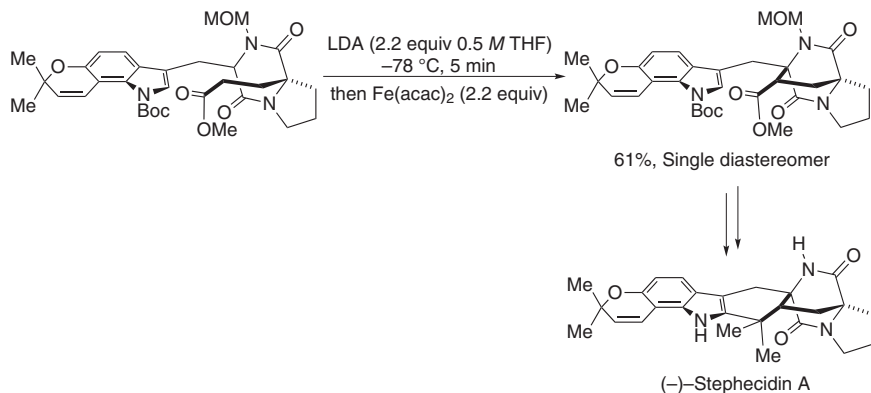
indicated that hydrogen transfer from alcohol to alkene occurred in discretely intermolecular fashion. Again low yield of the desired product in the presence of a radical scavenger (Scheme 84, Eq. 4) implied that radical pathway was followed.

In accordance with all of these results, the proposed catalytic cycle showed formation of a $\text{Fe}^{\text{IV}}-\text{H}$ active species, which was involved in an outer-sphere-type hydrogen radical transfer leading to the desired coupling product (Scheme 85) (102).

E. Oxidative Coupling of Two C–H Bonds

Irrespective of the different methods available for iron-catalyzed C–C coupling via C–H bond activation, direct application in total synthesis was restricted due to lack of control in selectivity and efficiency. Baran et al. (103) reported examples of iron mediated C–C bond formation by C–H transformation, which was directly applied in total synthesis (Scheme 86, LDA = lithium diisopropylamide).

In the total synthesis of anti-cancer natural products (e.g., stephacidins), Baran et al. (103) reported an unprecedented intermolecular oxidative C–C bond formation using $\text{Fe}(\text{acac})_3$ (103). In order to construct the bicyclic core of stepacidin alkaloids, this type of C–C coupling was critical especially with proper chemo- and stereoselectivity. A unique oxidation potential of the iron-based

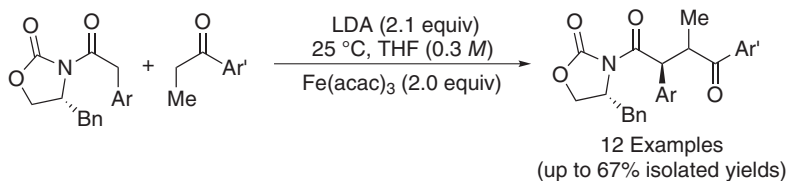


Scheme 86.

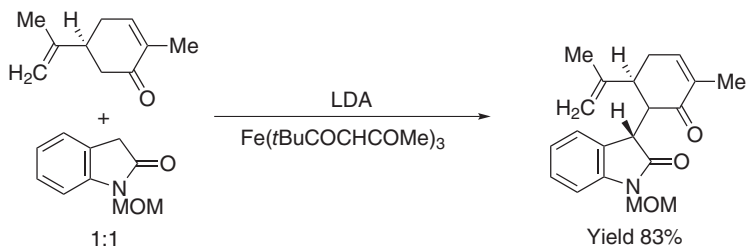
oxidant was proposed to control chemoselectivity. An easy formation of an iron-chelated transition state was proposed to control high stereoselectivity.

In another example, they reported iron-mediated intermolecular oxidative heterocoupling of two different carbonyl species to give 1,4-dicarbonyl species with a specific stereoselectivity due to the different coordinating nature of iron compared to copper (Scheme 87) (104). Mechanistic studies revealed nontemplated iron(III) mediated heterodimerization in this process with suppression of other possible side products from homodimerization, cross-homo Claisen condensation, cross-homo-aldol condensation, overoxidation, dehydrogenation, and α -oxidation.

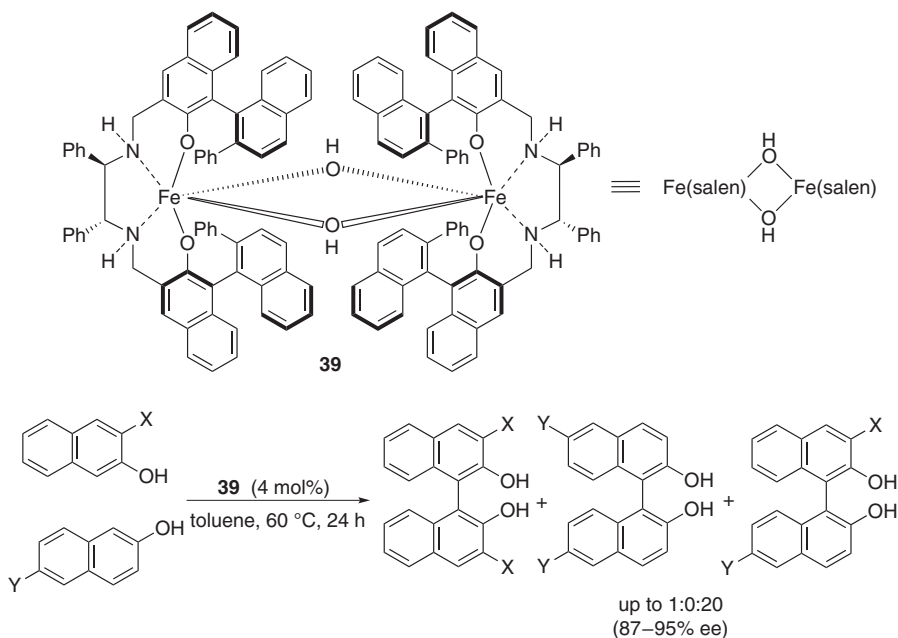
The same group reported another example of oxidative coupling between indinones and carvones, during the search for an alternate protocol to synthesize the core unit of hapalindoles, fischerindoles, and welwitindolinones, a class of indole-based heterocycles with a monoterpene unit attached at the C3 position (Scheme 88, MOM = methoxymethyl ether). It was found that with the indole type of moiety copper was best suited, where as for indinone the Fe based $\text{Fe}(t\text{BuCOCHCOMe})_3$ was found to give the highest yield (105).



Scheme 87.



Scheme 88.



Scheme 89.

Another case of oxidative cross-coupling of β -naphthols to give C1-symmetric 1,1'-bi-2-naphthols (BINOLs) was reported by Katsuki and co-workers (106) using the $[\text{Fe}(\text{salen})]$ complex (**39**) as an active catalyst (Scheme 89). High yield of cross-coupled product compared to competing homocoupled product, as well as high stereoselectivity proved this method to be advantageous compared to existing stereoselective homocoupling methodologies.

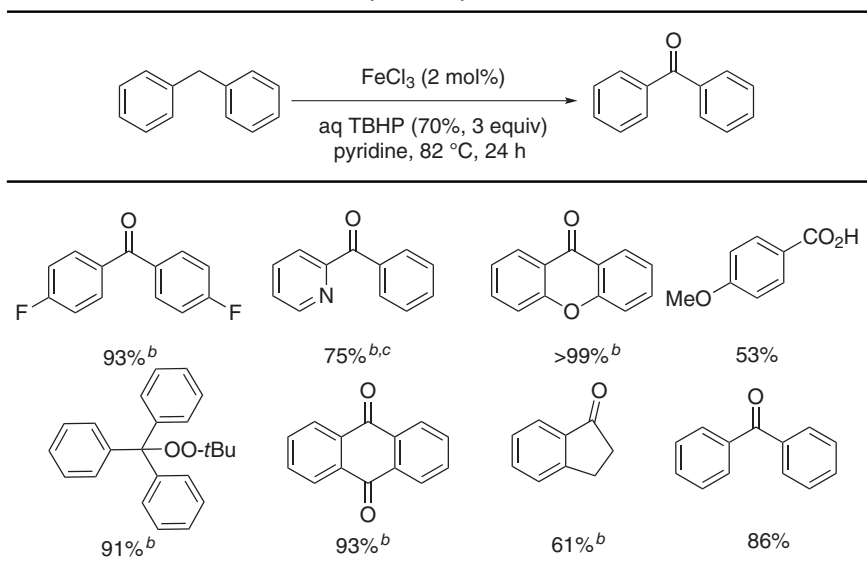
IV. THE C–H BOND OXIDATION

A. Hydroxylation

Various transformations in nature occur via C–H oxidation C–H activation. Different transition metal based enzymes accomplish C–H oxidation via the SET process (107). Most of these enzymes contain “Cu” and “Fe” as a metal cofactor. In organic transformation iron-catalyzed C–H oxidation was reported one century ago, which was summarized as Gif chemistry, Fenton chemistry, and other non-heme mimic systems (108). Recent iron-catalyzed C–H oxidations were mostly focused on sulfide oxidation, epoxidation, and olefin dihydroxylation.

Recent breakthroughs in iron-catalyzed C–H oxidation made this field more fascinating. In 2007, Nakanishi and Bolm (109), developed an efficient protocol for the C–H oxidation of benzylic compounds to their corresponding ketone under mild reaction conditions (109). The protocol was clean and efficient as it used an aqueous of TBHP as an oxidant. This reaction was compatible with various functionalized benzylic compounds (Table XV).

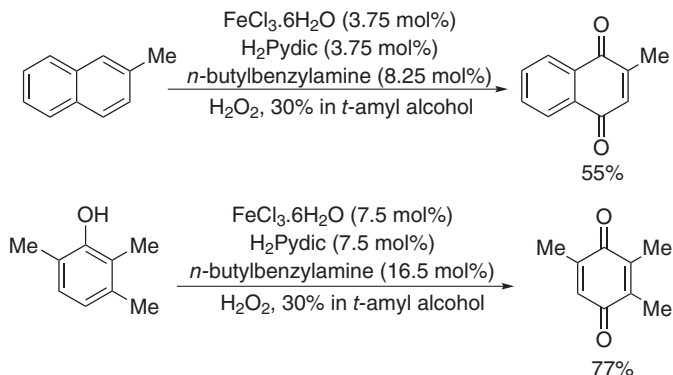
TABLE XV
Iron-Catalyzed Benzylic Oxidation^a



^a The compounds FeCl₃·6H₂O (2 mol%), TBHP (70%) in H₂O (3 equiv), and pyridine, 82 °C, 24 h.

^b All products were identified by comparison of their analytical data with those of previous reports or commercial materials.

^c At 110 °C, TBHP (70%) in H₂O (6 equiv).



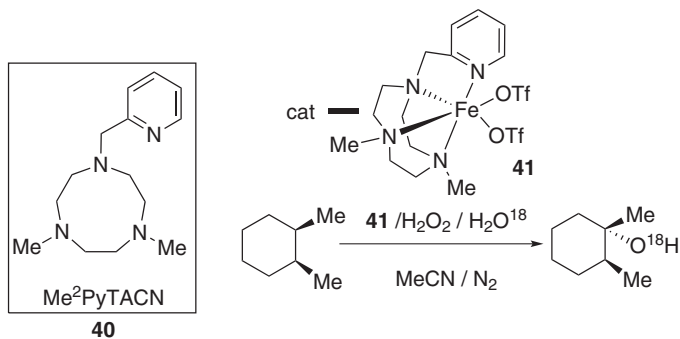
Scheme 90. The C–H hydroxylation by a non-heme iron catalyst.

Interestingly, when 4-methylanisole and diphenylmethanol were tested, corresponding overoxidation products, 4-methoxy benzoic acid and benzophenone, were obtained in high yields. Surprisingly the oxidation of triphenyl afforded *tert*-butyl triphenyl-peroxide in 91% yield instead of the corresponding alcohol product (Table XV).

Later in 2010, Beller and co-workers (110) reported an oxidation protocol for the sp^2 C–H bonds of phenols and arenes with a three-component catalyst system consisting of $\text{FeCl}_3 \cdot 6\text{H}_2\text{O}$, pyridine-2, 6-dicarboxylic acid (H_2pydic), and *n*-butylbenzylamine. A green and nontoxic oxidant H_2O_2 was used (110). Under optimum conditions the oxidation of 2,3,6-trimethylphenol (TMP) and 2-methylnaphthalene gave 77% and 55% isolated yields, respectively (Scheme 90).

Notably, the 2,3,6-trimethylbenzoquinone was the key intermediate for vitamin E synthesis, whereas the oxidation of 2-methyl naphthalene provided menadiione (viz, vitamin K_3 , menanaphthone), which serves as a precursor for the synthesis of various vitamin K derivatives (111).

It was a long-standing goal to develop a highly chemoselective and efficient alkane C–H oxidation by non-heme mimic systems. Recent improvements were more focused on developing synthetic models using a “green” oxidant (e.g., oxygen, air, or some hyperoxides). Que and co-workers (112) significantly contributed to non-heme systems in terms of building a mechanistic frame to understand metal-based C–H hydroxylation in non-heme systems. They reported the selective C–H alkane hydroxylation by the non-heme iron catalyst/ H_2O_2 in 1997. Que and co-workers (113) used multidentate nitrogen-containing ligand TPA [tris(2-pyridylmethyl)amine]. Later on, they developed different types of multidentate nitrogen-containing ligands with a modification in steric and electronic properties. These catalysts showed significantly improved activity toward C–H hydroxylation. Later on, Britovsek and co-workers (114) reported a valuable

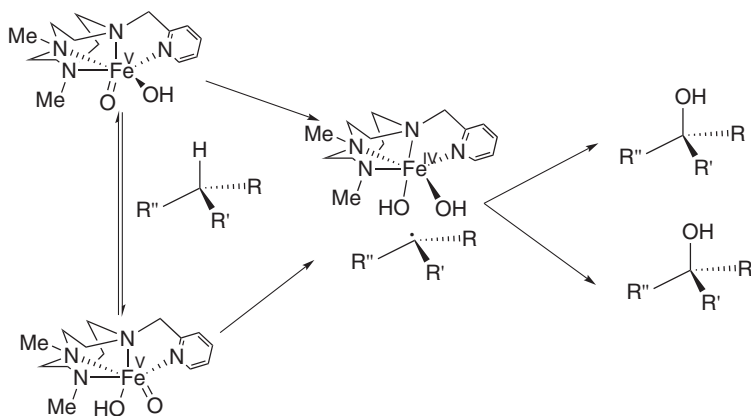


Scheme 91. Mechanism of iron-catalyzed C–O bond formation.

investigation on the synthesis and characterization of tetradentate nitrogen ligands based iron complexes, and their catalytic activity toward C–H oxidation. High-valent iron–oxo species could be accessed in non-heme ligand systems. A mechanistic framework also had been well established for non-heme iron-catalyzed C–H hydroxylation. Other non-heme enzymes (e.g., methane monooxygenase and Rieske dioxygenases) could successfully catalyze the C–H oxidation in nature, which inspired us to develop synthetic models for alkane C–H oxidation (108, 115). Que and Tolman (116) also discussed the critical fundamental principles, which were important for efficacy of their catalyst. Based on these principles great progress had been made toward the development of new ligands–catalysts and their catalytic application for alkane C–H bond oxidation.

Later, Que and co-workers (117) reported another N_4 -tetradentate ligated iron complex $[\text{Fe}^{\text{II}}(\text{CF}_3\text{SO}_3)_2(\text{Me}_2\text{PyTACN})]$, PyTACN = bis(2-pyridylmethyl)-1,4,7-triazacyclononane, with a distorted octahedral center. These complexes showed high catalytic activity for the oxidation of cyclohexane, as well as other tertiary C–H bonds of *cis*-1,2-dimethylcyclohexane, adamantane, and 2,3-dimethylbutane (Scheme 91).

The high levels of H_2O^{18} incorporations were obtained from the H_2O^{18} labeling experiment during the oxidation of alkanes with tertiary C–H bonds [e.g., adamantane (74%), *cis*-dimethylcyclohexane (*cis*-DMCH, 79%), and 2, 3-dimethylbutane (76%)] the % of O^{18} incorporations were denoted in the first brackets. The results were independent of the substrate concentration, which suggested that the $\text{OH}-\text{Fe}^{\text{V}}=\text{O}$ species was the only key oxidant toward alkane oxidation with iron complex $[\text{Fe}^{\text{II}}(\text{CF}_3\text{SO}_3)_2(\text{Me}_2\text{PyTACN})]$ (**41**). Obviously this oxidation process was significantly different from the $\text{Fe}(\text{TPA})$ complex [TPA = tris(2-pyridylmethyl) amine]. The new results were explained by an unusual rebound-like mechanism (Scheme 92). Notably, *cis* configuration of the two hydroxy groups in this catalytic system were also different from the stereo requirement of the *trans* configuration in



Scheme 92. Sets of iron complexes with TACN backbone ligands.

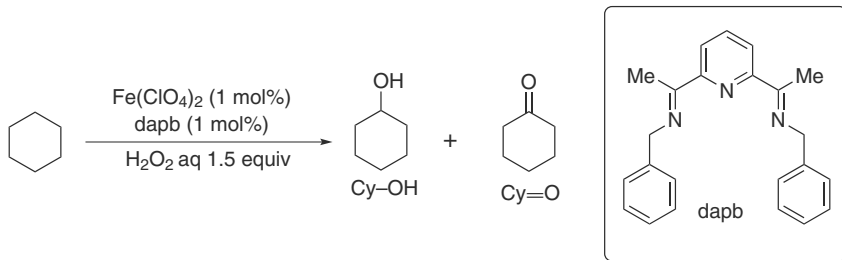
heme complexes and it was a unique feature in these non-heme iron catalytic systems.

Costas and co-workers (118) explored the iron complexes of the tetradentate ligand Me_2TACN to a “TACN” family, which had a common methylpyridine derived triazacyclononane (TACN) backbone (Scheme 92). These new families of iron complexes show unprecedented efficiency in the stereospecific oxidation of alkane C–H bonds and also dihydroxylation or epoxydation of alkenes.

In 2008, Reedijk and co-workers (119) described a simpler and more efficient method for oxidation of cyclohexane (CyH) by using a catalytic amount of iron salts $\text{Fe}(\text{ClO}_4)_2$ in acetonitrile and hydrogen peroxide as oxidant under mild conditions. The oxidation protocol afforded both cyclohexanol and cyclohexanone as a product (Scheme 93). Interestingly when the simple tridentate 2,6-bis[1-(benzylamino)ethyl]pyridine (dapb) was used in the reaction, the selectivity toward major products increased slightly.

Later in 2007, Chen and White (120) reported a selective aliphatic C–H oxidation by using the Fe(PDP) complex (**42**) [PDP=2-((S)-2-[(S)-1-(pyridin-2-ylmethyl)pyrrolidin-2-yl]pyrrolidin-1-yl)methyl]pyridine]. The rigid backbone of the PDP ligand in complex **42** (Scheme 94) played a vital role for selectivity in C–H hydroxylation (120).

The process was simple and clean. The electron-rich C–H bonds were selectively oxidized in the presence of electron-deficient C–H bonds, for example, the tertiary sp^3 C–H bond was preferentially oxidized over primary and secondary C–H bonds (Scheme 94). The presence of electron-withdrawing group on α or β to the carbon of the C–H bonds decreases the reactivity. Hence, the presence of electron-withdrawing groups (e.g., carbonyl, ester, acetate, and

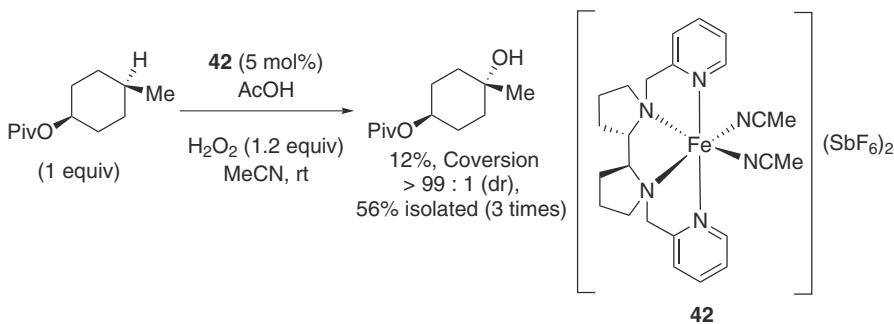


Entry	Catalyst	Major Products	Desired Product (%)	Byproducts (%)
1	With ligand	Cy-OH(37) : Cy=O(54)	91	9
2	Without ligand	Cy-OH(27): Cy=O(64)	87	13

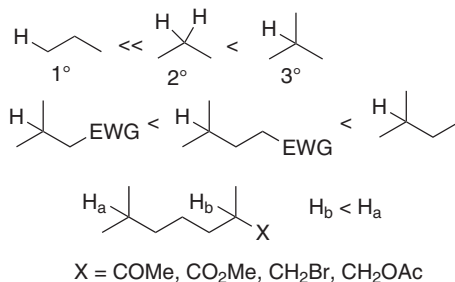
Scheme 93. Iron-catalyzed C–H oxidation of cyclohexane with and without ligand (Cy = cyclohexyl).

halogen functional groups) provided a better selectivity. The tertiary C–H bonds remote to these groups showed a much better reactivity (Scheme 95).

Based on the stereoselectivity outcome of these iron-catalyzed C–H oxidations, a concerted mechanism mediated by an electrophilic oxidant can be visualized. Further they applied their method to complex molecules like a natural product (+)-artemisinin in which the oxidation occur at the most electron-rich and least sterically hindered site. In some cases, these iron-catalyzed methods were high yielding and the reaction completed quickly compared to the enzymatic reaction (Scheme 96a).

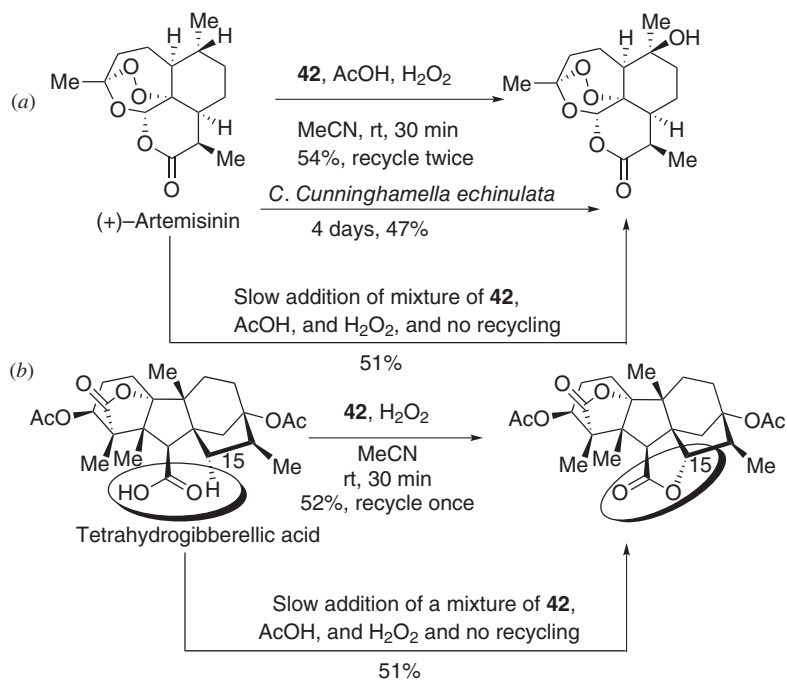


Scheme 94. Iron-catalyzed hydroxylation of unactivated sp^3 C–H bonds (Piv = pivaloyl)



Scheme 95. Reactivity pattern of different types of C–H bonds.

The presence of a carboxylic group acted as a directing group where the above discussed selectivity principle did not work. It generally formed lactone as the major product. For example, the tetrahydrogibberillic acid analogue under their reaction protocol produced lactone in 52% yield. Subsequently, a slow addition protocol was reported (121). Under a slow addition protocol, the reaction provided high conversion without decrease in site selectivity (Scheme 96b). This method



Scheme 96. Application of iron-catalyzed aliphatic C–H hydroxylation.

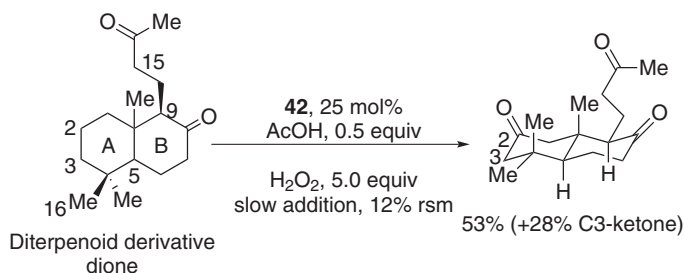
was applied in various diversified natural products, which showed a promising role in drug discovery.

Inspired by the initial success of developing a versatile method of iron-catalyzed sp^3 C–H hydroxylation, Chen and White (122) further explored their method with a new class of substrates, where a combined effect plays an important role for oxidation of secondary sp^3 C–H bonds (122). Clearly, a secondary C–H bond has less electron density compared to a tertiary C–H bond, but a secondary C–H bond has a higher steric accessibility than a tertiary C–H bond. Furthermore, secondary C–H bonds were present in the ring system (e.g., cyclohexane and decahydronaphthalene derivatives), where the combined effects were well pronounced in terms of their reactivity and selectivity. Contextually, the selective oxidation by a combined effect might provide a very useful method for methylene functionalization. Electronic, steric, stereoelectronic, and functional groups could determine the selectivity of C–H oxidation.

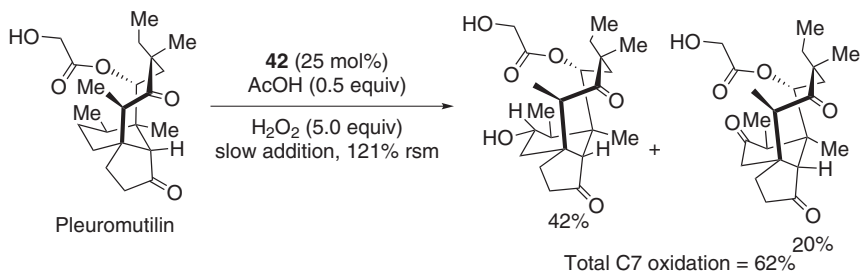
The diterpenoid-derived dione with 14 secondary C–H bonds and two tertiary C–H bonds were tested under optimum reaction conditions (Scheme 97). Based on selectivity principles, two tertiary C–H bonds were electronically and sterically deactivated due to the electron-withdrawing carbonyl group. The side chain and the B ring are electronically deactivated due to the presence of an electron-withdrawing carbonyl group. The C2 position in the A ring was the least bulky site, which was expected to be the most activated C–H bond in this case and the results from the reaction were also consistent with the prediction. The C2 oxidation product was obtained in 53% isolated yield and the C3 oxidation product in 28% yield, whereas 12% starting material was recovered.

Their method functioned well with a complex pleuromutilin derivative (Scheme 98). Dihydropleuromutilin derivative gave a C7 equatorial C–H bond hydroxylation product along with other oxidized products.

In 2009, Costas and co-workers (123) reported iron-catalyzed C–H oxidation with a different ligand backbone that afforded good regioselectivity with better



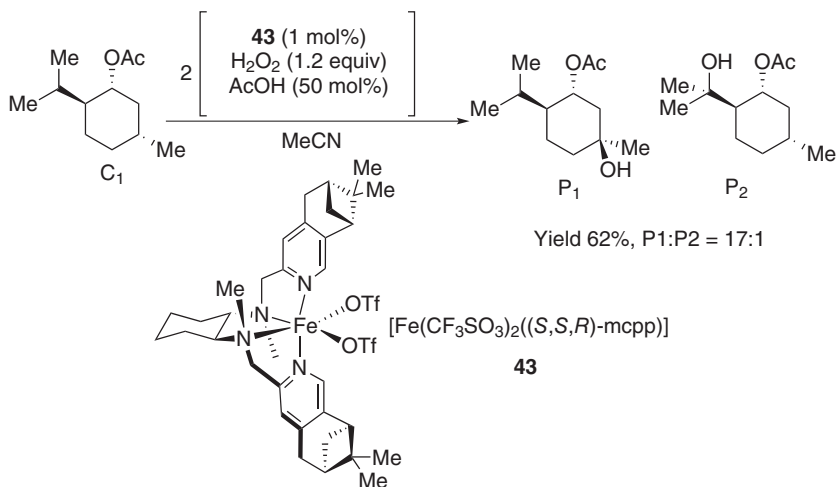
Scheme 97. Role of the combined effect toward high selectivity for secondary C–H bond hydroxylation (RSM = recovered starting material).



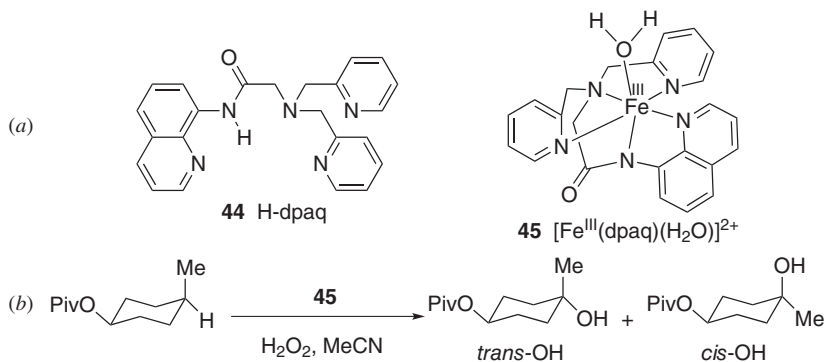
Scheme 98. Role of a combined effect toward the high diastereoselectivity of methylene oxidation.

yield (Scheme 99). Bulky hydrocarbon groups were introduced at the remote position of the pyridine ring, which helped to form a robust cavity. The iron complex $[\text{Fe}(\text{CF}_3\text{SO}_3)_2(\text{S,S,R})\text{-mcpp}]$ (**43**, mcpp = N1,N2-dimethyl-N1,N2-bis(pyridin-2-ylmethyl)cyclohexane-1,2-diamine) provided better selectivity and efficiency compared to White's catalyst. Costas's catalyst (**43**) with a much lower catalyst loading (1 mol%) accomplished the hydroxylation of (–)-acetoxyp-menthane preferentially at a more accessible (C1)–H bond. In this case, both electronic and steric factors played an important role in distinguishing different C–H bonds.

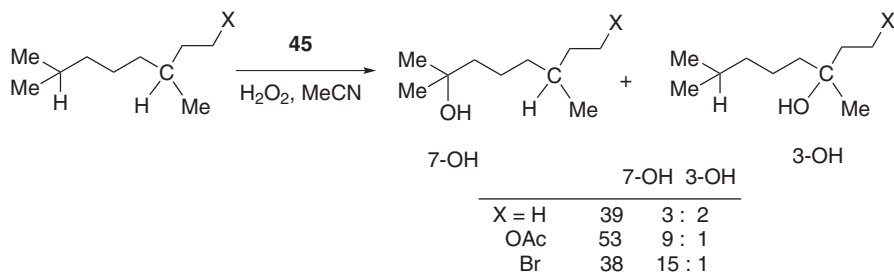
In 2012, Kodera and co-workers (124) reported another alternative protocol for an alkane C–H hydroxylation with a different type of iron complex (**45**) [iron(III)–monoamidate complex] as a catalyst and H_2O_2 as the oxidant. In the regioselective hydroxylation of *cis*-4-methylcyclohexyl-1-pivalate, catalyst **45** (Scheme 100a)



Scheme 99. Regiospecific hydroxylation by a robust non-heme iron catalyst.



Scheme 100. Regiospecific hydroxylation by an iron(III)–monoamidate complex [dpaq = 2-(bispyridin-2-ylmethylamino)-*N*-(quinolin-8-yl)acetamide] (**45**).



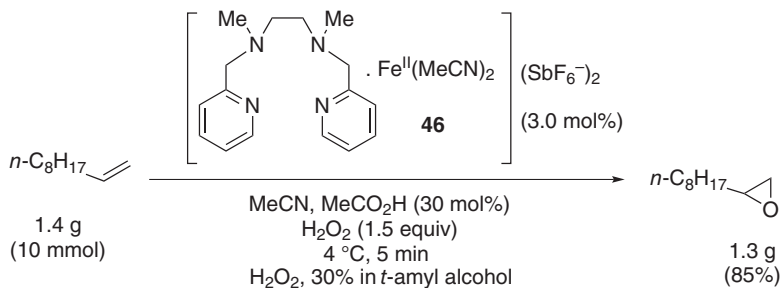
Scheme 101. Regiospecific hydroxylation by an iron(III)–monoamidate complex (**45**).

gave better selectivity (94% retention of configuration in 38% yield) in the formation of the *trans*-OH product compared to White and Costas's catalysts, but the yield was comparable to the White catalyst and lower than Costas catalyst (Scheme 100b).

The hydroxylation of 1-substituted 3,7-dimethyloctane with Kodera's catalyst provided better yields and selectivity compared to others. Preferential formation of 7-OH product over 3-OH (Scheme 101) is consistent with the selectivity rule discussed above. Unlike White and Costas catalyst, no *cis* labile position is available in Kodera's catalyst and acetic acid is not required for catalytic activity.

B. Epoxidation

Epoxides are an important class of compounds often used as the key precursors for synthesis of various drugs and natural products (125). Sharpless epoxidation of



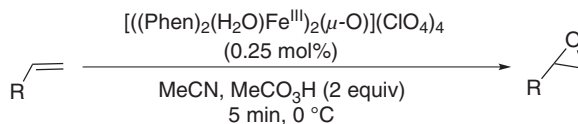
Scheme 102. Iron-catalyzed epoxidation

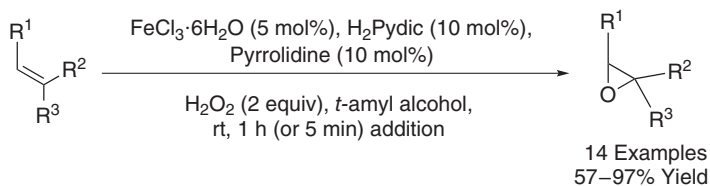
allylic alcohol and Katsuki–Jacobsen asymmetric epoxidation are historically significant in the development of epoxidation chemistry (126). First, iron-catalyzed epoxidation was reported in 2001 by Jacobsen and co-workers (127) with Fe–mep (**46**) in the presence of a catalytic amount of acetic acid (Scheme 102). Acetic acid plays a key role in order to form an iron- μ -oxo carboxylate bridged iron complex, which was most likely to be the active species as proposed by Jacobsen and co-workers (127).

Later on, Stack and co-workers (128) reported epoxidation by an μ -oxo-iron(III) dimer, $[\text{((Phen)}_2(\text{H}_2\text{O})\text{Fe}^{\text{III}})_2(\mu\text{-O})](\text{ClO}_4)_4$ in the presence of peracetic acid as the terminal oxidant. Their method can tolerate a wide range of alkenes including terminal alkenes (Scheme 103).

In 2002, Que and co-workers (129) developed a non-heme iron catalysts, $[\text{Fe}^{\text{II}}(5\text{-Me}_3\text{-TPA})(\text{MeCN})_2](\text{ClO}_4)_2$ and $[\text{Fe}^{\text{II}}(\text{bpmen})(\text{MeCN})_2](\text{SbF}_6)_2$, where bpmen = *N,N'*-dimethyl-*N,N'*-bis(pyridin-2-ylmethyl)ethane-1,2-diamine, for epoxidation of alkenes under neutral conditions. But in these cases, cis-diols were obtained as the major product and epoxides as minor products. Interestingly, the introduction of acetic acid as an additive suppressed the formation of cis-diols and provided epoxides as the major product. A high-valent iron oxo was proposed to be the active species for this reactions (130).

In this field, the major breakthrough came from Beller and co-workers (131) in 2007. They developed epoxidation using $\text{FeCl}_3 \cdot 6\text{H}_2\text{O}$ in combination with pyridine-2,6-dicarboxylic acid and pyrrolidine in the presence of H_2O_2 as the terminal

Scheme 103. Iron- μ -oxo carboxylate-bridged complex-catalyzed epoxidation.

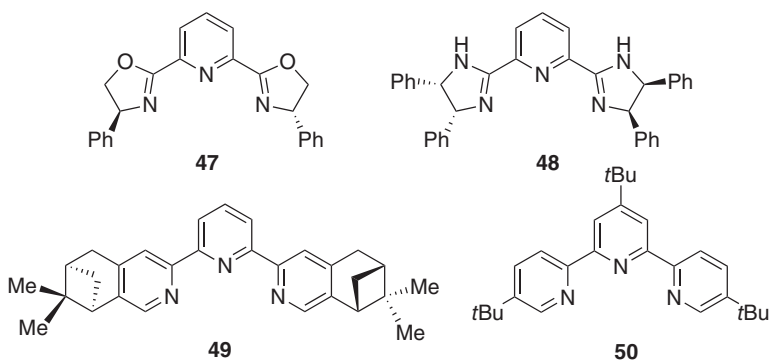
Scheme 104. The $\text{FeCl}_3 \cdot 6\text{H}_2\text{O}$ catalyzed epoxidation.

oxidant (Scheme 104). Aromatic olefins and 1,3-cyclooctadiene gave moderate-to-excellent yields under their standard reaction protocol.

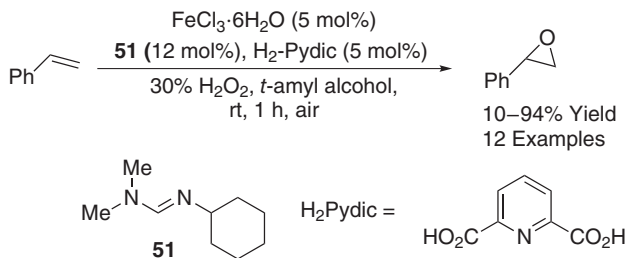
Later on, Beller and co-workers (132) developed a method, that could generate epoxides from both aliphatic and aromatic alkenes. Iron complexes in combination with various nitrogenous ligands (**47–50**) (Scheme 105) provided epoxides with good selectivity.

The formation of a red precipitate was observed under reaction conditions. From mass spectrometry analysis of the filtrate, it was found that the pybox ligand (**47**) decomposes into H_2Pydic and phenyl glycerol. After filtration, both the residue and filtrate showed similar reactivity, which implied that the filtrate contained decomposed ligand as well as iron (10). Based on these observations, they further optimized the iron source, H_2Pydic derivatives, and amine ligands in order to get better conditions.

Later they reported a few modified methods using different nitrogenous ligands (133). With formamidines (**51**) as ligands, they developed epoxidation for aromatic olefins and 1,3-dienes. Notably, both aromatic and aliphatic alkenes were tolerated with good selectivity (Scheme 106).

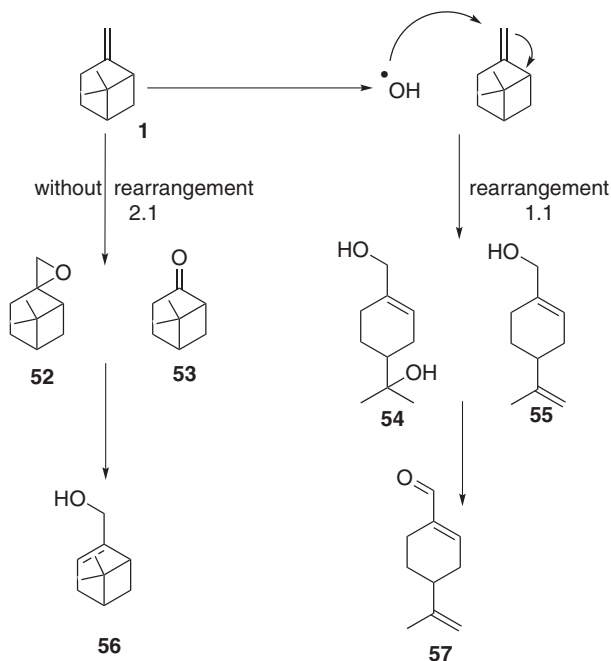


Scheme 105. Different ligands used in epoxidation.



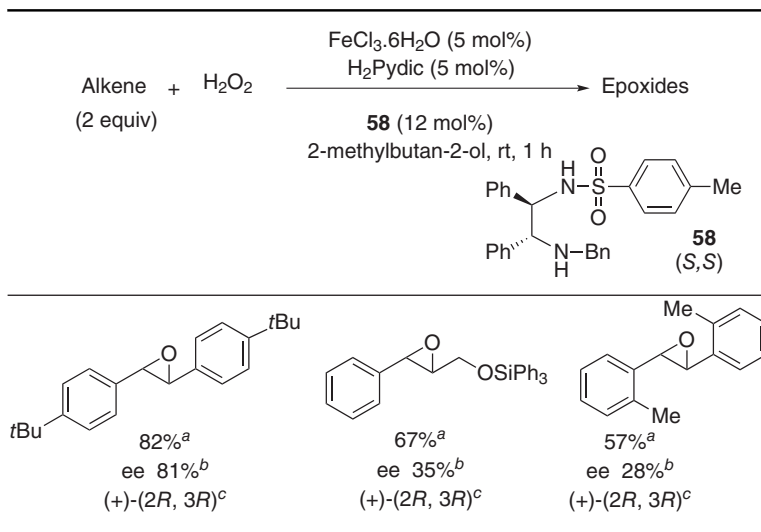
Scheme 106.

Control experiments with a radical inhibitor like TEMPO, butylphenylnitron (BPN), and duroquinone suppressed the product yield greatly. Notably, the presence of 1 equiv of TEMPO in their standard reaction stopped the reaction completely. A further control experiment with β -pinene as substrate gave the rearrangement products (**56** and **55**), which were in accord with the radical mechanism (Scheme 107). In 2012, Kozak and co-workers (134) developed



Scheme 107.

TABLE XVI
Iron-Catalyzed Asymmetric Epoxidation



^a Yield of isolated product.

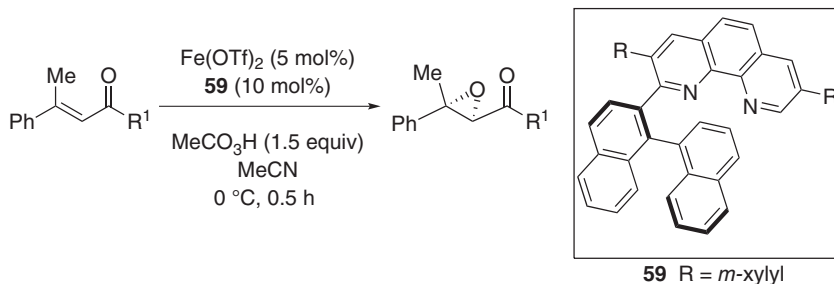
^b Assigned by comparing the retention times of enantiomer.

^c Determined by high-performance liquid chromatography (HPLC) on chiral columns by comparing the sign of the optical rotation.

epoxidation methods using *N*-methylimidazole as the organic base in acetone. Although their method showed poor selectivity for styrene, better selectivity was observed for larger alkenes.

First, the iron-catalyzed method for asymmetric epoxidation was reported by Que and co-workers (129) using $[\text{Fe}(\text{bpmcn})(\text{CF}_3\text{SO}_3)_2]$ (bpmcn = *N,N'*-bis(2-pyridylmethyl)-*N,N'*-dimethyl-1,2-cyclohexanediamine ligand). While studying the dihydroxylation of *trans*-2-heptene with H_2O_2 as oxidant, 12% ee for the epoxide byproduct was observed. In 2007, Beller and co-workers (135) developed an efficient method for iron-catalyzed asymmetric epoxidation using H_2O_2 as oxidant in the presence of a chiral sulfoxamide ligand (**58**). Various internal alkenes were tolerated under this protocol with good-to-excellent enantioselectivity (Table XVI).

In 2011, Beller and co-workers (136) reported epoxidation using molecular O_2 as oxidant, which showed high reactivity as well as selectivity in the presence of β -keto ester and imidazole as additives. Nishikawa and Yamamoto (137) developed asymmetric epoxidation for β,β -disubstituted enones by using $\text{Fe}(\text{OTf})_2$ with a chiral phenanthroline ligand (**59**) in the presence of peracetic acid as the terminal oxidant (Scheme 108). The reaction protocol provided epoxides of enones with high enantioselectivity (up to 92% ee).

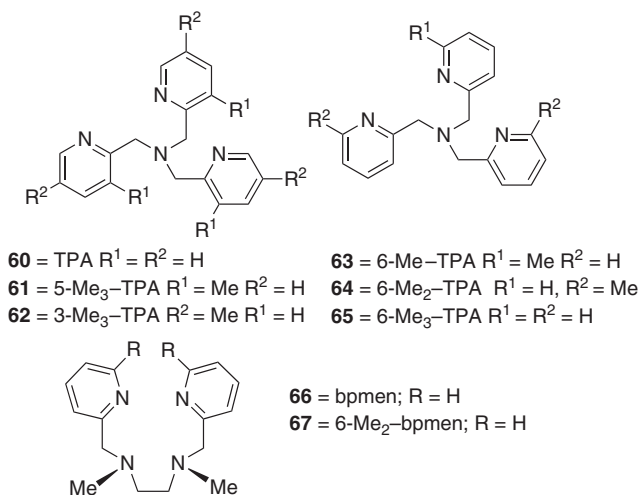


Scheme 108.

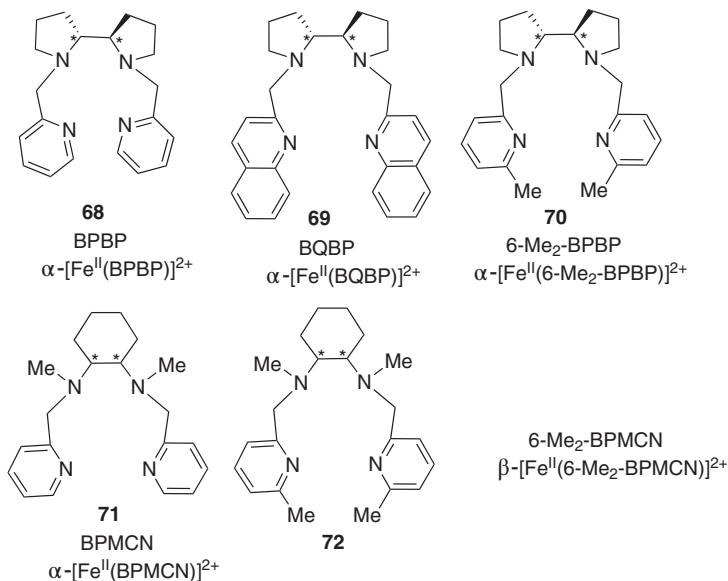
C. cis-Dihydroxylation

In nature, Riesky dioxygenases carry out dihydroxylation where iron is a metal cofactor (138). Inspired from nature, Que and co-workers (129) in 2002 developed the first iron-catalyzed synthetic non-heme systems for alkene dihydroxylation. They synthesized iron(II) complexes of the TPA family of ligands **60–65** (Scheme 109) and performed cis-dihydroxylation of 1-octene in MeCN using H₂O₂ as the terminal oxidant. Among these, TPA (**60**), TPA-5-Me₃ (**61**), and TPA-3-Me₃ (**62**) iron complexes gave 69–87% yield of the cis-dihydroxylation product. Minor amounts of epoxides were obtained as the byproduct.

Later on, they reported an asymmetric version of this cis-dihydroxylation reaction by using a chiral ligand backbone (Scheme 110) [1,1'-Bis(pyridin-2-



Scheme 109.



Scheme 110.

ylmethyl)2,2'-bipyrrolidine (BPBP); 1,1'-bis(quinolin-2-ylmethyl)-2,2'-bipyrrolidine (BQBP); *N,N'*-bis(2-pyridyl-methyl)-*N,N'*-dimethyl-1,2-cyclohexanediamine (BPMCN)] (139).

Among these sets of iron complexes (**68–72**), catalyst **70** was the most effective (97% ee) (Table XVII). Note that in all these cases there was a competition between epoxidation and cis-diol product formation.

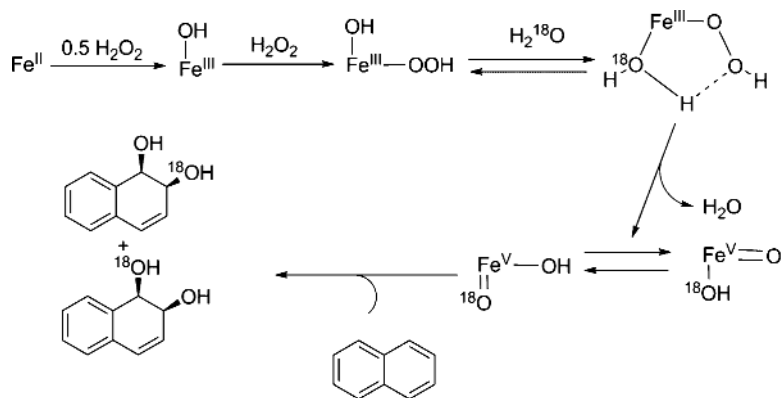
TABLE XVII
Asymmetric cis-Dihydroxylation of Olefins^a

Catalyst	Substrate	cis-Diol (%ee) ^b	Diol/Epoxide
68	<i>trans</i> -2-Heptene	38 (3)	1:4.6
69	<i>trans</i> -2-Heptene	78(3)	4:1
70	<i>trans</i> -2-Heptene	97(1)	26:1
70	<i>trans</i> -4-Octene	96(1)	13:1
70	1-Octene	76(1)	64:1
71	<i>trans</i> -2-Heptene	29	1:18
72^c	<i>trans</i> -2-Heptene	79	3.2:1

^a Reaction conditions: A 70-mm solution of H₂O₂ (10 equiv) in MeCN was delivered by syringe pump over a period of 20 min to a degassed and stirred solution of catalyst (0.7-mm) and substrate (0.35 m) at ambient temperature in air for **68** and **69** and under an Ar atmosphere for **70**.

^b Percent of ee of the predominant diol isomer.

^c Results were normalized to 10 equiv H₂O₂.



Scheme 111.

Later, in 2009 Que and co-workers (140) reported cis-dihydroxylation of the aromatic double bond of naphthalene using H₂O₂ as oxidant. Such a reaction mimics the activities of naphthalene dioxygenases. In order to establish the mechanism, they carried out an ¹⁸O labeling experiment. In the presence of either 10 equiv of 2% H₂¹⁸O₂ (100 equiv H₂O per H₂¹⁸O₂) or 10 equiv H₂O₂ and 1000 equiv H₂¹⁸O as oxidant > 90% singly labeled diol product was observed. This control experiment indicated that one O atom in cis-dihydroxylated product came from H₂O and another came from H₂O₂ (Scheme 111).

V. CROSS-COUPLING REACTIONS

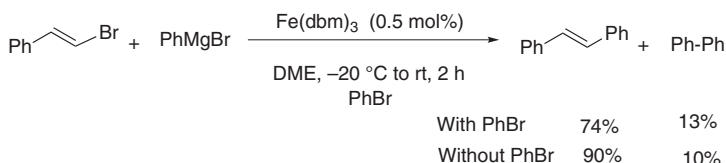
Metal-assisted cross-coupling reactions had gained immense importance toward the formation of C–C, C–X bonds over the last three to four decades due to their application in the synthesis of key precursors of various natural products and pharmaceuticals (141). In this context, iron-catalyzed coupling reactions are important, as most of the iron salts are environmentally benign and less expensive compared to the late transition metals that were well known for cross-coupling reactions (142). Nickel and palladium catalyzed cross-coupling reactions involving a wide range of organometallic reagents and organic electrophiles were widely studied (143). In 1972, Corriu and Masse (144a) Kumada and co-workers (144b) independently reported nickel-catalyzed coupling of Grignard reagents with alkenyl and aryl halides. However, iron-catalyzed coupling reaction of alkyl magnesium reagents with vinyl bromide was reported prior to 1972 (145). Following this work, iron sources were applied as catalyst for the cross-coupling reactions involving various coupling partners that were discussed in this subsection.

A. Alkenyl Derivatives as Coupling Partners

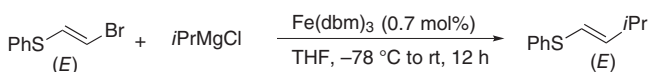
After Kochi's pioneering work, $\text{Fe}(\text{dbm})_3$ catalyzed cross-coupling between phenyl magnesium bromide and β -styrene bromide in bromobenzene was reported. The reaction showed selectivity toward the vinyl derivative yielding *trans*-stilbene and a trace amount of homocoupled biphenyl [Scheme 112, DME = dimethoxyethane, dbm = dibenzoylmethane (ligand)] (146). Bromothiophenes were also used as coupling partner with *i*PrMgCl, affording stereospecific *trans*- product in contrast to nickel- or palladium-catalyzed reactions where a mixture of isomers was observed (Scheme 113) (147).

Vinyl sulfones could be tolerated as electrophiles under these reaction conditions. However, they gave a mixture of (*E,Z*) isomers. The 1,4-addition product and reduction compounds were obtained as a byproduct (148). This methodology was applied in the synthesis of natural product pheromones (Scheme 114). Notably this reaction provided an olefin compound in the presence of *n*BuLi (149).

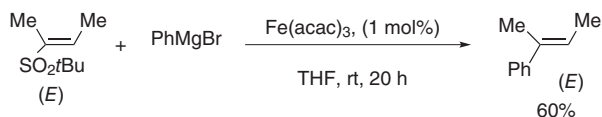
High selectivity (92% retention of configuration) was obtained when MeLi was used as the transmetalating agent (Scheme 115) (150).



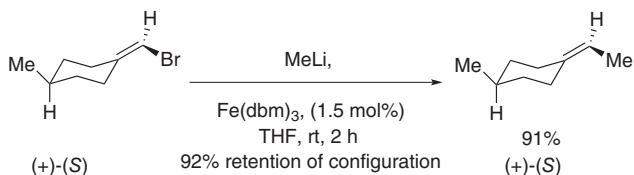
Scheme 112.



Scheme 113.

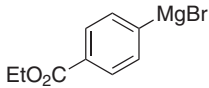
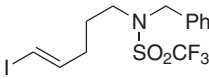
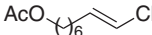
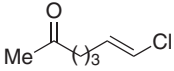
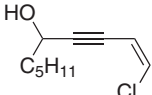
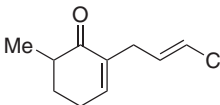
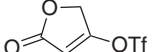
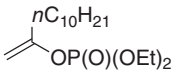
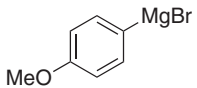



Scheme 114.



Scheme 115.

TABLE XVIII
Iron-Catalyzed Cross-Coupling Reactions of Grignard^a or Organomanganese^b
Reagents (RMX) With Alkenyl Halides (R'X)

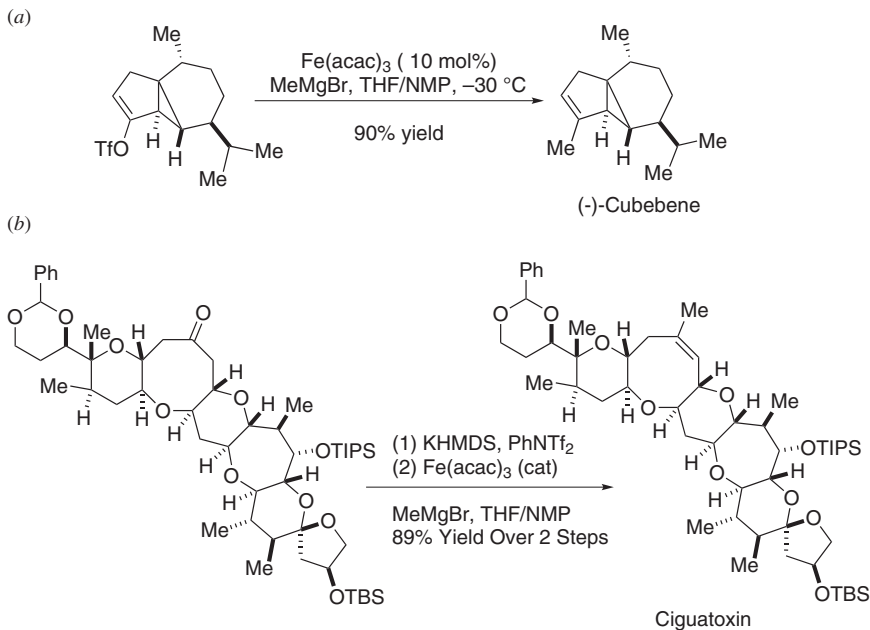
$\text{RMX} + \text{R}'\text{X} \xrightarrow{\text{Fe}(\text{acac})_3 \text{ cat}} \text{R}-\text{R}'$			
Entry	RMX	R'X	R-R' Yield (%)
1			69
2	<i>i</i> PrMgBr		72
3	<i>n</i> -BuMgBr		80
4 ^c	<i>c</i> -C ₆ H ₁₁ MgBr		82
5	<i>n</i> -BuMnCl		72
6	MeMgBr		70
7	<i>n</i> -BuMgBr		78
8			68

^aReactions performed with RMgBr (1.4 equiv) and Fe(acac)₃ (5 mol%) at -20 °C for 15 min in THF/NMP or at -5 °C for 15 min.

^bReaction performed with *n*-BuMnCl (1.4 equiv) and Fe(acac)₃ (3 mol%) in THF at rt 1 h (entry 6).

^cUsed 3 equiv of RMgBr.

Cahiez and co-workers (151) contributed significantly to improve the scope of an iron-catalyzed cross-coupling reaction by utilizing functionalized aryl Grignard reagents and vinyl halides (Table XVIII). Use of *N*-methylpyridine (NMP) as the solvent additive to THF dramatically increased the yield of the



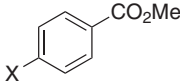
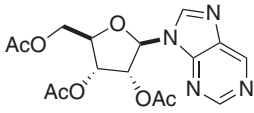
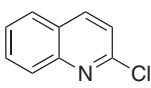
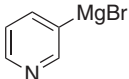
Scheme 116. Alkenyl triflate cross-coupling reactions in total synthesis [PhNTf₂ = *N*-phenyl-bis(trifluoromethanesulfonamide); TBS = *tert*-butyldimethylsilyl; TIPS = triisopropylsilyl; KHMDS = potassium bis(trimethylsilyl)amide].

cross-coupled product from 5 to 80%. Organomanganese reagents were tolerated as a coupling partner when Fe(acac)₃ was used as the catalyst (152). Different alkenyl derivatives (e.g., alkenyl sulfones, sulfides, phosphates, triflates, esters, ketones, enones, carbamates, and acetals) were well tolerated (151b, 153). These protocols were applied for the total synthesis of ciguatoxin(–)-cubebene (Scheme 116) and enantiopure bicyclic diene ligands (154). Notably, in these cases better yields were observed with iron compared to the Ni/Pd system (154b).

B. Aryl Derivatives as Coupling Partners

Application of iron-based organometallic compounds as a precatalyst in a cross-coupling reaction was explored by Fürstner and Leitner (155) (Table XIX). They used aryl halides in the presence of different iron sources (5 mol%, as a precatalyst), such as Fe(acac)₃, Fe(salen)Cl under mild reaction conditions (rt to –30 °C and < 1-h reaction time). Organomanganese, zinc, and magnesium derivatives

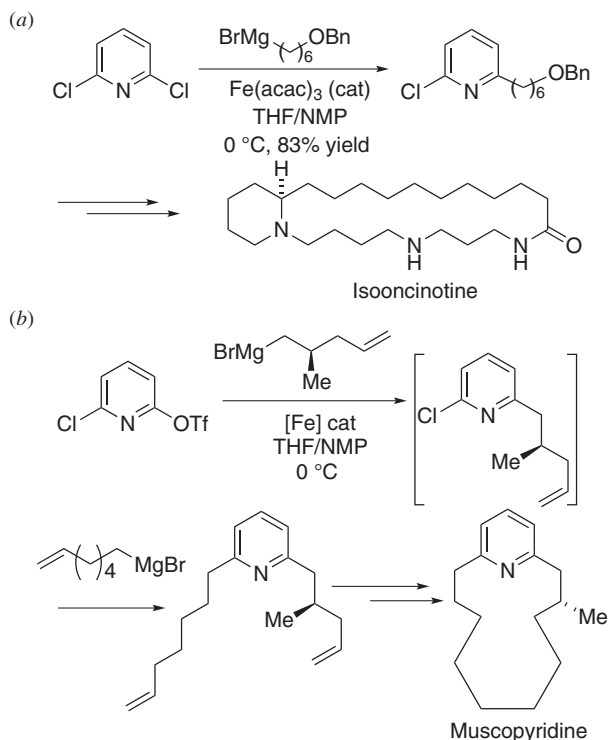
TABLE XIX
 Cross-Coupling Reactions of Organometallic Reagents (RMX) With Ar-X^a

Entry	Ar-X	RMX	Yield (%) of Product Ar-R
1		<i>n</i> -C ₆ H ₁₃ MgBr	83 (X = OTS)
2		Et ₃ ZnMgBr	93
3		C ₁₄ H ₂₉ MnCl	96
4		(C ₁₄ H ₂₉) ₂ MnCl	98
5		(C ₁₄ H ₂₉) ₂ MnMgCl	98
6		<i>n</i> -C ₄ H ₉ Li	0
7		<i>n</i> -C ₁₄ H ₂₉ MgBr	72
8		PhMgBr	71
9			63

^aReactions performed with RM (1.2–2.3 equiv) and Fe(acac)₃ (5 mol%) at 0 °C or at rt in THF/NMP for 10 min (Entries 1–6) or in THF at –30 °C for 1 h (Entries 7–9).

(both alkyl and aryl) were well tolerated, but no product was obtained in the case of organolithium derivatives. Aryl triflates, tosylates, and unactivated aryl derivatives (e.g., pyridines) were also compatible as electrophiles under these reaction conditions. Reaction in a THF/NMP mixture as solvent was completed within 15 min. The reaction was susceptible to steric effects as ortho substituted arenes gave a lower yield compared to para substituted arenes. Interestingly, selective monosubstitution was observed in the presence of more than one halide in the electrophile (153b). Unfortunately, the reaction suffered from the homocoupling of an aryl Grignard reagent, and is limited to only electron-deficient haloarenes.

The reaction protocol was applied in the synthesis of the intermediate of the immunosuppressive agent FTY720 (156). This method was applied in the total synthesis of spermidine alkaloid (–)-isooncinotine (Scheme 117a) and the olfactory macrocycle (+)-muscopyridine (Scheme 117b) (157, 158).

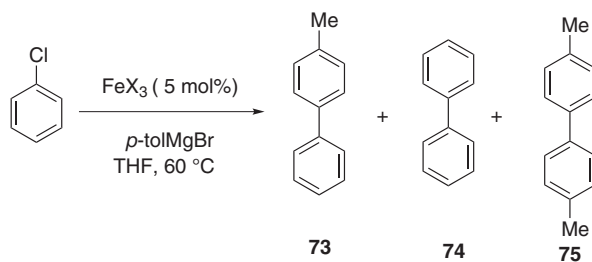


Scheme 117. Aryl electrophiles's cross-coupling reactions in total synthesis.

In 2007, Hatakeyama and Nakamura (159) reported that the presence of FeF_3 in combination with an *N*-heterocyclic carbene as ligand greatly reduced homocoupling of Grignard reagent (Scheme 118a). Nakamura's method was used by Hocek and Dvorakova (160) in regioselective monomethylation at the 6-position of 2,6-dichloropyridines, with MeMgCl , without any modification. In 2009, Lamaty and co-workers (161) reported both the alkylation and arylation of 4-chloro-pyrrolo[3,2-*c*]quinoline in the presence of a catalytic amount of iron salts (Scheme 118b).

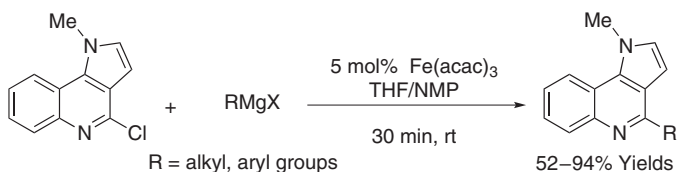
In 2012, Garg and co-workers (162) reported alkylation of aryl sulfamates and carbamates using iron catalysts and described the $\text{C}_{\text{sp}^2}\text{-C}_{\text{sp}^3}$ bond formation. Sulfamate and carbamate functional groups could be used as directing groups for various synthetic transformations in iron-catalyzed cross-couplings due to their high stability, easy availability, and low reactivity toward conventional $\text{Pd}(0)$ catalyzed methods (Scheme 119a). Recently, Knochel and co-workers (163) developed iron-catalyzed $\text{sp}^2\text{-sp}^2$ cross-coupling between *N*-heterocyclic chlorides/bromides and arylmagnesium reagents (Scheme 119b).

(a)



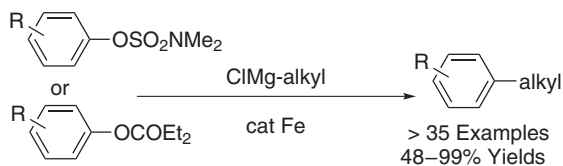
Entry	FeX ₃	L (mol %)	73:74:75
1	FeF ₃ ·3H ₂ O	SIPr·HCl (15)	98:<1:4
2	FeF ₃ ·3H ₂ O	–	6:trace:4
3	FeCl ₃	SIPr·HCl (15)	32:2:32
4	FeCl ₃	KF (20) SIPr·HCl (15)	92:1:8

(b)

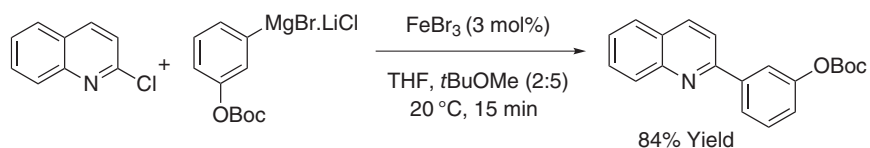


Scheme 118. In this scheme SIPr = 1,3-bis(2,6-disopropylphenyl)-imidazolidinium.

(a)



(b)



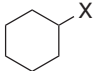
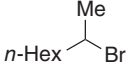

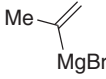
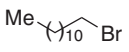
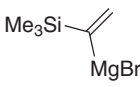
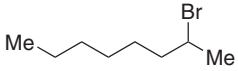
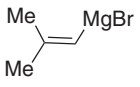
Scheme 119.

C. Alkyl Derivatives as Coupling Partners

Alkyl halides are traditionally challenging substrates for cross-coupling reactions due to their high-energy barrier in oxidative addition and favorable β -hydride elimination (164). Some early examples of iron-catalyzed cross-coupling were reported with alkyl halides, but these reactions suffered from homocoupling and conversion of the alkyl halide to the corresponding alkenes and alkanes (165). Efficient iron-catalyzed cross-coupling by using Grignard reagent and alkyl halide was reported by Nakamura et al. (166) (method A, Table XX). Iron(III) chloride (5 mol%) was used as catalyst in the presence of TMEDA (Scheme 120a, entry 3).

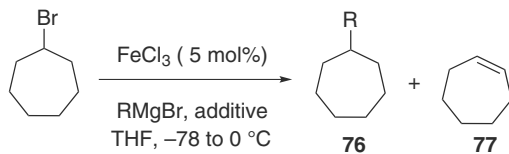
Nagano and Hayashi (167) used $\text{Fe}(\text{acac})_3$ for the same reaction using Et_2O under reflux conditions (method B). Use of solvent combination THF/NMP played a key role in the observed selectivity. In 2007, Cosy and co-workers (168a) (method C) and Cahiez and co-workers (168b) (method D) explored the scope of this reaction by using different alkyl halides as well as different alkenyl Grignard

TABLE XX
Cross-Coupling Reactions of Alkyl Halides (RX) With ArMgBr

Entry	R-X	ArMgBr	Method ^a	Yield (%)
1		Ph	A	99 (X = I, Br, Cl)
2	<i>n</i> -oct-X	Ph	A	91 (X = Br) 45 (X = Cl)
3		<i>p</i> -toyl	B	73 97 (X = 1)
4			C	80
5			C	6:2:2 (86)
6			D	72

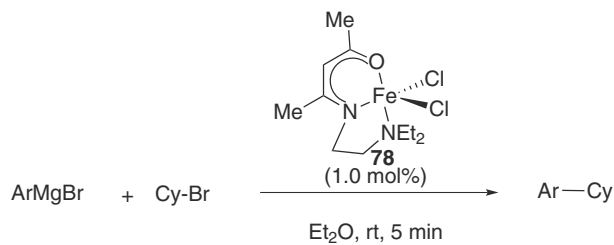
^a Method A: FeCl_3 (5 mol%), RX (1 equiv), ArMgBr (1.2 equiv, slow addition), and TMEDA (1.2 equiv, slow addition), in THF (-78 to 0°C), 0.5 h. Method B: $\text{Fe}(\text{acac})_3$ (5 mol%), RX (1 equiv), and ArMgBr (1.04 equiv) in refluxing Et_2O , 0.5 h.

(a)

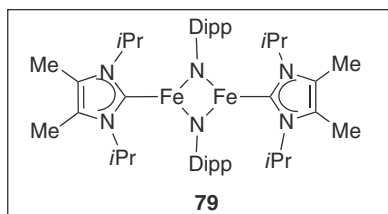
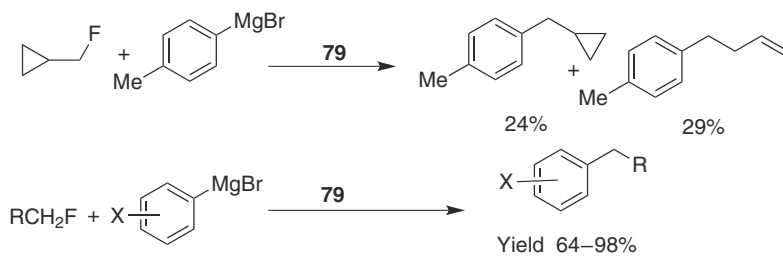


Entry	Additive	Yield (%) of 76 (R = Ph)	Yield (%) of 76 (R = H)	Yield (%) of 77
1	None	5	0	79
2	NMP	15	Trace	3
3	TMEDA	71	3	19

(b)



(c)



Scheme 120.

reagents as coupling partner in the presence of TMEDA as the additive (Table XX).

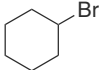
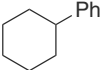


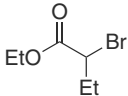
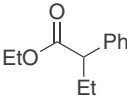
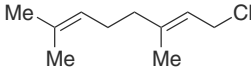
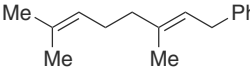
Later on this year (2007) Chai and co-workers (169) developed cross-coupling for unactivated alkyl halides and alkyl Grignard reagents in the presence of phosphine-based ligands, Xanthphos. In 2011, Asami and co-workers (170) reported the tridentate β -aminoketonato iron complex (**78**) as an efficient catalyst for a cross-coupling reaction between aryl magnesium bromides and alkyl halides (Scheme 120*b*).

Another approach for cross-coupling reactions involving nonactivated primary alkyl fluoride with aryl Grignard reagents was developed by Deng and co-workers (171) (in 2012) using a low-coordinate dinuclear iron complex $[(\text{IPr}_2\text{Me}_2)\text{Fe}(\mu_2\text{-NDipp})_2\text{Fe}(\text{IPr}_2\text{Me}_2)]$ (**79**, where Dipp = 2,6-diisopropylphenyl) as catalyst. This method for $\text{C}_{\text{sp}^3}\text{-F}$ bond arylation worked well for functionalized Grignard reagents and primary alkyl fluorides (Scheme 120*c*).

1. Low-Valent Iron Complex in Cross-Coupling Reactions

Iron-catalyzed alkylation of alkyl, allyl, and propargyl halides with an aryl Grignard reagent has been developed by using the low-valent ferrate complex $[\text{Fe}(\text{C}_2\text{H}_4)_4][\text{Li}(\text{tmeda})_2]$ as a precatalyst (172). This reaction tolerated various functional groups (e.g., esters, ketone, nitriles, isocyanides, or *tert*-amines) (Table XXI). A low-valent iron-catalyst can be synthesized on a large scale as

TABLE XXI
Alkylation Catalyzed by a Low-Valent Ferrate Complex

$\text{RX} + \text{PhMgBr} \xrightarrow[\text{THF, } -20^\circ\text{C}]{[\text{Fe}(\text{C}_2\text{H}_4)_4][\text{Li}(\text{tmeda})_2] (5 \text{ mol}\%)}$ R-Ph			
Entry	R-X	Product	Yield (%)
1			94
2			90
3			87
4			87

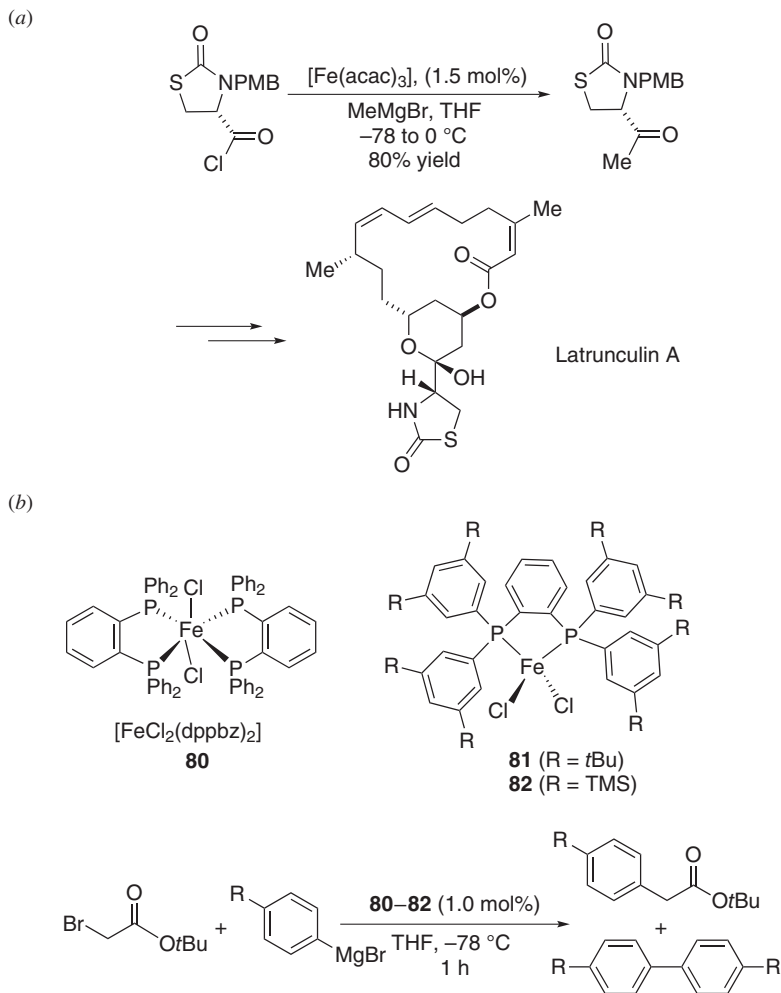
an air-sensitive crystalline material on treatment of ferrocene with lithium under an ethene atmosphere (173). Following the initial report from Fürstner and co-workers (172), a variety of catalyst systems were synthesized by only varying the ligand sets. Subsequently, the catalyst system was modified further to efficiently couple the alkyl electrophile and PhMgBr (174). The reaction protocol was found to be a good alternative of Jin and Nakamura's (175), condition, where TMEDA was used in more than stoichiometric amounts (176).

D. Acyl Derivatives as Coupling Partners

Selective monoaddition of a nucleophile to an activated acid derivative is a challenging task. In 1953, Cook and co-workers (177) successfully discovered the selective monoaddition of a nucleophile to an acid chloride catalyzed by FeCl₃. Such a reaction was used to synthesize 1,*n*-dicarbonyl compounds using di-Grignard reagents (178). Various functionalized acid chlorides, cyanides, and thioesters with primary, secondary, and tertiary alkyl and aryl Grignard reagents—diorganozinc derivatives afforded the corresponding products in good-to-excellent yields under mild reaction condition (Table XXII) (153b, 179). Total synthesis of (*Z*)-jasmone and dihydrojasmone were done using this reaction (180).

TABLE XXII
Cross-Coupling of Acid Chloride Derivatives With RMgX

Entry	R-X	RM	Product	Yield (%)
1				89
2				89
3		PhMgBr		79
5		<i>n</i> C ₆ H ₁₃ MgBr		90



Scheme 121. Iron-catalyzed acylation toward the synthesis of natural products (TMS = trimethylsilyl).

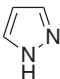
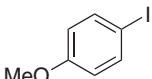
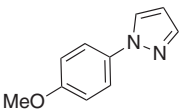
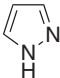
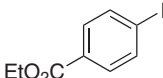
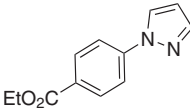
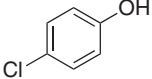
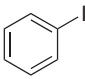
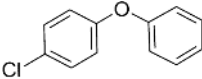
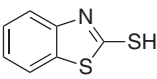
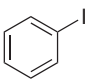
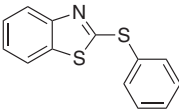
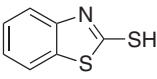
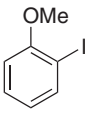
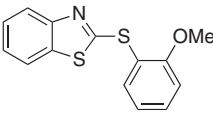
Fürstner et al. (181) synthesized the key building blocks for a concise total synthesis of the actin-binding macrolides of the latrunculin family, like latrunculin B (Scheme 121a) and the musk odorant (*R,Z*)-5-muscenone. In 2011, Jin and Nakamura (175) reported a simple and effective cross-coupling reaction of α -bromocarboxylic acid derivatives with aryl Grignard reagents. Better yields were obtained by using bisphosphine iron(II) complexes (**80–82**, Scheme 121b). The reaction proceeds at low temperature in a chemoselective manner to produce coupling products in good-to-excellent yields.

E. Iron-Catalyzed C–O, C–S, and C–N Cross-Coupling Reaction

Iron-catalyzed methods were also applicable for a carbon–heteroatom bond formation including C–N, C–O, and C–S. A cooperative catalyst system composed of $\text{Fe}(\text{acac})_3/\text{CuO}$ allowed *N*-arylation of aromatic heterocycles and lactams (182). Later, this type of C–N bond formation was done using $\text{FeCl}_3/\text{Fe}_2\text{O}_3$ in the presence of *N,N'*-dimethylethylenediamine (dmeda, ligand) (183). Although iron can catalyze an array of C–heteroatom coupling reactions, effect of metal contaminants in these cross-coupling reactions needs to be verified in light of recent developments reported by Buchwald and Bolm (88).

Amine-based ligand dmeda was also used for C–S bond formation (Table XXIII) (184). Recently, the phosphine-based ligand xantphos has also

TABLE XXIII
Iron-Catalyzed Carbon–Heteroatom Bond Formation

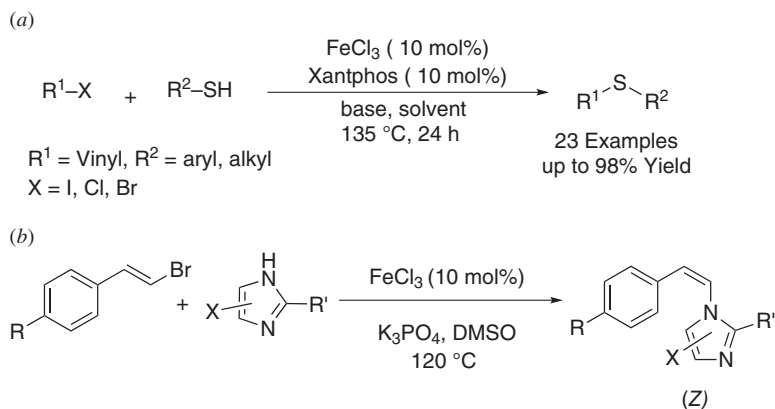
Entry	R–X	Ar–X	Product	Yield (%)
1				98 ^a
2				74 ^b
3				87 ^c
4				91 ^d
5				91 ^d

^a Conditions: CuO (10 mol%), $\text{Fe}(\text{acac})_3$ (30 mol%), Cs_2CO_3 (2 equiv), DMF, 90 °C, 30 h.

^b Conditions: FeCl_3 (10 mol%), dmeda (20 mol%), K_3PO_4 , PhMe, 135 °C, 24 h.

^c Conditions: FeCl_3 (10 mol%), $(t\text{BuCO})_2\text{CH}_2$ (20 mol%), Cs_2CO_3 , DMF, 135 °C.

^d Conditions: FeCl_3 (10 mol%), 20 mol% dmeda, NaOtBu , toluene, 135 °C.



Scheme 122.

been used for C–S bond formation with broad substrates studied by Lee and co-workers (185) (Scheme 122a). *S*-Vinylation is limited to 1-(2-bromovinyl)benzene and 1-(2-chlorovinyl)benzene. Related C–O bond formation was developed by using $\text{FeCl}_3/2,2,6,6\text{-tetramethyl-3,5-heptadione}$ system (Table XXIII) (186).

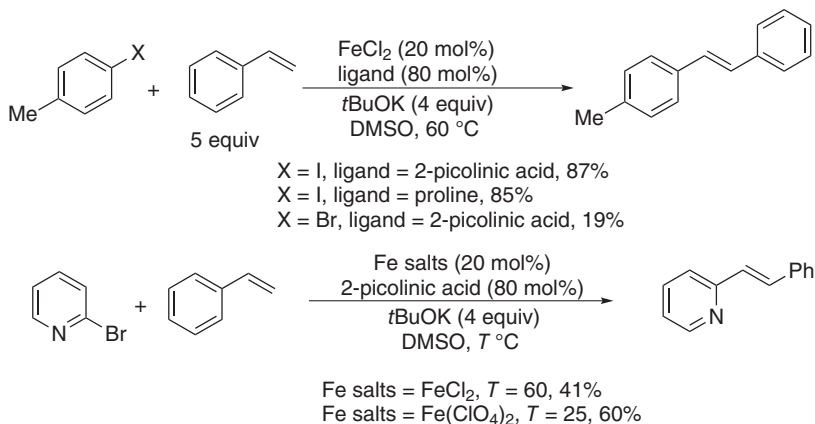
In 2009, Mao et al. (187) reported an iron-catalyzed cross-coupling reaction of vinyl bromides/chlorides with imidazoles in the absence of ligands and additives (Scheme 122b, dimethyl sulfoxide = DMSO, solvent). Notably (*E*)-vinyl bromides predominantly led to (*Z*)-products, while (*E*)-vinyl chlorides predominantly afforded (*E*)-isomers (Scheme 122b).

F. Iron-Catalyzed Mizoraki–Heck Reaction

One of the important methods for C–C bond formation is the Mizoraki–Heck reaction (188). Traditionally, palladium catalysts were used for this reaction. However, iron-catalyzed methods could provide a greener and sustainable approach. Consequently, the iron-catalyzed Mizoraki–Heck reaction between aryl–heteroaryl iodide and styrene was developed by Vogel and co-workers (189) in 2008. A proline or picolinic acid ligated iron(II) species (20 mol%) generated (*E*)-alkene in a stereoselective manner (Scheme 123).

G. Iron-Catalyzed Negishi Coupling Reaction

An iron-catalyzed Negishi reaction was reported by Nakamura M. and co-workers (190) in 2009. The polyfluorinated arylzinc reagents (Scheme 124b) and

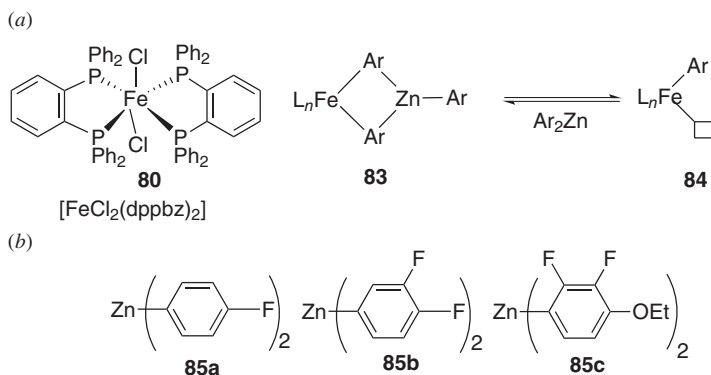


Scheme 123.

alkyl halides (Table XXIV) were coupled by using either iron-1,2-bis(diphenylphosphino)benzenedichloride (**80**) or a combination of FeCl_3 and dppbz[1,2-bis(diphenylphosphino)benzenedichloride].

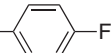
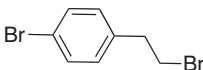
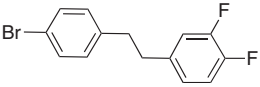
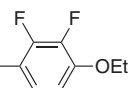
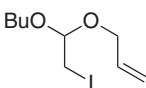
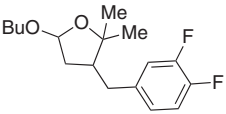
In 2009, Bedford et al. (191) explored the scope of an iron-catalyzed Negishi reaction with 2-halopyridine and pyrimidine substrates in a THF–toluene mixture (Table XXV). They proposed formation of an Fe–Zn bimetallic intermediate (**83**) for the success of **80** in the Negishi reaction. The arylzinc reagent helped to stabilize the putative active catalyst **84** (Scheme 124a) by preventing catalyst decomposition (191).

Nakamura and co-workers (192) reported a cross-coupling protocol between primary–secondary alkyl sulfonates and arylzinc reagents in the presence of FeCl_3

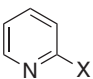
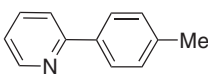
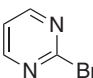
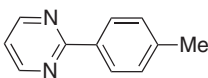
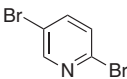
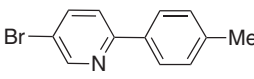


Scheme 124.

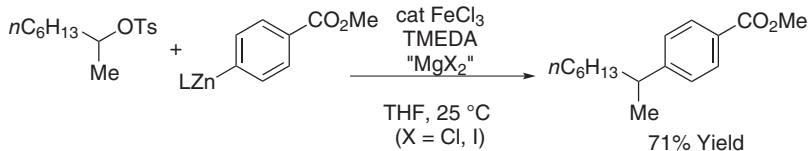
TABLE XXIV
 Cross-Coupling of Arylzinc Reagents and Alkyl Halides^a

$\text{R-X} \xrightarrow[\text{THF, 60}^\circ\text{C, 3 h}]{\text{ZnAr}_2(1.2 \text{ equiv})\text{FeCl}_3(3 \text{ mol}\%) \text{ with additive or } \text{FeCl}_2(\text{dppbz})_2(3 \text{ mol}\%)} \text{R-Ar}$					
Entry	R-X	Ar ₂ Zn	Product	Yield (%) ^b	Condition
1	cHep-Br	85a	cHep- 	92	(60 °C, 3 h)
2		85b		77 ^c	(60 °C, 15 h)
3 ^{d,e}	C ₁₀ H ₂₁ I	85c	C ₁₀ H ₂₁ - 	91	(60 °C, 24 h)
4		85b		85	(60 °C, 15 h)

^aReactions were carried out on a 1.0–2.0-mmol scale.^bIsolated yield.^cThe ¹H NMR yield.^dUsed 3 mol% of FeCl₃ and 9 mol% of dppbz.^eUsed 1.5 equiv of Ar₂Zn.
 TABLE XXV
 Iron-Catalyzed Negishi Coupling of Halopyridines^a

$\text{Heteroaryl-X} + \text{Zn(4-tolyl)}_2 \xrightarrow{\text{80 (5 mol\%)}} \text{Heteroaryl-Ar}$			
Entry	Heteroaryl Halide	Product	Yield (%)
1			65 ^b
2			58(58)
3			56(50)

^aConditions: Heteroarylhalide (1.0 mmol), Zn(4-tolyl)₂ (0.25 M in THF, 4.8 mL), 1 (0.05 mmol), toluene (6 mL), 100 °C, 4 h.^bUsed 1 equiv Zn(4-tolyl).



Scheme 125.

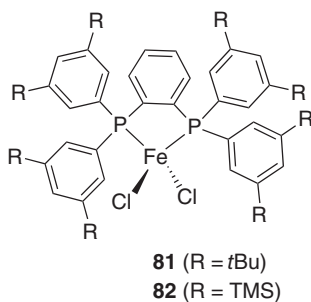
and TMEDA. The arylzinc reagent was prepared from aryllithium or magnesium reagents with ZnI_2 . *In situ* formation of alkyl halides from sulfonates avoided discrete preparation of secondary alkyl halides and gave high product selectivity (Scheme 125).

H. Suzuki–Miyaura Coupling Reaction

Nakamura and co-workers (193) developed iron-catalyzed Suzuki–Miyaura coupling using iron(II) chloride–diphosphine complexes (**81**, **82**) (Scheme 126) as catalyst with magnesium bromide, lithium aryl borates. Primary and secondary alkyl halides were successfully employed as the coupling partners for this reaction.

The reaction protocol was applicable for arylboronic acid and pinacol esters possessing methoxy, dimethylamino, halides, and alkoxy carbonyl functional groups (Table XXVI). The reaction occurred via formation of *in situ* borate with butyl- or *tert*-butyllithium (192).

A stereospecific cross-coupling between alkenylboronates and alkyl halides catalyzed by iron–bisphosphine complexes (**81**) was reported in 2012 by Nakamura and co-workers (194) (Table XXVII). An *in situ* generated lithium alkenylborate was the active alkenylation agent for this reaction.



Scheme 126. Iron-bisphosphine complexes (192).

TABLE XXVI
Substrate Scope of Suzuki–Miyaura Coupling of Alkyl Halides

$$R'-X + \left[\begin{array}{c} \text{Me} \\ | \\ \text{R}'-\text{B} \\ / \quad \backslash \\ \text{Ar} \quad \text{O} \\ | \quad | \\ \text{Me} \quad \text{Me} \end{array} \right]^- \text{M}^+ \xrightarrow[\text{THF, 0–40 } ^\circ\text{C}]{\begin{array}{c} \mathbf{81} \text{ or } \mathbf{82} \text{ (1–5 mol\%)} \\ \text{MgBr}_2 \text{ (0–20 mol\%)} \end{array}} R'-\text{Ar}$$

R' = 1°, 2°, alkyl, R = Et, Bu, *t*Bu, Ar = aromatic group, M = Li or MgBr

Entry ^a	Alkyl–X	Coupling Product	Yield (%) ^b
1 ^c			99 (R'' = H)
2	cHept–Br	cHept––R''	98 (R'' = OMe)
3 ^{d-f}			90 (R'' = CO ₂ Me)
4 ^{d-f}			81 (R'' = CO ₂ Et)
5 ^{d-f}			74 (R'' = CO ₂ <i>t</i> Pr)
6			79
7 ^{f,g}			90
8 ^e			83 ^h

^aReaction was carried out at 40 °C for 3–4 h on a 0.44–1.0-mmol scale using 3 mol% **82**. Arylborates were prepared from arylboronic acid pinacol ester and *t*BuLi.

^bIsolated yield.

^cUsing 1 mol% **82**.

^dUsing 1 mol% **82**.

^eUsed 5 mol% **82**.

^fAt 25 °C for 3–8 h.

^gUsed BuLi instead of *t*BuLi.

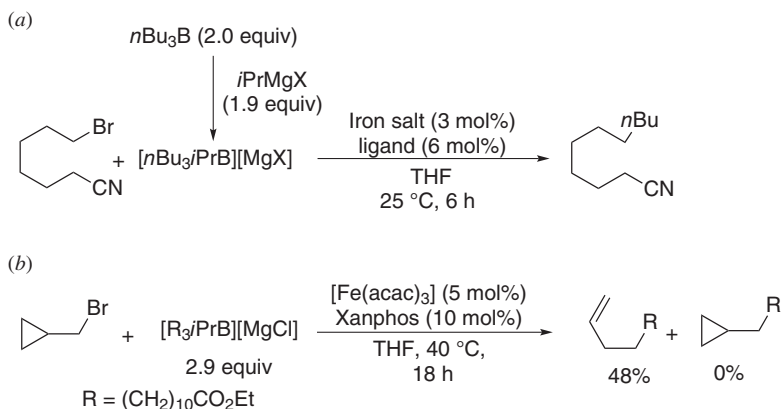
^hThe *cis*–*trans* ratio: 42:58.

The reaction protocol was also applied to alkyl–alkyl Suzuki–Miyaura coupling in the presence of [Fe(acac)₃] (3 mol%)–xanthphos(6 mol%) and a stoichiometric amount of *i*PrMgCl (Scheme 127*a*). Here *i*PrMgCl acted as an efficient activator for trialkylboranes by forming magnesium tetraalkylborate, which was the key

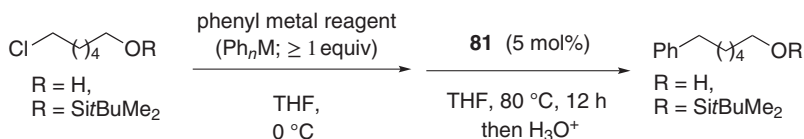
TABLE XXVII
Substrate Scope of Alkyl-Alkenyl Suzuki–Miyaura Coupling

Entry	R–X	Coupling Product	Yield (%) (<i>E/Z</i>)
1			98 (>99% <i>E</i>)
2			98 (>99% <i>E</i>)
3			98 (>99% <i>E</i>)
4			98 (>99% <i>E</i>)
5			98 98 (>99% <i>E</i>)

transmetalating agent for this reaction (195). A radical clock experiment (Scheme 127*b*) gave a ring-opening cross-coupling product, which indicated the formation of an alkyl radical intermediate. This radical intermediate was suggested to trigger the Suzuki–Miyaura coupling. Recently, a modified protocol with iron–bisphosphine complexes (**81**, **82**) was developed with unprotected nonactivated halohydrins and aryl aluminium reagents as the coupling partners. In this report, a free alcohol group formed an alkoxide, which in turn accelerated the reaction and enhanced the diastereoselectivity (Scheme 128) (196).



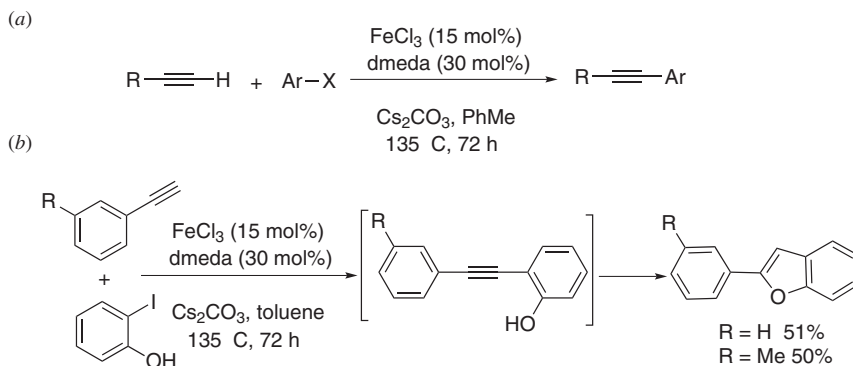
Scheme 127.



Scheme 128.

I. Sonogashira Reaction

The iron-catalyzed Sonogashira reaction was developed in 2008 by Bolm and co-workers (197), with the use of FeCl₃, an amine-based ligand dmeda, and Cs₂CO₃ as a base in toluene (Scheme 129*a*). Use of an iron-based catalyst for this reaction instead of Pd/Cu made this method economical. Various functional groups were well tolerated on both the coupling partners. Furthermore, iron-catalyzed domino Sonogashira/hydroxylation of alkynes also was reported (Scheme 129*b*). Notably, in 2009, Buchwald and Bolm (88) reported the effect of metal contaminants in these cross-coupling reactions and concluded that these reactions were likely catalyzed by trace copper impurities rather than iron. Their correspondence raised the question about the role of iron in the Sonogashira reaction and related cross-coupling reactions.



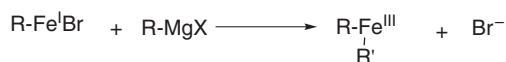
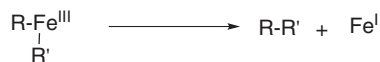
Scheme 129. Iron-catalyzed Sonogashira reaction.

J. Mechanism of Cross-Coupling Reactions

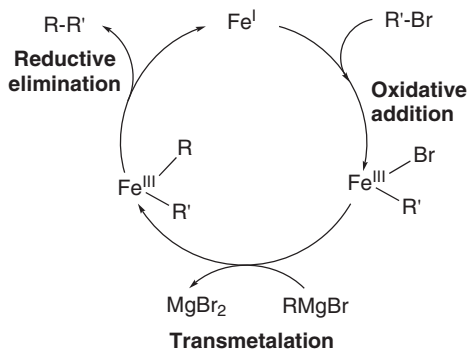
Initial mechanistic studies by Kochi (145) suggested that the iron(II) and iron(III) species rapidly oxidize Grignard reagent to give a reduced soluble form of iron that was most likely Fe(I). They also proposed that cross-coupling was independent of the concentration of alkyl magnesium halide and first order with respect to alkenyl halide and iron catalyst. Based on these observations, Kochi proposed a catalytic pathway involving oxidative (ox) addition, transmetalation, and then reductive elimination (Scheme 130*a* and *b*) similar to Pd catalyzed cross-coupling reactions.

Fürstner et al. (199) proposed the formation of a low-valent ferrate complex as the active species for their cross-coupling reactions based on their experimental data and literature reports (173, 198). At first, there was an *in situ* formation of $[\text{Fe}^{(-II)}(\text{MgX})_2]$ (ferrate complex) and subsequently it was oxidatively added between the R–X bond. The formation of this type of ferrate complex was reported in the literature with the X-ray crystal structure of $[\text{Cp}(\text{dppe})\text{Fe}(\text{MgBr})\cdot 3\text{THF}]$. It has a covalent-bond character between the Fe and Mg centers. Such an observation supported the idea that iron can remain covalently bonded to magnesium in $[\text{Fe}(\text{MgX})_2]$, the “Inorganic Grignard Reagent” (173, 198). They found that finely dispersed $\text{Fe}(0)^*$ particles in THF dissolved slowly on treatment with an excess of $n\text{C}_{14}\text{H}_{29}\text{MgBr}$ and the resulting solution catalyzed the cross-coupling reaction (Scheme 131). Further, iron complexes of different oxidation states -2 , 0 , $+1$, $+2$ and $+3$ were prepared, which were devoid of stabilizing ligands, and were tested for their activity toward the cross-coupling reaction. It was observed that nucleophiles (e.g., MeLi, PhLi, or PhMgBr) were unable to undergo β -hydride elimination. Rather, they rapidly reduce Fe^{3+} to Fe^{2+} and then alkylated

(a)

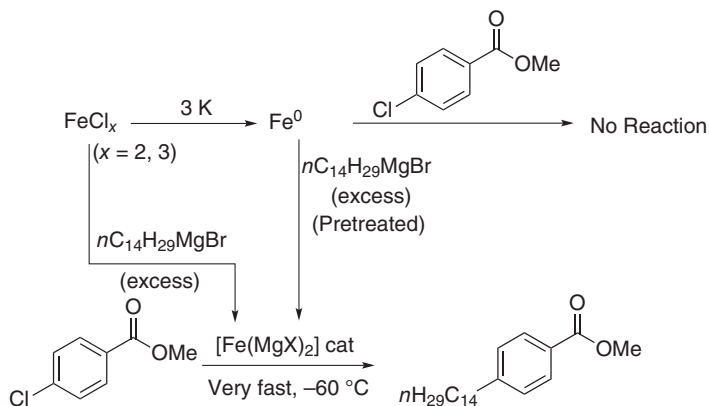
Initiation**Propagation–Oxidative Addition–Reduction Elimination****Propagation (II) Substitution****Termination**

(b)



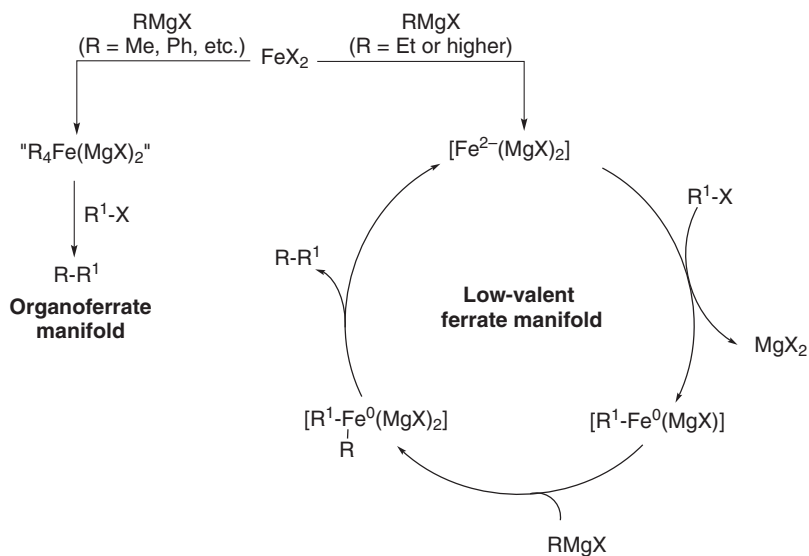
Scheme 130.

the metal center. The resulting homoleptic organoferrate complexes, like $[(\text{Me}_4\text{Fe}(\text{MeLi})\text{Li}(\text{OEt}_2)_2)]$, which was characterized by X-ray crystallography, transferred their organic ligand to activate electrophilic partner (173). However, the nucleophile, which underwent β -hydride elimination, was likely to follow a low-valent ferrate mechanism. Consequently, the reaction mechanism was dependent on substrates and the redox couple of iron in the solution. Based on these detailed studies, they had proposed both an organoferrate manifold and a low-valent redox manifold for these coupling reactions (Scheme 132) (199).

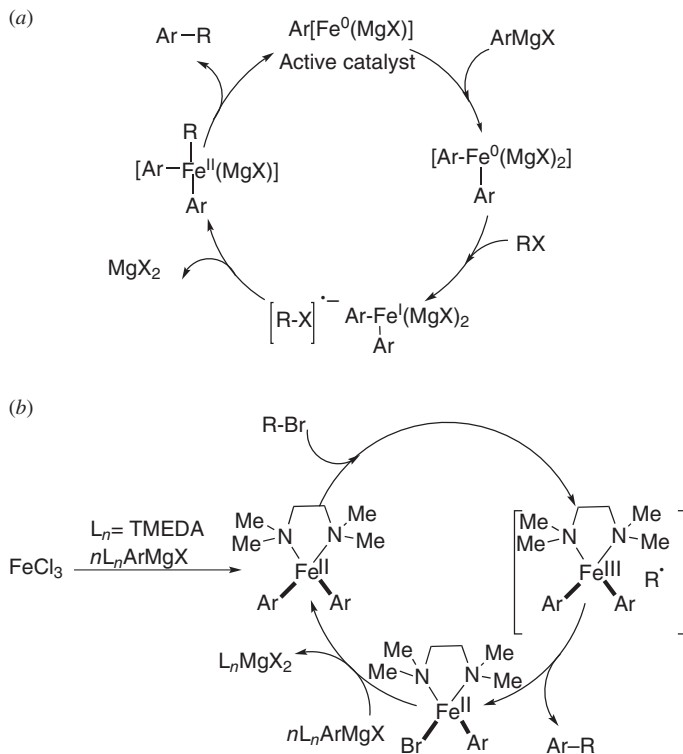


Scheme 131.

Later, Holzer and Hoffman (200) found a sufficient amount of racemization for chiral substrates under iron-catalyzed cross-coupling in contrast to Ni/Pd catalyzed reactions, which gave products without any loss in optical purity. On the basis of these observations, an SET mechanism (radical mechanism) was proposed rather than transmetalation.



Scheme 132.

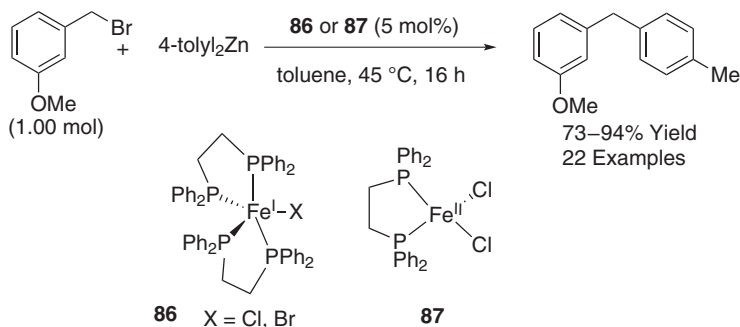


Scheme 133.

Cahiez et al. (176) proposed the Fe(0)/iron(II) cycle via formation of an alkyl radical anion (Scheme 133a). Cossy and co-workers (168a) also proposed a radical-based oxidative addition and a “radical clock” experiment was successfully carried out that further supported their hypothesis.

In 2009, Nagashima and co-workers (201) proposed an iron(II)–iron(III) catalytic cycle on the basis of the isolation of catalytically competent intermediates of both iron(II) and iron(III) complexes. Once again, their “radical clock” experiment confirmed a radical intermediate during these reactions (Scheme 133b).

In 2008 and 2009, Norrby and co-workers (202) supported the iron(I)/iron(III) cycle, which was proposed 40 years ago by Kochi on the basis of their mechanistic and computational studies. More recently in 2012, Bedford and co-workers (203) reported that iron(I) was the lowest kinetically reasonable oxidation state in a representative Negishi cross-coupling reaction with aryl zinc reagents and benzyl bromide on the basis of the isolation of the catalytically competent Fe(I) species.



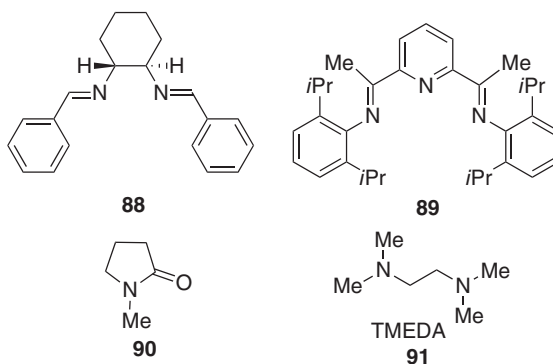
Scheme 134.

Interestingly, better results were obtained in the presence of iron(I) phosphine compared to the iron(II) phosphine complexes for reaction between aryl/alkyl halide and an arylzinc reagent (204) (Scheme 134).

As discussed above, the iron-catalyzed cross-coupling reaction mechanism is versatile and varies with the nature of the coupling partners and on the reaction condition. Formation of a radical intermediate is likely, and the iron(I)–iron(III) catalytic cycle is more accepted compared to others.

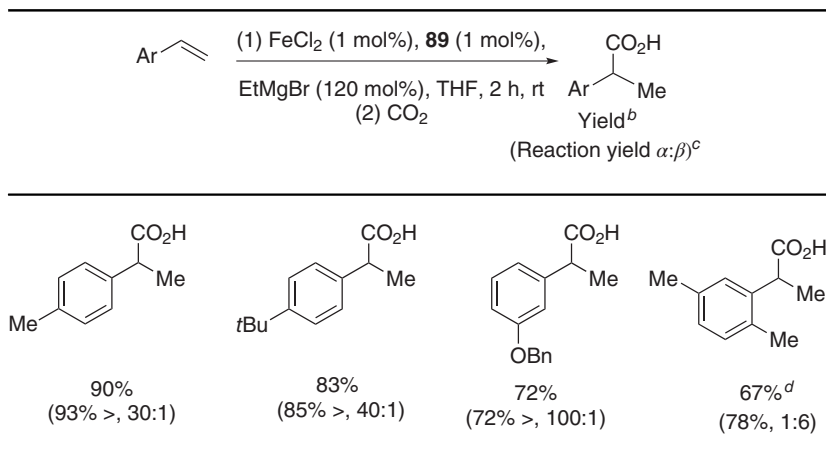
K. Hydrocarboxylation

The iron-catalyzed hydrocarboxylation reaction was first reported by Greenhalgh and Thomas (205). Bench-stable FeCl_2 was used as an iron precatalyst in the presence of different amine ligands (Scheme 135; **88–91**). It was observed that FeCl_2 –bis(imino)pyridine ligands (**88–89**) and hydride source (EtMgBr , 1.2



Scheme 135.

TABLE XXVIII
Substrates Scope of Hydrocarboxylation^a



^a Condition: 0.7 mmol of 1, 1 mol% FeCl₂, 1 mol% 7, THF (0.15 M), rt; (1) 120 mol% EtMgBr (3 M in Et₂O), 2 h. (2) CO₂, 30 min.

^b Isolated yield α -product.

^c Reaction yield and regioselectivity determined by proton nuclear magnetic resonance (¹H NMR) using an internal standard.

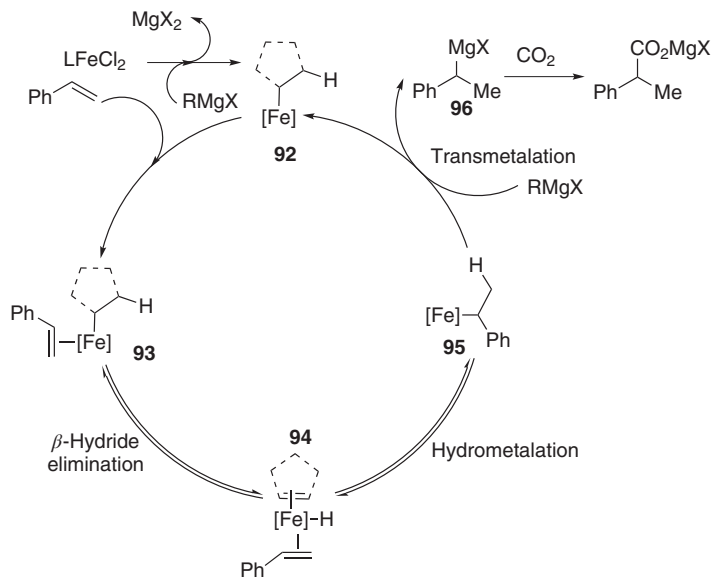
^d Used 120 mol% cyclopentylmagnesium bromide (2 M in Et₂O); isolated yield of β -product.

equiv) gave the best yield of α -aryl carboxylic acid in the presence of CO₂ at atmospheric pressure (Table XXVIII).

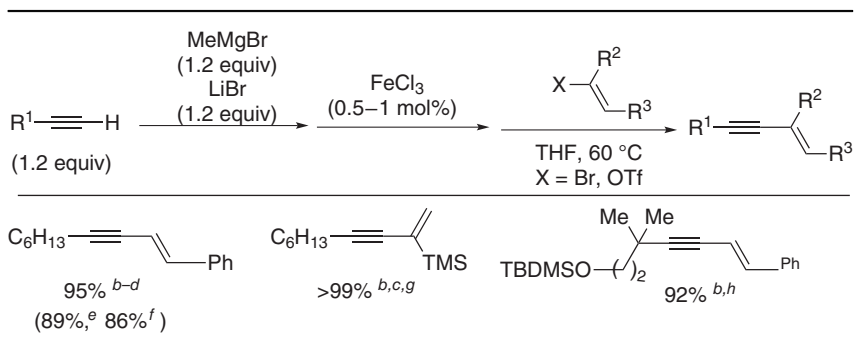
A mechanistic investigation was carried out with methanol-*d*₄ instead of CO₂. In this experiment, 1-deuteroethylbenzene was observed as the main product, which indicated the possibility of α -aryl organometallic species formation. Such α -aryl organometallic species (**93**) could be formed from **92**. Subsequently, **93** underwent β -hydride elimination, hydrometalation, and transmetalation to form α -aryl organometallic species (**96**). The nucleophile **96** attacked CO₂ to give the desired product (Scheme 136).

L. Enyne Cross-Coupling Reaction

Conjugated enynes were the key structural motif of various bioactive molecules, drug intermediates, and organic electronic materials (206). Generally, Pd was known to catalyze the synthesis of these types of molecules via the C_{sp}–C_{sp}² coupling reaction. Nakamura and co-workers (207) first reported the FeCl₃ catalyzed enyne cross-coupling in 2008 (Table XXIX, TBDMS = *tert*-butyldimethylsilyl). Lithium bromide was used as the crucial additive and FeCl₃ efficiently catalyzed the cross-coupling of alkynyl Grignard reagent with alkenyl bromides–triflates.



Scheme 136. Mechanism of hydrocarboxylation.

TABLE XXIX
Iron-Catalyzed Enyne Cross-Coupling^a

^a Reactions were carried out at $60\text{ }^\circ\text{C}$ for 24 h on a 1.0 mmol scale in the presence of 1 mol% of FeCl_3 unless otherwise noted (TBDMS = *tert*-butyldimethylsilyl).

^b Isolated yield.

^c Used 0.5 mol% of FeCl_3 .

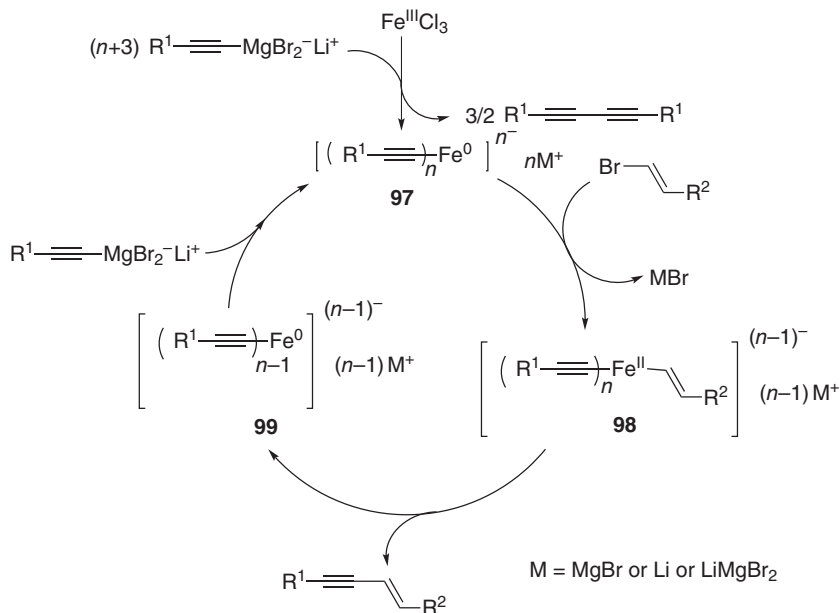
^d Ratio was (*E/Z*) 88:12.

^e Used 0.5 mol% of FeCl_2 .

^f Used 0.5 mol% of $\text{Fe}(\text{acac})_3$.

^g Reaction time was 12 h.

^h Ratio was (*E*)/(*Z*) 85:15.



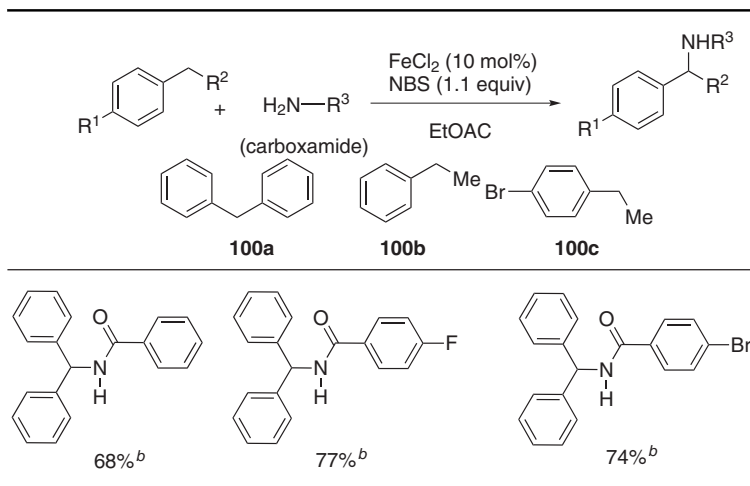
Scheme 137.

They proposed the mechanism of enyne cross-coupling via formation of the alkenyl iron complex **97**. Subsequently, oxidative addition of alkenyl bromide to **97** resulted in the formation of high-valent ferrate (**98**), which underwent reductive elimination to give the desired product. The presence of a lithium salt was important to reduce Fe^{III} to the low-valent ferrate complex **97** (Scheme 137).

VI. DIRECT C–N BOND FORMATION VIA C–H OXIDATION

Transition metal mediated C–N bond formation methods via C–H activation are important for the synthesis of nitrogen-containing organic compounds (208). Nitrene intermediates or derivatives were used as the nitrogen source in most cases (1d, 209). Often, hazardous compound PhI=NTs is used for C–N bond formation. Consequently, use of amines and amides as the nitrogen source is challenging and more sustainable (1d).

In 2008, Fu and co-workers (210) reported an efficient, inexpensive, and air-stable catalyst–oxidant (FeCl₂–NBS) system for amidation of benzylic sp³ C–H in ethyl acetate under mild conditions. The reaction tolerated a variety of substrates with variations in benzylic sp³ C–H bonds (**100a–100c**) and carboxamide–sulfonamide (Table XXX). The NBS played a vital role as an oxidant and radical initiator.

TABLE XXX
 Substrate Scope for C–H Amidation^a


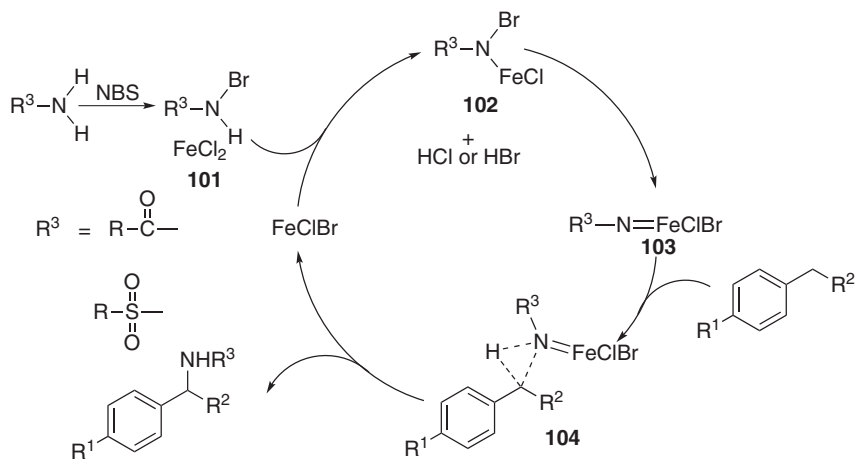
^aReaction conditions: benzylic reagent (1.2 mmol), amide–sulfonamide (1.0 mmol), NBS (1.1 mmol), and FeCl₂ (0.1 mmol).

^bIsolated yield.

The reaction occurred via formation of the *N*-bromocarboxamide and *N*-bromosulfonamide intermediate **101**. Subsequently, it formed intermediate **102** as an active species through proton exchange. Then it formed the iron–nitrene complex **103**, which upon reacting with benzylic sp³ C–H bonds, formed intermediate **104** to provide the desired amidation product (Scheme 138).

Later in 2010, Li and co-workers (211) developed an iron-catalyzed C–N bond-formation method without using a nitrene source (Scheme 139). Their method included oxidative C–N bond formation of azoles and ether with good-to-excellent yields. Iron(III) chloride was used as the catalyst and TBHP as the oxidant (and radical initiator too). This combination activated the α -C–H bonds of ethers. Subsequently, nucleophilic attack from azoles generated an oxidative C–N bond with ethers. Under standard reaction protocol, imidazole and its derivatives gave a high yield for such oxidative coupling with THF (Scheme 139a). It was also observed that benzimidazoles underwent oxidative C–N bond formation with ethers in moderate-to-good yield (Scheme 139b).

The reaction occurred via formation of a radical and hydroxyl anion from TBHP in the presence of iron(II). The hydroxyl anion abstracted a proton from azole and the *t*BuO[•] generated a radical in ether. This ether was oxidized to an oxonium ion in the presence of iron(III). Subsequently, it was attacked by an azole anion in order to form a C–N bond (Scheme 140).



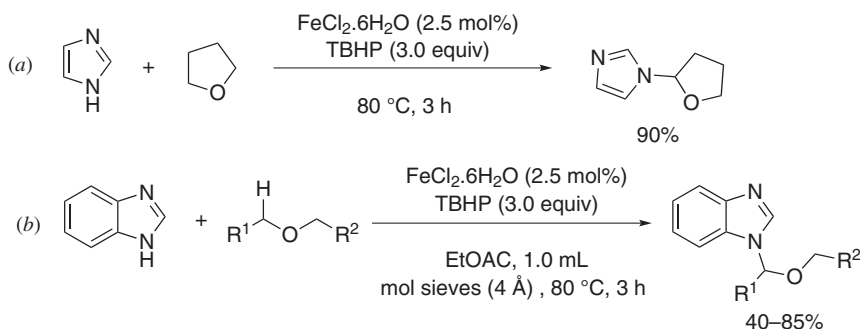
Scheme 138. Proposed mechanism of benzylic sp^3 C–H amidation.

Later in 2012, Xia and Chen (212) reported oxidative C–N bond formation between azole derivatives and amides–sulfonamides via activation of sp^3 C–H bond adjacent to the nitrogen atom, with good-to-excellent yields (Scheme 141).

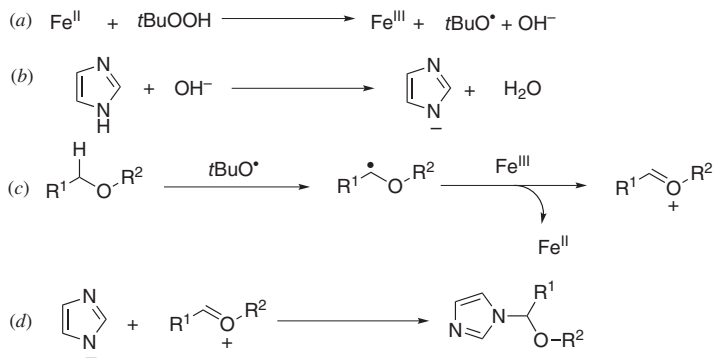
Formation of a radical adjacent to nitrogen (**105**) was proposed, which was followed by oxonium ion (**106**) formation. Subsequently, nucleophilic attack occurred from azole, which gave the desired product (Scheme 142).

Iron-catalyzed direct amination was developed in 2011 by Yu and co-workers (213). They used FeCl_3 –benzoxazoles with formamide and different secondary amines as nitrogen sources via decarbonylation (Table XXXI).

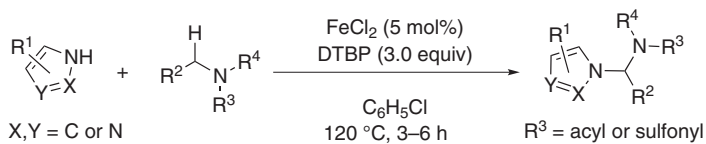
They proposed a Lewis acid catalyzed mechanism where FeCl_3 coordinated to a nitrogen atom and facilitated nucleophilic attack (Scheme 143).



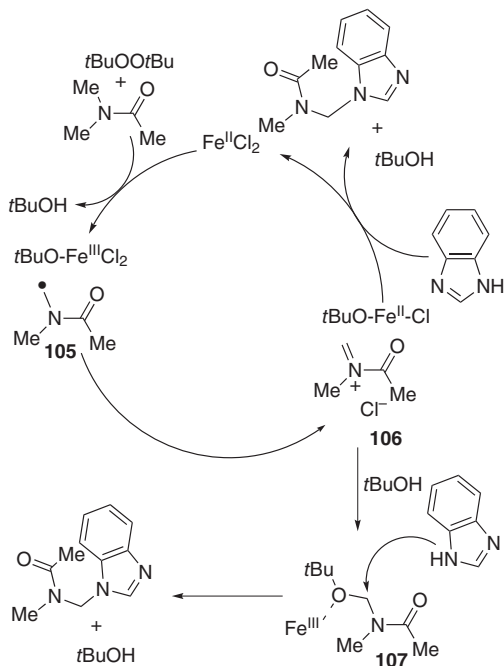
Scheme 139. Iron-catalyzed oxidative C–N bond formation.



Scheme 140.

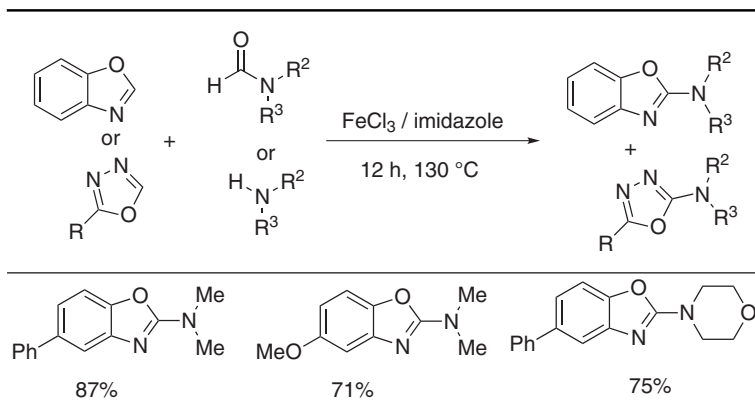


Scheme 141.

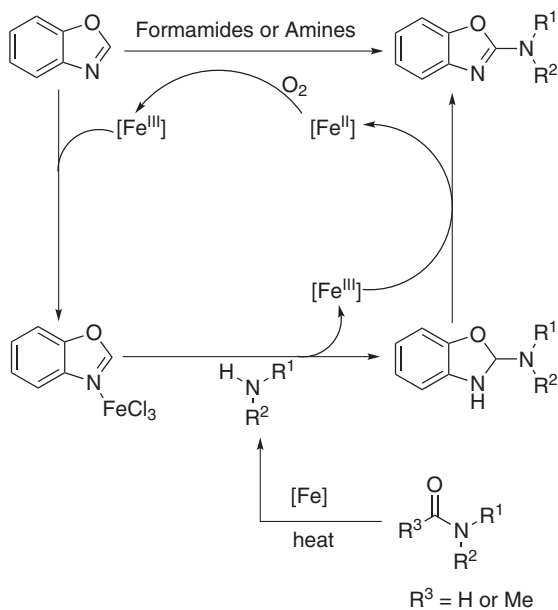


Scheme 142.

TABLE XXXI
Iron-Catalyzed Decarbonylative Amination^a



^aConditions: DMF (solvent) (2 mL), FeCl₃ (0.25 equiv), imidazole (2.0 equiv), 130 °C, 12 h, under air. Yields were isolated yields, formamide or amine was the nitrogen source.



Scheme 143. Mechanism of iron-catalyzed decarbonylative amination.

VII. IRON-CATALYZED AMINATION

Amine compounds are important in the pharmaceuticals industry and different amine-based pesticides are widely used to protect crops. Hence, syntheses of different amine compounds are important.

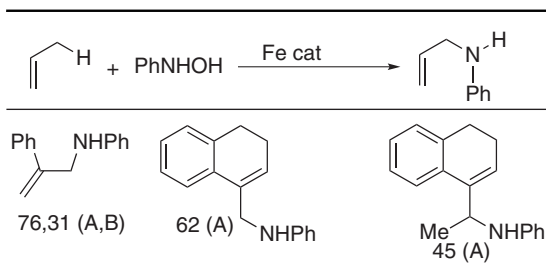
A. Allylic Aminations

Amine compounds could be synthesized by allyl amination where nitrogen-based compounds added to unsaturated compounds (214). Allylic amination was first reported by Johannsen and Jorgenson (215) and Srivastava and Nicholas (216) independently in 1994 using allylic compounds and a phenylhydroxylamine in the presence of an iron phthalocyanine complex (method A) or a mixture of $\text{FeCl}_2 \cdot 4\text{H}_2\text{O}/\text{FeCl}_3 \cdot 6\text{H}_2\text{O}$ (method B) (Table XXXII).

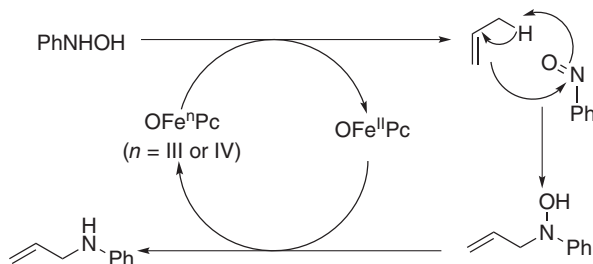
Olefins generally gave low-to-moderate yields of allyl amines in this reaction via a formal heteroene process (215). Iron-phthalocyanine (FePc) gave an amination product with limited substrates, mainly olefins conjugated to aromatic rings. On the other hand, use of an $\text{Fe}^{\text{II}}/\text{Fe}^{\text{III}}$ catalyst system was more beneficial than FePc as it gave good yields with nonterminal acyclic olefins. The later catalytic system (method B), with a mixture of $\text{FeCl}_2 \cdot 4\text{H}_2\text{O}/\text{FeCl}_3 \cdot 6\text{H}_2\text{O}$, showed better activity when PhNHOH was changed to 2,4-dinitrophenyl-hydroxylamine (217). Poor results were obtained from both catalyst systems due to the decomposition of phenylhydroxylamine to aniline, azobenzene, and azoxybenzene in the presence of iron complexes (218).

Two different sets of mechanisms were proposed based on the different catalytic systems. Here FePc generally underwent an “-NR” transfer mechanism “off” the metal (Scheme 144). The iron catalyst played an important role in

TABLE XXXII
Allylic Aminations of Olefins^a



^a Method A: Reaction performed with FePc (5 mol%), olefin (5 equiv), and PhNHOH (1 equiv) in toluene under reflux for 10 h. Method B: Reaction performed with $\text{FeCl}_2 \cdot 4\text{H}_2\text{O}/\text{FeCl}_3 \cdot 6\text{H}_2\text{O}$ (9:1, 10 mol%), olefin (1 equiv), and PhNHOH (2 equiv) in dioxane at 80 °C.



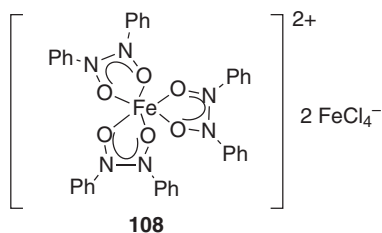
Scheme 144.

forming nitrosobenzene from phenylhydroxylamine and in the formation of an allylic amine from hydroxylamine via a hetero-ene reaction of PhNO with alkene (219).

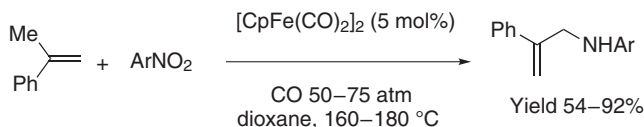
In the case of a second catalytic system (method B), Nicholas and co-workers (220) showed that reaction occurred via formation of an azo-dioxide complex (**108**) (Scheme 145).

Later, Srivastava and Nicholas (221) reported that nitroarenes could also be used as an aminating reagent in the presence of $[\text{CpFe}(\text{CO})_2]_2$ as catalyst under a CO atmosphere at high temperature (Scheme 146).

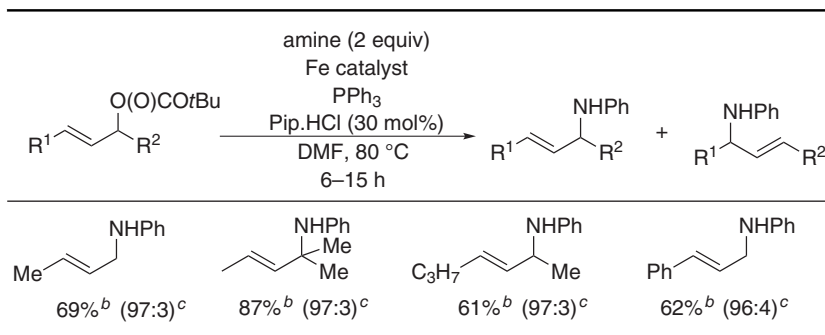
An iron-cyclopentadienyl-dicarbonyl complex also catalyzed allylation of styrene nitroaryl compounds having electron-withdrawing groups. The reaction temperature and pressure can be reduced (222) under a photoassisted condition.



Scheme 145.



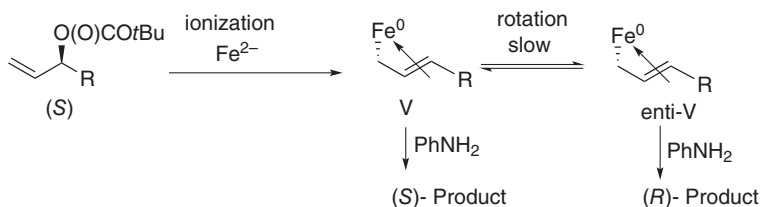
Scheme 146.

TABLE XXXIII
 Amination of Allyl Carbonates^a


^a All reactions were performed on a 1-mmol scale.

^b Yield of isolated product.

^c Regioselectivity of the crude product according to gas chromatography (GC) integration is given in parenthesis.



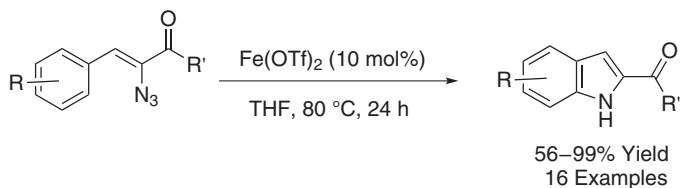
Scheme 147.

Later in 2006, Plietker (223) reported a regio- and stereoselective allylic amination of allyl carbonates with secondary amines using a $[\text{Bu}_4\text{N}][\text{Fe}(\text{CO})_3(\text{NO})]$ and triphenyl phosphine combination as the catalyst. The presence of a catalytic amount of piperidinium chloride (Pip.HCl) as a buffer retarded the decomposition of the catalyst. The variation in carbonate and amine partners provided good-to-excellent yield with high regioselectivity (Table XXXIII).

The reaction occurred via the formation of an σ -allyl metal intermediate (Scheme 147), and therefore provided high regio- and stereospecificity (223).

B. Intramolecular Allylic Amination

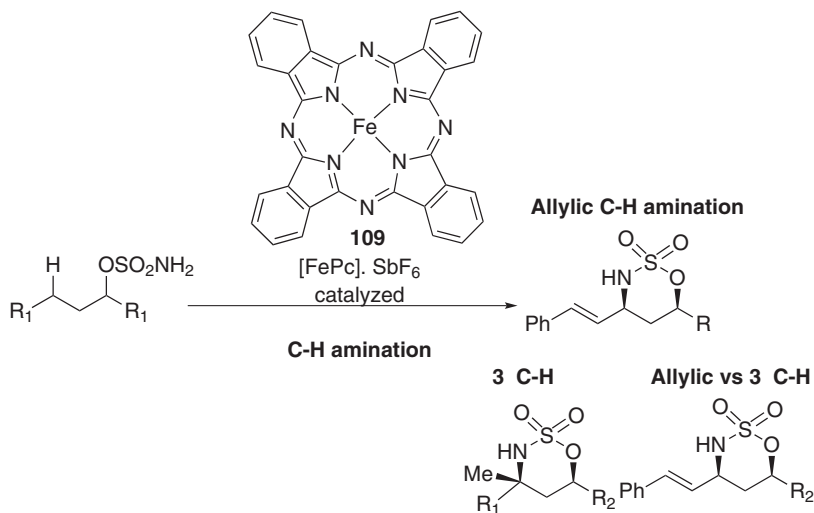
In 2011, Bonnamour and Bolm (224) developed an intramolecular C–H amination of azidoacrylates toward the synthesis of indole derivatives using an



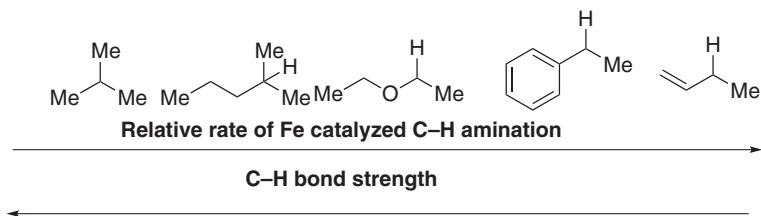
Scheme 148.

iron(II) triflate as catalyst. This reaction tolerated various functional groups including methoxy, alkyl, trifluoromethyl, halo, and phenyl groups at the para position of the aryl ring (Scheme 148).

The field of nitrenoid-based C–H amination was pioneered by Breslow and Gellman (225) by using Fe (TPP). Paradine and White (226) developed a highly selective intramolecular C–H amination by using an inexpensive, nontoxic [Fe^{III}Pc] catalyst, where Pc = phthalocyanine (**109**). This method showed a strong preference for allylic C–H amination over aziridinations (Scheme 149). A selectivity pattern emerged for the C–H amination: allylic > benzylic > ethereal > 3° > 2° >> 1°. In the case of polyolefinic substrates, the selectivity was controlled by an electronic and steric character. As expected, the relative rate of C–H amination inversely varied with bond strength (Scheme 150) (226). Allylic



Scheme 149.



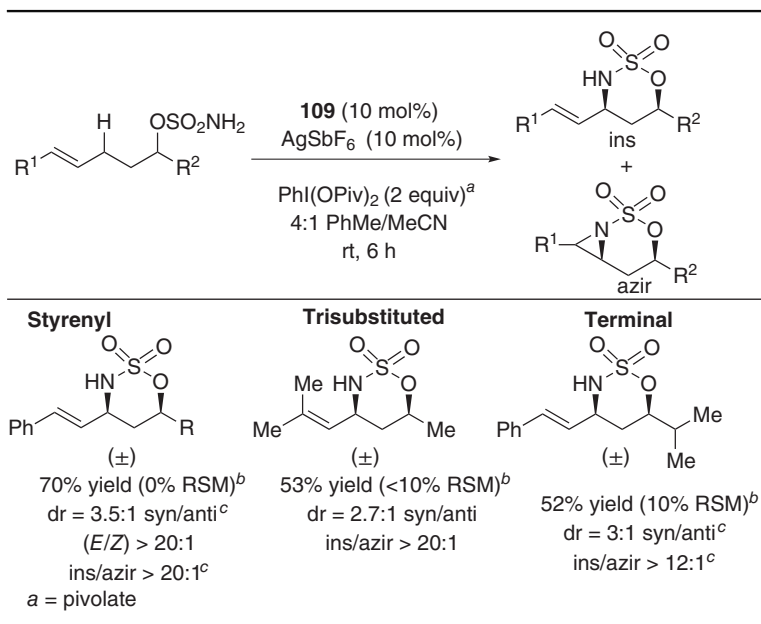
Scheme 150.

substrates with a wide variety of substituents were successfully employed for such amination reactions (Table XXXIV).

A stepwise mechanism was considered based on experimental observations. However, the stereoretentive nature of C–H amination for 3° aliphatic C–H bonds suggested a rapid radical rebound mechanism.

Later, Sun and co-workers (227) reported an FeCl_3 catalyzed intramolecular allylic amination toward the synthesis of dihydroquinolines and quinolones

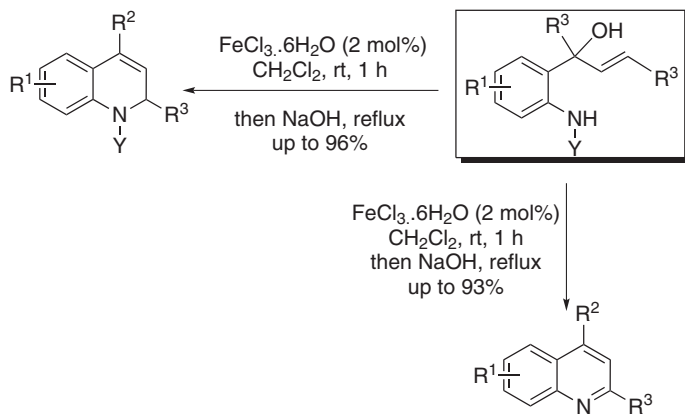
TABLE XXXIV
Intramolecular C–H Amination



^a Pivalate = Piv.

^b Isolated yields (syn + anti); % RSM in parentheses.

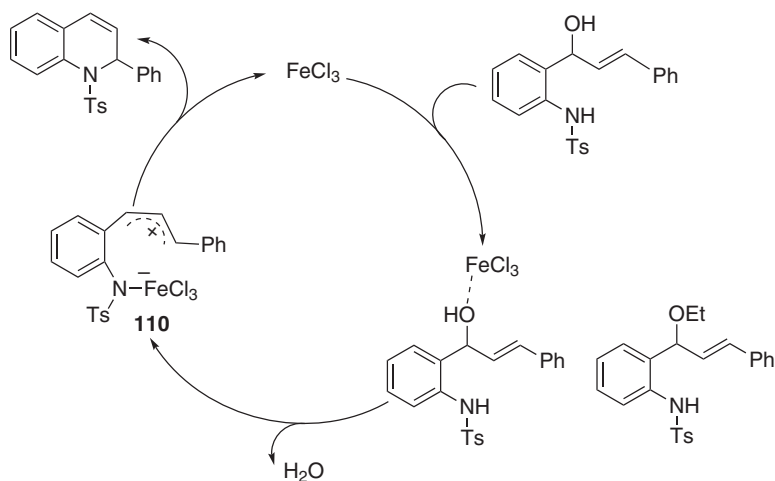
^c All product ratios were determined by ¹H NMR analysis of the crude reaction mixture.



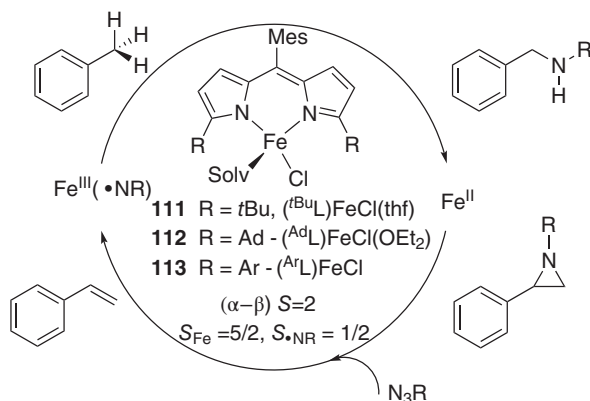
Scheme 151.

(Scheme 151). No stereoretentivity was observed with pure enantiomeric substrates. Hence, it was proposed that the reaction occurred via formation of the carbocationic intermediate (**110**) (Scheme 152).

In 2011, Betley and co-workers (228) employed an iron complex of the dipyrromethane ligand scaffolds bearing large aryl groups for C–H amination. The use of a bulky ligand provided a high-spin iron complex ($S = 2$), which was the catalytically active species. Reaction of iron complexes (**111–113**) with alkyl azides provided C–H amination for toluene and aziridine in the case of styrene



Scheme 152.



Scheme 153.

(Scheme 153 Ad = adamantyl, Ar = aryl). The complex (^{Ad}L)FeCl(OEt₂) (**112**) gave a better yield compared to **111** and **113**. They were able to isolate a high-spin iron complex, (^{Ar}L)FeCl(N(*p-t*BuC₆H₄)) during the reaction of (^{Ar}L)FeCl(OEt₂) (**113**) with *p-t*BuC₆H₄N₃ (**228**). A radical rebound-like mechanism by hydrogen-atom abstraction was proposed based on their experimental findings.

VIII. SULFOXIDATIONS AND SYNTHESIS OF SULFOXIMINES, SULFIMIDES, AND SULFOXIMIDES

A. Sulfoxidation

Sulfoxides are an important class of compounds since they were used for various ligand syntheses. Selective oxidation of sulfide was reported in the literature by using an iron catalyst in the presence of different oxidants (e.g., H₅IO₆, HNO₃, or other terminal oxidants) (**229**). Asymmetric sulfoxides were usually synthesized using titanium, vanadium, and manganese complexes. But those were less effective for practical use. One of the earlier methods iron porphyrin in the presence of iodosyl benzene, gave a moderate enantioselectivity (<55% ee) (**230**). Fontcave and co-workers (**231**) employed **114** as a ligand for iron-catalyzed sulfoxidation, however, they got low enantioselectivity (ee_{max} = 40%) (Scheme 154).

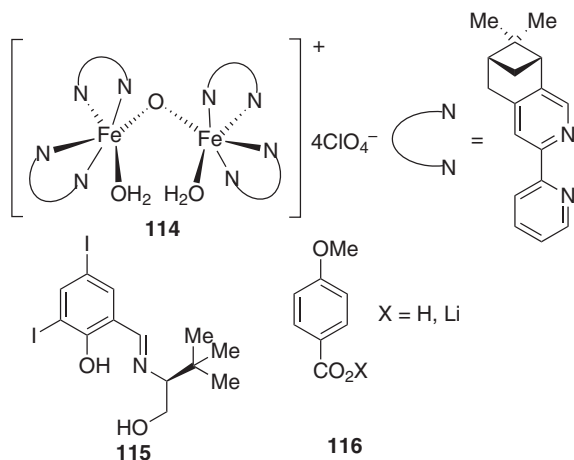
Legros and Bolm (**232**) reported the major breakthrough in iron-catalyzed asymmetric sulfoxidation. A highly enantioselective sulfide oxidation with optical purity (ee = 96%) was described under clean reaction condition (Table XXXV). More challenging substrates (e.g., phenyl ethyl and phenyl benzyl sulfides) were

TABLE XXXV
Iron-Catalyzed Asymmetric Sulfoxidation

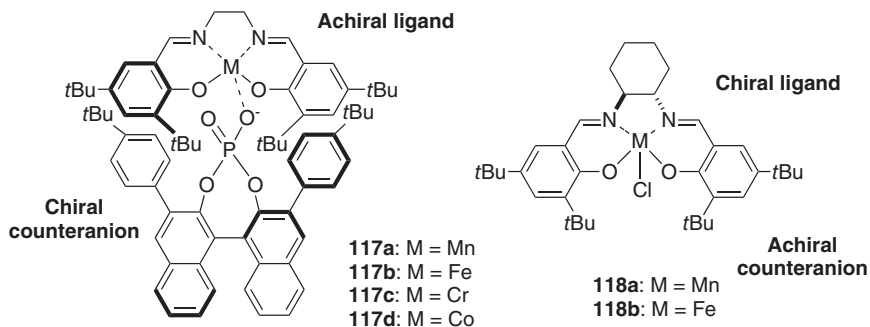
Entry	Sulfide	Product	
		Yield (%)	ee (%)
1	Ph-S-Me	63	90
2	Ph-S-Et	56	82
3	Ph-S-CH ₂ Ph	73	79
4	Ph-S-CH ₂ -CH=CH ₂	63	71

well tolerated with excellent enantioselectivity under their reaction protocol. The reaction was chemoselective since in phenyl allyl sulfide only the sulfur atom was oxidized and the double bond remained unaffected (233). This method was useful for the asymmetric synthesis of sulindac (> 90% ee), a biologically active chiral sulfoxide (234).

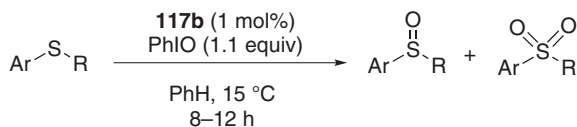
An iron(III)–salen complex with H₂O₂ could also catalyze the oxidation of organic sulfides and sulfoxides, in which an iron high-valent oxo (Fe^{IV}=O) species was proposed to be the active species (235).



Scheme 154.



Scheme 155.

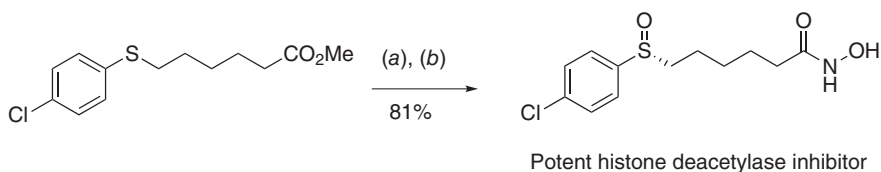


Scheme 156.

Later in 2012, Liao and List (236) reported a highly active and enantioselective sulfoxidation catalyst using an iron(III)–salen cation (**118b**) and a chiral phosphate counteranion (**117a–117d**) (Scheme 155). They used **117b** as the chiral catalyst in combination with PhIO as the terminal oxidant (Scheme 156). This reaction was the first example of an asymmetric counteranion directed catalysis (236).

Their methodology had a potential application toward the enantioselective synthesis of hydroxamic acid (Scheme 157), which is a potent histone deacetylase inhibitor.

Very recently, Chen and co-workers (237) developed another protocol of sulfoxidation using $\text{Fe}(\text{acac})_3$ (1 mol%) and polyethylene glycol as an additive and O_2 as the oxidant.



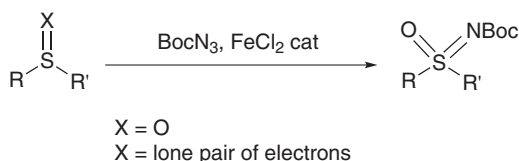
(a) **117b** (2 mol%), PhIO (1.20 equiv), EtOAc, 10 °C, 12 h
 (b) aq NH_2OH , KOH, MeOH/THF

Scheme 157.

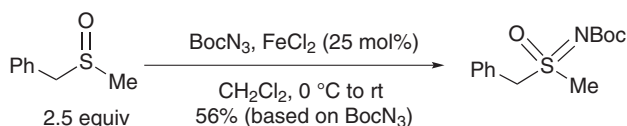
B. Synthesis of Sulfoximines, Sulfimides, and Sulfoximides

Nitrene transfer was a key process for the synthesis of various classes of organic compounds (e.g., aziridination and different nitrogen-containing compounds). It was also utilized in the synthesis of N-substituted sulfimides. Bach and Kober (238) first reported the iron-catalyzed method for the synthesis of sulfoximides using FeCl_3 /*tert*-butyloxycarbonyl azide (BocN_3) (Scheme 158). Instead of using FeCl_3 in a stoichiometric amount, it could be used in a catalytic amount (25–50 mol%) in their modified condition (Scheme 159). The nitrene could transform sulfoxide and sulfide to sulfoximides and sulfimides, respectively.

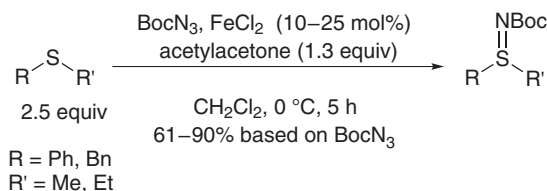
These reactions were stereospecific and could be utilized for the synthesis of chiral ligands. Optically pure sulfoxides could be converted into sulfoximides. Subsequently, free NH_2 -sulfoximine was obtained after Boc cleavage. Bolm and co-workers (239) synthesized chiral sulfoximines as ligands for enantioselective synthesis. Syntheses of sulfoximines by imidation of sulfides and sulfimides were obtained in moderate-to-good yield in the presence of acetylacetonone or DMF (Scheme 160).



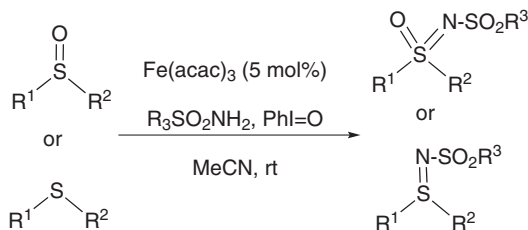
Scheme 158.



Scheme 159.



Scheme 160.



Scheme 161.

Later, Mancheno and Bolm (240) developed stereospecific methods for sulfoximine synthesis using $\text{Fe}(\text{acac})_3$ as a catalyst (Scheme 161). Unfortunately, the reaction was susceptible toward steric effect.

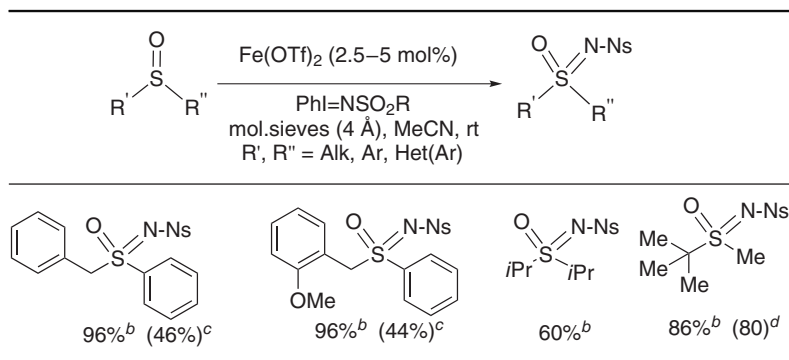
Subsequently, they reported a modified method, which tolerated challenging substrates including benzyl, sterically demanding alkyl, and heteroaryl substituted sulfoxides at rt (Table XXXVI) (241).

1. Mechanism

An $\text{Fe}(\text{V})$ -nitrene complex $[(\text{Cl})\text{Fe}^{\text{V}}=\text{NR}]$ was proposed as a imidation reagent in the catalytic cycle (Scheme 162).

Darcel and co-workers (242) developed a sulfonylimines synthesis under neutral condition starting from an aldehyde (Scheme 163).

TABLE XXXVI
Iron-Catalyzed Sulfoximide Synthesis^a

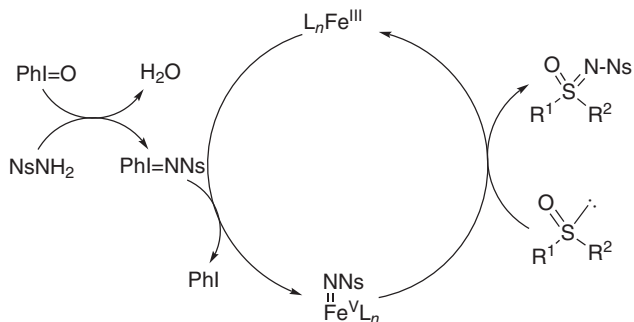


^a Reaction conditions: sulfoxide (1 equiv), $\text{Fe}(\text{OTf})_2$, $\text{PhI}=\text{NNs}$ ($\text{Ns} = 2$ or 4 -nitrobenzenesulfonyl) (1.3 equiv), and molecular sieves 4 \AA in acetonitrile (0.1 M) at rt.

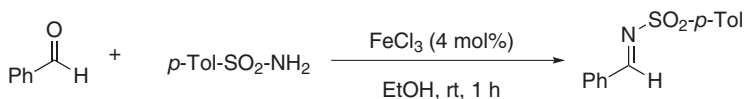
^b After column chromatography.

^c Yield obtained by using 10 mol% of $\text{Fe}(\text{acac})_3$ as catalyst.

^d Reference (240).



Scheme 162.



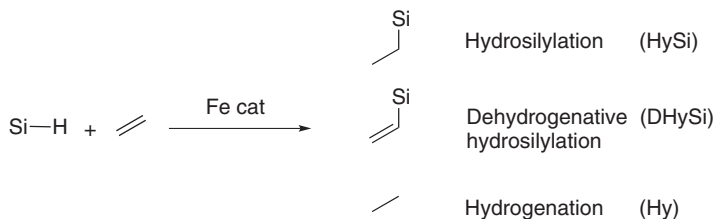
Scheme 163.

IX. REDUCTION REACTIONS

A. Hydrosilylation of Alkenes

Organosilicon compounds can be found in numerous consumer goods that are associated with our daily life (e.g., oil, grease, rubbers, cosmetics, and medicinal compounds). Most of them contain Si–C bonds that need to be synthesized artificially, as they do not exist in nature. Addition of Si–H across an unsaturated double or triple bond provides the most convenient and widely used approach to form such organosilicon. This method is termed as hydrosilylation (HySi) and it requires a transition metal catalyst (Scheme 164).

One of the major problems regarding hydrosilylation of alkenes and alkynes is the selectivity issue, as side reactions (e.g., DHySi and Hy) may decrease the turn



Scheme 164. Iron-catalyzed reactions of alkene and hydrosilane (243).

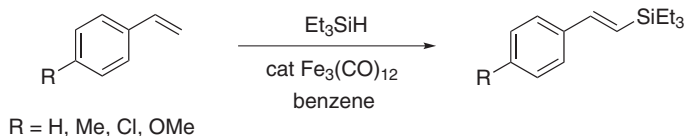
over number (TON) and can generate unwanted side products in a significant amount (Scheme 164). The success of this method, therefore, lies in discovering highly reactive yet selective reaction conditions that will not only ensure high-catalytic turnover, but also make the process economical and environmentally benign as organosilicons are generated on the millions of tons scale.

Traditionally, for over three decades, among transition metal catalysts, platinum-based Spier's catalyst ($\text{Pt}_2(\text{[(CH}_2=\text{CH)SiMe}_2\text{]}_2\text{O})_3$) and Karstedt's catalyst ($\text{H}_2\text{PtCl}_6 \cdot 6\text{H}_2\text{O}/i\text{PrOH}$) have been regarded to be very powerful and are often employed for commercial purposes. In 2007, worldwide consumption of platinum by the silicone industry was estimated to be 5.6 metric tons and most of them were not recovered (244). Also, Rh and lanthanide-based catalysts have been reported to affect HySi. The high cost, limited availability, and toxic nature of precious metals imposed a scientific challenge to discover catalytic systems based on earth-abundant first-row transition metals, particularly iron.

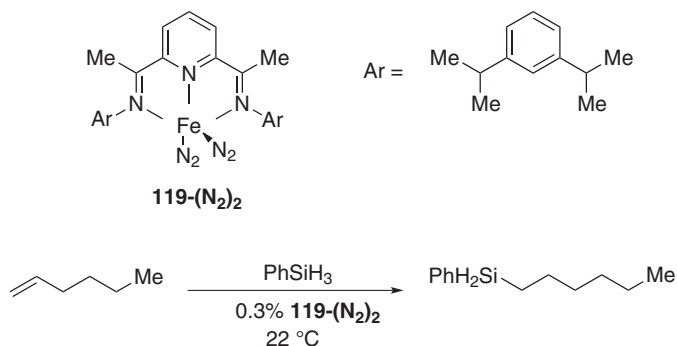
Nesmeyanov et al. (244b) reported the first iron-catalyzed HySi reaction in 1962, where $\text{Fe}(\text{CO})_5$ served as the catalyst in the reaction of alkenes and tertiary silanes. Products from both HySi and DHySi were generated depending on the substrate and reaction condition. In 1977, Schroeder and Wrighton (244c) disclosed a photoreaction of R_3SiH and alkenes involving the same catalyst, $\text{Fe}(\text{CO})_5$. Later, they proposed a mechanism of iron-catalyzed HySi for the $\text{Cp}^*\text{Fe}(\text{CO})_2\text{R}$ catalytic system ($\text{Cp}^* = \eta^5\text{-C}_5\text{Me}_5$, R = alkyl, silyl) that included the insertion of a C=C double bond into an Fe–Si bond.

Completely selective DHySi was realized by Murai and co-workers (245) in 1993 as vinyl silanes were obtained from the reaction of styrenes and Et_3SiH in the presence of $\text{Fe}_3(\text{CO})_{12}$ (Scheme 165). Other metals of the same group (Ru, Os) were also effective, but iron exhibited complete selectivity. However, the reaction suffered a serious drawback, since 1-hexene afforded a complex mixture that contained vinylsilane, alkylsilane, and allylsilane.

On the other hand, selective hydrosilylation of alkenes by inexpensive iron catalysts eluded researchers, until Chirik and co-workers (246) made a significant breakthrough in 2004 (Scheme 166). By using a well-characterized iron bis(imino)pyridine dinitrogen complex (**119**), they successfully hydrosilylated a number of unactivated olefins with PhSiH_3 , whereas with Ph_2SiH_2 , a slower reaction rate was observed. The method was also compatible with alkynes and with PhSiH_3 . However, due to the steric



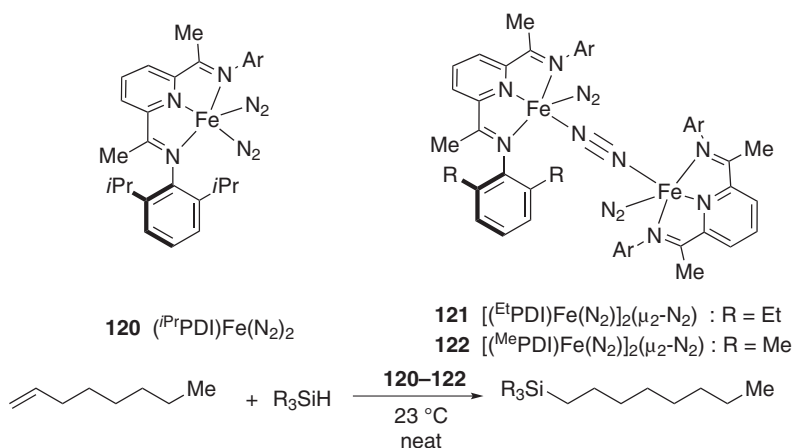
Scheme 165. Selective DHySi of styrenes catalyzed by triiron decacarbonyl.



Scheme 166. Selective hydrosilylation of alkenes catalyzed by an iron bis(imino)pyridine dinitrogen complex.

hindrance of the bulky silylalkene, no further reaction was observed even with a large excess of phenylsilane.

Unfortunately, this catalyst was unreactive toward the most commercially relevant silicon hydrides, the tertiary silanes (e.g., Et_3SiH). To overcome this, Chirik and co-workers (244) carried out a series of reactions under solvent-free conditions with iron bis(imino)pyridine complexes containing both linear and bridging nitrogen ligands. By manipulating the size of the 2,6-aryl substituent of the bis(imino)pyridine ligand (*i*Pr, Et) (**120**, **121**), they were successful in employing a number of tertiary silanes as efficient silylating agents under ambient conditions, though Et_3SiH remained unreactive (Scheme 167). With a sterically



Scheme 167. Iron-catalyzed selective hydrosilylation of alkenes.

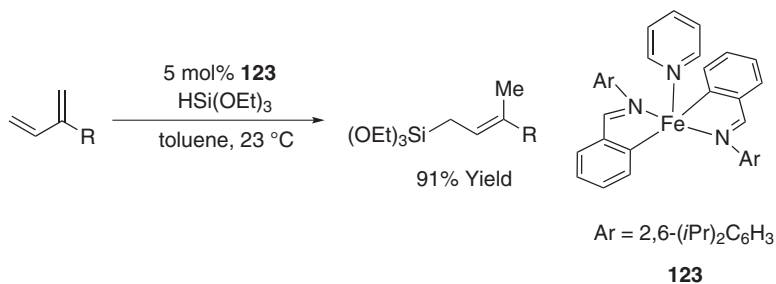
less hindered methyl as the substituent (**122**), the most active catalytic system was discovered as a complete conversion of Et_3SiH and 1-octene was observed after 45 min at 23 °C. This method was also applicable to styrene, as well as with amino substituted olefins. Notably, in the case of a platinum catalysts, the amino group often serves as a catalyst poison. Further, this catalytic system was successfully applied in cross-linking of silicone fluids, thus promising a viable alternative to the use of a precious platinum catalysts for such a purpose.

The problem of limited accessibility, as well as the air and moisture sensitivity of iron–bis(imino)pyridine dinitrogen complexes, was overcome in 2012, by the same group. In that year they prepared a series of iron dialkyl complexes containing either bis(imino)pyridine or terpyridine ligands that served as efficient pre-catalysts in the hydrosilylation reaction (247). At the same time, Nakazawa and co-workers (248) independently reported selective single–double hydrosilylation of 1-octene by iron complexes containing terpyridine as ancillary ligands.

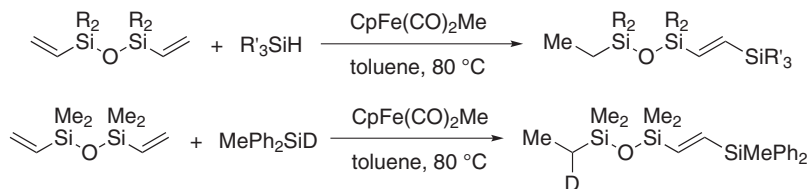
Meanwhile, Ritter and co-workers (249) reported a very efficient iron-catalyzed hydrosilylation of a 1,4-diene by a well-defined low-valent iron complex (**123**) (Scheme 168). In the presence of redox active imino pyridine ligands, a number of substituted dienes underwent hydrosilylation that provided allylsilanes in excellent yields and selectivities.

In 2012, unprecedented reactivity of $\text{CpFe}(\text{CO})_2\text{Me}$ was exhibited in the reaction of 1,3-divinyldisiloxane with hydrosilane by Nakazawa and co-workers (241) (Scheme 169). In this reaction, one of the vinyl groups was dehydrogenatively silylated, while the other vinyl group was hydrogenated.

This reaction is a combination of DHySi and Hy, which are regarded as unwanted side reactions in hydrosilylation chemistry, and from the reaction outcome it can very well be termed as HySi. It was observed that two vinyl groups and an oxygen atom connecting the vinylsilyl group were necessary for the success of the reaction. A labeling experiment with MePh_2SiD indicated that hydrogen atoms from the silylated vinyl group and tertiary silane were responsible for hydrogenation of the other vinyl group.



Scheme 168. Iron-catalyzed hydrosilylation of 1,4-diene.



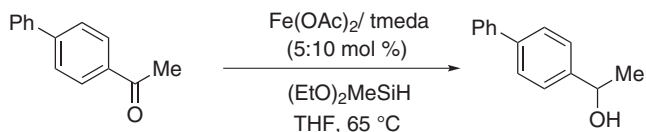
Scheme 169. A different iron-catalyzed “hydrosilylation” reaction.

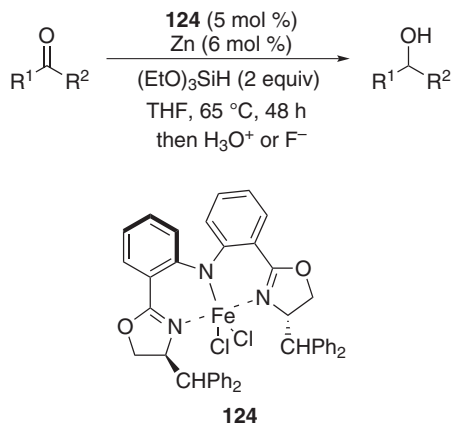
B. Hydrosilylation of Aldehydes and Ketones

Reduction of aldehydes and ketones to the corresponding alcohols is a fundamental transformation in synthetic chemistry. Although numerous methods are reported for reduction, the lack of chemoselectivity, sensitivity, and toxicity of the reagents available call for the discovery of mild and easy to handle reaction conditions. Hydrosilylation can be envisaged as a useful alternative in this regard. Unfortunately, hydrosilanes by themselves are unreactive toward the carbonyl compounds and a transition metal catalyst is needed for the success of the reaction. In recent decades, several transition metals ranging from Rh, Ru, and Ir to Ti, Zn, Sn, and Cu have been explored. But the cost of the metals, toxicity arising from the waste, and residual toxicity in the product emphasizes the need for more sustainable and greener protocols. Iron due to its relatively lower toxicity, inexpensiveness, and abundance in the earth has drawn significant attention from the scientific community.

In 2007, Nishiyama (250) disclosed a hydrosilylation reaction of aromatic and aliphatic ketones by using readily available $\text{Fe}(\text{OAc})_2/\text{tmeda}$ in conjunction with $(\text{EtO})_2\text{MeSiH}$ as the hydride source (Scheme 170). Surprisingly, reaction did not proceed in the absence of ligand; *tmeda* presumably helped the catalyst system to be homogeneous by facile coordination with iron. By using a chiral ligand (e.g., *bopa-tb* in place of *tmeda*), up to 79% ee was achieved. But, competing DH_2Si produced silyl enol ether in a significant amount since in most of the cases starting material was recovered (2–51%) after work up. However, replacing *tmeda* by thiophene-2-carboxylate as the ligand greatly improved the selectivity, as corresponding alcohols were obtained in excellent yields (> 90%) with no or a trace amount of starting material recovered.

To address the enantioselectivity issue, they prepared an iron catalyst based on NCN type ligands, bis(oxazolinyphenyl), amine) (phebox and bis(oxazolinyl)

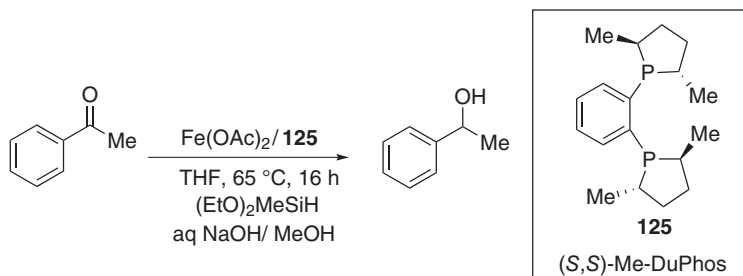
Scheme 170. The $\text{Fe}(\text{OAc})_2/\text{tmeda}$ catalyzed hydrosilylation of ketones.



Scheme 171. Enantioselective iron-catalyzed hydrosilylation of ketones.

pyridine (251a), plus $\text{Fe}_2(\text{CO})_9$. However, only up to 66% ee with an (*R*) configuration of the product alcohol was obtained with this catalytic system. Note, with the same ligand, an Ru catalyst yielded alcohol of absolute configuration (*S*) with 77% ee. Improved stereoselectivity was observed with bis(oxazolinylphenyl)amine (Bopa) ligand in conjunction with iron (up to 88% ee) (**124**) and cobalt (up to 98% ee). In all these cases, (*R*) products were obtained. Addition of Zn powder to an Fe–Bopa catalytic system dramatically altered the outcome, as alcohol product was obtained with an absolute configuration (*S*) (Scheme 171) (251b).

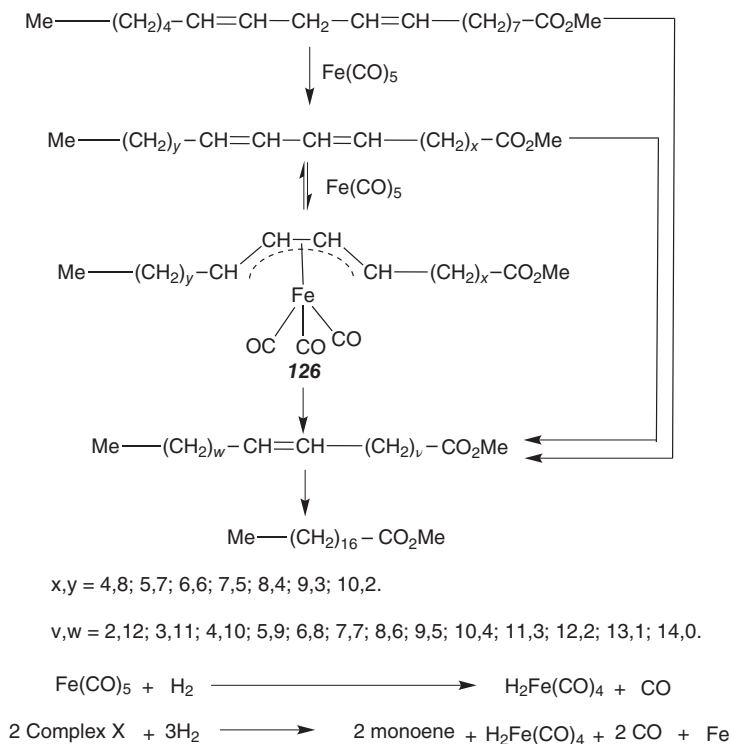
Electron-rich phosphine ligands (**125**) were applied in conjunction with iron for enantioselective hydrosilylation of ketones (up to 99% ee) (Scheme 172) (252a). Earlier, Beller and co-workers (252b) utilized most inexpensive hydrosilane, PMHS (polymethylhydrosiloxan) to reduce aldehydes by $\text{Fe}(\text{OAc})_2/\text{PCy}_3$. A broad range of aromatic, aliphatic, and heteroaromatic aldehydes were successfully converted to alcohols with excellent yields under a particularly mild reaction

Scheme 172. Highly enantioselective hydrosilylation of ketones by use of an iron–phosphine catalyst [DuPhos = 1,2-bis((2*R*,5*R*)-2,5-di-*i*-isopropylphospholano)benzene].

condition. Meanwhile, Yang and Tilley (253) made use of a simple iron amide catalyst $[\text{Fe}(\text{N}(\text{SiMe}_3)_2)_2]$ to generate alkoxysilanes in high yields from the corresponding aldehydes and ketones.

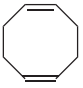
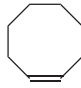
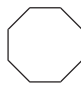

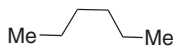
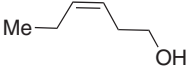
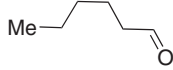
C. Hydrogenation of C–C Unsaturated Bonds

Iron complexes have high complexing affinity toward the C–C unsaturated bonds, which can cause a problem for hydrogenation due to deactivation of the catalyst by forming a stable complex. In 1965, Frankel et al. (254) reported homogeneous hydrogenation of methyl linoleate using $\text{Fe}(\text{CO})_5$ as the precatalyst under a nitrogen (250 psi) and hydrogen atmosphere (400 psi) at 180°C for successive hydrogenation. In the presence of the iron–carbonyl complex, the double-bond isomerizes and forms the conjugated diene leading to the stable complex **126**. High temperature and pressure was used to decompose this catalyst poisoning complex (**126**). Under reaction conditions, an iron carbonyl compound results in the formation of $\text{H}_2\text{Fe}(\text{CO})_4$, which is considered to be the hydrogenating agent (Scheme 173) (254).



Scheme 173. The $\text{Fe}(\text{CO})_5$ catalyzed hydrogenation of olefin.

TABLE XXXVII
Photoassisted Hydrogenation of the olefin by $\text{Fe}(\text{CO})_5$

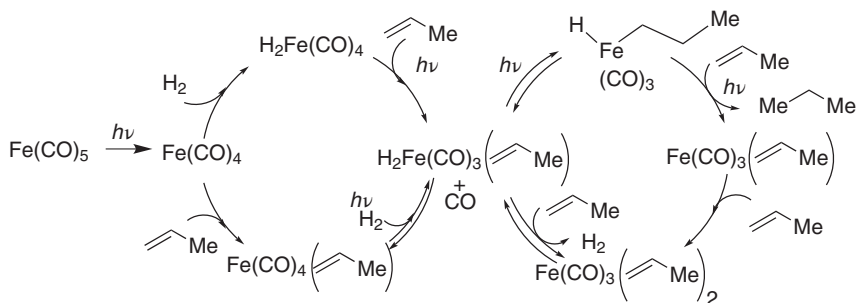
Entry	Olefin	Irradiation Time (min)	$0.011 M \text{Fe}(\text{CO})_5$ in benzene or toluene H_2 gas (10–14 psi) $\xrightarrow{25^\circ\text{C, near-UV radiation}}$ Hydrogenated product	
			Product(s)	Conversion (%)
1		60		8.9
				7.3
2		60		30.8
3		60	Linear hexenes	~100
				

With fully hydrogenated product, a mixture of double-bond isomerized monoenoic fatty esters have been observed with considerable cis–trans isomerization (254).

After Frankel's pioneering work in 1976 on hydrogenation under thermal conditions, Schroeder and Wrighton's (255) group carried out the photocatalyzed hydrogenation of the olefin using the same iron–carbonyl precatalyst. In the presence of radiation (UV), $\text{Fe}(\text{CO})_5$ performed the hydrogenation of an alkene under a milder condition than before (Table XXXVII). Again, positional isomerization of the double bond is the main limitation of this method. The olefin with the alcohol moiety produced only the corresponding aldehyde.

Schroeder and Wrighton (255) proposed that photoirradiation initiates the dissociation of the pentacarbonyl iron complex to the tetracarbonyl iron complex, which under photolytic or thermal conditions, forms the $\text{H}_2\text{Fe}(\text{CO})_3(\pi\text{-alkene})$ species (Scheme 174). Under a photoinduced condition, a $\text{H}_2\text{Fe}(\text{CO})_3(\pi\text{-alkene})$ complex performs hydrogenation through the iron monohydride, $\text{HFe}(\text{CO})_3(\text{alkyl})$, complex. Surprisingly, in the presence of the 1,3-dienes, the hydrogenation reactions are totally quenched due to the formation of a stable (1,3-diene) $\text{Fe}(\text{CO})_3$ complex, which cannot be dissociated under the reaction condition.

Meanwhile, in 1972 Noyori et al. (256) demonstrated another route for the iron pentacarbonyl mediated olefin hydrogenation of α,β -unsaturated ketones (Scheme 175). In the presence of base and protonated solvent, the iron pentacarbonyl

Scheme 174. Mechanism for the $\text{Fe}(\text{CO})_5$ catalyzed photoassisted hydrogenation of olefin.

Scheme 175.

complex generates a hydrido-iron complex. They also proposed the formation of an iron π -enolate intermediate.

This method showed selectivity toward the olefin moiety in the presence of a conjugated ketone, aldehyde, ester, and nitrile entities. Contrary to earlier reports, no isomerization of the double bond occurred. Steric hindrance near an olefin moiety decreases the reductive efficiency of the complex, for example, yield of the hydrogenation decreases from 2-cyclohexenone to 2-methyl-2-cyclohexenone (Table XXXVIII) (256).

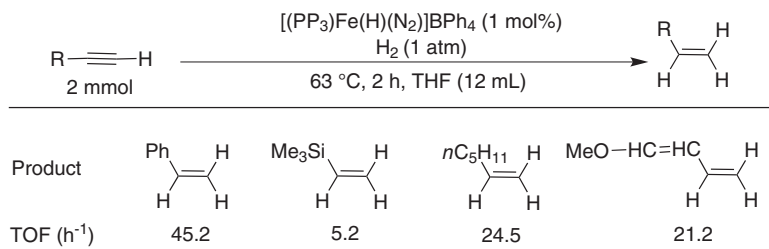
Selective hydrogenation of alkyne has also been achieved by using the iron(II)-*cis*-hydride- η^2 - H_2 complex. Bianchini and co-workers (257) showed that terminal alkynes are preferentially hydrogenated over a double bond present in the same substrate (Scheme 176). Trimethylsilane containing a terminal alkyne gave a low turnover frequency (TOF) value for the desired hydrogenated product due to formation of diene.

According to the reported hypotheses (Scheme 177) (257), one phosphine ligating site of a tetra-phosphine bound iron(II) center unlocks from the metal center to allow alkyne coordination. Subsequent hydride transfer to the alkyne results in the iron-vinyl complex. Subsequently, a proton from dihydrogen to the vinyl moiety is transferred through an intramolecular acid-base reaction as the oxidation of iron(II) to iron(IV) is less likely. In the final step, molecular hydrogen again coordinates with the iron center regenerating the active complex.

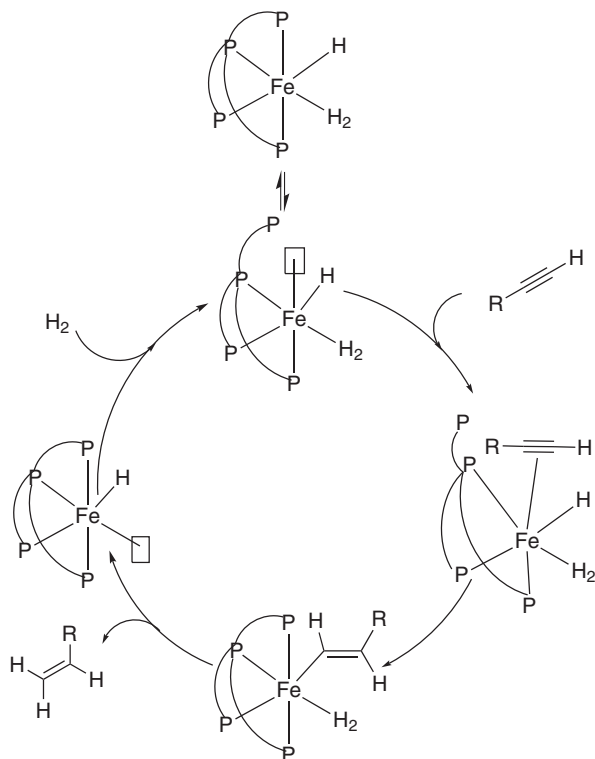
Brown and Peters (258) reported a tris(phosphino)borato-ligated iron(III)-imide complex that can perform partial hydrogenation of benzene (Scheme 178). The iron(III) hydride species is formed by a hydrogenolytic cleavage of the imide

TABLE XXXVIII
Substrate Scope for Hydrogenation with a Hydridoiron Complex

$\text{R}^1\text{-CH=CH-C(=O)R}^2 \xrightarrow[\text{MeOH} + \text{H}_2\text{O} (2 \text{ mL}) (v/v \text{ 95:5})]{\text{Fe(CO)}_5 (4 \text{ equiv}), \text{NaOH} (2 \text{ equiv})} \text{R}^1\text{-CH}_2\text{-CH}_2\text{-C(=O)R}^2$					
Entry	Substrate	Temp. (°C)	Time (h)	Product	Yield (%)
1		20	12		>98
2		20	10		96
3		60	24		35
4		20	12		98
5		20	48		90
6		20	36		92



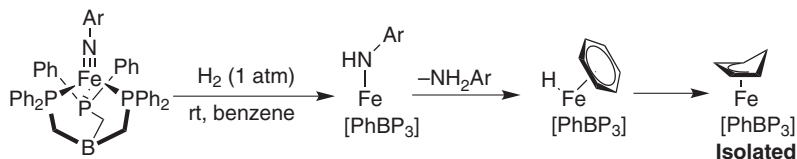
Scheme 176. Hydrogenation of the alkyne iron(II)-cis-hydride complex.



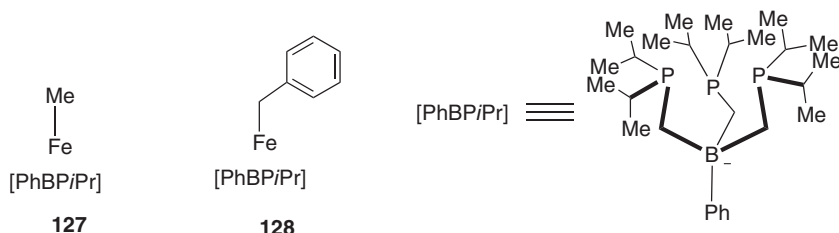
Scheme 177. Catalytic cycle for hydrogenation of alkyne.

complex under a hydrogenation atmosphere and has been suggested to be the active species for hydrogenation. Subsequently, a class of tris(phosphino)borato-ligated iron(III) alkyl and hydride complexes were prepared for olefin and alkyne hydrogenations (Scheme 179) (259).

Simple aromatic and aliphatic alkenes were hydrogenated efficiently following Peter's condition. Catalyst **127** was found to be more active since it is hydrogenated more easily than **128**. Double-bond isomerization of 1-hexene was observed



Scheme 178. Hydrogenation of benzene by tris(phosphino)borato-ligated iron(III) hydride.



Scheme 179. Catalyst for hydrogenation of unsaturated C–C bond.

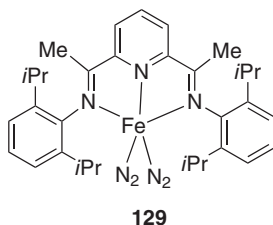
during the course of hydrogenation. Alkyne is quantitatively hydrogenated to alkane after successive double hydrogenations (Table XXXIX) (259). The TOF is calculated after >95% conversion of the starting materials.

In their search for a better hydrogenation catalyst, Chirik and co-workers (246) reported bis(imino)pyridine-iron(0)-bis(nitrogen) complex (**129**) (Scheme 180), which can facilitate hydrogenation of a different functionalized alkene and alkyne (Schemes 179–181). The π -acidic imine ligand moiety was chosen to provide stability for the iron(0) oxidation state. During deuteration of norbornene under the same reaction condition, *exo*, *exo*-2,3-norborane was generated through a *cis*-addition toward the double bond. Geometrical and stereochemical (*cis*–*trans*) isomerizations of the double bond were detected during the course of hydrogenation (246).

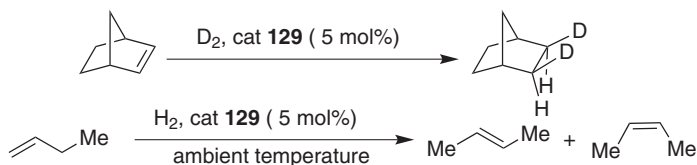
A wide range of functionalized alkenes and a disubstituted alkyne were hydrogenated using a catalytic amount of bis(imino)pyridine-iron(0)-bis(nitrogen) complex (**129**) (260). Amino olefins were hydrogenated to amino alkanes without any N–H trans-hydrogenation and the hydrogenation ability was increased with the N-alkylated substrates. Alkenes with various oxygen-containing functional groups and a fluorinated moiety can be tolerated. Di- and trisubstituted alkenes were readily hydrogenated. In the case of an α,β -unsaturated ketone, conversion sharply decreases due to the decomposition of the catalyst. Notably, olefin with a

TABLE XXXIX
Hydrogenation by Tris(phosphino)borato-Ligated Iron(III) Alkyl Complexes

Entry	Catalyst	Substrate	127 or 128 (10 mol%), 50°C		
			Alkene or Alkyne	Alkene	TOF (h ⁻¹)
			H ₂ (atm)	Time (min)	
1	127	Styrene	4	78	7.7
2	128	Ethylene	4	25	24.0
3	127	1-Hexene	1	115	5.2
4	128	1-Hexene	1	130	4.6
5	128	2-Pentyne	1	370	1.6



Scheme 180.



Scheme 181. Bis(imino)pyridine iron(0)-bis(nitrogen) complex for alkene hydrogenation.

conjugated ester moiety was selectively hydrogenated. Functional groups (e.g., amine or carbonyl) coordinate with the iron center prior to hydrogenation and hydrogenation TOF is inversely proportional to the strength of this coordination (Table XL) (260).

In 2012, Beller and co-workers (261) introduced the transfer hydrogenation of the terminal alkyne to the corresponding alkene using formic acid as the hydrogen source (Table XLI). Formic acid releases carbon dioxide and hydrogen, which coordinates to the metal center and performs the hydrogenation. By using deuterated formic acid (DCOOH) in place of HCOOH, deuterium was incorporated into the reduced alkene (261). A number of aliphatic alkynes, heterocyclic alkynes, and aromatic terminal alkynes bearing electron-donating and electron-withdrawing groups have been hydrogenated efficiently and selectively.

D. Hydrogenation of Ketones

Ketones are widely available precursors, for synthesizing enantiopure secondary alcohols. Optically active secondary amines, lactones, and so on, can be prepared from enantiopure alcohols, which are widely used in fragrances, pharmaceuticals, and in the beverage industry. Asymmetric hydrogenation is usually achieved using a chiral environment around the metal center. However, selectivity toward keto functionality in the presence of other unsaturated moieties is a challenging task.

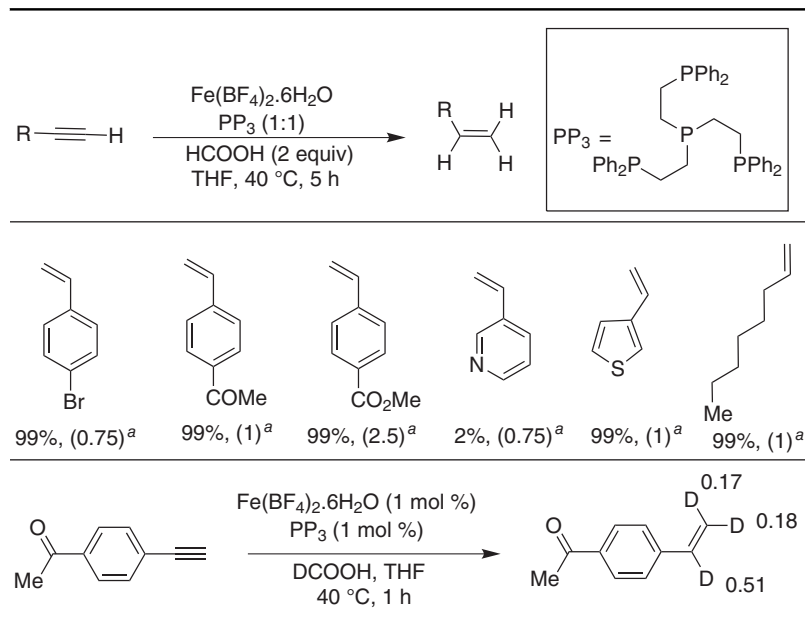
TABLE XL
Olefin Hydrogenation Using Bis(imino)pyridine-Iron(0)-bis(nitrogen) Catalyst

$\text{R}-\text{CH}=\text{CH}_2 \xrightarrow[4 \text{ atm H}_2, 23 \text{ }^\circ\text{C}]{\text{cat } \mathbf{129} \text{ (5 mol \%)}} \text{R}-\text{CH}_2-\text{CH}_3$				
Entry	Substrate	Time (min)	Conversion (%)	TOF (h ⁻¹)
1		5	>99	>240
2		900	3	0.04
3		5	>99	>240
4		5	>99	>240
5			No conversion	
6		1440 ^a	20	3
7		60 ^a	95	320

^aCatalyst loading 0.3 mol%.

Bianchini et al. (262) explored the iron-catalyzed reduction of ketone in 1993. A trihydride iron(II) catalyst, [(PP₃)Fe(H)(H₂)]BPh₄, was used for transfer hydrogenation, where a superstoichiometric (20 equiv) cyclopentanol or isopropyl alcohol was the hydride source. Reduction of ketone in the presence of an olefin is extremely challenging since the C=C bond is more easily reducible than the C=O bond. Increasing the size of the olefin substituent (R₁), decreases the chance of C=C hydrogenation. A large substituent at ketone (R₂) makes it less polarizable and decreases the probability of hydrogenation of the keto-group. Thus, it was possible to keep C=C unaffected even with a conjugated electron-withdrawing group (Table XLII) (262).

TABLE XLI
Iron-Catalyzed Selective Hydrogenation of Terminal Alkynes

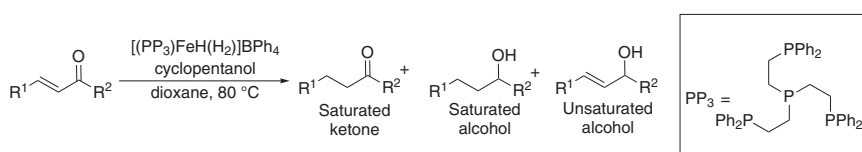


^aThe values in parentheses are the catalyst loading in mol%.

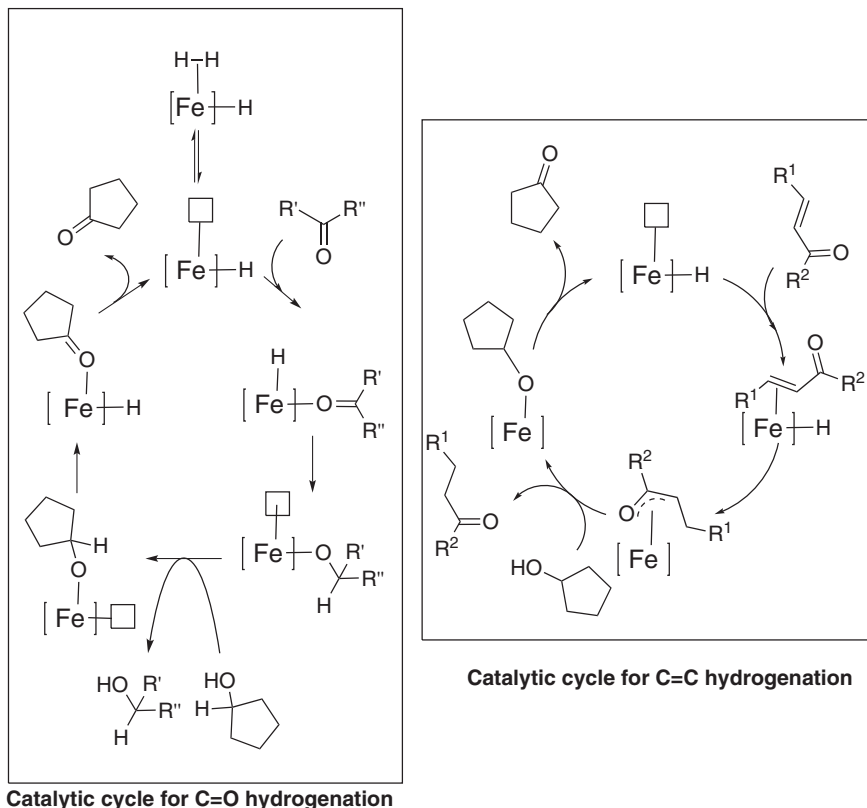
Further interrogation showed that in the presence of H₂ gas, catalytic activity was totally stopped. This result suggested that hydrogen gas coordinates with the metal center and inhibits the substrate to bind with the metal center. For ketone hydrogenation, a catalytic cycle was proposed (Scheme 182) (262), where (a) at first the ketone coordinates with the metal center (may be in either η^1 or η^2 fashion), (b) then the hydride from the metal center is transferred to the keto carbon center through a four-member transition state, (c) the secondary alcohol coordinates with the metal, breaking the M–O bond of the reduced ketone, and (d) finally, the secondary alcohol donates a hydride to the metal center and departs as the ketone. A similar mechanism also has been proposed for the competing hydrogenation of an olefin. In the case of olefin hydrogenation, the C=C bond first coordinates with the metal center in η^2 -fashion and goes through a π -oxa-allyl intermediate. Therefore, any steric hindrance near the keto group prefers olefin hydrogenation more and vice versa.

In 2007, Casey and co-workers (263) reported the first iron-catalyzed efficient chemoselective H₂ hydrogenation of a ketone using the similar catalyst active center of Shvo's ketone hydrogenation catalyst, which replaced ruthenium with iron (**130**) (Table XLIII). Successful hydrogenation with aliphatic and aromatic ketones has proved the utility of this method. Further, the reported reaction condition was milder

TABLE XLII
Chemoselective-Transfer Hydrogenation of α,β -Unsaturated Ketones



Entry	Substrates	Yield of Saturated Ketone (%)	Yield of Saturated Alcohol (%)	Yield of Unsaturated Alcohol (%)
1	$R^1 = Ph; R^2 = Me$ 	0 	0 	95
2	$R^1 = Ph; R^2 = Ph$ 	30 	0 	0
3	$R^1 = Me; R^2 = Ph$ 	7 	0 	0
4	$R^1 = Me; R^2 = Et$ 	19 	0 	0
5	$R^1 = H; R^2 = Et$ 	100 	0 	0
6		0 	44 	28
7		0 	0 	31
8		No reaction	-	-



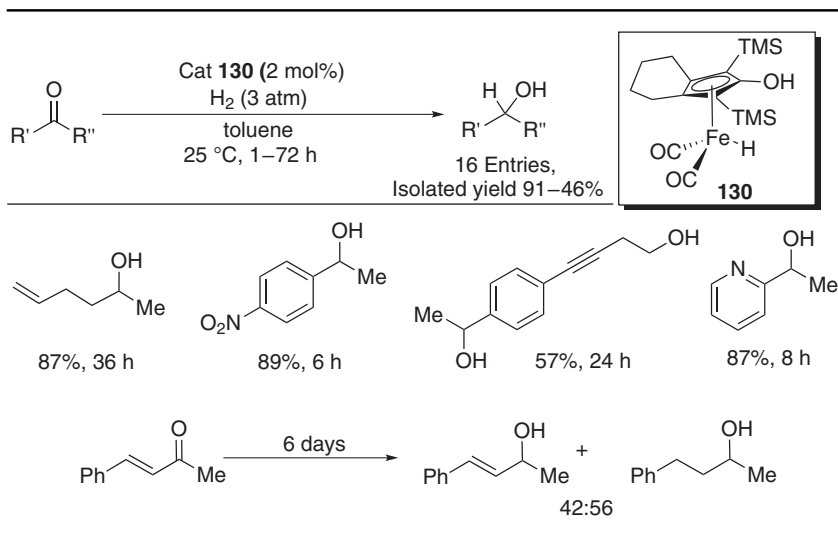
Scheme 182. Catalytic cycle for transfer hydrogenation of α,β -unsaturated ketones.

than Shvo's reaction condition. Functional groups including a nitro and a double bond at the homoallylic position were well tolerated in this system. A ketone with a pyridine moiety was also hydrogenated efficiently. High diastereoselectivity has also been observed in the case of benzoin (*meso/dl* = 25). Under hydrogenation condition, esters, epoxides, alkynes, and alkenes were survived well. Unfortunately, selective hydrogenation of α,β -unsaturated ketone failed to be impressive.

Casey and co-workers (263b) first established the mechanistic details of hydrogenation with Shvo's catalyst. Detailed studies on the hydrogenation of benzaldehyde revealed first-order dependence with respect to both the aldehyde and the catalyst. In addition, a primary kinetic isotope effect for transfer of both RuD and OD was also observed. Since transfer of ^{13}C O from labeled catalyst has not occurred, they proposed an outer-sphere mechanism as depicted in Scheme 183 (263b).

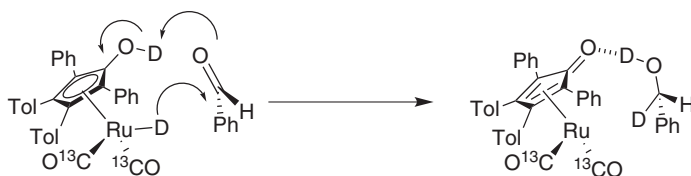
In the case of an iron-based catalyst, Casey's group found similar experimental results and concluded that the iron catalyst is also going through the same

TABLE XLIII
Substrate Scope for Hydrogenation Explored by Casey's Group

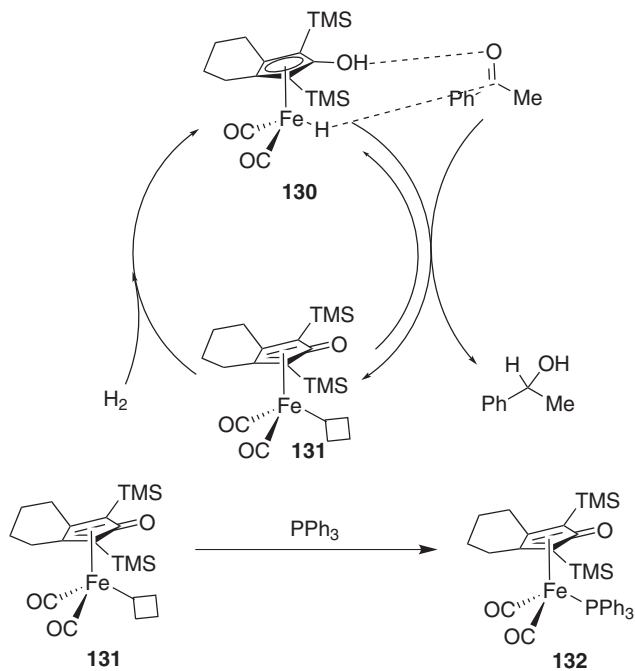


mechanistic pathway as that of ruthenium (Scheme 184) (263a). In the first step, the hydroxyl proton is transferred to the keto-oxygen and hydride is transferred to the keto-carbon. Consequently, hydrogen gas regenerates the catalyst and completes the catalytic cycle. In addition, the proposed intermediate (**131**) was trapped by PPh_3 , which provides further support to this hypothesis. Also, there was no rate dependence on the concentration of PPh_3 . *In situ*, they quantitatively measured the rate of hydrogenation by ReactIR and concluded that hydrogen transfer from the catalyst is the rate-determining step and first order with respect to the catalyst.

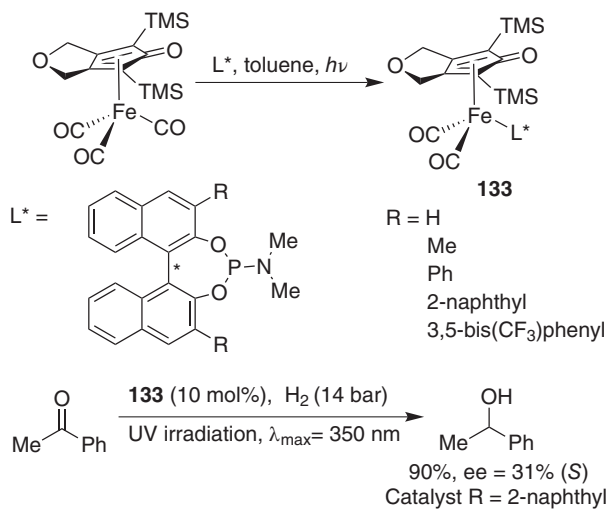
Casey's iron cyclopentadienone catalyst (**130**) with a chiral ligand environment was capable of chiral hydrogenation. In 2012, Berkessel et al. (264) developed a chiral precatalyst (**133**) that replaced one CO of Casey's catalyst with a chiral phosphoramidite ligand under photoirradiation (Scheme 185).



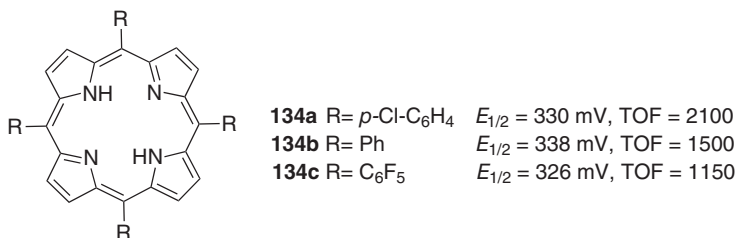
Scheme 183. Labeling experiment on hydrogenation with Shvo' catalyst.



Scheme 184. Outer-sphere mechanism for transfer hydrogenation of ketones.

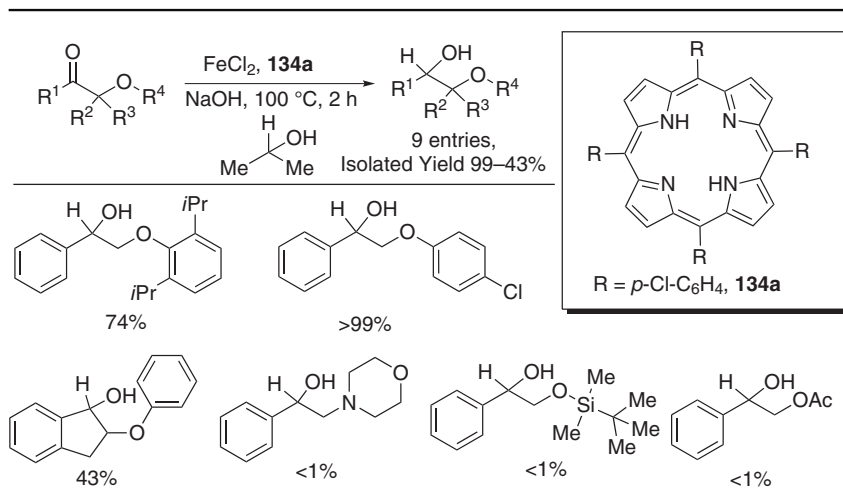


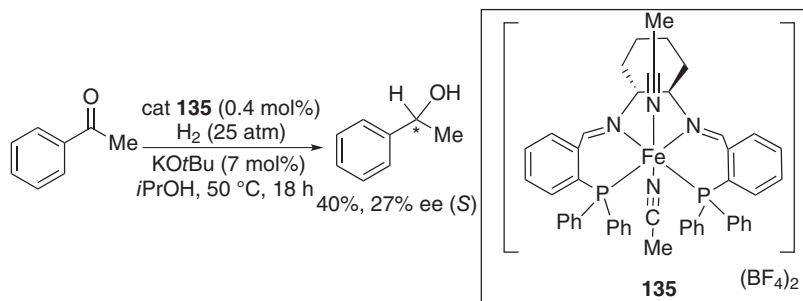
Scheme 185. Enantioselective hydrogenation of a ketone using a chiral phosphoramidite.



Scheme 186. Porphyrin ligands used in transfer-hydrogenation reactions.

Iron–porphyrin systems are also known for transfer hydrogenation. In 2008 Beller and co-workers (265) tested a class of porphyrin derivatives (**134a–134c**) and discovered ligand **134a** (Scheme 186), which showed a good catalytic system with FeCl₂ (Table XLIV) (265). Substitution at the meso-phenylic moiety of the porphyrin system is responsible for tuning the oxidation potential of iron(II) to iron(III). Unfortunately, no clear correlation between the catalytic activity and the oxidation potential can be outlined. Different types of 2-alkoxy- and 2-aryloxy ketones were tested and most of them had shown good-to-moderate yields. Increasing the bulkiness simultaneously at the 2- and 6-positions, yield of hydrogenation reaction decreased. However, a substrate without a six substitution gave a good yield. Unfortunately, other hydroxyl protecting groups like silyl and acetyl were unsuccessful.

 TABLE XLIV
 Substrate Scope for Transfer Hydrogenation Using an Iron–Porphyrin Complex


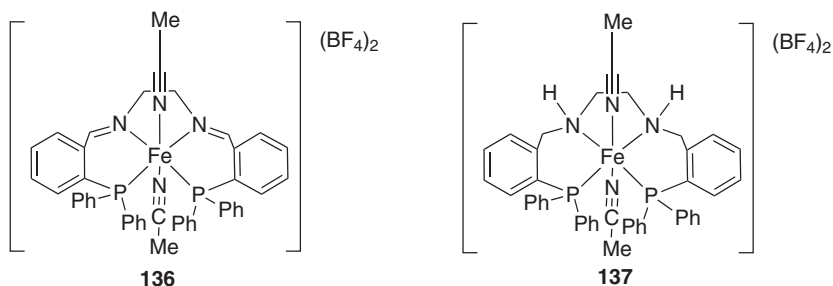


Scheme 187. Asymmetric hydrogenation using iron complexes containing a P–N–N–P based ligand.

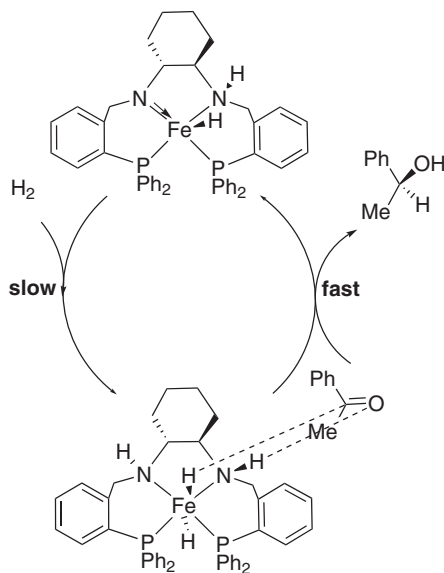
Earlier asymmetric hydrogenation of ketones has been reported with a ruthenium-based catalyst containing P–N–N–P based chiral ligands (Gao's catalyst). Using a P–N–N–P chelated iron catalyst (**135**), Morris and co-workers (266) in 2009 reported hydrogenation under a high-pressured hydrogen atmosphere (Scheme 187). Unfortunately, they failed to extend their substrate scope beyond acetophenone.

Catalyst **136** with P–N–N–P and **137** with P–NH–NH–P ligand systems gave a similar result in the hydrogenation of acetophenone (Scheme 188) (266b). Their similar activity suggested that these two systems go through the same active intermediate. It was also assumed that iron-catalyzed reactions are going through the same reaction pathway as the ruthenium based catalyst *trans*-[RuH₂(P–NH–NH–P)]. Density functional theory (DFT) calculations also proved that iron would have similar activation barriers for ruthenium in the catalytic cycle (266b).

An outer-sphere mechanism was proposed for catalyst **135**, where the N–H proton binds with the carbonyl oxygen and the M–H hydride attacks the carbonyl carbon. Therefore, the alcohol was generated along with an unsaturated imido complex, which cleaved the hydrogen molecule heterolytically and regenerated the



Scheme 188. Iron catalysts for hydrogenation with a P–N–N–P and P–NH–NH–P based ligand.



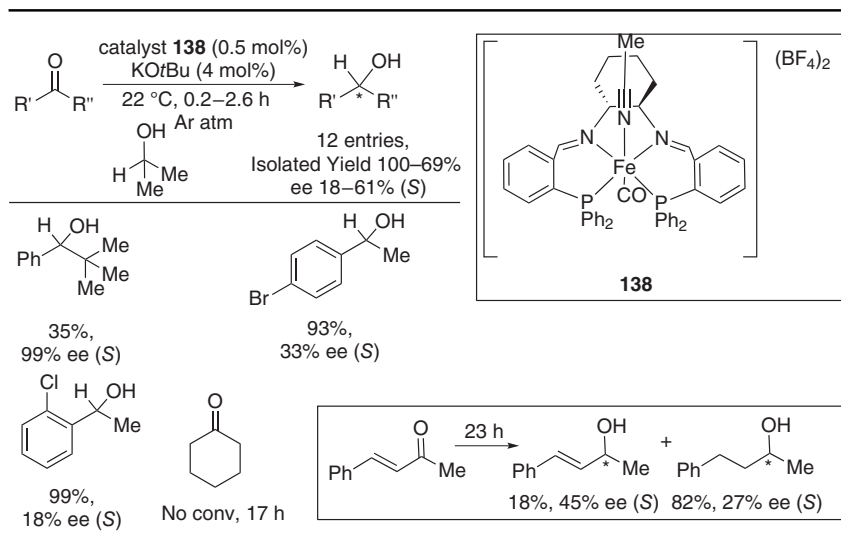
Scheme 189. Iron-catalyzed asymmetric hydrogenation of ketones.

active catalyst. The regeneration step required a high-activation energy and therefore a high-pressure hydrogen atmosphere was needed for smooth functioning of the catalytic cycle (Scheme 189) (266b, 267).

A suitable chiral ligand for iron can promote hydrogenation in an asymmetric fashion. For example, Morris and co-workers (266a, 267–268) found that catalyst **138** was suited for transfer hydrogenation using isopropyl alcohol as the hydride source, as well as the solvent. Functional group variability and moderate-to-good enantioselectivity were notable features of this method. They found that the substituent next to the keto group determined the conversion, as well as the stereoselectivity. From acetophenone to *tert*-butylphenyl ketone, conversion decreased, but selectivity increased. On the other hand, cyclohexylphenyl ketone showed low conversion and less stereoselectivity compared to acetophenone. Unlike the meta position, the π -electron-donating moiety at the para position of the aromatic ketone decreased the stereoselectivity. The method failed to generate the expected product from α,β -unsaturated ketones (Table XLV) (266a). Catalyst **138** followed the same mechanistic pathway as catalyst **135** except for the last step, where a secondary alcohol regenerated the active catalyst (269).

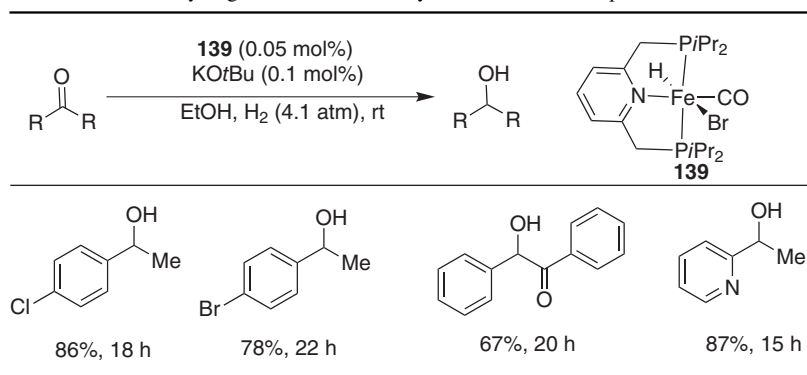
After considerable progress in the development of a phosphorous nitrogen-based iron complex for ketone hydrogenation, Milstein and co-workers (270) reported iron–pincer complexes as effective hydrogenation catalysts (Table XLVI). Even at rt

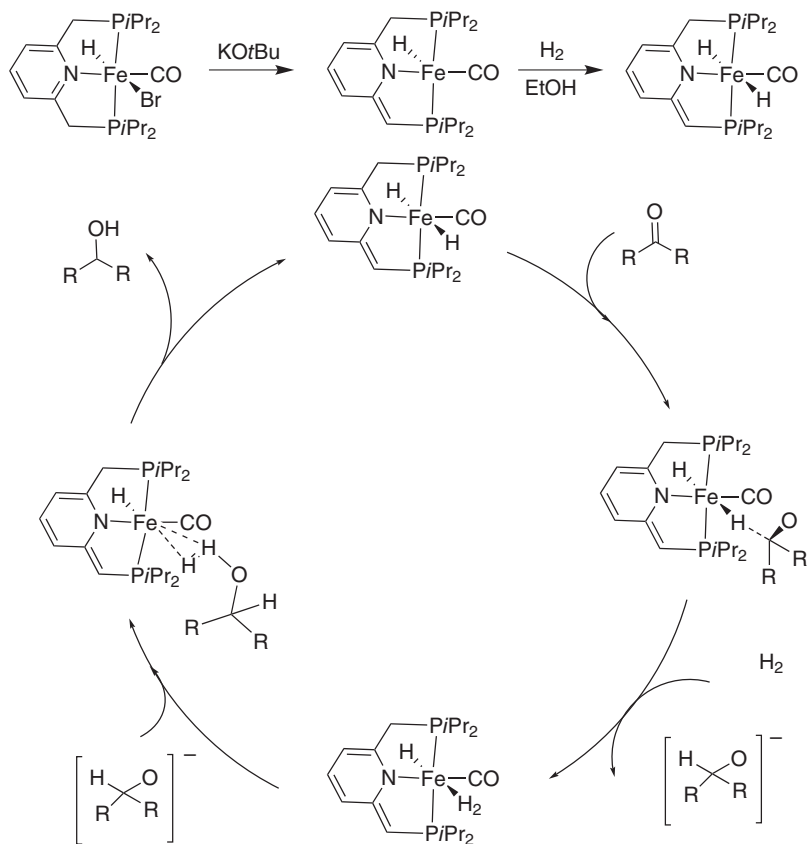
TABLE XLV
Substrate Scope for Iron-Catalyzed Asymmetric-Transfer Hydrogenation



(26–28 °C) and at a relatively low hydrogen pressurized atmosphere (4.1 atm) iron–pincer complex [(*i*PrPNP)FeH(CO)Br] [*i*PrPNP = 2,6-bis(diisopropylphosphino)methylpyridine] (**139**) showed hydrogenation with a broader substrate scope. Halide substituted aromatic ketones and ketones with a pyridine moiety were well tolerated.

TABLE XLVI
Hydrogenation of Ketones by an Iron–Pincer Complex





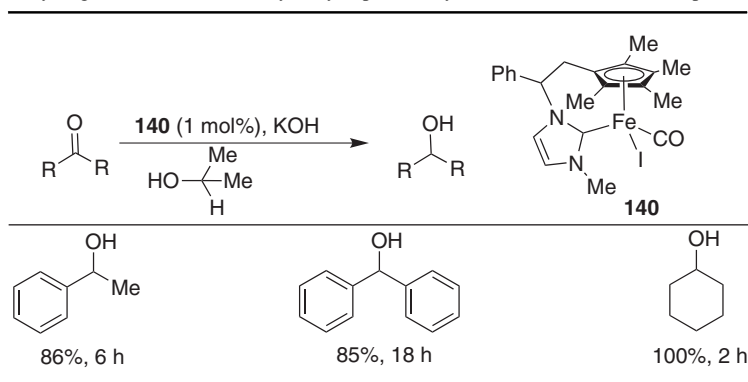
Scheme 190. Catalytic cycle for hydrogenation of ketones with an iron-pincer complex.

The hydrogenation of ketones by the $[(iPrPNP)FeH(CO)Br]$ complex putatively underwent a direct reduction mechanism. The DFT studies by Yang (271) showed that the pincer ligand was not involved in hydride transfer to the ketone carbon, as well as the H_2 molecule cleavage by the hydrido-alkoxo species (Scheme 190). Calculations also showed that the choice of $EtOH$ as the solvent is crucial for H_2 cleavage.

Further studies discovered a tetrahydridoborate iron-pincer complex $[(iPrPNP)FeH(CO)(\eta^1-BH_4)]$ that can promote hydrogenation of ketones with almost the same efficiency without any base (272).

Royo and co-workers (273) reported transfer hydrogenation of ketones using a cyclopentadienyl functionalized NHC iron complex (Table XLVII). Their piano-stool type iron complex (**140**) can accomplish hydrogenation in the presence of

TABLE XLVII
Hydrogenation of a Ketone by a Cyclopentadienyl Functionalized NHC Complex



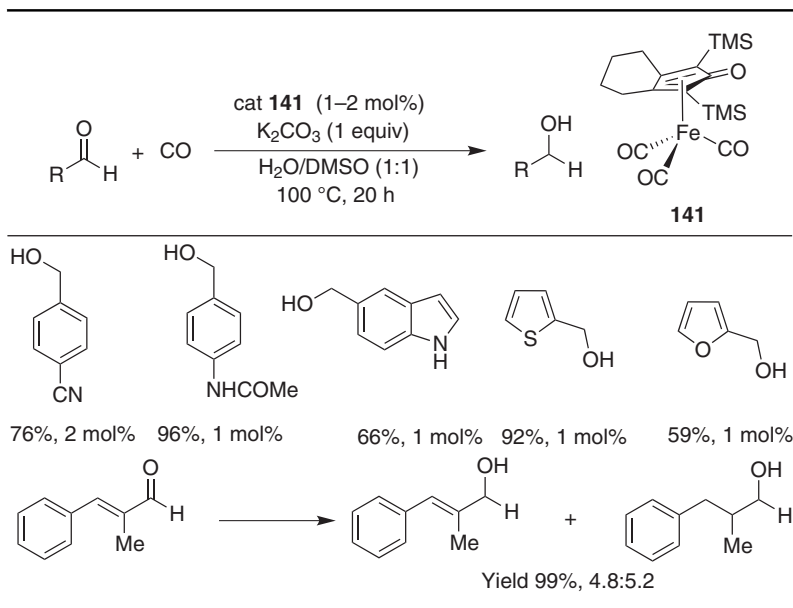
isopropyl alcohol as the hydride source. In 2012, Hashimoto et al. (274) applied an iron(II)-N-heterocyclic carbene complex for transfer hydrogenation. They explored a number of monodentate NHC ligands with an iron(II) complex for catalytic study. Iron NHC complexes $(IMes)_2FeCl_2$, $trans-(IMes)_2FeMe_2$, $(IEtPh^*)_2FeCl_2$ [$IMes = 1,3$ -bis(2,4,6-trimethylphenyl)imidazole-2-ylidene] and $[IEtPh^* = 1,3$ -bis(*R*)-1'-phenylethyl]imidazole-2-ylidene] were efficient in catalytic-transfer hydrogenation.

Recently, Beller and co-workers (275) published reduction of an aldehyde in a water-gas shift condition using Knolker's iron cyclopentadienone complex (**141**) as catalyst (Table XLVIII). They used K_2CO_3 as the base and water as the cosolvent under a CO atmosphere. In their reduction protocol, aromatic and aliphatic aldehyde as well as α,β -unsaturated aldehydes can be employed. Presumably, hydroxide attacked the CO coordinated to the metal center and formed CO_2 and an iron-hydride species. This iron-hydride species was responsible for the reduction.

E. Hydrogenation of Imines

Chiral amine moieties are found in numerous drug and pesticide molecules. The most convenient way of preparing stereochemically active amines is the hydrogenation of imines in an asymmetric way. As expected, plenty of catalytic methods based on transition metals were developed in the past two decades. Iron is most acceptable among other transition metals due to its natural abundance and biorelevance. The reduction of imines is more challenging since they are much more sensitive toward hydrolysis and other side reactions. This problem is settled

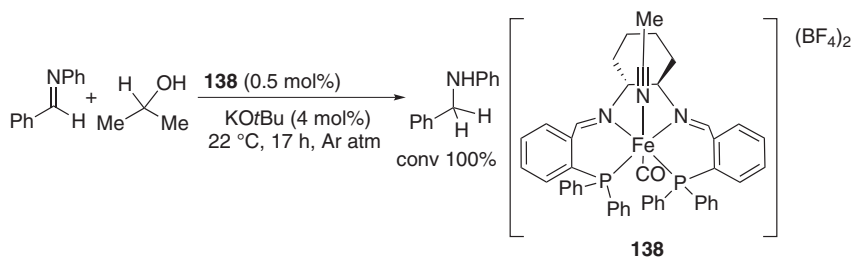
TABLE XLVIII
Iron-Catalyzed Reduction of Aldehyde Using a Water–Gas Shift Condition



by electronic or steric protection (e.g., phosphinoyl, sulfonyl) of imines prior to hydrogenation and then deprotection.

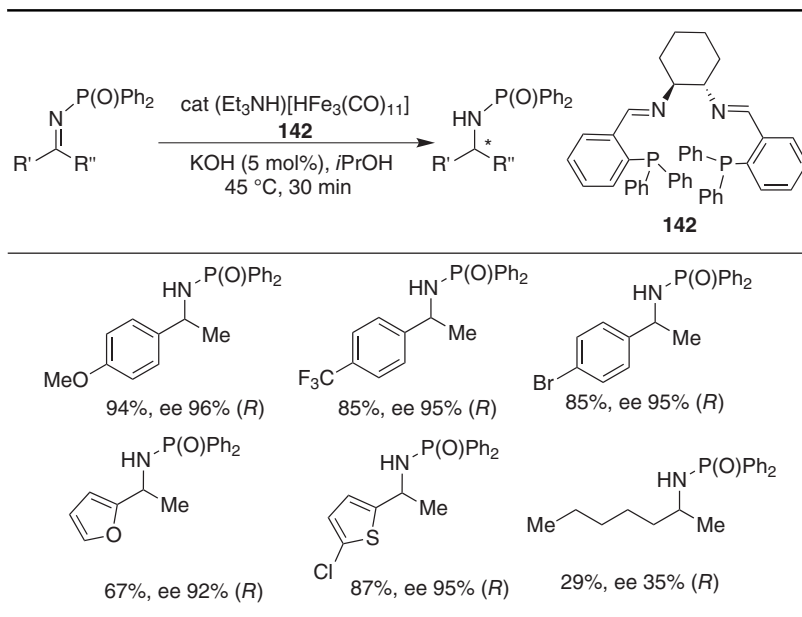
In 2008, Morris and co-workers (266a) showed that the iron–PNNP [P(2)(N2)] ligated complex (**138**) can hydrogenate *N*-benzylideneaniline (Ph-CH=NPh) (Scheme 191). Unfortunately, the same condition completely failed for *N*-(1-phenylethylidene)aniline (Ph-CMe=NPh).

After Morris, Beller and co-workers (276) reported the iron-catalyzed asymmetric hydrogenation of imines (Table XLIX). They used the iron(II) hydride



Scheme 191. Hydrogenation of imine by an Fe^{II} -PNNP ligated complex.

TABLE XLIX
Asymmetric Hydrogenation of *N*-(Diphenylphosphinyl)imines

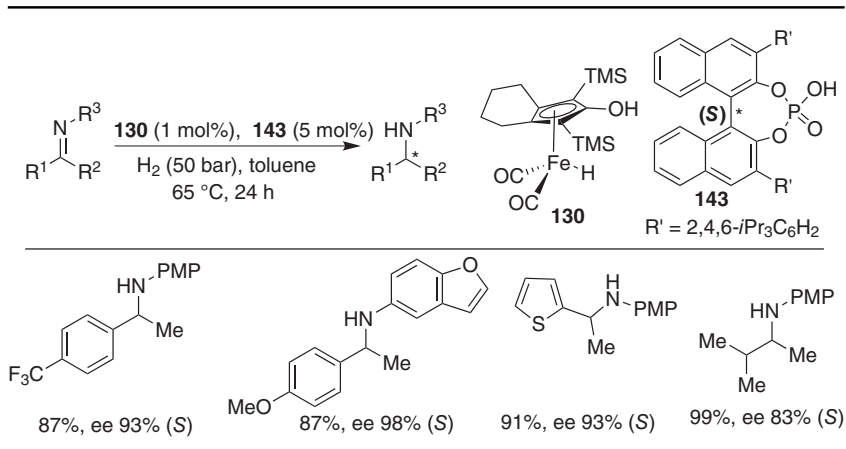


carbonyl complex with the chiral PNNP ligand (**142**) for asymmetric hydrogenation of *N*-(diphenylphosphinyl)imines. Aromatic and heterocyclic imines were efficiently hydrogenated with up to 99% ee. But, aliphatic imines failed to give a meaningful conversion, as well as stereoselectivity.

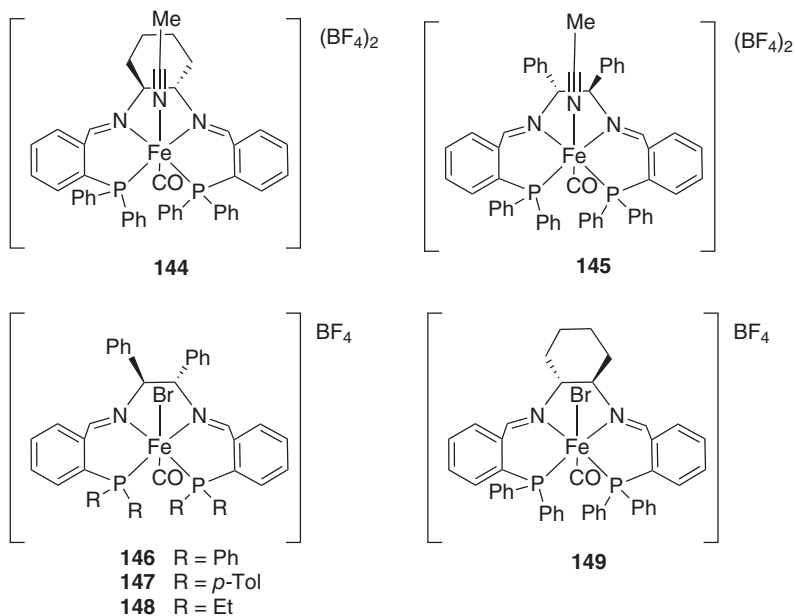
A year later, the asymmetric hydrogenation reaction of *N*-(1-phenylethylidene)aniline (Ph-CMe=NPh) was demonstrated by Beller and co-workers (277) using the Knolker iron cyclopentadienone complex (**130**) with a chiral phosphate ligand (**143**) (Table L). It is notable that this type of imine was unreactive toward Morris's catalyst. In the current reaction protocol, a class of aromatic ketamines was hydrogenated stereoselectively.

In 2012, Morris and co-workers (278) demonstrated a class of iron–PNNP based precatalyst for asymmetric-transfer hydrogenation of *N*-(diphenylphosphinyl)imines. They observed that the catalytic activity was dependent on the substituent on the phosphorous atom or the type of diamine. Catalyst **148** gave very low hydrogenation conversion due to the presence of an electron-donating ethyl group on the phosphorous atom. However, catalyst **146** was efficient in conversion, as well as in stereoselectivity. Aromatic and heterocyclic *N*-(diphenylphosphinyl)-imines were efficiently hydrogenated with good conversion and excellent stereoselectivity (Scheme 192).

TABLE L
Hydrogenation of Imine by the Knolker Iron Cyclopentadienone Complex^a



^a *p*-Methoxyphenyl = PMP.



Scheme 192. Hydrogenation of the imine by a Knolker iron–cyclopentadienone complex.

F. Reduction of Nitroarene to Anilines

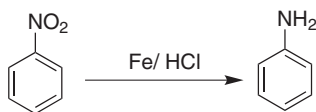
In synthetic chemistry, reduction of diverse functional groups is an indispensable protocol. Hydrogenation of nitro compounds to the corresponding amines is considered as one of the most important and classical methods for the production of amines. Since amine derivatives are valuable intermediates for the manufacture of many agrochemicals, pharmaceuticals, dyes, and pigments, it is important to develop economically feasible catalytic processes for this transformation.

The selective reduction of the nitro group is often difficult when other reducible groups (e.g., carbon-carbon or carbon-nitrogen double or triple bonds, carbonyl or benzyl groups, and multiple Cl, Br, or I substituents) are present in the same molecule. Continuous progress has been made and is still going on in this area to produce a catalytic method based on iron that can selectively reduce the nitro group to the corresponding amines. In this section, iron-based nitro reduction has been compiled.

Bachamp (279a) used iron in a stoichiometric amount for the reduction of nitro compounds to amines with Fe/HCl (Scheme 193). This reaction was originally used to produce large amounts of aniline for industry, but this reaction is the most vigorous reduction method producing merely the amino products. Therefore, if the aromatic moiety contains substituents prone to being reduced (e.g., carbonyl, cyano, azo, or further nitro groups) a significant amount of the byproducts will be produced.

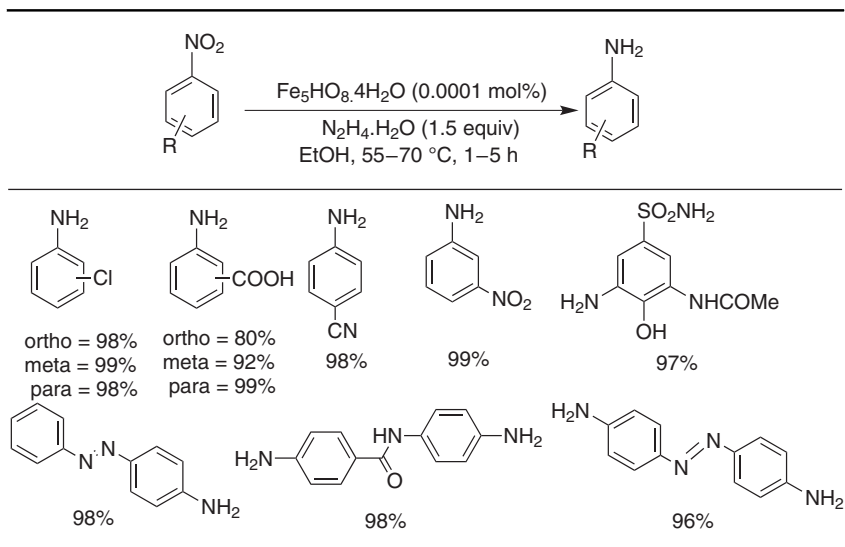
In 1998, Lauwiner et al. (279) applied an iron oxide-hydroxide as a catalyst for the reduction of various substituted nitroarenes to produce the corresponding amines (Table LI). Hydrazine hydrate was applied as the hydrogen source. Various functional groups (e.g., halide, hydroxyl, amide, and acid) were well tolerated. The important finding was that regioselective reduction of 1,3-dinitrobenzene produce the corresponding 3-nitroanilines, but the method was not applicable for 1,2- and 1,4-dinitrobenzene. In most cases, an excellent yield was reported. The reaction kinetics was measured to determine the dependence of the rate of reduction on the nature and position of additional substituents other than the nitro group. It was observed that the rate is enhanced by electron-withdrawing substituents and decreased by electron-donating groups (279).

The same group reported the reduction of a series of monosubstituted 3- and 4-nitrophenylazobenzenes with hydrazine hydrate in the presence of the iron oxide-hydroxide catalyst (Scheme 194) (280). Their study revealed that selectivity for the nitro group reduction versus that of the azo bridge in substituted



Scheme 193.

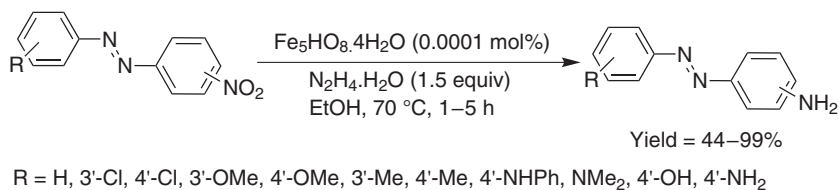
TABLE LI
Iron Oxide–Hydroxide Catalyzed Reduction of Substituted Nitroarenes



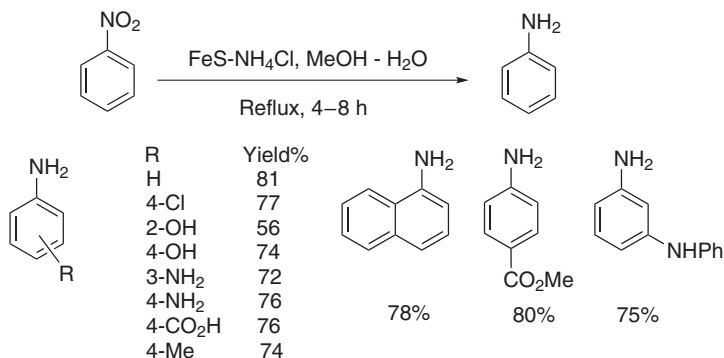
nitrophenylazobenzenes is higher than for the para nitro group than for the azo bridge, than for the corresponding meta counterparts. This selectivity was enhanced with the stronger electron-attracting properties of the substituent. Moreover, the selectivity for the reduction of the nitro group versus that of the azo function can be enhanced by increasing the reaction temperature (280).

Desai et al. (281) applied mild, neutral, ecofriendly, and a useful $\text{FeS}-\text{NH}_4\text{Cl}-\text{MeOH}-\text{H}_2\text{O}$ system for the reduction of nitroarenes to anilines (Scheme 195).

In 2003, Sonavane et al. (282) applied recyclable trivalent iron substituted hexagonal mesoporous aluminophosphate (FeHMA), for catalytic-transfer hydrogenation of aromatic nitro compounds using isopropyl alcohol as donor (Table LII). High chemo- and regioselectivity was reported in the studied substrates. The catalyst



Scheme 194.



Scheme 195.

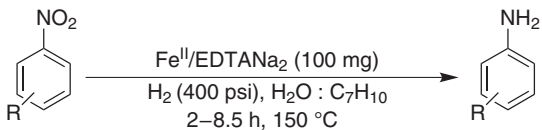
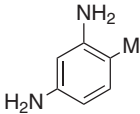
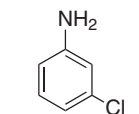
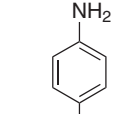
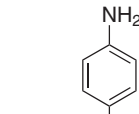
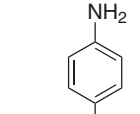
was recycled up to six times without any loss in selectivity. It was observed that the regioselectivity depended on the reaction time (282).

In 2004, Deshpande et al. (282b) reported chemoselective reduction of substituted nitroarenes that correspond to amines by using water soluble iron ethylenediaminetetraacetic acid disodium salt ($\text{Fe}^{\text{II}}/\text{EDTANa}_2$) with molecular hydrogen (Table LIII). They applied this catalyst for hydrogenation in a biphasic toluene–water system to achieve selectivity and recyclability. Catalyst remained in the aqueous phase, while the nitro substrate and the product formed in the organic layer. A comparison of reactivity of this water soluble iron salt showed little decrease in activity, which may be due to the coordination of EDTANa_2 and also due to the fact that catalyst remained in the aqueous phase. Excellent chemoselectivity with a

TABLE LII
The FeHMA Catalyzed Transfer Hydrogenation of Aromatic Nitro Compounds

	$\xrightarrow[\text{KOH (20 mmol), MeCH(OH)Me (20 mL)}]{\text{FeHMA (100 mg)}}$					
First run 82% Six run 81%	First run 74% Six run 74%	First run 83% Six run 83%	First run 83% Six run 83%	First run 80% Six run 80%		

TABLE LIII
 $\text{Fe}^{\text{II}}/\text{EDTANa}_2^a$ Catalyzed Hydrogenation of Aromatic Nitro Compounds

				
 Yield = 84.6% TOF (h^{-1}) = 134	 Yield = 99.0% TOF (h^{-1}) = 434	 Yield = 99.0% TOF (h^{-1}) = 208	 Yield = 85.8% TOF (h^{-1}) = 393	 Yield = 90.1% TOF (h^{-1}) = 99

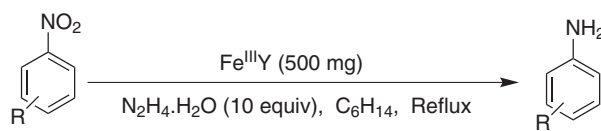
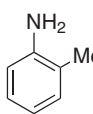
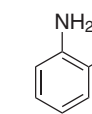
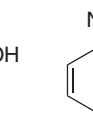
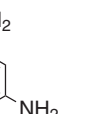
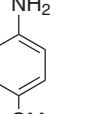
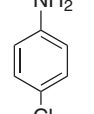
^aEthylenediaminetetraacetic acid = EDTA.

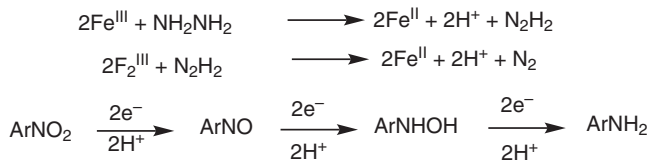
good-to-excellent yield was observed in most of the studied substrates with a TOF (h^{-1}) range between 99 and 529.

A solid-supported catalysis has a number of advantages over conventional solution-phase reaction because of the good dispersion of active sites leading to more reactivity (Table LIV). Kumarraja and Pitchumani (283) applied the iron(III) cation exchanged faujasite zeolite for selective reduction of nitro arenes to the corresponding amines with hydrazine hydrate. A nonpolar solvent (e.g., hexane) was used. Polar solvents lead to a decrease in yield by occupying the zeolite cavity and thereby forcing the substrate into the solvent phase.

Kumarraja and Pitchuman (283) author also proposed an electron-transport based mechanism for the reduction (Scheme 196). Hydrazine hydrate leads to the

TABLE LIV
 The Iron(III) Cation Exchanged Faujasite Zeolite-Catalyzed Reduction of Aromatic Nitro Compounds

					
 91%	 91%	 100%	 100%	 63%	 88%



Scheme 196.

one-electron reduction of ferric ion to the ferrous ion and generation of a proton. Finally, oxidation of ferrous ion to ferric ion leads to electron transfer to nitrobenzene. An initial four-electron process leads to hydroxylamine, which was finally reduced to aniline in a two-electron process.

Liu et al. (284) applied activated iron for the reduction of nitroarenes (Table LV). Iron powder was preactivated by hydrochloric acid and then used as a catalyst for the reaction. Other tested acids (e.g. acetic acid, sulfuric acid, and phosphoric acid) did not provide the appropriate yield of the desired amine. Liu et al. (284) had also activated iron with zinc powder in the presence of ammonium chloride. Similar results were obtained as in the case of the acid-activated iron catalyst. Though an excess of iron metal (5 equiv) was used, a sensitive functional group (e.g., cyano, olefin double bond, and carbonyl) were well tolerated.

Shi et al. (285) applied $\text{Fe}_2\text{O}_3\text{-MgO}$ as a catalyst for the reduction of the pharmaceutically important sulfur-containing nitro compounds to amines by using hydrazine hydrate as the hydrogen source (Table LVI). Sulfur-containing compounds are generally considered difficult because of the poisoning of the catalyst, but Shi et al. (285) applied $\text{Fe}_2\text{O}_3\text{-MgO}$ successfully to obtain good yields of the corresponding sulfur-containing amines.

Gamble et al. (286) applied iron powder for selective reduction of nitro compounds under ultrasonic irradiation (35 kHz) (Table LVII). It was proposed

TABLE LV
Activated Iron-Catalyzed Reduction of Nitroarenes

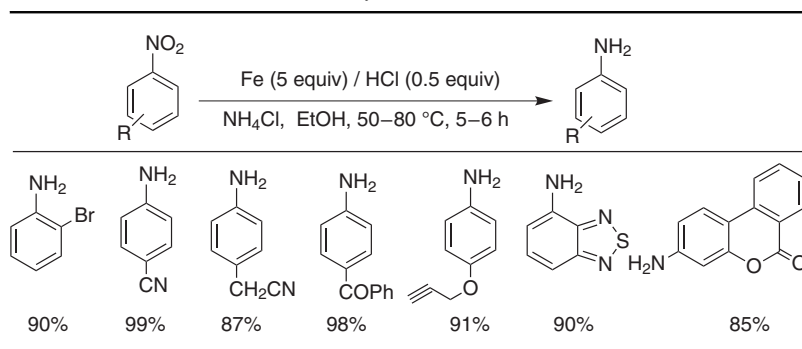
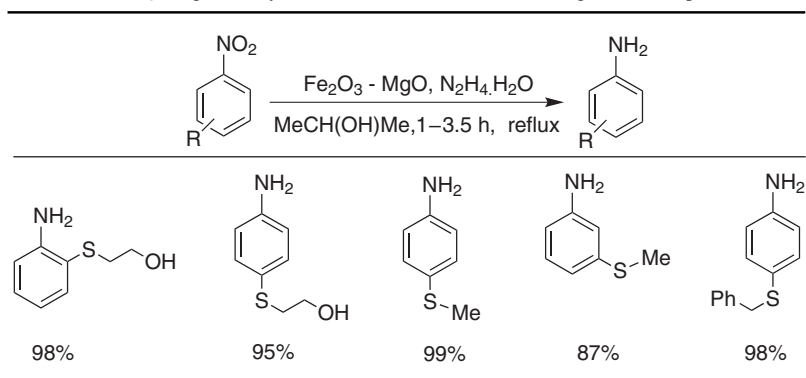


TABLE LVI
The Fe₂O₃-MgO Catalyzed Reduction of Sulfur-Containing Nitro Compounds



that ultrasonication helps in cleaning and activation of the surface of metal reagents, consequently resulting in the activation of the metal catalyst. Tri- or tetrasubstituted substrates were tested for the reduction. Good yields were reported in most cases.

Iron-catalyzed reduction of nitro compounds to amines was mostly carried out using hydrazine hydrate as the hydrogen source. In 2010, Chandrappa et al. (287) for the first time carried out rapid catalytic transfer hydrogenation using a stoichiometric amount of an Fe-CaCl₂ combination in a water: ethanol mixture (Table LVIII). Various functional groups (e.g., cyano, carbonyl, halide, and amide) were well tolerated.

TABLE LVII
Iron Powder Catalyzed Reduction of Nitro Compounds Under Ultrasonic Irradiation

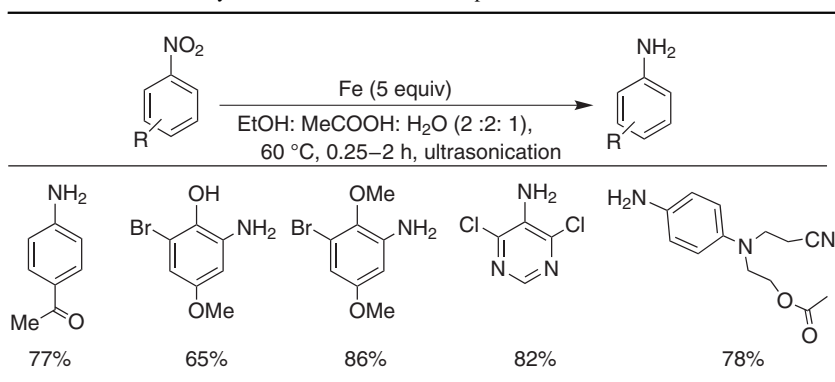
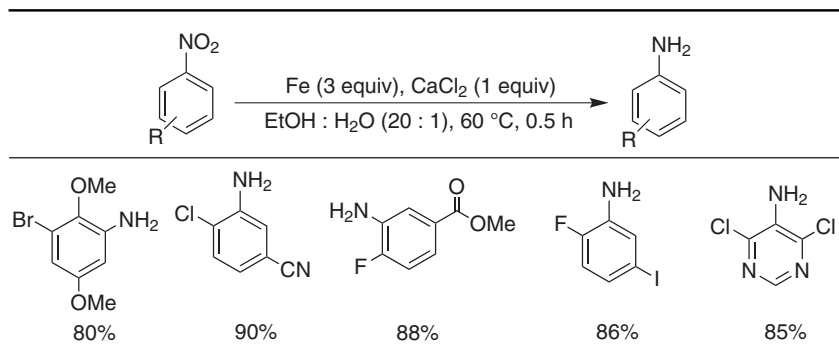
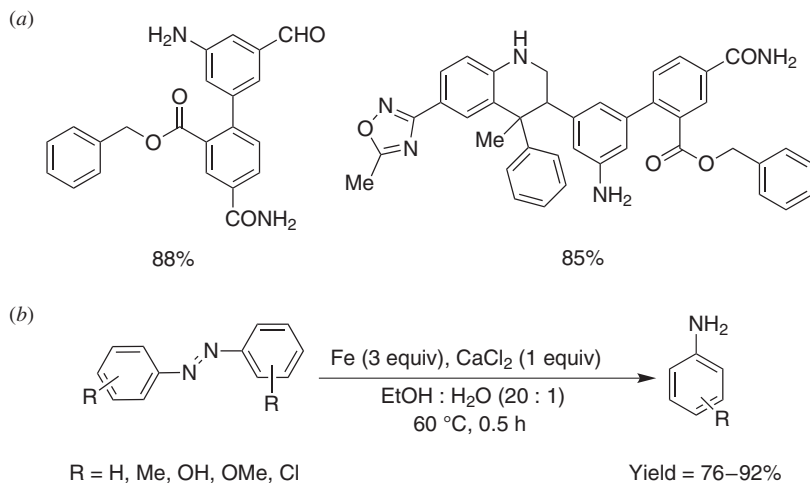


TABLE LVIII
The Fe/CaCl₂ Catalyzed Reduction of Nitro Compounds

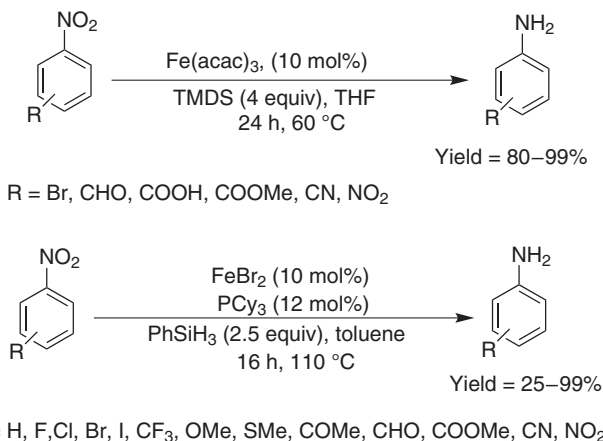


Most importantly, good yields were obtained in the multisubstituted macro-molecules as well (Scheme 197a). This method was also applicable for the reduction of azo compounds to the corresponding amines (Scheme 197b) (287).

In 2010, Beller and co-workers (289) and Lemaire and co-workers (288) independently reported the iron-catalyzed reduction of nitro compounds to the corresponding amines by using silanes as the hydrogen source (Scheme 198). These requests gave the first report on the use of an iron–silane combination for nitro reduction. Beller and co-workers (289) applied ferrous bromide, phosphine



Scheme 197.

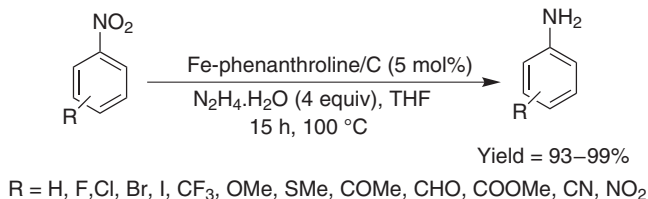


Scheme 198.

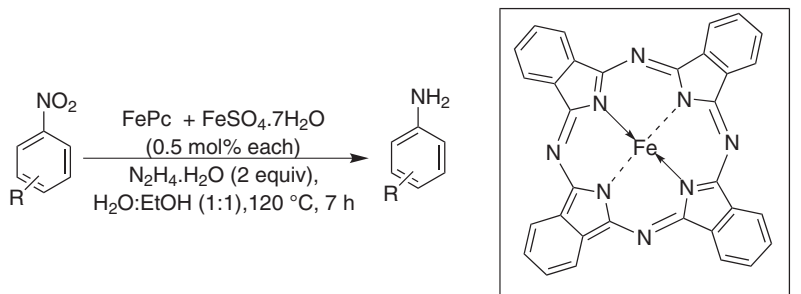
ligand and triphenyl silane, whereas Lemaire and co-workers (288) applied $\text{Fe}(\text{acac})_3$ and 1,1,3,3-tetramethyldisiloxane (TMDSO) without using any ligand, but the substrate scope was much less.

In 2011, Beller and co-workers (289) applied Fe–phenanthroline–C as a heterogeneous catalyst for highly chemoselective reduction of nitro aromatic compounds (Scheme 199). The combination of $\text{Fe}(\text{OAc})_2$ –phenanthroline–C provided only 10% conversion even after 24 h, but the pyrolysis of the *in situ* generated $\text{Fe}(\text{OAc})_2$ –phenanthroline complex supported on carbon led to full conversion of the nitro compounds to the corresponding amines. Challenging functional groups (e.g., halide, cyano, ester, double, and triple bonds) were well tolerated [289].

Sharma et al. (290) applied a combination of iron phthalocyanine and an iron salt for a highly chemo- and regioselective reduction of aromatic nitro compounds in a green solvent (water–ethanol) system using hydrazine hydrate as the hydrogen source (Scheme 200). Iron phthalocyanine and iron sulfate were also studied as a separate catalyst, but the combination of both produce a better result than



Scheme 199.



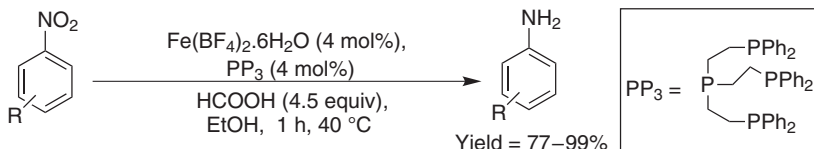
R = -F, -Cl, -Br, -I, -OH, -OMe, -COOH, -CN, -COOMe, -CONH₂, -NO₂, -NHCH₂Ph
 Pc = Phthalocyanine

Scheme 200.

individuals do. The reduction sensitive functional group was well tolerated. The most important finding of this method was the regioselective reduction of the nitro group and tolerance of an *N*-benzyl and an *O*-benzyl functional group, which are generally considered acid–base sensitive.

Beller and co-workers (291) further reported the first base-free catalytic-transfer hydrogenation of nitroarenes (Scheme 201). An iron-based catalyst and a phosphine ligand combination was applied in the presence of formic acid as the hydrogen source at ambient temperature in a green solvent (ethanol). This method avoids the use of any base, which is generally required for the catalytic-transfer hydrogenation. High chemoselectivity with good-to-excellent yield was reported for most of the studied substrates (291).

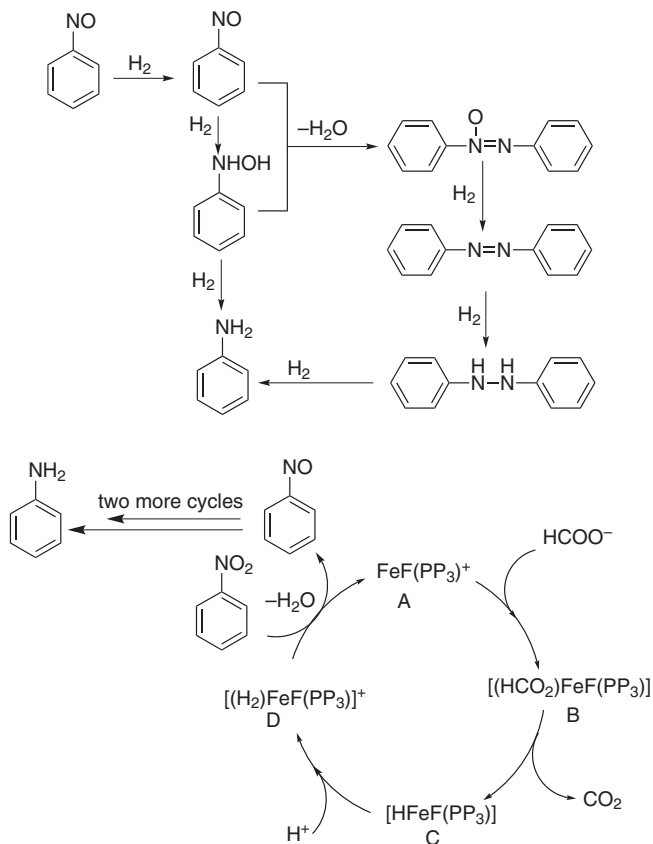
To confirm that the nitro group is reduced by catalytic-transfer hydrogenation and not by hydrogen generated from dehydrogenation of the formic acid, the reduction was performed under a 5-bar hydrogen pressure in the presence of an iron catalyst. No reduction was observed, which confirmed the catalytic-transfer hydrogenation. Beller and co-workers (291) also analyzed the gas phase of the reaction mixture. A 3.2: 1 ratio of carbon monoxide to hydrogen was observed. This ratio showed that only 31% of the consumed formic acid was decomposed to hydrogen showing the necessity of using 4.5 equiv of acid.



R = F, Cl, Br, I, CF₃, OMe, SMe, COMe, CHO, COOMe, CN, NO₂

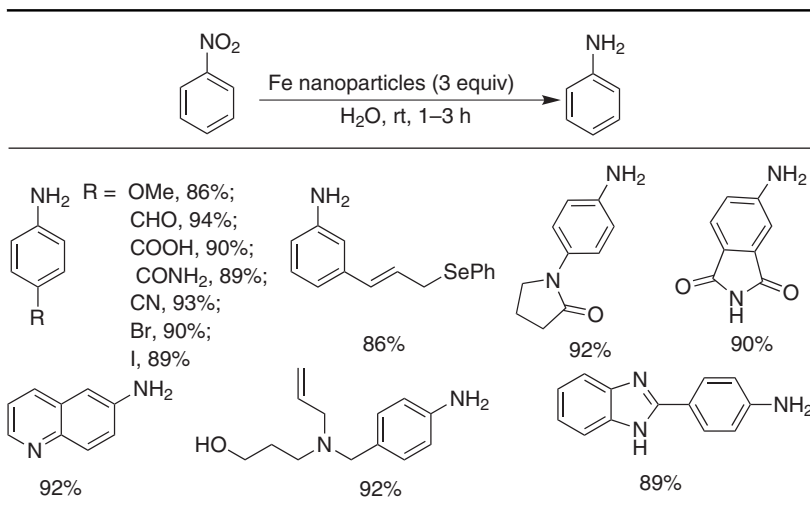
Scheme 201.

Reduction of a nitro group to an amine can proceed by two mechanisms: through hydroxylamine or through azobenzene. To confirm which pathway was followed, the authors analyzed the reaction mixture and only a small quantity of azobenzene (<1%) was observed. Further, the direct reduction of azobenzene resulted in only a 48% conversion and 5 % yield of aniline clearly indicating the direct reduction pathway in their reaction. On the basis of these results and isolated iron complexes, it was proposed that the $[\text{FeF}(\text{PP}_2)]^+$ (A) cation act as the active catalyst. This cation coordinated to formate leading to the neutral complex (B). A β -hydride elimination from B resulted in complex C, with the elimination of carbon dioxide. This reaction was followed by protonation of complex C by formic acid leading to the iron dihydride complex D that reduced the nitrobenzene to nitrosobenzene. This cycle was repeated two more times to yield aniline (Scheme 202).



Scheme 202.

TABLE LIX
Iron Nanoparticle-Catalyzed Reduction of Nitro Compounds



Nanoparticles have unique properties compared to the bulk material due to their high surface-to-volume ratio. Iron nanoparticles have been applied for the selective reduction of aromatic nitro compounds in water without using any additional hydrogen source at rt (Table LIX). It was proposed that the hydrogen coordinated iron nanoparticles are responsible for the hydride atom. This weak hydride acted as a target specific reducing agent for the highly electrophilic nitro group. Good-to-excellent yield was observed with high chemoselectivity in most of the substrates. In this method, an excess amount of iron nanoparticles (i.e., 3 equiv) was applied, which need improvements.

Cantillo et al. (292) applied *in situ* formed iron nanoparticles in a catalytic manner for the reduction of nitro compounds using a microwave. Hydrazine hydrate was used as the hydrogen source and the reaction time was 2–8 min. This method has the advantage of being homogenous as the colloidal nanocrystals remain in the solution. Then nanocrystals start to aggregate forming a precipitate, and therefore making the reaction mixture heterogeneous. After completion, the nanocrystals can be removed easily by using a magnet. Products were purified simply by filtration and excellent yields were observed for all the selected substrates. This method was also applied for the synthesis of amines up to the gram scale using a continuous-flow method.

G. Hydrogenation of Carbon Dioxide and Bicarbonate

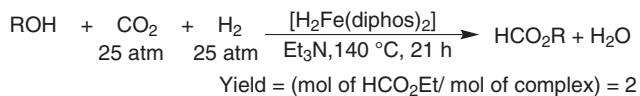
Carbon dioxide is a widely available carbon source and also has a greenhouse effect on the environment. Therefore, the reduction of carbon dioxide to formate is a breakthrough from both the industrial, as well as the environmental, viewpoint. For the same reason, a number of methods involving rhodium, ruthenium, iridium, and palladium were developed in the last 20 years. In 1975, Inoue et al. (293) reported that group 7 transition metal complexes including iron could generate formate from carbon dioxide, hydrogen, and alcohol in the presence of a tertiary amine. The iron complex $[\text{H}_2\text{Fe}(\text{diphos})_2]$ was tested with high pressurized CO_2 and H_2 at 140°C (Scheme 203, diphos = 1,2-bis(diphenylphosphino)ethane).

In 1978, Evans and Newell (294) reported an anionic iron-hydride complex $[\text{HFe}(\text{CO})_4]^-$ for carbon dioxide reduction. Their method suffered from the use of a high-pressure gas and high temperature. Later, Jessop and co-workers (295) designed a high-pressure combinatorial screening process using pressure sustainable apparatus (up to 200 bar). Their process established that a catalytic amount of FeCl_3 , depe ($\text{C}_2\text{PCH}_2\text{CH}_2\text{PC}_2$) and DBU (1,8-diazabicyclo[5.4.0]undec-7-ene) is essential for generation of formate under 100-bar hydrogen and carbon dioxide atmosphere.

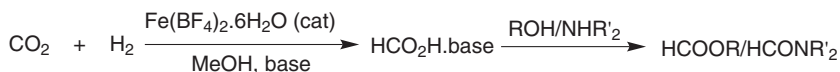
Beller and co-workers (296) reduced bicarbonate to formate (and formamide) in the presence of catalytic $\text{Fe}(\text{BF}_4)_2 \cdot 6\text{H}_2\text{O}$ and PP_3 as ligand [$\text{PP}_3 = \text{P}(\text{CH}_2\text{CH}_2\text{PPh}_2)_3$]. A reasonable TON = 610 was attained under 60 bar H_2 at 80°C (Scheme 204).

In 2012, Beller and co-workers (296) reported an improved version for hydrogenation of carbon dioxide and bicarbonate using a catalytic amount of $\text{Fe}(\text{BF}_4)_2 \cdot 6\text{H}_2\text{O}$. Their catalytic proposal included formation of $[\text{FeH}(\text{H}_2)(\text{PP}_3)]$ from $\text{Fe}(\text{BF}_4)_2$ in the presence of H_2 gas and base (Scheme 205) (297). Afterward, reaction of carbon dioxide and hydride, generated formate. Both the $[\text{FeH}(\text{H}_2)(\text{PP}_3)]^+$ and $[\text{FeH}(\text{CO}_2)(\text{PP}_3)]^+$ intermediates were characterized by nuclear magnetic resonance (NMR) spectroscopy. In the last step, H_2 gas regenerated the catalytic species and removed formic acid.

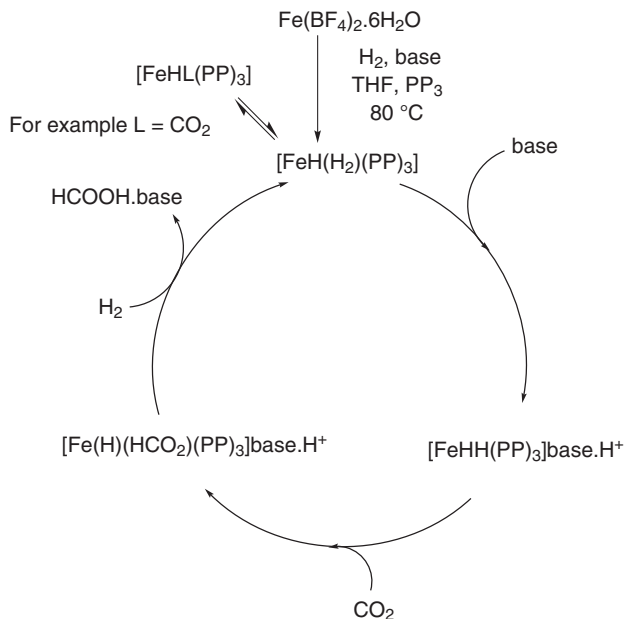
A number of pincer complexes were reported with higher row transitional metals (Ir, Ru) for CO_2 hydrogenation. The strong donating ability of the pincer



Scheme 203. Hydrogenation of Carbon Dioxide Using $[\text{H}_2\text{Fe}(\text{diphos})_2]$.

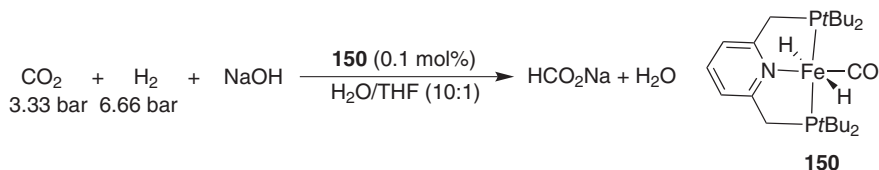


Scheme 204. Catalytic hydrogenation of CO_2 and formation of formate ester and formamides.

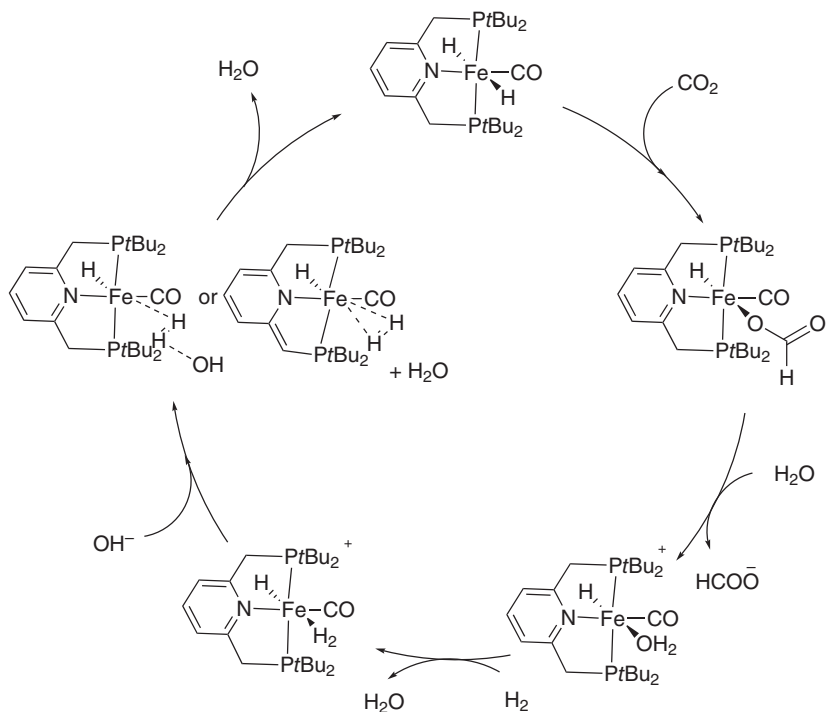


Scheme 205. Mechanism for hydrogenation catalyzed by $\text{Fe}(\text{BF}_4)_2 \cdot 6\text{H}_2\text{O}$.

ligands facilitated the insertion of carbon dioxide into the metal-hydride bonds. In 2011, Milstein and co-workers (298) studied the iron–pincer complex *trans*- $[(t\text{Bu-PNP})\text{Fe}(\text{H})_2(\text{CO})]$ (**150**) for effective hydrogenation of carbon dioxide and bicarbonates (Scheme 206). In their hydrogenation protocol, carbon dioxide was hydrogenated under low-pressure hydrogen (6.66 bar) and a carbon dioxide (3.33 bar) atmosphere with a TOF of 156 h^{-1} . Hydride directly attacked CO_2 generating formate, which was subsequently replaced by the cosolvent water. This water molecule was displaced by H_2 in the next step. In a final step of the catalytic cycle, *trans*- $[(t\text{Bu-PNP})\text{Fe}(\text{H})_2(\text{CO})]$ (**150**) was regenerated through the heterolytic cleavage of the H_2 molecule in the presence of base or dearomatization and successive proton transfer (Scheme 207) (298).



Scheme 206. Hydrogenation of carbon dioxide using an iron–pincer complex.



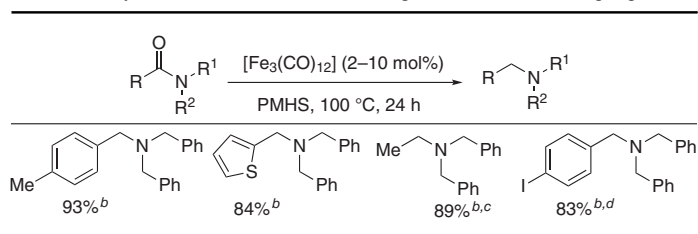
Scheme 207. Hydrogenation of carbon dioxide with an iron-pincer complex.

H. Amide Reduction

Beller and co-workers (299) developed a very convenient and general method of amide reduction for the synthesis of amine derivatives. During their study on iron-catalyzed dehydrations of primary amides in the presence of polymethylhydrosilanes (PMHS) as the reducing agent, a secondary amine was obtained as the byproduct. From their details investigation, they were able to develop a method for amide reduction. They used a $\text{Fe}_3(\text{CO})_{12}$ complex as the catalyst in the presence of PMHS as the reducing agent. This finding was the first report of an iron-catalyzed hydrosilylation of amides to an amine (Table LX).

The iron precursor formed an activated species that resulted in hydrosilylations of the carbonyl group in the amide to generate *O*-silylated *N,O*-acetal (**151**). Subsequently, **151** transformed to **152**, which was further reduced to the amine with a second equivalent of activated species (Scheme 208).

TABLE LX
Iron-Catalyzed Reduction of Amides Using PMHS as a Reducing Agent^a

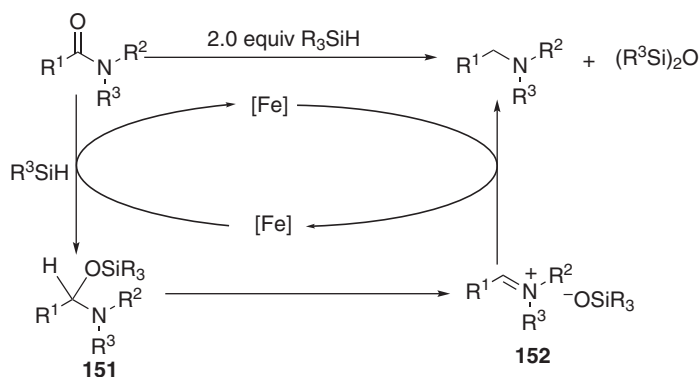


^a Reaction conditions: Amide (1 mol), $[\text{Fe}_3(\text{CO})_{12}]$ (2–10 mol%), PMHS (4–8 mmol), $n\text{Bu}_2\text{O}$ (5 mL).

^b Yield of isolated product.

^c Toluene as solvent.

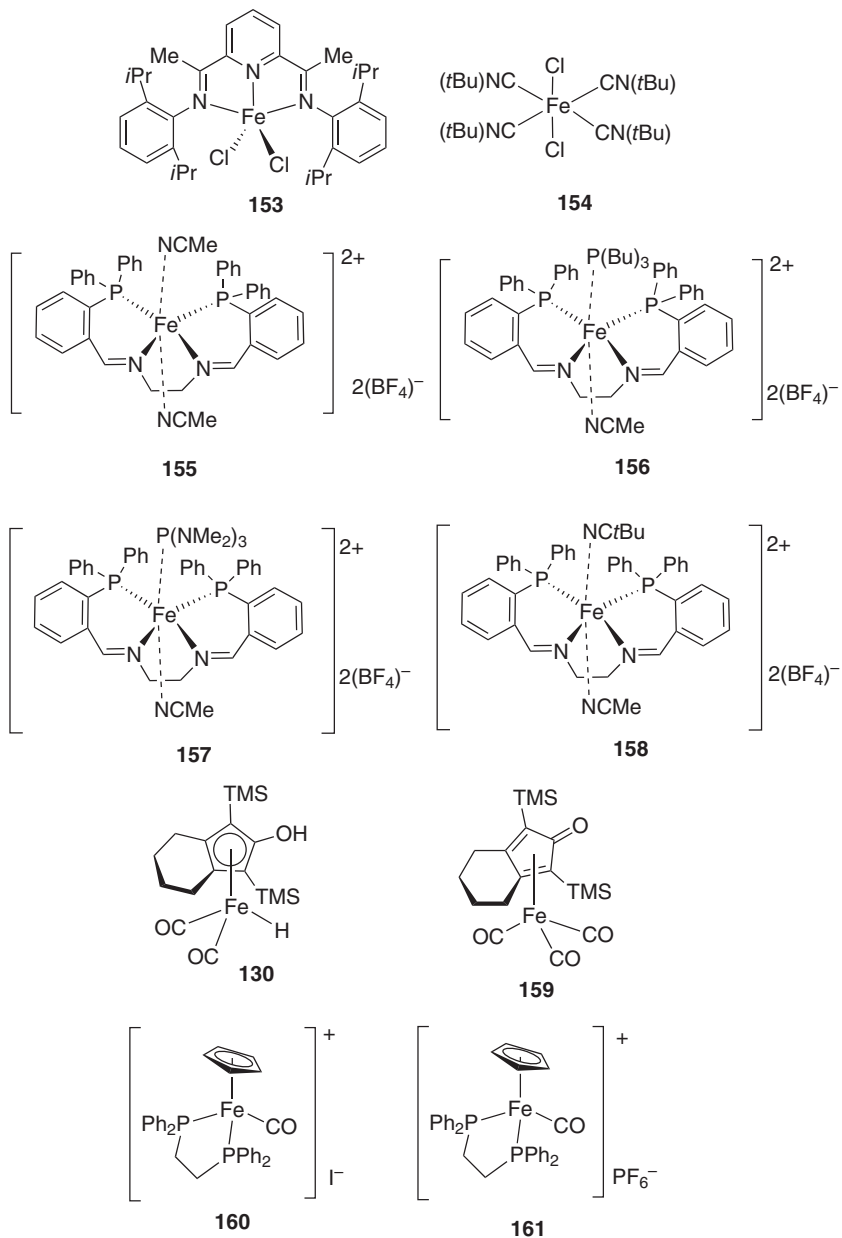
^d Contained 10% tribenzylamine.



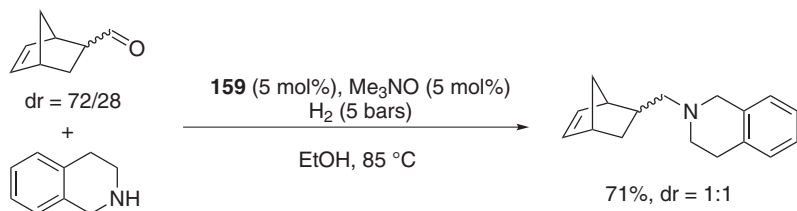
Scheme 208. Mechanism of reduction of amides.

I. Reductive Aminations

Amine compounds are very important for pharmaceuticals and natural product synthesis (300). Reductive amination of carbonyl compounds is one of the alternative protocols for synthesis of amine compounds. Renaud and co-workers (301) developed an iron-catalyzed reductive amination method. They synthesized different iron(II) complexes (**153–158**, (Scheme 209) (266a, 302). Interestingly, full conversion of starting material into the desired product was obtained by using



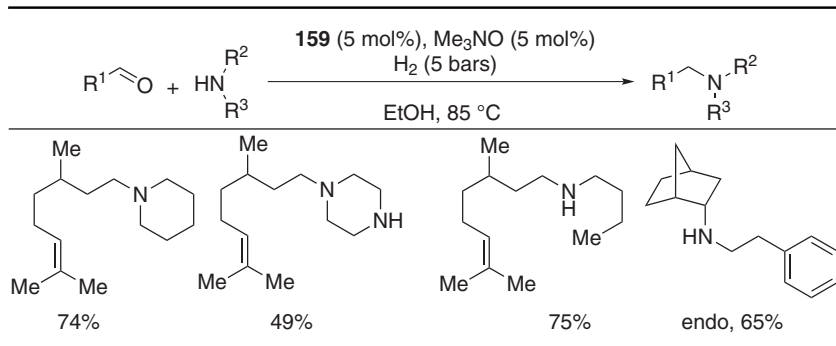
Scheme 209.



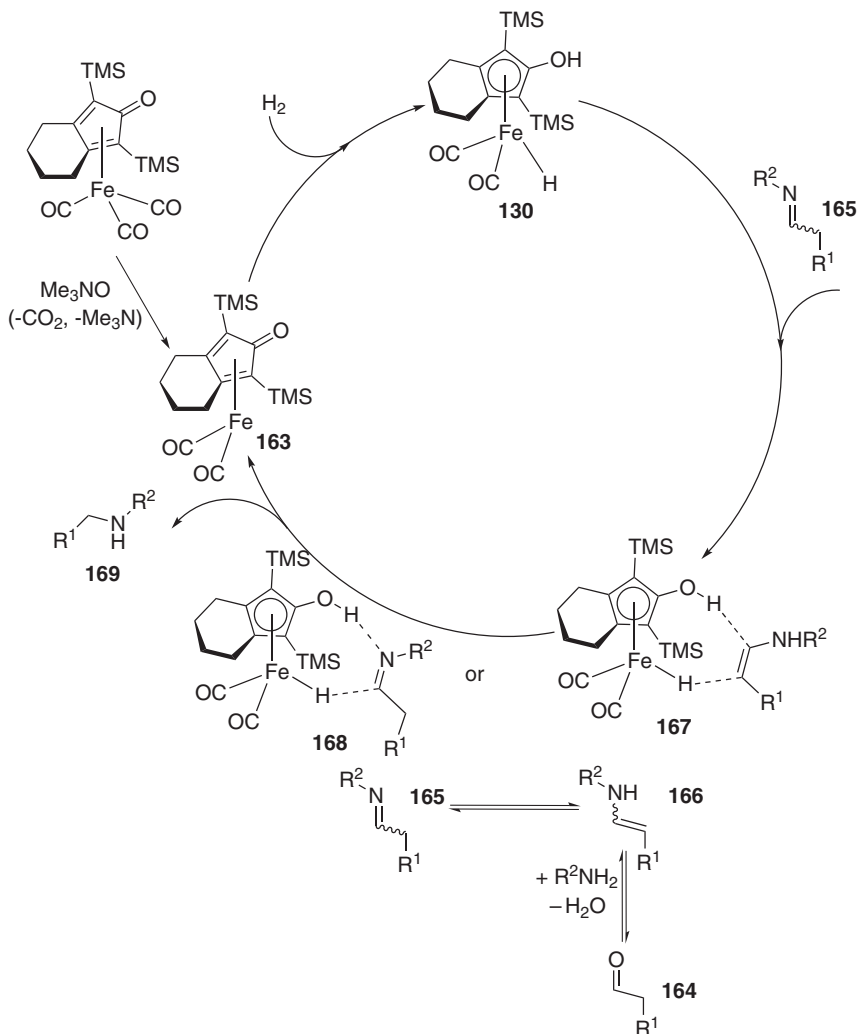
Scheme 210.

the Knolker complex **130** (263a, 264, 277, 303). Complex **130** was air sensitive and decomposed quickly. But, its related complex **159** (Scheme 209, Scheme 210) was air stable but unable to show activity toward reductive amination. Interestingly, when it was treated with trimethylamine *N*-oxide, which oxidatively removed CO ligand from **159** and generated a 16e species (**163**, Scheme 211). Subsequently, **163** reacted with hydrogen to form **130** *in situ*, which showed full conversions with moderate yield and selectivity. Note, other piano-stool complexes, **160** and **161**, failed to give product. The reaction tolerated both primary and secondary amines, as well as both aliphatic and aromatic aldehydes, to provide alkylated amines in good-to-excellent yields (Table LXI). Control experiments between norbornene carboxaldehyde and tetrahydroisoquinoline were carried out under standard reaction protocol (Scheme 210). This reaction provided an amine product in 71% yield and 1:1 mixtures of diastereomers. Based on these observations, imine (**165**)/enamine (**166**) equilibrium was proposed in the mechanism (Scheme 211).

TABLE LXI
Substrates Scope of Reductive Amination by a Knolker Complex^a



^aThe hydrogenation reactions were carried out with aldehyde (1 mmol) and amine (1.2 mmol) in the presence of an iron precatalyst (5 mol%) and trimethyl-*N*-oxide (5 mol%) in ethanol (2 mL) under 5 bar of hydrogen at 85 °C.

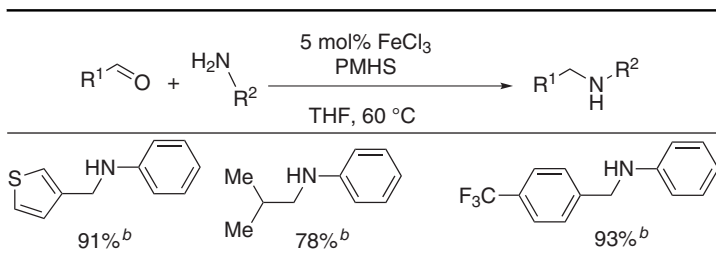


Scheme 211. Mechanism of reductive amination by a Knolker complex.

The *in situ* generated **130** then led to activation of **165** (or **166**) via coordination through the hydroxy group and generated intermediates **167** and **168** (Scheme 211). Subsequently, addition of hydride provided reduced amine and with regeneration of the unsaturated iron(0) complex (**163**).

In 2008, Bhagane and co-workers (304) synthesized amines via reductive amination using an iron(II)/EDTA complex with molecular hydrogen as the

TABLE LXII
Reductive Amination Using FeCl_3 as Catalyst^a



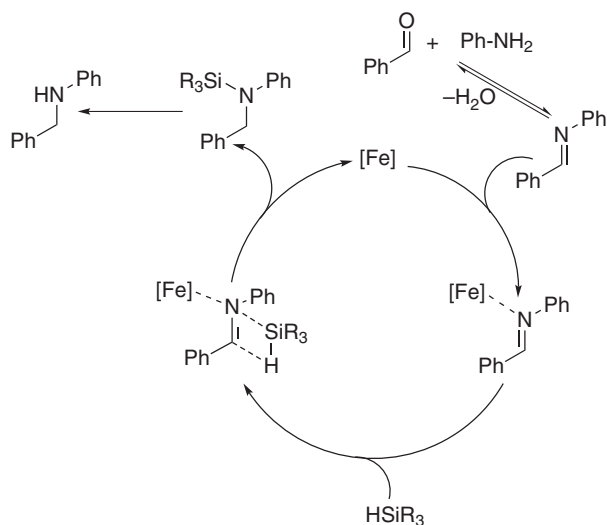
^aReaction conditions: FeCl_3 (0.12 mmol, 5 mol%), aldehyde (2.4 mmol), amine (2.4 mmol), PMHS (0.5 mL), THF (2.0 mL), 60 °C, 24 h. All products were characterized by GC-MS (mass spectrometry) and ^1H NMR.

^bIsolated yield.

hydrogen source. Later Enthaler reported a very effective method for reductive amination by using $\text{FeCl}_3/\text{PMHS}$ (Table LXII). This reaction tolerated a wide range of aromatics aldehydes (Table LXII) (305).

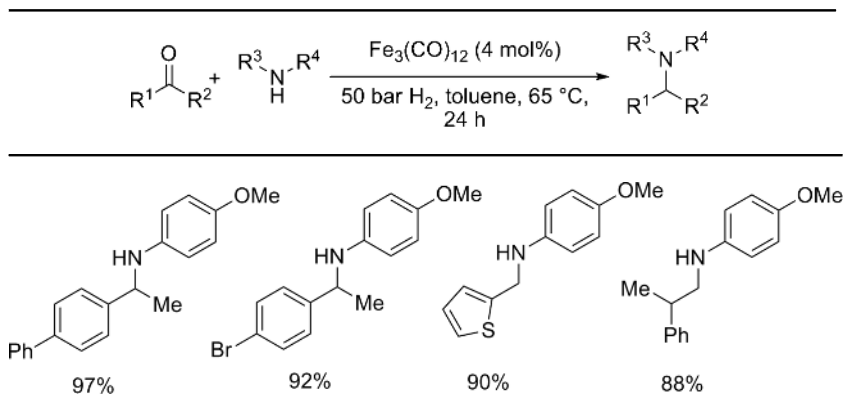
The reaction was proposed to undergo a Lewis acid catalyzed imine formation followed by the reduction of this imine (Scheme 212).

Later, Beller and co-workers (306) reported another alternative protocol of reductive amination between a ketone-aldehyde and an amine. In Beller's report,

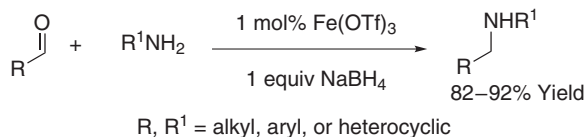


Scheme 212. Mechanism of reductive amination using FeCl_3 as catalyst.

TABLE LXIII
Reductive Amination of Ketones and Aldehydes with an Amine in the Presence of H₂^a



^aGeneral reaction condition: 0.5-mmol aldehyde, 0.75 mmol amine, 0.02 mmol Fe₃(CO)₁₂, 50 bar, H₂, 65 °C, 24 h.



Scheme 213. Reductive amination using Fe(OTf)₃/NaBH₄.

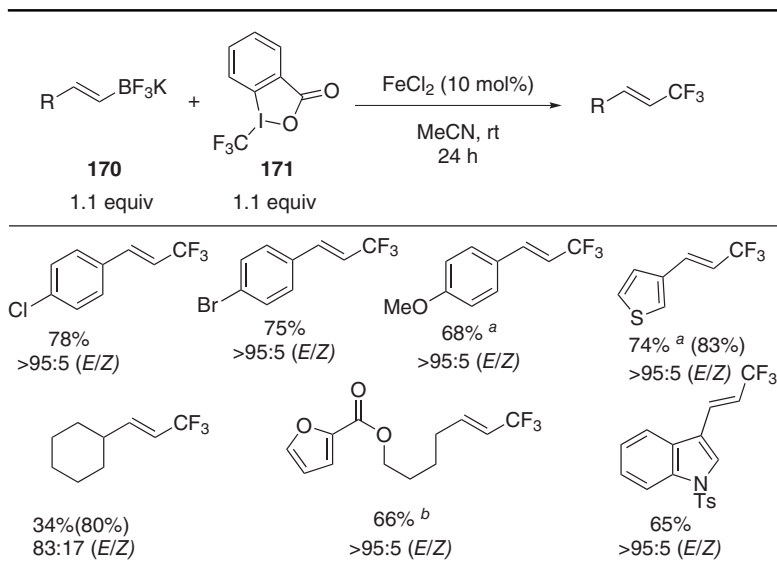
the iron carbonyl complex was used as the catalyst in the presence of molecular hydrogen (Table LXIII).

In 2012, Bandichhor and co-workers (307) reported another protocol for reductive amination using Fe(OTf)₂ as the catalyst and NaBH₄ as a reducing agent (Scheme 213).

X. TRIFLUOROMETHYLATION

The introduction of the trifluoromethyl group (–CF₃) into organic molecules is crucial for the discovery of biologically active compounds (308). The CF₃ group can act as a useful biostere of a methyl group and also it does not suffer from metabolic oxidation. In 2012, Buchwald and co-workers (309) developed a facile method for trifluoromethylation of potassium vinyltrifluoroborates using catalytic amounts of FeCl₂ and Togni's reagent (**171**) (Table LXIV) as the trifluoromethyl

TABLE LXIV
Trifluoromethylation Reaction with Iron Catalysis^a

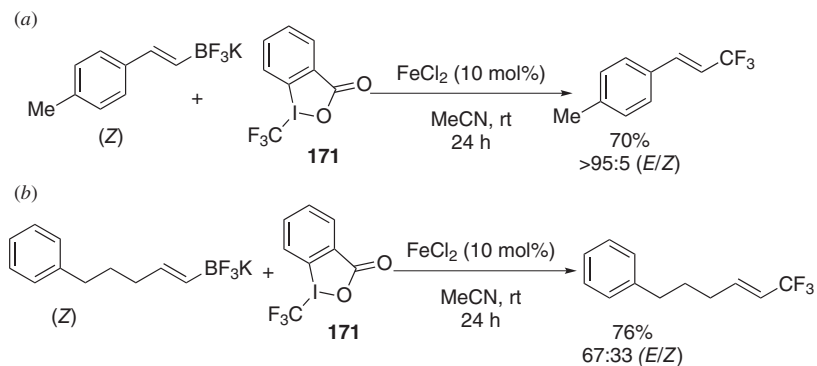


^a Reaction conditions: compound **170** (1.1–0.55 mmol, 1.1 equiv), **171** (1.0–0.5 mmol, 1.0 equiv), FeCl_2 (10 mol%), $[\text{171}]_{t=0} = 0.40 \text{ M}$. Contains 10–15 mol% of a protodeboronated side product.

^b Here 15 mol% FeCl_2 was used.

source. This method works efficiently for different aryl, heteroaryl, and aliphatic compounds (Table XLIV).

Some trifluoromethylated substrates gave a considerable amount of (E/Z) isomers (Scheme 214). According to Parsons et al. (309), such observations



Scheme 214. Selectivity in the formation of trifluoromethylated product.

disfavor transmetalation–reductive elimination type mechanism. Interestingly, $\text{Sn}(\text{OTf})_2$ provided a similar selectivity and yields of the desired product. Notably, irrespective of the geometry of the potassium trifluoroborate starting material, same product was obtained. All these observations supported formation of a cationic intermediate by Lewis acid catalysis.

XI. CONCLUSION

Efforts toward the development of sustainable, efficient, and selective processes for the synthesis of fine chemicals and pharmaceuticals are undoubtedly increasing. Designing environmentally benign methods for the construction of highly valuable building blocks from renewable raw materials remain a challenging task. In this context, catalysis based on abundant, inexpensive, and relatively nontoxic metals can play a pivotal role in the chemist's synthetic toolbox. Recently, catalysts based on iron metal have emerged as sustainable alternatives to precious metal-based catalysts in a range of synthetic applications. The wealth of knowledge concerning reaction pathways that is available for transition metal catalyzed reactions will continue to advance the growth of well-defined catalytic systems with iron. Handling of a number of useful "ligand–iron" complexes is often problematic due to their air sensitivity. Expensive and toxic late transition metals are used as an alternative for a given reaction. Consequently, designing and developing air stable, robust, and easy to handle iron catalyst should be a primary goal for aspiring chemists.

Acknowledgments

This work is supported by DST-India. Financial support received from CSIR-India (fellowships to S.R., A.M., and S.M.) and UGC-India (fellowship to T.P.) is gratefully acknowledged.

ABBREVIATIONS

acac	Acetylacetonate
BINAP	2,2'-Bis(diphenylphosphino)-1,1'-binaphthyl
BINOL	1,1'-Bi-2-naphthol
Bn	Benzyl
BNP	Bis-Binaphthylporphyrin
Boc	<i>tert</i> -Butyloxycarbonyl
BocN ₃	<i>N-tert</i> -Butyloxycarbonyl azide

Bopa	Bis(oxazolinyphenyl)amine
BPBP	1,1'-Bis(pyridin-2-ylmethyl)-2,2'-bipyrrolidine
BPMCN	<i>N,N'</i> -Bis(2-pyridyl-methyl)- <i>N,N'</i> -dimethyl-1,2-cyclohexanediamine bpmcn (ligand)
bpmen	<i>N,N'</i> -Dimethyl- <i>N,N'</i> -bis(pyridin-2-ylmethyl)ethane-1,2-diamine
BPN	Butylphenylnitron
BQBP	1,1'-Bis(quinolin-2-ylmethyl)-2,2'-bipyrrolidine
BTA	bis[(trifluoromethyl)sulfonyl]-amide
Bu	Butyl
CDA	Cross-dehydrogenative arylation
CDC	Cross-dehydrogenative coupling
CHT	Cyclohepta-1,3,5-triene
COD	1,5-cyclooctadiene
COX	Acyl halide
Cp	Cyclopentadienyl
Cy	Cyclohexyl
CyH	Cyclohexane
Cyclen	1,4,7,10-Tetraazacyclododecane
dach	1,2-Diaminocyclohexane
dapb	2,6-Bis[1-(benzylemino)ethyl]pyridine
DBFOX	4,6-Dibenzofurandilyl-2,2'-bis(4-phenyloxazoline)
DBM	Dibenzoylmethane (solvent), dbm (ligand)
DBU	1,8-Diazabicyclo[5.4.0]undec-7-ene
DCE	1,2-Dichloroethane
DCIB	1,2-Dichloroisobutane
DCM	Dichloromethane
dppbz	1,2-Bis(diphenylphosphino)benzenedichloride
DDQ	2,3-Dichloro-5,6-dicyano-1,4-benzoquinone
de	Diastereomeric excess
depe	Cy ₂ PCH ₂ CH ₃ PCy ₂
DFT	Density functional theory
DHySi	Dehydrogenative hydrosilylation
diphos	1,2-Bis(diphenylphosphino)ethane
Dipp	2,6-Diisopropylphenyl
DMAP	4-Dimethylaminopyridine
DMCH	Dimethyl cyclohexane
DME	Dimethoxyethane
dmeda	<i>N,N'</i> -Dimethylethylenediamine (solvent) dmeda (ligand)
DMF	<i>N,N'</i> -Dimethylformamide
DMSO	Dimethyl sulfoxide (solvent), dmsol (ligand)
dpaq	2-(Bis(pyridin-2-ylmethyl)amino- <i>N</i> -(quinolin-8-yl)acetamide
dppbz	1,2-Bis(diphenylphosphino)benzene

dppe	1,2-Bis(diphenylphosphino)ethane
dppp	1,3-Bis(diphenylphosphino)propane
DTPB	Di-(<i>tert</i> -butyl)peroxide
dtbpy	4,4'-Di- <i>tert</i> -butyl-2,2'-bipyridine
D ₄ -TpAP	H ₂ [HPhH(dach) ₂] where 1,2-diaminocyclohexane (dach)
dr	Diastereomeric ratio
DuPhos	(-)-1,2-bis((2 <i>S</i> ,5 <i>S</i>)-2,5-di- <i>i</i> -propylphospholano)benzene
EDA	Ethyldiazoacetate
EDTA	Ethylenediaminetetraacetic acid
ee	Enantiomeric excess
emim	Ethyl methyl imidazolium
EWG	Electron-withdrawing group
FTMS	Fourier transform mass spectrometer
GC	Gas chromatography
HMA	Hexagonal mesoporous aluminophosphate
HMDS	Bis(trimethylsilyl)amide
¹ H NMR	Proton nuclear magnetic resonance
HPLC	High-performance liquid chromatography
H ₂ Pydic	Pyridine-2,6-dicarboxylic acid
HOMO	Highest occupied molecular orbital
Hy	Hydrogenation
HySi	Hydrosilylation
IEtPh	1,3-Bis(<i>R</i>)-1'-phenylethyl)imidazole-2-ylidene)
INAS	Intramolecular nucleophilic acyl substitution
IMes	1,3-Bis(2,4,6-trimethylphenyl)imidazole-2-ylidene
Ipr	1,3-Bis(2,6-diisopropylphenyl)-2,3-dehydro-1 <i>H</i> -imidazole
<i>i</i> PrPNP	2,6-Bis(diisopropylphosphinomethyl)pyridine
KHMDS	Potassium bis(trimethylsilyl)amide
KIE	Kinetic isotopic effect
LDA	Lithium diisopropylamide
LiHMDS	Lithium bis(trimethylsilyl)amide
LUMO	Lowest unoccupied molecular orbital
mcpp	N1,N2-dimethyl-N1,N2-bis(pyridin-2-ylmethyl)cyclohexane-1,2-diamine
mep	<i>N,N'</i> -Dimethyl- <i>N,N'</i> -bis(2-pyridylmethyl)ethane
Mes	2,4,6-Trimethylphenyl
MOM	Methoxymethyl ether
NBS	<i>N</i> -Bromosuccinamide
NHC	<i>N</i> -Heterocyclic carbene
N-IBN	<i>N</i> -(2-Iodophenyl) methyl
NMP	<i>N</i> -methylpyridine
NMR	Nuclear magnetic resonance
NTs	Tosylaziridine

OTf	Trifluoromethanesulfonate
OMP	<i>o</i> -methoxyphenyl
Pc	Phthalocyanine
PDI	(<i>N,N'</i> E, <i>N,N'</i> E)- <i>N,N'</i> -(1,1')-(Pyridine-2,6-diyl)bis(ethan-1-yl-1-ylidene))bis(2,6-diisopropylaniline)
PDP	PDP=2-((S)-2-[(S)-1-(pyridin-2-ylmethyl)pyrrolidin-2-yl]pyrrolidin-1-yl)methylpyridine
phebox	Bis(oxazoliny)phenyl
Phen	1,10-Phenanthroline
PhNTf ₂	<i>N</i> -Phenyl-bis(trifluoromethanesulfonimide)
PhINTs	<i>N</i> -Tosyliminobenzylidiodinane
Pip	Piperidinium
Piv	Pivaloyl
PMB	4-Methoxybenzyl bromide
PMHS	Polymethylhydrosiloxane
PMP	<i>p</i> -Methoxyphenyl
PNNP	[P(2)(N2)] ligad set
Pr	Propyl
PrPNP	2,6-Bis(diisopropylphosphinomethyl)pyridine
pybox	Bis(oxazoliny)pyridine
PyTACN	Bis(2-pyridylmethyl)-1,4,7-triazacyclononane
rt	Room temperature
RM	Organometalic reagent
RSM	Recovered starting material
salen	<i>N,N'</i> -Bis(3,5-di- <i>tert</i> -butylsalicylidene)-1,2-cyclohexanediamino
SET	Single-electron transfer
SIPr	1,3-Bis(2,6-diisopropylphenyl)-imidazolidinium
TACN	Triazacyclononane
TBA	Tetrabutylammonium
TBDMS	<i>tert</i> -Butyldimethylsilyl
TBDPS	<i>tert</i> -Butyldiphenylsilane
TBHP	<i>tert</i> -Butyl hydrogen peroxide
TBS	<i>tert</i> -Butyldimethylsilyl
TEMPO	2,2,6,6-Tetramethyl-piperidin-1-yl)oxyl
tf	Trifluoromethylsulfonyl
TFA	Trifluoroacetic acid
THF	Tetrahydrofuran (solvent), thf (ligand)
THP	Tetrahydropyran
TIP	Tetrakis(imino)pyracene
TIPS	Triisopropylsilyl
TMDSO	1,1,3,3-Tetramethyldisiloxane
TMEDA	<i>N,N,N,N'</i> -Tetramethylethane-1,2-diamine (solvent), tmeda (ligand)

TMP	2,3,6-Trimethylphenol
TMS	Trimethylsilyl
TON	Turn over number
TPA	Tris(2-pyridylmethyl)amine
TPP	Tetraphenylporphyrin
TOF	Turn over frequency
tol	Tolyl
Tosyl	4-Toluenesulfonyl
TTP	<i>meso</i> -Tetra- <i>p</i> -tolylporphyrin
UV	Ultraviolet
VCP	Vinylcyclopropane

REFERENCES

1. (a) C. Bolm, J. Legros, J. Le Paih, and L. Zani, *Chem. Rev.*, *104*, 6217 (2004); (b) S. Enthaler, K. Junge, and M. Beller, *Angew. Chem. Int. Ed.*, *47*, 3317 (2008); (c) A. Correa, O. G. Mancheno, and C. Bolm, *Chem. Soc. Rev.*, *37*, 1108 (2008); (d) C. L. Sun, B. J. Li, and Z. J. Shi, *Chem. Rev.*, *111*, 1293 (2011); (e) K. Gopalaiah, *Chem. Rev.* *113*, 3248 (2013).
2. H. Ohara, T. Itoh, M. Nakamura, and E. Nakamura, *Chem. Lett.*, 624 (2001).
3. H. Ohara, H. Kiyokane, and T. Itoh, *Tetrahedron Lett.*, *43*, 3041 (2002).
4. M. Rosenblum and D. Scheck, *Organometallics*, *1*, 397 (1982).
5. M. W. Bouwkamp, A. C. Bowman, E. Lobkovsky, and P. J. Chirik, *J. Am. Chem. Soc.*, *128*, 13340 (1982).
6. S. K. Russell, E. Lobkovsky, and P. J. Chirik, *J. Am. Chem. Soc.*, *133*, 8858 (2011).
7. A. P. Dieskau, M. S. Holzwarth, and B. Plietker, *J. Am. Chem. Soc.*, *134*, 5048 (2012).
8. J. M. Fan, L. F. Gao, and Z. Y. Wang, *Chem. Commun.*, 5021 (2009).
9. H. S. Wu, B. Wang, H. Q. Liu, and L. Wang, *Tetrahedron*, *67*, 1210 (2011).
10. E. P. Kundig, C. M. Saudan, and F. Viton, *Adv. Synth. Catal.*, *343*, 51 (2002).
11. W. S. Jen, J. J. M. Wiener, and D. W. C. MacMillan, *J. Am. Chem. Soc.*, *122*, 9874 (2000).
12. C. Breschi, L. Piparo, P. Pertici, A. M. Caporusso, and G. Vitulli, *J. Organomet. Chem.*, *607*, 57 (2000).
13. F. Knoch, F. Kremer, U. Schmidt, U. Zenneck, P. LeFloch, and F. Mathey, *Organometallics*, *15*, 2713 (1996).
14. K. Ferre, L. Toupet, and V. Guerchais, *Organometallics*, *21*, 2578 (2002).
15. N. Saino, D. Kogure, and S. Okamoto, *Org. Lett.*, *7*, 3065 (2005).
16. N. Saino, D. Kogure, K. Kase, and S. Okamoto, *J. Organomet. Chem.*, *691*, 3129 (2006).
17. A. Furstner, K. Majima, R. Martin, H. Krause, E. Kattinig, R. Goddard, and C. W. Lehmann, *J. Am. Chem. Soc.*, *130*, 1992 (2008).

18. Y. Yu, J. M. Smith, C. J. Flaschenriem, and P. L. Holland, *Inorg. Chem.*, **45**, 5742 (2006).
19. C. X. Wang, X. C. Li, F. Wu, and B. S. Wan, *Angew. Chem. Int. Ed.*, **50**, 7162 (2011).
20. B. R. D'Souza, T. K. Lane, and J. Louie, *Org. Lett.*, **13**, 2936 (2011).
21. E. J. Corey, N. Imai, and H. Y. Zhang, *J. Am. Chem. Soc.*, **113**, 728 (1991).
22. M. P. Sibi, S. Manyem, and H. Palencia, *J. Am. Chem. Soc.*, **128**, 13660 (2006).
23. N. Khiar, I. Fernandez, and F. Alcudia, *Tetrahedron Lett.*, **34**, 123 (1993).
24. S. Matsukawa, H. Sugama, and T. Imamoto, *Tetrahedron Lett.*, **41**, 6461 (2000).
25. S. Kanemasa, Y. Oderaotoshi, H. Yamamoto, J. Tanaka, E. Wada, and D. P. Curran, *J. Org. Chem.*, **62**, 6454 (1997).
26. S. Kanemasa, Y. Oderaotoshi, S. Sakaguchi, H. Yamamoto, J. Tanaka, E. Wada, and D. P. Curran, *J. Am. Chem. Soc.*, **120**, 3074 (1998).
27. H. Usuda, A. Kuramochi, M. Kanai, and M. Shibasaki, *Org. Lett.*, **6**, 4387 (2004).
28. Y. Shimizu, S. L. Shi, H. Usuda, M. Kanai, and M. Shibasaki, *Angew. Chem. Int. Ed.*, **49**, 1103 (2010).
29. M. E. Bruin and E. P. Kundig, *Chem. Commun.*, 2635 (1998).
30. R. Bakhtiar, J. J. Drader, and D. B. Jacobson, *J. Am. Chem. Soc.*, **114**, 8304 (1992).
31. K. Fujiwara, T. Kurahashi, and S. Matsubara, *J. Am. Chem. Soc.*, **134**, 5512 (2012).
32. (a) G. Wuitschik, M. Rogers-Evans, A. Buckl, M. Bernasconi, M. Marki, T. Godel, H. Fischer, B. Wagner, I. Parrilla, F. Schuler, J. Schneider, A. Alker, W. B. Schweizer, K. Muller, and E. M. Carreira, *Angew. Chem. Int. Ed.*, **47**, 4512 (2008); (b) G. Wuitschik, M. Rogers-Evans, K. Muller, H. Fischer, B. Wagner, F. Schuler, L. Polonchuk, and E. M. Carreira, *Angew. Chem. Int. Ed.*, **45**, 7736 (2006).
33. W. A. Donaldson, *Tetrahedron*, **57**, 8589 (2001).
34. (a) J. Salaun, *Chem. Rev.*, **89**, 1247 (1989); (b) M. P. Doyle and D. C. Forbes, *Chem. Rev.*, **98**, 911 (1998).
35. M. Brookhart and W. B. Studabaker, *Chem. Rev.*, **87**, 411 (1987).
36. P. W. Jolly and R. Pettit, **88**, 5045 (1966).
37. W. J. Seitz, A. K. Saha, and M. M. Hossain, *Organometallics*, **12**, 2604 (1993).
38. (a) S. K. Edulji and S. T. Nguyen, *Organometallics*, **22**, 3374 (2003); (b) S. K. Edulji, and S. T. Nguyen, *Pure. Appl. Chem.*, **76**, 645 (2004).
39. X. Morise, M. L. H. Green, P. Braunstein, L. H. Rees, and I. C. Veil, *New J. Chem.*, **27**, 32 (2003).
40. J. R. Wolf, C. G. Hamaker, J. P. Djukic, T. Kodadek, and L. K. Woo, *J. Am. Chem. Soc.*, **117**, 9194 (1995).
41. G. D. Du, B. Andrioletti, E. Rose, and L. K. Woo, *Organometallics*, **21**, 4490 (2002).
42. I. Nicolas, T. Roisnel, P. Le Maux, and G. Simonneaux, *Tetrahedron Lett.*, **50**, 5149 (2009).
43. B. Morandi and E. M. Carreira, *Science*, **335**, 1471 (2012).
44. B. Morandi, A. Dolva, and E. M. Carreira, *Org. Lett.*, **14**, 2162 (2012).

45. (a) M. Schlosser, *Angew. Chem. Int. Ed.*, **45**, 5432 (2006); (b) C. Isanbor and D. O'Hagan, *J. Fluorine Chem.*, **127**, 303 (2006).
46. B. Morandi and E. M. Carreira, *Angew. Chem. Int. Ed.*, **49**, 938 (2010).
47. B. Morandi, J. Cheang, and E. M. Carreira, *Org. Lett.*, **13**, 3080 (2011).
48. (a) I. D. G. Watson, L. L. Yu, and A. K. Yudin, *Acc. Chem. Res.*, **39**, 194 (2006); (b) B. Zwanenburg and P. ten Holte, *Top. Curr. Chem.*, **216**, 93 (2001); (c) W. McCoull and F. A. Davis, *Synthesis*, 1347 (2001); (d) S. Lociuero, L. Pellacani, and P. A. Tardella, *Tetrahedron Lett.*, **24**, 593 (1983); (e) S. Fioravanti, M. A. Loreto, L. Pellacani, and P. A. Tardella, *J. Org. Chem.*, **50**, 5365 (1985); (f) D. A. Evens, M. M. Faul, and M. T. Bilodeau, *J. Am. Chem. Soc.*, **116**, 2742 (1994); (g) K. Surendra, N. S. Krishnaveni, and K. R. Rao, *Tetrahedron Lett.*, **46**, 4111 (2005); (h) M. S. Reddy, M. Narender, and K. R. Rao, *Tetrahedron Lett.*, **46**, 1299 (2005).
49. M. Nakanishi, A. F. Salit, and C. Bolm, *Adv. Synth. Catal.*, **350**, 1835 (2008).
50. A. C. Mayer, A. F. Salit, and C. Bolm, *Chem. Commun.*, 5975 (2008).
51. A. Marti, L. Richter, and C. Schneider, *Synlett*, 2513 (2011).
52. (a) A. M. Caporusso, L. Lardicci, and G. Giacomelli, *Tetrahedron Lett.*, 4351 (1977); (b) A. M. Caporusso, G. Giacomelli, and L. Lardicci, *J. Chem. Soc., Perkin Trans. 1*, 3139 (1979).
53. M. Nakamura, A. Hirai, and E. Nakamura, *J. Am. Chem. Soc.*, **122**, 978 (2000).
54. M. Hojo, Y. Murakami, H. Aihara, R. Sakuragi, Y. Baba, and A. Hosomi, *Angew. Chem. Int. Ed.*, **40**, 621 (2001).
55. D. H. Zhang and J. M. Ready, *J. Am. Chem. Soc.*, **128**, 15050 (2006).
56. E. Shirakawa, T. Yamagami, T. Kimura, S. Yamaguchi, and T. Hayashi, *J. Am. Chem. Soc.*, **127**, 17164 (2005).
57. E. Shirakawa, D. Ikeda, S. Masui, M. Yoshida, and T. Hayashi, *J. Am. Chem. Soc.*, **134**, 272 (2012).
58. T. Yamagami, R. Shintani, E. Shirakawa, and T. Hayashi, *Org. Lett.*, **9**, 1045 (2007).
59. E. Shirakawa, D. Ikeda, T. Ozawa, S. Watanabe, and T. Hayashi, *Chem. Commun.*, 1885 (2009).
60. L. Adak and N. Yoshikai, *Tetrahedron* **68**, 5167 (2012).
61. S. Ito, T. Itoh, and M. Nakamura, *Angew. Chem. Int. Ed.*, **50**, 454 (2011).
62. J. Cabral, P. Laszlo, L. Mahe, M. T. Montaufier, and S. L. Randriamahefa, *Tetrahedron Lett.*, **30**, 3969 (1989).
63. (a) J. Christoffers, *Chem Commun*, 943 (1997); (b) J. Christoffers, *Tetrahedron Lett.*, **39**, 7083 (1998).
64. (a) J. Christoffers, *Eur. J. Org. Chem.*, 1259 (1998); (b) S. Pelzer, T. Kauf, C. van Wullen, and J. Christoffers, *J. Organomet. Chem.*, **684**, 308 (2003).
65. J. Christoffers, *Eur. J. Org. Chem.*, 759 (1998).
66. J. Christoffers and A. Mann, *Eur. J. Org. Chem.*, 1977 (2000).
67. (a) J. Christoffers and A. Mann, *Eur. J. Org. Chem.*, 1475 (1999); (b) J. Christoffers, *J. Prakt. Chem.-Chem. Ztg.*, **341**, 495 (1999).

68. K. Shimizu, M. Miyagi, T. Kan-no, T. Kodama, and Y. Kitayama, *Tetrahedron Lett.*, **44**, 7421 (2003).
69. G. A. Molander and C. R. Harris, *Chem. Rev.*, **96**, 307 (1996).
70. (a) G. A. Molander and J. B. Etter, *Tetrahedron Lett.*, **25**, 3281 (1984); (b) G. A. Molander and J. B. Etter, *J. Org. Chem.*, **51**, 1778 (1986).
71. G. A. Molander and J. A. McKie, *J. Org. Chem.*, **56**, 4112 (1991).
72. G. A. Molander and J. A. McKie, *J. Org. Chem.*, **58**, 7216 (1993).
73. G. A. Molander and S. R. Shakya, *J. Org. Chem.*, **59**, 3445 (1994).
74. M. S. Kharasch, P. S. Skell, and P. Fisher, *J. Am. Chem. Soc.*, **70**, 1055 (1948).
75. J. Elzinga and H. Hogeveen, *J. Org. Chem.*, **45**, 3957 (1980).
76. (a) T. Susuki and J. Tsuji, *J. Org. Chem.*, **35**, 2982 (1970); (b) R. Davis, J. L. A. Durrant, N. M. S. Khazal, and T. E. Bitterwolf, *J. Organomet. Chem.*, **386**, 229 (1990).
77. L. Forti, F. Ghelfi, and U. M. Pagnoni, *Tetrahedron Lett.*, **37**, 2077 (1996).
78. L. Forti, F. Ghelfi, E. Libertini, U. M. Pagnoni, and E. Soragni, *Tetrahedron*, **53**, 17761 (1997).
79. (a) T. K. Hayes, A. J. Freyer, M. Parvez, and S. M. Weinreb, *J. Org. Chem.*, **51**, 5501 (1986); (b) T. K. Hayes, R. Villani, and S. M. Weinreb, *J. Am. Chem. Soc.*, **110**, 5533 (1988); (c) G. M. Lee, M. Parvez, and S. M. Weinreb, *Tetrahedron*, **44**, 4671 (1988); (d) G. M. Lee and S. M. Weinreb, *J. Org. Chem.*, **55**, 1281 (1990).
80. J. Norinder, A. Matsumoto, N. Yoshikai, and E. Nakamura, *J. Am. Chem. Soc.*, **130**, 5858 (2008).
81. N. Yoshikai, A. Matsumoto, J. Norinder, and E. Nakamura, *Angew. Chem. Int. Ed.*, **48**, 2925 (2009).
82. L. Ilies, J. Okabe, N. Yoshikai, and E. Nakamura, *Org. Lett.*, **12**, 2838 (2010).
83. N. Yoshikai, A. Mieczkowski, A. Matsumoto, L. Ilies, and E. Nakamura, *J. Am. Chem. Soc.*, **132**, 5568 (2010).
84. L. D. Tran and O. Daugulis, *Org. Lett.*, **12**, 4277 (2010).
85. J. Wang, S. Wang, G. Wang, J. Zhang, and X. Q. Yu, *Chem. Commun.*, **48**, 11769 (2012).
86. F. Vallee, J. J. Mousseau, and A. B. Charette, *J. Am. Chem. Soc.*, **132**, 1514 (2010).
87. W. Liu, H. Cao, and A. W. Lei, *Angew. Chem. Int. Ed.*, **49**, 2004 (2010).
88. S. L. Buchwald and C. Bolm, *Angew. Chem. Int. Ed.*, **48**, 5586 (2009).
89. (a) H. Chen, S. Schlecht, T. C. Semple, and J. F. Hartwig, *Science*, **287**, 1995 (2000); (b) V. Ritleng, C. Sirlin, and M. Pfeffer, *Chem. Rev.*, **102**, 1731 (2002); (c) T. Naota, H. Takaya, and S.-I. Murahashi, *Chem. Rev.*, **98**, 2599 (1998); (d) B. A. Arndtsen, R. G. Bergman, T. A. Mobley, and T. H. Peterson, *Acc. Chem. Res.*, **28**, 154 (1995); (e) A. S. Goldman, *Nature (London)*, **366**, 514 (1993).
90. C.-J. Li, *Acc. Chem. Res.*, **42**, 335 (2009).
91. Z. Li, L. Cao, and C.-J. Li, *Angew. Chem., Int. Ed.*, **46**, 6505 (2007).
92. S.-I. Murahashi, N. Komiya, and H. Terai, *Angew. Chem., Int. Ed.*, **44**, 6931 (2005).
93. Z. Li, R. Yu, and H. Li, *Angew. Chem., Int. Ed.*, **47**, 7497 (2008).

94. H. Li, Z. He, X. Guo, W. Li, X. Zhao, and Z. Li, *Org. Lett.*, **11**, 4176 (2009).
95. Y. Zhang and C.-J. Li, *Eur. J. Org. Chem.*, **2007**, 4654 (2007).
96. Y.-Z. Li, B.-J. Li, X.-Y. Lu, S. Lin, and Z.-J. Shi, *Angew. Chem., Int. Ed.*, **48**, 3817 (2009).
97. C.-X. Song, G.-X. Cai, T. R. Farrell, Z.-P. Jiang, H. Li, L.-B. Gan, and Z.-J. Shi, *Chem. Commun.*, 6002 (2009).
98. X. Guo, R. Yu, H. Li, and Z. Li, *J. Am. Chem. Soc.*, **131**, 17387 (2009).
99. C. M. R. Volla and P. Vogel, *Org. Lett.*, **11**, 1701 (2009).
100. (a) R. Shang, Y. Fu, Y. Wang, Q. Xu, H.-Z. Yu, and L. Liu, *Angew. Chem. Int. Ed.*, **48**, 9350 (2009); (b) Z.-M. Sun and P. Zhao, *Angew. Chem. Int. Ed.*, **48**, 6726 (2009); (c) F. Zhang and M. F. Greaney, *Angew. Chem. Int. Ed.*, **49**, 2768 (2010).
101. H.-P. Bi, W.-W. Chen, Y.-M. Liang, and C.-J. Li, *Org. Lett.*, **11**, 3246 (2009).
102. S.-Y. Zhang, Y.-Q. Tu, C.-A. Fan, F.-M. Zhang, and L. Shi, *Angew. Chem., Int. Ed.*, **48**, 8761 (2009).
103. P. S. Baran, B. D. Hafensteiner, N. B. Ambhaikar, C. A. Guerrero, and J. D. Gallagher, *J. Am. Chem. Soc.*, **128**, 8678 (2006).
104. M. P. DeMartino, K. Chen, and P. S. Baran, *J. Am. Chem. Soc.*, **130**, 11546 (2008).
105. J. M. Richter, Y. Ishihara, T. Masuda, B. W. Whitefield, T. s. Llamas, A. Pohjakallio, and P. S. Baran, *J. Am. Chem. Soc.*, **130**, 17938 (2008).
106. H. Egami, K. Matsumoto, T. Oguma, T. Kunisu, and T. Katsuki, *J. Am. Chem. Soc.*, **132**, 5886 (2010).
107. (a) I. Fridovich, *Science*, **201**, 875 (1978); (b) S. H. Han, B. Zheng, D. G. Schatz, E. Spanopoulou, and G. Kelsoe, *Science*, **274**, 2094 (1996); (c) P. L. Roach, I. J. Clifton, C. M. H. Hensgens, N. Shibata, C. J. Schofield, J. Hajdu, and J. E. Baldwin, *Nature (London)*, **387**, 827 (1997); (d) P. C. Ford, B. O. Fernandez, and M. D. Lim, *Chem. Rev.*, **105**, 2439 (2005).
108. (a) D. H. R. Barton and D. Doller, *Acc. Chem. Res.*, **25**, 504 (1992); (b) D. H. R. Barton, *Chem. Soc. Rev.*, **25**, 237 (1996); (c) D. H. R. Barton, *Tetrahedron*, **54**, 5805 (1998); (d) P. Stavropoulos, R. Celenligil-Cetin, and A. E. Tapper, *Acc. Chem. Res.*, **34**, 745 (2001); (e) M. J. Perkins, *Chem. Soc. Rev.*, **25**, 229 (1996); (f) D. T. Sawyer, A. Sobkowiak, and T. Matsushita, *Acc. Chem. Res.*, **29**, 409 (1996); (g) C. Walling, *Acc. Chem. Res.*, **31**, 155 (1998); (h) P. A. MacFaul, D. D. M. Wayner, and K. U. Ingold, *Acc. Chem. Res.*, **31**, 159 (1998); (i) S. Goldstein and D. Meyerstein, *Acc. Chem. Res.*, **32**, 547 (1999); (j) M. Fontecave, S. Menage, and C. Duboc-Toia, *Coord. Chem. Rev.*, **178**, 1555 (1998); (k) M. Costas, K. Chen, and L. Que, Jr., *Coord. Chem. Rev.*, **200**, 517 (2000); (l) M. Costas, M. P. Mehn, M. P. Jensen, and L. Que, *Chem. Rev.*, **104**, 939 (2004); (m) E. Y. Tshuva and S. J. Lippard, *Chem. Rev.*, **104**, 987 (2004).
109. M. Nakanishi and C. Bolm, *Adv. Synth. Catal.*, **349**, 861 (2007).
110. K. Moller, G. Wienhofer, K. Schroder, B. Join, K. Junge, and M. Beller, *Chem. Eur. J.*, **16**, 10300 (2010).
111. (a) F. Shi, M. K. Tse, and M. Beller, *J. Mol. Catal. A: Chem.*, **270**, 68 (2007); (b) F. Shi, M. K. Tse, and M. Beller, *Adv. Synth. Catal.*, **349**, 303 (2007); (c) G. Wienhofer,

- K. Schroder, K. Moller, K. Junge, and M. Beller, *Adv. Synth. Catal.*, 352, 1615 (2010); (d) M. Periasamy and M. V. Bhatt, *Tetrahedron Lett.*, 4561 (1978); (e) A. Bohle, A. Schubert, Y. Sun, and W. R. Thiel, *Adv. Synth. Catal.*, 348, 1011 (2006); (f) T. Takai, E. Hata, and T. Mukaiyama, *Chem. Lett.*, 885 (1994); (g) R. Song, A. Sorokin, J. Bernadou, and B. Meunier, *J. Org. Chem.*, 62, 673 (1997).
112. C. Kim, K. Chen, J. H. Kim, and L. Que, Jr., *J. Am. Chem. Soc.*, 119, 5964 (1997).
113. K. Chen and L. Que, Jr., *J. Am. Chem. Soc.*, 123, 6327 (2001).
114. (a) G. J. P. Britovsek, J. England, and A. J. P. White, *Inorg Chem*, 44, 8125 (2005); (b) J. England, G. J. P. Britovsek, N. Rabadia, and A. J. P. White, *Inorg. Chem.*, 46, 3752 (2007); (c) J. England, C. R. Davies, M. Banaru, A. J. P. White, and G. J. P. Britovsek, *Adv. Synth. Catal.*, 350, 883 (2008); (d) J. England, R. Gondhia, L. Bigorra-Lopez, A. R. Petersen, A. J. P. White, and G. J. P. Britovsek, *Dalton Trans.*, 5319 (2009); (e) O. Y. Lyakin, K. P. Bryliakov, G. J. P. Britovsek, and E. P. Talsi, *J. Am. Chem. Soc.*, 131, 10798 (2009).
115. (a) M. Merckx, D. A. Kopp, M. H. Sazinsky, J. L. Blazyk, J. Muller, and S. J. Lippard, *Angew. Chem. Int. Ed.*, 40, 2782 (2001); (b) M. M. Abu-Omar, A. Loaiza, and N. Hontzeas, *Chem. Rev.*, 105, 2227 (2005).
116. L. Que and W. B. Tolman, *Nature (London)*, 455, 333 (2008).
117. A. Company, L. Gomez, M. Guell, X. Ribas, J. M. Luis, L. Que, and M. Costas, *J. Am. Chem. Soc.*, 129, 15766 (2007).
118. A. Company, L. Gomez, X. Fontrodona, X. Ribas, and M. Costas, *Chem. Eur. J.*, 14, 5727 (2008).
119. B. Retcher, J. S. Costa, J. K. Tang, R. Hage, P. Gamez, and J. Reedijk, *J. Mol. Catal. A: Chem.*, 286, 1 (2008).
120. M. S. Chen and M. C. White, *Science*, 318, 783 (2007).
121. N. A. Vermeulen, M. S. Chen, and M. C. White, *Tetrahedron*, 65, 3078 (2009).
122. M. S. Chen and M. C. White, *Science*, 327, 566 (2010).
123. L. Gomez, I. Garcia-Bosch, A. Company, J. Benet-Buchholz, A. Polo, X. Sala, X. Ribas, and M. Costas, *Angew. Chem. Int. Ed.*, 48, 5720 (2009).
124. Y. Hitomi, K. Arakawa, T. Funabiki, and M. Kodera, *Angew. Chem. Int. Ed.*, 51, 3448 (2012).
125. (a) K. A. Jorgensen, Wiley-VCH, Weinheim 2, 1998; (b) U. Sundermeier, C. Döbler, and M. Beller, *Modern Oxidation Methods*, Wiley-VCH, Weinheim, 2004.
126. (a) Y. Shi, *Acc. Chem. Res.*, 37, 488 (2004); (b) E. N. Jacobsen and M. H. Wu, *Comprehensive Asymmetric Catalysis*, Vol. 2, 1999; (c) T. Katsuki, *Comprehensive in Asymmetric Catalysis*, Vol. 2, Springer, Berlin, 1999.
127. M. C. White, A. G. Doyle, and E. N. Jacobsen, *J. Am. Chem. Soc.*, 123, 7194 (2001).
128. G. Dubois, A. Murphy, and T. D. P. Stack, *Org. Lett.*, 5, 2469 (2003).
129. J. Y. Ryu, J. Kim, M. Costas, K. Chen, W. Nam, and L. Que, *Chem. Commun.*, 1288 (2002).
130. R. Mas-Balleste and L. Que, *J. Am. Chem. Soc.*, 129, 15964 (2007).
131. G. Anilkumar, B. Bitterlich, F. G. Gelalcha, M. K. Tse, and M. Beller, *Chem. Commun.*, 289 (2007).

132. B. Bitterlich, G. Anilkumar, F. G. Gelalcha, B. Spilker, A. Grotevendt, R. Jackstell, M. K. Tse, and M. Beller, *Chem. Asian J.*, **2**, 521 (2007).
133. (a) F. G. Gelalcha, G. Anilkumar, M. K. Tse, A. Brueckner, and M. Beller, *Chem. Eur. J.*, **14**, 7687 (2008); (b) B. Bitterlich, K. Schroder, M. K. Tse, and M. Beller, *Chem. Eur. J. Org. Chem.*, 4867 (2008); (c) S. Enthaler, K. Schroder, S. Inoue, B. Eckhardt, K. Junge, M. Beller, and M. Driess, *Eur. J. Org. Chem.*, 4893 (2010); (d) K. Schroder, K. Junge, A. Spannenberg, and M. Beller, *Catal. Today*, **157**, 364 (2010); (e) K. Schroder, S. Enthaler, B. Join, K. Junge, and M. Beller, *Adv. Synth. Catal.*, **352**, 1771 (2010).
134. K. Hasan, N. Brown, and C. M. Kozak, *Green Chem.*, **13**, 1230 (2012).
135. F. G. Gelalcha, B. Bitterlich, G. Anilkumar, M. K. Tse, and M. Beller, *Angew. Chem. Int. Ed.*, **46**, 7293 (2007).
136. K. Schroder, B. Join, A. J. Amali, K. Junge, X. Ribas, M. Costas, and M. Beller, *Angew. Chem. Int. Ed.*, **50**, 1425 (2011).
137. Y. Nishikawa and H. Yamamoto, *J. Am. Chem. Soc.*, **133**, 8432 (2011).
138. (a) D. J. Ferraro, L. Gakhar, and S. Ramaswamy, *Biochem. Biophys. Res. Commun.*, **338**, 175 (2005); (b) S. Beil, B. Happe, K. N. Timmis, and D. H. Pieper, *Eur. J. Biochem.*, **247**, 190 (1997).
139. K. Suzuki, P. D. Oldenburg, and L. Que, Jr., *Angew. Chem. Int. Ed.*, **47**, 1887 (2008).
140. Y. Feng, C. Y. Ke, G. Q. Xue, and L. Que, Jr., *Chem. Commun.*, **50** (2009).
141. (a) F. Dietrich and P. J. Stang, *Metal-Catalyzed Cross-Coupling Reactions*, Wiley–VCH, Weinheim, 1998; (b) N. Miyaura, *Cross-Coupling Reaction. A Practical Guide*, Vol. 219, Springer, Berlin, 2002.
142. M. Beller, A. Zapf, and W. Magerlein, *Chem. Eng. Technol.*, **24**, 575 (2001).
143. (a) L. Acemoglu and J. M. J. Williams, in *Handbook of Organopalladium Chemistry for Organic Synthesis*, John Wiley & Sons, Inc., New York, 2002; (b) J. Tsuji, *Palladium Reagents and Catalysts: Innovation in Organic Synthesis*, John Wiley & Sons, Inc., New York, 1996; (c) B. M. Trost, and T. R. Verhoeven, Vol. 8, *Pergamon, Oxford*, 1982.
144. (a) J. P. Corriu and J. P. Masse, *J. Chem. Soc. Chem. Commun.*, 144 (1972); (b) K. Tamao, K. Sumitani, and M. Kumada, *J. Am. Chem. Soc.*, **94**, 4374 (1972).
145. (a) M. Tamura and J. Kochi, *J. Am. Chem. Soc.*, **93**, 1487 (1971); (b) M. Tamura and J. K. Kochi, *Bull. Chem. Soc. Jpn.*, **44**, 3063 (1971); (c) M. Tamura and J. Kochi, *Synthesis*, 303 (1971); (d) J. K. Kochi, *Acc. Chem. Res.*, **7**, 351 (1974); (e) S. M. Neumann and J. K. Kochi, *J. Org. Chem.*, **40**, 599 (1975); (f) R. S. Smith and J. K. Kochi, *J. Org. Chem.*, **41**, 502 (1976); (g) J. K. Kochi, *J. Organomet. Chem.*, **653**, 11 (2002).
146. (a) G. A. Molander, B. J. Rahn, D. C. Shubert, and S. E. Bonde, *Tetrahedron Lett.*, **24**, 5449 (1983); (b) H. Felkin, P. J. Knowles, and B. Meunier, *J. Organomet. Chem.*, **146**, 151 (1978).
147. V. Fiandanese, G. Miccoli, F. Naso, and L. Ronzini, *J. Organomet. Chem.*, **312**, 343 (1986).

148. (a) J. L. Fabre, M. Julia, and J. N. Verpeaux, *Tetrahedron Lett.*, **23**, 2469 (1982); (b) J. L. Fabre, M. Julia, and J. N. Verpeaux, *Bull. Soc. Chim. Fr.*, 772 (1985); (c) E. Alvarez, T. Cuvigny, C. H. Dupenhoat, and M. Julia, *Tetrahedron*, **44**, 111 (1988); (d) E. Alvarez, T. Cuvigny, C. H. Dupenhoat, and M. Julia, *Tetrahedron*, **44**, 119 (1988).
149. (a) L. Jin, M. Julia, and J. N. Verpeaux, *Synlett*, 215 (1994); (b) I. Daub, A. K. Habermann, A. Hobert, and M. Julia, *Eur. J. Org. Chem.*, 163 (1999).
150. H. M. Walborsky and R. B. Banks, *J. Org. Chem.*, **46**, 5074 (1981).
151. (a) W. Dohle, F. Kopp, G. Cahiez, and P. Knochel, *Synlett*, 1901 (2001); (b) G. Cahiez and H. Avedissian, *Synthesis*, 1199 (1998).
152. (a) G. Cahiez and S. Marquais, *Tetrahedron Lett.*, **37**, 1773 (1996); (b) A. Furstner and H. Brunner, *Tetrahedron Lett.*, **37**, 7009 (1996); (c) G. Cahiez and S. Marquais, *Pure Appl. Chem.*, **68**, 53 (1996).
153. (a) A. Furstner and R. Martin, *Chem. Lett.*, **34**, 624 (2005); (b) B. Scheiper, M. Bonnekessel, H. Krause, and A. Furstner, *J. Org. Chem.*, **69**, 3943 (2004); (c) K. Itami, S. Higashi, M. Mineno, and J. Yoshida, *Org. Lett.*, **7**, 1219 (2005).
154. (a) A. Furstner and P. Hannen, *Chem. Eur. J.*, **12**, 3006 (2006); (b) G. Berthon-Gelloz and T. Hayashi, *J. Org. Chem.*, **71**, 8957 (2006).
155. (a) A. Furstner and A. Leitner, *Angew. Chem. Int. Ed.*, **41**, 609 (2002); (b) A. Furstner, A. Leitner, M. Mendez, and H. Krause, *J. Am. Chem. Soc.*, **124**, 13856 (2002).
156. G. Seidel, D. Laurich, and A. Furstner, *J. Org. Chem.*, **69**, 3950 (2004).
157. B. Scheiper, F. Glorius, A. Leitner, and A. Furstner, *Proc. Ind. Natl. Sci. Acad.*, **101**, 11960 (2004).
158. A. Furstner, A. Leitner, *Angew. Chem. Int. Ed.*, **42**, 308 (2003).
159. T. Hatakeyama and M. Nakamura, *J. Am. Chem. Soc.*, **129**, 9844 (2007).
160. M. Hocek and H. Dvorakova, *J. Org. Chem.*, **68**, 5773 (2003).
161. E. Colacino, H. Benakki, F. Guenoun, J. Martinez, and F. Lamaty, *Synth. Commun*, **39**, 1583 (2009).
162. A. L. Silberstein, S. D. Ramgren, and N. K. Garg, *Org. Lett.*, **14**, 3796 (2012).
163. O. M. Kuzmina, A. K. Steib, D. Flubacher, and P. Knochel, *Org. Lett.*, **14**, 4818 (2012).
164. A. C. Frisch and M. Beller, *Angew. Chem. Int. Ed.*, **44**, 674 (2005).
165. M. Tamura and J. Kochi, *J. Organomet. Chem.*, **31**, 289 (1971).
166. (a) M. Nakamura, K. Matsuo, S. Ito, and B. Nakamura, *J. Am. Chem. Soc.*, **126**, 3686 (2004); (b) M. Nakamura, S. Ito, K. Matsuo, and E. Nakamura, *Synlett*, 1794 (2005).
167. T. Nagano and T. Hayashi, *Org. Lett.*, **6**, 1297 (2004).
168. (a) A. Guerinot, S. Reymond, and J. Cossy, *Angew. Chem. Int. Ed.*, **46**, 6521 (2007); (b) G. Cahiez, C. Duplais, and A. Moyeux, *Org. Lett.*, **9**, 3253 (2007).
169. K. G. Dongol, H. Koh, M. Sau, and C. L. L. Chai, *Adv. Synth. Catal.*, **349**, 1015 (2007).
170. Y. Yamaguchi, H. Ando, M. Nagaya, H. Hinago, T. Ito, and M. Asami, *Chem. Lett.*, **40**, 983 (2011).

171. Z. B. Mo, Q. Zhang, and L. Deng, *Organometallics*, *31*, 6518 (2012).
172. R. Martin and A. Furstner, *Angew. Chem. Int. Ed.*, *43*, 3955 (2004).
173. K. Jonas, L. Schieferstein, C. Kruger, and Y. H. Tsay, *Angew. Chem. Int. Ed.*, *18*, 550 (1979).
174. (a) R. B. Bedford, D. W. Bruce, R. M. Frost, and M. Hird, *Chem. Commun.*, 4161 (2005); (b) K. Bica and P. Gaertner, *Org. Lett.*, *8*, 733 (2006); (c) R. R. Chowdhury, A. K. Crane, C. Fowler, P. Kwong, and C. M. Kozak, *Chem. Commun.*, 94 (2008).
175. M. Jin and M. Nakamura, *Chem. Lett.*, *40*, 1012 (2011).
176. G. Cahiez, V. Habiak, C. Duplais, and A. Moyeux, *Angew. Chem. Int. Ed.*, *46*, 4364 (2007).
177. W. C. Percival, R. B. Wagner, and N. C. Cook, *J. Am. Chem. Soc.*, *75*, 3731 (1953).
178. F. Babudri, A. Dettolo, V. Fiandanese, G. Marchese, and F. Naso, *J. Organomet. Chem.*, *405*, 53 (1991).
179. (a) B. D. Sherry and A. Furstner, *Acc. Chem. Res.*, *41*, 1500 (2008); (b) C. Cardellicchio, V. Viandanese, G. Marchese, and L. Ronzini, *Tetrahedron Lett.*, *26*, 3595 (1985); (c) C. Duplais, F. Bures, I. Sapountzis, T. J. Korn, G. Cahiez, and P. Knochel, *Angew. Chem. Int. Ed.*, *43*, 2968 (2004).
180. V. Fiandanese, G. Marchese, and F. Naso, *Tetrahedron Lett.*, *29*, 3587 (1988).
181. (a) A. Furstner, D. De Souza, L. Parra-Rapado, and J. T. Jensen, *Angew. Chem. Int. Ed.*, *42*, 5358 (2003); (b) K. Lehr and A. Furstner, *Tetrahedron*, *68*, 7695 (2012).
182. M. Taillefer, N. Xia, and A. Ouali, *Angew. Chem. Int. Ed.*, *46*, 934 (2007).
183. A. Correa and C. Bolm, *Angew. Chem. Int. Ed.*, *46*, 8862 (2007).
184. A. Correa, M. Carril, and C. Bolm, *Angew. Chem. Int. Ed.*, *47*, 2880 (2008).
185. Y. Y. Lin, Y. J. Wang, C. H. Lin, J. H. Cheng, and C. F. Lee, *J. Org. Chem.*, *77*, 6100 (2012).
186. O. Bistri, A. Correa, and C. Bolm, *Angew. Chem. Int. Ed.*, *47*, 586 (2008).
187. J. C. Mao, G. L. Xie, J. M. Zhan, Q. Q. Hua, and D. Q. Shi, *Adv. Synth. Catal.*, *351*, 1268 (2009).
188. (a) T. Mizoroki, K. Mori, and A. Ozaki, *Bull. Chem. Soc. Jpn.*, *44*, 581 (1971); (b) R. F. Heck and J. P. Nolley, *J. Org. Chem.*, *37*, 2320 (1972).
189. R. Loska, C. M. R. Volla, and P. Vogel, *Adv. Synth. Catal.*, *350*, 2859 (2008).
190. T. Hatakeyama, Y. Kondo, Y. I. Fujiwara, H. Takaya, S. Ito, E. Nakamura, and M. Nakamura, *Chem. Commun.*, 1216 (2009).
191. R. B. Bedford, M. Huwe, and M. C. Wilkinson, *Chem. Commun.*, 600 (2009).
192. S. Ito, Y. Fujiwara, E. Nakamura, and M. Nakamura, *Org. Lett.*, *11*, 4306 (2009).
193. T. Hatakeyama, T. Hashimoto, Y. Kondo, Y. Fujiwara, H. Seike, H. Takaya, Y. Tamada, T. Ono, and M. Nakamura, *J. Am. Chem. Soc.*, *132*, 10674 (2010).
194. T. Hashimoto, T. Hatakeyama, and M. Nakamura, *J. Org. Chem.*, *77*, 1168 (2012).
195. T. Hatakeyama, T. Hashimoto, K. Kathiriarachchi, T. Zenmyo, H. Seike, and M. Nakamura, *Angew. Chem. Int. Ed.*, *51*, 8834 (2012).
196. S. Kawamura, T. Kawabata, K. Ishizuka, and M. Nakamura, *Chem. Commun.*, *48*, 9376 (2012).

197. M. Carril, A. Correa, and C. Bolm, *Angew. Chem. Int. Ed.*, **47**, 4862 (2008).
198. B. Bogdanovic and M. Schwickardi, *Angew. Chem. Int. Ed.*, **39**, 4610 (2000).
199. A. Furstner, R. Martin, H. Krause, G. Seidel, R. Goddard, and C. W. Lehmann, *J. Am. Chem. Soc.*, **130**, 8773 (2008).
200. B. Holzer and R. W. Hoffmann, *Chem. Commun.*, 732 (2003).
201. D. Noda, Y. Sunada, T. Hatakeyama, M. Nakamura, and H. Nagashima, *J. Am. Chem. Soc.*, **131**, 6078 (2009).
202. (a) J. Kleimark, A. Hedstrom, P. F. Larsson, C. Johansson, and P. O. Norrby, *Chemcatchem*, **1**, 152 (2009); (b) A. Hedstrom, U. Bollmann, J. Bravidor, and P. O. Norrby, *Chem. Eur. J.*, **17**, 11991 (2011).
203. C. J. Adams, R. B. Bedford, E. Carter, N. J. Gower, M. F. Haddow, J. N. Harvey, M. Huwe, M. A. Cartes, S. M. Mansell, C. Mendoza, D. M. Murphy, E. C. Neeve, and J. Nunn, *J. Am. Chem. Soc.*, **134**, 10333 (2012).
204. R. B. Bedford, E. Carter, P. M. Cogswell, N. J. Gower, M. F. Haddow, J. N. Harvey, D. M. Murphy, E. C. Neeve, and J. Nunn, *Angew. Chem. Int. Ed.*, **51**, 5435 (2012).
205. M. D. Greenhalgh and S. P. Thomas, *J. Am. Chem. Soc.*, **134**, 11900 (2012).
206. (a) R. Chinchilla, C. Najera, *Chem. Rev.*, **107**, 874 (2007); (b) H. Doucet and J. C. Hierso, *Angew. Chem. Int. Ed.*, **46**, 834 (2007).
207. T. Hatakeyama, Y. Yoshimoto, T. Gabriel, and M. Nakamura, *Org. Lett.*, **10**, 5341 (2008).
208. (a) T. E. Muller and M. Beller, *Chem. Rev.*, **98**, 675 (1998); (b) R. N. Salvatore, C. H. Yoon, and K. W. Jung, *Tetrahedron*, **57**, 7785 (2001); (c) P. Muller and C. Fruit, *Chem. Rev.*, **103**, 2905 (2003).
209. (a) J. L. Liang, J. S. Huang, X. Q. Yu, N. Y. Zhu, and C. M. Che, *Chem. Eur. J.*, **8**, 1563 (2002); (b) Y. Cui and C. He, *J. Am. Chem. Soc.*, **125**, 16202 (2003); (c) Z. G. Li, D. A. Capretto, R. Rahaman, and C. A. He, *Angew. Chem. Int. Ed.*, **46**, 5184 (2007).
210. Z. Wang, Y. M. Zhang, H. Fu, Y. Y. Jiang, and Y. F. Zhao, *Org. Lett.*, **10**, 1863 (2008).
211. S. G. Pan, J. H. Liu, H. R. Li, Z. Y. Wang, X. W. Guo, and Z. P. Li, *Org. Lett.*, **12**, 1932 (2010).
212. Q. Q. Xia and W. Z. Chen, *J. Org. Chem.*, **77**, 9366 (2012).
213. J. A. Wang, J. T. Hou, J. Wen, J. Zhang, and X. Q. Yu, *Chem. Commun.*, **47**, 3652 (2011).
214. (a) M. Johannsen and K. A. Jorgensen, *Chem. Rev.*, **98**, 1689 (1998); (b) Y. Tamaru, and M. Kimura, *Synlett*, 749 (1997).
215. M. Johannsen and K. A. Jorgensen, *J. Org. Chem.*, **59**, 214 (1994).
216. R. S. Srivastava and K. M. Nicholas, *Tetrahedron Lett.*, **35**, 8739 (1994).
217. S. Singh and K. M. Nicholas, *Synth. Commun.*, **31**, 3087 (2001).
218. (a) J. E. Kmieciak, *J. Org. Chem.*, **30**, 2014 (1965); (b) D. Mulvey and W. A. Waters, *J. Chem. Soc., Perkin Trans. 2*, 1868 (1977).
219. M. Johannsen and K. A. Jorgensen, *J. Org. Chem.*, **60**, 5979 (1995).

220. (a) R. S. Srivastava, M. A. Khan, and K. M. Nicholas, *J. Am. Chem. Soc.*, **118**, 3311 (1996); (b) R. S. Srivastava and K. M. Nicholas, *J. Am. Chem. Soc.*, **119**, 3302 (1997).
221. (a) R. S. Srivastava and K. M. Nicholas, *Chem. Commun.*, 2705 (1998); (b) M. K. Kolel-Veetil, M. A. Khan, and K. M. Nicholas, *Organometallics*, **19**, 3754 (2000).
222. R. S. Srivastava, M. Kolel-Veetil, and K. M. Nicholas, *Tetrahedron Lett.*, **43**, 931 (2002).
223. B. Plietker, *Angew. Chem. Int. Ed.*, **45**, 6053 (2006).
224. J. Bonnamour and C. Bolm, *Org. Lett.*, **13**, 2012 (2011).
225. (a) R. Breslow and S. H. Gellman, *J. Chem. Soc. Chem. Commun.*, 1400 (1982); (b) R. Breslow and S. H. Gellman, *J. Am. Chem. Soc.*, **105**, 6728 (1983).
226. S. M. Paradine and M. C. White, *J. Am. Chem. Soc.*, **134**, 2036 (2012).
227. Z. Wang, S. Li, B. Yu, H. Wu, Y. Wang, and X. Sun, *J. Org. Chem.*, **77**, 8615 (2012).
228. E. R. King, E. T. Hennessy, and T. A. Betley, *J. Am. Chem. Soc.*, **133**, 4917 (2011).
229. (a) S. S. Kim, K. Nehru, S. S. Kim, D. W. Kim, and H. C. Jung, *Synthesis*, 2484 (2002); (b) A. R. Suarez, A. M. Baruzzi, and L. I. Rossi, *J. Org. Chem.*, **63**, 5689 (1998).
230. (a) J. T. Groves and P. Viski, *J. Org. Chem.*, **55**, 3628 (1990); (b) E. Baciocchi, M. F. Gerini, and A. Lapi, *J. Org. Chem.*, **69**, 3586 (2004).
231. (a) C. Duboc-Toia, S. Menage, R. Y. N. Ho, L. Que, C. Lambeaux, and M. Fontecave, *Inorg. Chem.*, **38**, 1261 (1999); (b) Y. Mekmouche, H. Hummel, R. Y. N. Ho, L. Que, V. Schunemann, F. Thomas, A. X. Trautwein, C. Lebrun, K. Gorgy, J. C. Lepretre, M. N. Collomb, A. Deronzier, M. Fontecave, and S. Menage, *Chem. Eur. J.*, **8**, 1196 (2002).
232. (a) J. Legros and C. Bolm, *Angew. Chem. Int. Ed.*, **42**, 5487 (2003); (b) J. Legros and C. Bolm, *Angew. Chem. Int. Ed.*, **43**, 4225 (2004).
233. J. Legros and C. Bolm, *Chem. Eur. J.*, **11**, 1086 (2005).
234. (a) A. Korte, J. Legros, and C. Bolm, *Synlett*, 2397 (2004); (b) J. Legros, J. R. Dehli, and C. Bolm, *Adv. Synth. Catal.*, **347**, 19 (2005).
235. A. M. I. Jayaseeli and S. Rajagopal, *J. Mol. Catal. A: Chem.*, **309**, 103 (2009).
236. S. H. Liao and B. List, *Adv. Synth. Catal.*, **354**, 2363 (2012).
237. B. Li, A. H. Liu, L. N. He, Z. Z. Yang, J. Gao, and K. H. Chen, *Green Chem.*, **14**, 130 (2012).
238. (a) T. Bach and C. Korber, *Tetrahedron Lett.*, **39**, 5015 (1998); (b) T. Bach and C. Korber, *Eur. J. Org. Chem.*, 1033 (1999).
239. (a) C. Bolm, K. Muniz, N. Aguilar, M. Kesselgruber, and G. Raabe, *Synthesis*, 1251 (1999); (b) H. Okamura and C. Bolm, *Chem. Lett.*, **33**, 482 (2004); (c) M. Reggelin and C. Zur, *Synthesis*, 1 (2000).
240. O. G. Mancheno and C. Bolm, *Org. Lett.*, **8**, 2349 (2006).
241. O. G. Mancheno, J. Dallimore, A. Plant, and C. Bolm, *Org. Lett.*, **11**, 2429 (2009).
242. X. F. Wu, C. Vovard-Le Bray, L. Bechki, and C. Darcel, *Tetrahedron*, **65**, 7380 (2009).
243. R. N. Naumov, M. Itazaki, M. Kamitani, and H. Nakazawa, *J. Am. Chem. Soc.*, **134**, 804 (2012).

244. (a) A. M. Tondreau, C. C. H. Atienza, K. J. Weller, S. A. Nye, K. M. Lewis, J. G. P. Delis, and P. J. Chirik, *Science*, **335**, 567 (2012); (b) A. N. Nesmeyanov, R. Kh. Freedline, E. C. Chukovskaya, R. G. Petrova, A. B. Belyarsky, *Tetrahedron*, **17**, 61 (1962); (c) M. A. Schroeder and M. S. Wrighton, *J. Organomet. Chem.*, **128**, 345 (1977).
245. F. Kakiuchi, Y. Tanaka, N. Chatani, and S. Murai, *J. Organomet. Chem.*, **456**, 45 (1993).
246. S. C. Bart, E. Lobkovsky, and P. J. Chirik, *J. Am. Chem. Soc.*, **126**, 13794 (2004).
247. A. M. Tondreau, C. C. H. Atienza, J. M. Darmon, C. Milsmann, H. M. Hoyt, K. J. Weller, S. A. Nye, K. M. Lewis, J. Boyer, J. G. P. Delis, E. Lobkovsky, and P. J. Chirik, *Organometallics*, **31**, 4886 (2012).
248. K. Kamata, A. Suzuki, Y. Nakai, and H. Nakazawa, *Organometallics*, **31**, 3825 (2012).
249. J. Y. Wu, B. N. Stanzl, and T. Ritter, *J. Am. Chem. Soc.*, **132**, 13214 (2010).
250. H. Nishiyama and A. Furuta, *Chem. Commun.*, 760 (2007).
251. (a) S. Hosokawa, J. Ito, and H. Nishiyama, *Organometallics*, **29**, 5773 (2010); (b) T. Inagaki, A. Ito, J. Ito, and H. Nishiyama, *Angew. Chem. Int. Ed.*, **49**, 9384 (2010).
252. (a) N. S. Shaikh, S. Enthaler, K. Junge, and M. Beller, *Angew. Chem. Int. Ed.*, **47**, 2497 (2008); (b) N. S. Shaikh, K. Junge, and M. Beller, *Org. Lett.*, **9**, 5429 (2007).
253. J. A. Yang and T. D. Tilley, *Angew. Chem. Int. Ed.*, **49**, 10186 (2010).
254. E. N. Frankel, E. A. Emken, and V. L. Davison, *J. Org. Chem.*, **30**, 2739 (1965).
255. M. A. Schroeder and M. S. Wrighton, *J. Am. Chem. Soc.*, **98**, 551 (1976).
256. R. Noyori, I. Umeda, and T. Ishigami, *J. Org. Chem.*, **37**, 1542 (1972).
257. C. Bianchini, A. Meli, M. Peruzzini, P. Frediani, C. Bohanna, M. A. Esteruelas, and L. A. Oro, *Organometallics*, **11**, 138 (1992).
258. S. D. Brown and J. C. Peters, *J. Am. Chem. Soc.*, **126**, 4538 (2004).
259. E. J. Daida and J. C. Peters, *Inorg. Chem.*, **43**, 7474 (2004).
260. R. J. Trovitch, E. Lobkovsky, E. Bill, and P. J. Chirik, *Organometallics*, **27**, 1470 (2008).
261. G. Wienhofer, F. A. Westerhaus, R. V. Jagadeesh, K. Junge, H. Junge, and M. Beller, *Chem. Commun.*, **48**, 4827 (2012).
262. C. Bianchini, E. Farnetti, M. Graziani, M. Peruzzini, and A. Polo, *Organometallics*, **12**, 3753 (1993).
263. (a) C. P. Casey and H. R. Guan, *J. Am. Chem. Soc.*, **129**, 5816 (2007); (b) C. P. Casey, S. E. Beetner, and J. B. Johnson, *J. Am. Chem. Soc.*, **130**, 2285 (2008).
264. A. Berkessel, S. Reichau, A. von der Hoh, N. Leconte, and J. M. Neudorfl, *Organometallics*, **30**, 3880 (2011).
265. S. Enthaler, B. Spilker, G. Erre, K. Junge, M. K. Tse, and M. Beller, *Tetrahedron*, **64**, 3867 (2008).
266. (a) C. Sui-Seng, F. Freutel, A. J. Lough, and R. H. Morris, *Angew. Chem. Int. Ed.*, **47**, 940 (2008); (b) C. Sui-Seng, F. N. Haque, A. Hadzovic, A. M. Puetz, V. Reuss, N. Meyer, A. J. Lough, M. Z. D. Iuliis, and R. H. Morris, *Inorg. Chem.*, **48**, 735 (2009).
267. R. H. Morris, *Chem. Soc. Rev.*, **38**, 2282 (2009).

268. (a) A. Mikhailine, A. J. Lough, and R. H. Morris, *J. Am. Chem. Soc.*, **131**, 1394 (2009); (b) N. Meyer, A. J. Lough, and R. H. Morris, *Chem. Eur. J.*, **15**, 5605 (2009).
269. (a) P. O. Lagaditis, A. J. Lough, and R. H. Morris, *Inorg. Chem.*, **49**, 10057 (2010); (b) P. E. Sues, A. J. Lough, and R. H. Morris, *Organometallics*, **30**, 4418 (2011); (c) D. E. Prokopchuk, J. F. Sonnenberg, N. Meyer, M. Z. D. Iulius, A. J. Lough, and R. H. Morris, *Organometallics*, **31**, 3056 (2012); (d) D. E. Prokopchuk and R. H. Morris, *Organometallics*, **31**, 7375 (2012).
270. R. Langer, G. Leitus, Y. Ben-David, and D. Milstein, *Angew. Chem. Int. Ed.*, **50**, 2120 (2011).
271. X. Z. Yang, *Inorg. Chem.*, **50**, 12836 (2011).
272. R. Langer, M. A. Iron, L. Konstantinovski, Y. Diskin-Posner, G. Leitus, Y. Ben-David, and D. Milstein, *Chem. Eur. J.*, **18**, 7196 (2012).
273. V. Kandepi, J. M. S. Cardoso, E. Peris, and B. Royo, *Organometallics*, **29**, 2777 (2010).
274. T. Hashimoto, S. Urban, R. Hoshino, Y. Ohki, K. Tatsumi, and F. Glorius, *Organometallics*, **31**, 4474 (2012).
275. A. Tlili, J. Schranck, H. Neumann, and M. Beller, *Chem. Commun.*, **18**, 15935 (2012).
276. S. L. Zhou, S. Fleischer, K. Junge, S. Das, D. Addis, and M. Beller, *Angew. Chem. Int. Ed.*, **49**, 8121 (2010).
277. S. L. Zhou, S. Fleischer, K. Junge, and M. Beller, *Angew. Chem. Int. Ed.*, **50**, 5120 (2011).
278. A. A. Mikhailine, M. I. Maishan, and R. H. Morris, *Org. Lett.*, **14**, 4638 (2012).
279. (a) A. Bechamp, *Annal. Chim.*, **42**, 186 (1854); (b) M. Lauwiner and P. Rys, J. Wissmann, *Appl. Catal., A*, **172**, 141 (1998).
280. M. Lauwiner, R. Roth, and P. Rys, *Appl. Catal., A*, **177**, 9 (1999).
281. D. G. Desai, S. S. Swami, S. K. Dabhade, and M. G. Ghagare, *Synth. Commun.*, **31**, 1249 (2001).
282. (a) S. U. Sonavane, S. K. Mohapatra, R. V. Jayaram, and P. Selvam, *Chem. Lett.*, **32**, 142 (2003); (b) R. M. Deshpande, A. N. Mahajan, M. M. Diwakar, P. S. Ozarde, and R. V. Chaudhari, *J. Org. Chem.*, **69**, 4835 (2004).
283. M. Kumarraja and K. Pitchumani, *Appl. Catal., A*, **265**, 135 (2004).
284. Y. G. Liu, Y. S. Lu, M. Prashad, J. Repic, and T. J. Blacklock, *Adv. Synth. Catal.*, **347**, 217 (2005).
285. Q. X. Shi, R. W. Lu, Z. X. Zhang, and D. F. Zhao, *Chin. Chem. Lett.*, **17**, 441 (2006).
286. A. B. Gamble, J. Garner, C. P. Gordon, S. M. J. O'Conner, and P. A. Keller, *Synth. Commun.*, **37**, 2777 (2007).
287. S. Chandrappa, K. Vinaya, T. Ramakrishnappa, and K. S. Rangappa, *Synlett*, 3019 (2010).
288. L. Pehlivan, E. Metay, S. Laval, W. Dayoub, P. Demonchaux, G. Mignani, and M. Lemaire, *Tetrahedron Lett.*, **51**, 1939 (2010).
289. R. V. Jagadeesh, G. Wienhofer, F. A. Westerhaus, A. E. Surkus, M. M. Pohl, H. Junge, and K. Junge, and M. Beller, *Chem. Commun.*, **47**, 10972 (2011).

290. U. Sharma, P. K. Verma, N. Kumar, V. Kumar, M. Bala, and B. Singh, *Chem. Eur. J.*, **17**, 5903 (2011).
291. G. Wienhofer, I. Sorribes, A. Boddien, F. Westerhaus, K. Junge, H. Junge, R. Llusar, and M. Beller, *J. Am. Chem. Soc.*, **133**, 12875 (2011).
292. D. Cantillo, M. Baghbanzadeh, and C. O. Kappe, *Angew. Chem. Int. Ed.*, **51**, 10190 (2012).
293. Y. Inoue, Y. Sasaki, and H. Hashimoto, *J. Chem. Soc., Chem. Commun.*, 718 (1975).
294. G. O. Evans and C. J. Newell, *Inorg. Chim. Acta*, **31**, L387 (1978).
295. C. C. Tai, T. Chang, B. Roller, and P. G. Jessop, *Inorg. Chem.*, **42**, 7340 (2003).
296. C. Federsel, A. Boddien, R. Jackstell, R. Jennerjahn, P. J. Dyson, R. Scopelliti, G. Laurency, and M. Beller, *Angew. Chem. Int. Ed.*, **49**, 9777 (2010).
297. C. Ziebart, C. Federsel, P. Anbarasan, R. Jackstell, W. Baumann, A. Spannenberg, and M. Beller, *J. Am. Chem. Soc.*, **134**, 20701 (2012).
298. R. Langer, Y. Diskin-Posner, G. Leitus, L. J. W. Shimon, Y. Ben-David, and D. Milstein, *Angew. Chem. Int. Ed.*, **50**, 9948 (2011).
299. S. Zhou, K. Junge, D. Addis, S. Das, and M. Beller, *Angew. Chem. Int. Ed.*, **48**, 9507 (2009).
300. B. Merla and N. Risch, *Synthesis*, 1365 (2002).
301. A. Pagnoux-Ozherelyeva, N. Pannetier, M. D. Mbaye, S. Gaillard, and J. L. Renaud, *Angew. Chem. Int. Ed.*, **51**, 4976 (2012).
302. (a) P. O. Lagaditis, A. J. Lough, and R. H. Morris, *J. Am. Chem. Soc.*, **133**, 9662 (2011); (b) A. Mikhailine, A. J. Lough, and R. H. Morris, *J. Am. Chem. Soc.*, **131**, 1394 (2009); (c) C. P. Casey, and H. R. Guan, *J. Am. Chem. Soc.*, **131**, 2499 (2009).
303. J. P. Hopewell, J. E. D. Martins, T. C. Johnson, J. Godfrey, and M. Wills, *Org. Biol. Chem.*, **10**, 134 (2012).
304. M. D. Bhor, M. J. Bhanushali, N. S. Nandurkar, and B. M. Bhanage, *Tetrahedron Lett.*, **49**, 965 (2008).
305. S. Enthaler, *Chemcatchem*, **2**, 1411 (2010).
306. S. Fleischer, S. L. Zhou, K. Junge, and M. Beller, *Chem. Asian J.*, **6**, 2240 (2011).
307. N. U. Kumar, B. S. Reddy, V. P. Reddy, and R. Bandichhor, *Tetrahedron Lett.*, **53**, 4354 (2012).
308. K. Muller, C. Faeh, and F. Diederich, *Science*, **317**, 1881 (2007).
309. A. T. Parsons, T. D. Senecal, and S. L. Buchwald, *Angew. Chem. Int. Ed.*, **51**, 2947 (2012).